

University of Warwick institutional repository: <http://go.warwick.ac.uk/wrap>

A Thesis Submitted for the Degree of PhD at the University of Warwick

<http://go.warwick.ac.uk/wrap/3097>

This thesis is made available online and is protected by original copyright.

Please scroll down to view the document itself.

Please refer to the repository record for this item for information to help you to cite it. Our policy information is available from the repository home page.

**Annexin IV:
a pronephros specific gene with a role in pronephric development**

Rachel Alice Seville B.Sc. (Hons.)

Thesis submitted for the degree of Doctor of Philosophy

University of Warwick

**Cell and Molecular Development Research Group
Department of Biological Sciences
University of Warwick**

November 2001

Table of contents

| | |
|-------------------|-------|
| Table of contents | i |
| Table of figures | viii |
| Table of tables | xiii |
| Acknowledgements | xiv |
| Declaration | xv |
| Abstract | xvi |
| Abbreviations | xviii |

Chapter 1: Introduction

| | | |
|------------|--|-----------|
| 1.1 | The vertebrate kidney | 1 |
| 1.2 | The pronephros | 1 |
| 1.2.1 | The <i>Xenopus</i> pronephros structure and function | 3 |
| 1.2.2 | The organogenesis of the <i>Xenopus</i> pronephros | 5 |
| 1.2.3 | The zebrafish pronephros structure and function | 8 |
| 1.2.4 | The zebrafish pronephros organogenesis | 8 |
| 1.3 | The molecular markers of pronephric development | 11 |
| 1.3.1 | LIM class transcription factors | 11 |
| 1.3.2 | Paired-box transcription factors | 13 |
| 1.3.3 | Hepatocyte nuclear factors (HNF) | 15 |
| 1.3.4 | Wilms' Tumor | 15 |
| 1.3.5 | Helix-loop-helix transcription factors | 16 |
| 1.3.6 | Vascular Endothelial Growth Factor (VEGF) | 17 |
| 1.3.7 | Wingless family members (wnt) | 17 |
| 1.3.8 | Frizzled Receptors of wnt family ligands | 18 |
| 1.3.9 | Bone Morphogenetic Proteins (BMP). | 18 |
| 1.3.10 | Hedgehog family | 19 |
| 1.3.11 | Glial-derived neurotrophic factor | 19 |
| 1.3.12 | Fibroblast growth factor pathway | 20 |
| 1.3.13 | The Notch and Delta family | 20 |
| 1.3.14 | Integrins and cadherins | 22 |
| 1.3.15 | Cold-inducible RNA binding protein (CIRP) | 22 |

| | | |
|--------|---|----|
| 1.3.16 | Other useful markers of pronephric components | 23 |
| 1.4 | Mutagenesis studies in the zebrafish pronephros | 24 |
| 1.5 | Specification and induction of the pronephros in <i>Xenopus</i> | 27 |
| 1.6 | Pronephric cell lineages in Zebrafish | 31 |
| 1.7 | In vitro induction of pronephric tissues | 33 |
| 1.8 | Cloning of <i>Xenopus laevis</i> annexin 4 (<i>Xanx-4</i>) | 33 |
| 1.9 | The aims of this thesis | 38 |

Chapter 2 Materials and Methods

| | | |
|-------|--|----|
| 2.1 | Materials | 40 |
| 2.2 | Media and stock solutions | 40 |
| 2.3 | Vectors | 41 |
| 2.4 | DNA techniques | |
| 2.4.1 | Agarose gel electrophoresis | 41 |
| 2.4.2 | Restriction enzyme digests | 41 |
| 2.4.3 | DNA minipreps | 42 |
| 2.4.4 | Ligation of DNA into plasmid vectors | 42 |
| 2.4.5 | Preparation of the <i>myc-Xanx-4</i> and <i>Xanx-4-MUT</i> inserts and their ligation into plasmid vectors. | 42 |
| 2.4.6 | Transformation of plasmid DNA into competent <i>E. coli</i> | 44 |
| 2.4.7 | DNA sequencing | 45 |
| 2.5 | RNA techniques | |
| 2.5.1 | RNA extraction from embryos and animal caps | 45 |
| 2.5.2 | Reverse Transcription PCR | 46 |
| 2.5.3 | <i>In vitro</i> transcription of mRNA | 49 |
| 2.5.4 | Wholemout in situ hybridization | 49 |
| 2.5.5 | Northern blot analysis | 50 |
| 2.6 | Protein techniques | |
| 2.6.1 | Protein expression in oocytes | 51 |
| 2.6.2 | Protein extraction from oocytes and embryos | 51 |
| 2.6.3 | Sucrose gradient fractionation of oocytes | 51 |
| 2.6.4 | <i>In vitro</i> translation | 52 |
| 2.6.5 | Western immunoblot analysis | 52 |

| | | |
|-------------|--|-----------|
| 2.7 | Wholemout immunohistochemistry | 53 |
| 2.8 | Histology | 54 |
| 2.8.1 | Acrylamide embedding and cryostat sectioning | 54 |
| 2.8.2 | Histological staining | 54 |
| 2.9 | Embryo manipulations | 54 |
| 2.9.1 | <i>In vitro</i> fertilization of <i>Xenopus</i> eggs | 54 |
| 2.9.2 | Micro-injection of embryos | 55 |
| 2.10 | Bespoke oligonucleotides for gene expression perturbation | 55 |
| 2.10.1 | dsRNA consructs | 56 |
| 2.10.2 | siRNA constructs | 57 |
| 2.10.3 | Morpholinos | 59 |

Chapter 3: Characterisation of the clone K2

| | | |
|------------|--|-----------|
| 3.1 | Introduction | 60 |
| 3.2 | Results | 62 |
| 3.2.1 | The cDNA clone K2 identified as <i>Xenopus laevis</i> annexin IV | 62 |
| 3.2.2 | <i>Xanx-4</i> is expressed at the right time to have a role in pronephric specification and organogenesis. | 66 |
| 3.2.3 | <i>Xanx-4</i> transcripts are present throughout the <i>Xenopus</i> oocyte | 66 |
| 3.2.4 | <i>Xanx-4</i> protein is localised to all fractions of <i>Xenopus</i> oocytes | 68 |
| 3.2.5 | Expression of <i>Xanx4</i> transcripts is restricted to the otic vesicle and to the pronephric tubules in <i>Xenopus laevis</i> embryos | 70 |
| 3.2.6 | Expression of <i>Xanx4</i> and protein is restricted to the apical surface of pronephric tubules in <i>Xenopus laevis</i> embryos | 73 |
| 3.2.7 | Expression of <i>Xanx-4</i> restricted to specific organs in adult frog. | 76 |
| 3.3 | Discussion | 79 |
| 3.3.1 | Sequence analysis, protein structure and motifs | 79 |
| 3.3.2 | Maternal Expression of <i>Xanx-4</i> | 80 |
| 3.3.3 | Zygotic embryonic Expression of <i>Xanx-4</i> | 81 |
| 3.3.4 | Expression of <i>Xanx-4</i> in the adult frog | 83 |
| 3.3.5 | In conclusion | 84 |

Chapter 4 The effect of overexpression of *Xanx-4* on pronephric structure in *Xenopus laevis*.

| | | |
|------------|--|-----------|
| 4.1 | Introduction | 85 |
| 4.2 | Injected <i>Xanx-4</i> mRNA translates into a 34 kDa protein at high level in oocytes | 89 |
| 4.3 | Targeting of the <i>Xanx-4</i> mRNA to the pronephric anlagen | 89 |
| 4.4 | Analysis of the <i>Xanx-4</i> mRNA injected embryos by wholemount antibody 3G8 and 4A6 staining | 92 |
| 4.5 | Longevity of injected message | 95 |
| 4.6 | Discussion | 97 |

Chapter 5: Perturbation of *Xanx-4* expression in *Xenopus laevis* by double stranded RNA

| | | |
|------------|--|-----------|
| 5.1 | Introduction | 99 |
| 5.1.1 | Studying gene activity in <i>Xenopus</i> by loss-of-function experiments | 99 |
| 5.1.1.1 | The dominant-negative approach | 99 |
| 5.1.1.2 | Antisense DNA and RNA | 100 |
| 5.1.1.3 | Rescue of dominant-negative and antisense induced phenotypes | 101 |
| 5.1.2 | Transgene induced gene silencing | 102 |
| 5.1.3 | Transgene silencing in plants (co-suppression) | 102 |
| 5.1.4 | Gene silencing in fungi (Quelling) | 104 |
| 5.1.5 | RNA interference (RNAi) | 104 |
| 5.1.5.1 | <i>Caenorhabditis elegans</i> | 105 |
| 5.1.5.2 | <i>Drosophila melanogaster</i> | 107 |
| 5.1.5.3 | Zebrafish | 111 |
| 5.1.5.4 | Mouse | 112 |
| 5.1.5.5 | Mammalian cell line studies | 112 |
| 5.1.5.6 | <i>Xenopus</i> | 113 |
| 5.1.5.7 | <i>Trypanosoma brucei</i> | 114 |
| 5.1.5.8 | Planarians | 114 |
| 5.1.5.9 | <i>Hydra magnipapillata</i> | 115 |
| 5.1.6 | The specificity, length, localisation, delivery and heritability | |

| | | |
|------------|--|------------|
| | of dsRNA for RNAi | 115 |
| 5.1.7 | The current model of RNAi induced mRNA degradation | 117 |
| 5.1.8 | Aims | 120 |
| 5.2 | Results | |
| 5.2.1 | Production of single stranded and double stranded RNAs | 121 |
| 5.2.2 | RNAi prevents translation of exogenous mRNA in <i>Xenopus</i> oocytes | 126 |
| 5.2.3 | Interference of endogenous <i>Xanx-4</i> expression by RNAi in <i>Xenopus</i> oocytes | 128 |
| 5.2.4 | Effect of RNAi on exogenous <i>Xanx-4</i> mRNA in <i>Xenopus</i> oocytes | 131 |
| 5.2.4 | Interference of endogenous <i>Xanx-4</i> expression by RNAi in <i>Xenopus</i> embryos. | 133 |
| 5.2.6 | Persistence of dsRNA in <i>Xenopus</i> embryos | 136 |
| 5.2.7 | Effect of RNAi on exogenous <i>Xanx-4</i> mRNA in <i>Xenopus</i> embryos | 136 |
| 5.3 | The use of synthetic short interfering RNA (siRNA) to perturb <i>Xanx-4</i> expression in <i>Xenopus laevis</i> | |
| 5.3.1 | The advent of synthetic siRNA | 139 |
| 5.3.2 | The design and preparation of the <i>Xanx-4</i> siRNA | 141 |
| 5.3.3 | Testing the effect of <i>Xanx-4</i> siRNA <i>in vitro</i> | 141 |
| 5.3.4 | <i>Xanx-4</i> siRNA does not have a marked effect on the level of <i>Xanx-4</i> mRNA in <i>Xenopus laevis</i> embryos | 143 |
| 5.3.5 | <i>Xanx-4</i> siRNA double stranded produces a reduced tubule phenotype in <i>Xenopus laevis</i> embryos | 146 |
| 5.4 | Discussion | 149 |
| 5.4.1 | RNAi effects on <i>Xanx-4</i> mRNA translation in <i>Xenopus</i> oocytes | 150 |
| 5.4.2 | RNAi effects on <i>Xanx-4</i> mRNA translation in embryos | 152 |
| 5.4.3 | The effects of <i>Xanx-4</i> siRNA in <i>Xenopus laevis</i> | 153 |
| 5.4.4 | Conclusion | 154 |

Chapter 6: Perturbation of the expression of *Xanx-4* using morpholino technology

| | | |
|------------|---|------------|
| 6.1 | Introduction | 155 |
| 6.1.1 | The use of morpholinos in <i>Xenopus</i> | 157 |
| 6.1.2 | Zebrafish | 162 |
| 6.1.3 | Mouse | 164 |
| 6.1.4 | Chick | 165 |
| 6.1.5 | Sea urchin | 165 |
| 6.1.6 | Morpholinos in cell lines and <i>in vivo/ in vitro</i> for therapeutics | 165 |
| 6.1.7 | Caged RNA/DNA | 166 |
| 6.1.8 | Summary | 167 |
| 6.2 | Results | |
| 6.2.1 | <i>Xanx-4</i> MO1 blocks translation of <i>Xanx-4</i> mRNA | 167 |
| 6.2.2 | <i>Xanx-4</i> knockout using MO1 produces pronephric tubules with an enlarged diameter | 171 |
| 6.2.3 | <i>Xanx-4</i> MO1 phenotype can be rescued by co-injection with <i>Xanx-4</i> mRNA | 180 |
| 6.2.4 | Analysis of the expression of pronephric molecular markers in <i>Xanx-4</i> overexpression and <i>Xanx-4</i> morpholino treated embryos | 182 |
| 6.2.5 | The issue of a true rescue. | 188 |
| 6.2.6 | Design and preparation of mutant <i>Xanx-4</i> mRNA | 189 |
| 6.2.7 | The effectiveness of <i>Xanx-4</i> MO2 with <i>Xanx-4</i> mRNA and <i>Xanx-4</i> -MUT mRNA <i>in vitro</i> | 189 |
| 6.2.7.1 | <i>Xanx-4</i> MO2 blocks translation of <i>Xanx-4</i> mRNA <i>in vitro</i> | 189 |
| 6.2.7.2 | <i>Xanx-4</i> MO2 can not block translation of <i>Xanx-4</i> -MUT mRNA | 191 |
| 6.2.8 | <i>Xanx-4</i> MO2 produces the same aberrant pronephric tubule phenotype, observed using <i>Xanx-4</i> MO1, which can be rescued by <i>Xanx-4</i> -MUT mRNA | 194 |
| 6.2.9 | Summary | 196 |
| 6.3 | Discussion | 198 |
| 6.3.1 | <i>Xanx-4</i> morpholinos are specific and potent inhibitors of <i>Xanx-4</i> gene expression in <i>Xenopus laevis</i> . | 198 |

| | | |
|-------|--|-----|
| 6.3.2 | <i>Xanx-4</i> depletion in <i>Xenopus laevis</i> results in enlarged and shortened pronephric tubules | 199 |
| 6.3.3 | A novel strategy for quantitation of pronephric tubule phenotype reveals an increased number of cells in the circumference of the pronephric tubules | 200 |
| 6.3.4 | <i>Xanx-4</i> depleted tubule phenotype can be rescued by <i>Xanx-4</i> mRNA | 201 |
| 6.3.5 | Pronephric tubule phenotype is a result of morphological perturbation | 202 |
| 6.3.6 | Possible explanations for enlarged tubule phenotype | 203 |

Chapter 7: Discussion - Annexins and their biological roles, and the potential role of *Xanx-4* in pronephric development

| | | |
|-----|------------------------------|-----|
| 7.1 | The annexin family | 206 |
| 7.2 | Summary and final discussion | 219 |

| | | |
|--|---------------------|------------|
| | Bibliography | 228 |
|--|---------------------|------------|

Appendices

Table of figures

| | | |
|--------------|---|----|
| Figure 1.1: | Organisation of the nephrons of the pronephros, mesonephros and metanephros. | 2 |
| Figure 1.2: | Schematic representation of the pronephros in <i>Xenopus laevis</i> . | 4 |
| Figure 1.3: | The segregation of the pronephric anlagen from the intermediate mesoderm. | 6 |
| Figure 1.4: | Pronephric tubule formation in <i>Xenopus laevis</i> . | 7 |
| Figure 1.5: | The zebrafish pronephros. | 9 |
| Figure 1.6: | The four-step model of zebrafish pronephric development. | 10 |
| Figure 1.7: | A selection of <i>in situ</i> patterns for marker genes of the pronephros in <i>Xenopus laevis</i> . | 12 |
| Figure 1.8: | The onset of pronephric gene expression in <i>Xenopus laevis</i> . | 25 |
| Figure 1.9: | Specification and patterning of intermediate mesoderm forming the lineage of the pronephric components during pronephrogenesis. | 29 |
| Figure 1.10: | Patterning of the intermediate mesoderm giving rise to the components of the zebrafish pronephros. | 32 |
| Figure 1.11: | Tissue types induced by activin in <i>Xenopus</i> and newt animal caps. | 34 |
| Figure 1.12: | Induction of pronephric tubules in animal caps of <i>Xenopus laevis</i> . | 36 |
| Figure 1.13: | Preparation of the subtracted probe. | 37 |
| Figure 3.1: | <i>Xenopus laevis</i> annexin 4 nucleotide sequence and deduced amino acid sequence. | 63 |
| Figure 3.2: | <i>Xenopus laevis</i> annexin 4 predicted 321 amino acid sequence aligned against deduced amino acid sequences of annexin 4 cloned and sequenced in other vertebrate species. | 64 |
| Figure 3.3: | Motif diagram of <i>Xenopus laevis</i> annexin 4 deduced protein sequence. | 65 |
| Figure 3.4: | <i>Xanx-4</i> is expressed at the right time to have a role in pronephric specification and organogenesis. | 67 |
| Figure 3.5: | <i>Xanx-4</i> transcripts are present throughout the <i>Xenopus laevis</i> oocyte. | 69 |

| | | |
|--------------|---|-----|
| Figure 3.6: | Xanx-4 protein is localised to all fractions of the <i>Xenopus</i> oocyte | 71 |
| Figure 3.7: | Wholemount in situ hybridisation of <i>Xenopus laevis</i> embryos using <i>Xanx-4</i> DIG labelled antisense RNA probe. | 74 |
| Figure 3.8: | Wholemount anti-annexin-4 antibody staining on <i>Xenopus laevis</i> embryos. | 77 |
| Figure 3.9: | Northern blot analysis of RNA isolated from dissected adult organs. | 78 |
| Figure 4.1: | Nomenclature of blastomeres at 32-cell stage <i>Xenopus laevis</i> blastula embryo. | 88 |
| Figure 4.2 : | Expression of <i>Xanx-4</i> in oocytes. | 90 |
| Figure 4.3: | Targeting injection of <i>Xenopus laevis</i> embryos. | 90 |
| Figure 4.4: | Analysis of <i>Xanx-4</i> overexpression on pronephric phenotype. | 91 |
| Figure 4.5: | Morphogenic analysis of <i>Xanx-4</i> overexpressing embryos. | 93 |
| Figure 4.6: | RT-PCR stage series showing longevity of injected <i>Xanx-4</i> mRNA. | 96 |
| Figure 5.1: | A proposed model for RNA interference (RNAi). | 119 |
| Figure 5.2: | PCR products amplified from <i>Xanx-4</i> cDNA used to generate dsRNA templates. | 122 |
| Figure 5.3: | Generation of dsRNAs from PCR templates for use in RNAi experiments. | 123 |
| Figure 5.4: | Generation of control ssRNAs and dsRNAs. | 124 |
| Figure 5.5: | The mRNAs, ssRNAs and dsRNAs used in RNAi experiments. | 125 |
| Figure 5.6: | <i>Xanx-4</i> dsRNA-Long-1 and dsRNA-Short prevents translation of exogenous <i>Xanx-4</i> mRNA in <i>Xenopus</i> oocytes | 127 |
| Figure 5.7: | The effect of control <i>Xanx-4</i> ssRNAs and dsRNAs compared to <i>Xanx-4</i> dsRNA-Short and dsRNA-Long-1 on the translation of exogenous <i>Xanx-4</i> mRNA in oocytes. | 129 |
| Figure 5.8: | Interference of endogenous <i>Xanx-4</i> expression by <i>Xanx-4</i> dsRNA and ssRNA in <i>Xenopus</i> oocytes determined by RT-PCR. | 130 |

| | | |
|--------------|---|-----|
| Figure 5.9: | The effect of <i>Xanx-4</i> dsRNA and ssRNA on exogenous <i>Xanx-4</i> mRNA in <i>Xenopus</i> oocytes as determined by RT-PCR. | 132 |
| Figure 5.10: | The interference of endogenous <i>Xanx-4</i> expression by <i>Xanx-4</i> dsRNA-Long-1 in stage 13 <i>Xenopus</i> embryos determined by RT-PCR. | 134 |
| Figure 5.11: | The interference of endogenous <i>Xanx-4</i> expression by <i>Xanx-4</i> dsRNAs and ssRNAs in stage 20 <i>Xenopus</i> embryos determined by RT-PCR. | 135 |
| Figure 5.12: | Longevity of <i>Xanx-4</i> dsRNAs in <i>Xenopus</i> embryos determined by a stage series and RT-PCR. | 137 |
| Figure 5.13: | The effect of <i>Xanx-4</i> dsRNAs and ssRNAs on exogenous <i>Xanx-4</i> mRNA in <i>Xenopus</i> embryos. | 140 |
| Figure 5.14: | The sequence and position of <i>Xanx-4</i> siRNA. | 142 |
| Figure 5.15 | The testing of <i>Xanx-4</i> siRNA <i>in vitro</i> using rabbit reticulocyte lysate system. | 144 |
| Figure 5.16: | The effect of <i>Xanx-4</i> siRNA on <i>Xanx-4</i> mRNA in <i>Xenopus laevis</i> embryos by RT-PCR. | 145 |
| Figure 5.17: | <i>Xanx-4</i> siRNA produces a reduced tubule phenotype in <i>Xenopus</i> embryos. | 147 |
| Figure 5.18: | <i>Xanx-4</i> siRNA produces a reduced tubule phenotype in <i>Xenopus</i> embryos: scoring analysis. | 148 |
| Figure 6.1: | The structure of DNA and morpholino oligonucleotides. | 156 |
| Figure 6.2: | The position and sequence of the <i>Xanx-4</i> morpholinos MO1 and MO2 in relation to <i>Xanx-4</i> coding region. | 168 |
| Figure 6.3: | <i>Xanx-4</i> MO specificity <i>in vitro</i> . | 170 |
| Figure 6.4: | <i>Xanx-4</i> MO specificity <i>in vivo</i> . | 172 |
| Figure 6.5: | Depletion of <i>Xanx-4</i> in embryos by injection of <i>Xanx-4</i> MO1 results in enlarged pronephric tubule phenotype. | 173 |
| Figure 6.6: | Wholemount pronephric phenotype scoring analysis of <i>Xanx-4</i> depleted embryos and embryos over-expressing <i>Xanx-4</i> . | 175 |
| Figure 6.7: | Cryostat transverse sections of stage 40 <i>Xenopus</i> pronephroi stained with tubules specific antibody 3G8 and counterstained with Hoescht. | 176 |

| | | | |
|--------------|--|-----|---|
| Figure 6.8: | A pronephric tubule section and a schematic representation of the same section. | 178 | — |
| Figure 6.9: | Graphical representation of data collected from cell counts of complete serial sections of pronephric tubules from embryos depleted or over-expressing <i>Xanx-4</i> MO. | 179 | — |
| Figure 6.10: | The enlarged pronephric tubule phenotype produced by injection of <i>Xanx-4</i> MO can be rescued by co-injection with <i>Xanx-4</i> mRNA. | 181 | |
| Figure 6.11: | Examples of the cryostat transverse sections of stage 40 <i>Xenopus</i> pronephroi stained with tubules specific antibody 3G8 and counterstained with Hoescht, showing <i>Xanx-4</i> mRNA is able to rescue MO1 induced phenotype. | 183 | |
| Figure 6.12: | Graphical representation of data collected from cell counts of complete serial sections of pronephric tubules from embryos with depleted <i>Xanx-4</i> expression or rescued by co-injection of <i>Xanx-4</i> mRNA. | 184 | |
| Figure 13: | Analysis of the effects of <i>Xanx-4</i> depletion or over-expression on the expression of pronephric marker genes by RT-PCR. | 186 | |
| Figure 14: | Analysis of the effects of <i>Xanx-4</i> depletion or over-expression on the expression of pronephric marker genes by <i>in situ</i> hybridisation. | 187 | |
| Figure 6.15: | The preparation of <i>Xanx-4</i> -MUT mRNA template. | 190 | |
| Figure 6.16: | <i>Xanx-4</i> MO2 blocks translation of <i>Xanx-4</i> mRNA <i>in vitro</i> . | 192 | |
| Figure 6.17: | <i>Xanx-4</i> MO2 does not block translation of <i>Xanx-4</i> -MUT mRNA <i>in vitro</i> . | 193 | |
| Figure 6.18: | <i>Xanx-4</i> MO2 produces the same aberrant pronephric tubule phenotype as MO1, which can be rescued by co-injection with <i>Xanx-4</i> -MUT, analysed by wholemount antibody 3G8 staining of stage 40 injected embryos. | 195 | |
| Figure 6.19: | Wholemount pronephric phenotype scoring analysis of <i>Xanx-4</i> depleted embryos and embryos rescued with <i>Xanx-4</i> -MUT mRNA. | 197 | |
| Figure 7.1: | Annexin family members share a highly conserved domain structure. | 207 | |

| | | |
|-------------|---|-----|
| Figure 7.2: | Ribbon diagram of the membrane bound form of annexin protein. | 209 |
| Figure 7.3: | Annexins bind to phospholipid membranes in ordered arrays. | 210 |

Table of tables

| | | |
|------------|---|----|
| Table 1.1: | Aberrant pronephric phenotypes isolated from a zebrafish mutant screen. | 26 |
| Table 2.1 | RT-PCR primers | 48 |
| Table 2.2 | Primers for preparation of myc-Xanx-4 and Xanx-4-MUT | 44 |
| Table 2.3 | Primers for preparation of dsRNA | 56 |

Acknowledgements

Thanks to Liz Jones for her enthusiasm, advice and her empathy during some of my darkest hours. Thanks to Debbie Clements for technical advice, to Surinder Bhamra for *in situs* and friendship and to Sarb for K2 clone. Thanks to all of my family for their love and support, in particular to Karen and Mick for looking after me whilst I was writing up and to Jonathan for interesting discussions. Thanks to Mark for his love and his help in carrying the load.

Thank you to my Mum and Dad for being wonderful role models, for the Nature and the Nurture so selflessly given.

This research was funded by the BBSRC

Declaration.

All the results presented in this thesis were obtained by the author.

The majority of micro-injections were performed by Dr. E. A. Jones. The majority of hormone injections given to *Xenopus* females were performed by Mr B. Taylor. The majority of the *in situ* hybridisations were carried out by Mr S. Bhamra.

All sources of information have been acknowledged by means of reference.

A study of *Xenopus laevis* Enhancer of Zest (XEZ) was conducted during the course of this research which is not contained in this thesis, a reprint of this work can be found at the rear of this thesis.

Abstract

Vertebrate kidney organogenesis is characterised by the successive formation of the pronephros, the mesonephros and the metanephros. They all have a similar function and organisation and all arise from mesodermal tissue, with their differences being that of temporal and spatial organisation. The pronephros is the first to form and is the functional embryonic kidney of lower vertebrates and although it is vestigial in higher vertebrates, it is a necessary precursor for the other kidney types. The *Xenopus* pronephros is a simple paired organ; each nephron consists of a single large glomus, one set of tubules and a single duct. Previous work done in our laboratory demonstrates that the tubules and duct are specified at stages 12.5 and 14 respectively and the glomus is specified at stage 12.5. The kidney unit functions to control water balance and dispose of wastes. The simple organisation of the pronephros and the amenability of *Xenopus laevis* embryos to manipulation make the *Xenopus* pronephros an attractive system in which to study organogenesis. It has been shown that pronephric tubules can be induced to form in presumptive ectodermal tissue by treatment with RA and activin. Members of this laboratory have used this system in a subtractive hybridisation screen that resulted in the cloning of *Xenopus laevis* annexin IV (*Xanx-4*). In this thesis it has been demonstrated that *Xanx-4* transcripts are specifically located to the developing pronephric tubules, and the protein to the luminal surface of these tubules. Temporal expression shows zygotic transcription is upregulated at the time of pronephric tubule specification. The temporal and spatial expression pattern of *Xanx-4* suggests it may have a role in pronephric tubule development. Overexpression of *Xanx-4* yields no apparent phenotype. Depletion of *Xanx-4* by dsRNA was tested and was shown to specifically reduce levels of *Xanx-4* protein in oocytes. *Xanx-4* siRNA was also tested for efficacy and was shown to cause a reduced pronephric tubule phenotype. However analysis of the effects of dsRNA and siRNA on mRNA levels have proved inconclusive and cast doubt on the usefulness of dsRNAs in *Xenopus laevis*. Further studies on RNAi in *Xenopus* will be required before it can be judged a reliable method for interfering with gene expression. *Xanx-4* depletion, using morpholinos produces a shortened, enlarged tubule phenotype. The phenotype observed can be rescued by coinjection of *Xanx-4* mRNA. Thus, *Xanx-4* can be successfully depleted in embryos using morpholino oligos. Although the function of annexins is not yet clear, studies have suggested a

role for annexins in a number of cellular processes. It is argued that the enlarged pronephric tubule phenotype observed in the Xanx-4 depleted embryos is the consequence of aberrant control of cell division in the extending pronephric tubules. Further work will be required to substantiate this theory.

Abbreviations

| | |
|------------|---|
| ATP | adenosinetriphosphate |
| BMP | bone morphogenetic protein |
| bp | base pairs |
| BSA | bovine serum albumin |
| cDNA | complementary deoxyribonucleic acid |
| Ci | Curie |
| dGTP | deoxy guanosine triphosphate |
| DNA | deoxyribo nucleic acid |
| DNase | deoxyribonuclease |
| dNTPs | deoxyribonucleoside triphosphates |
| dsRNA | double stranded ribonucleic acid |
| dsRNA-Ann | double stranded ribonucleic acid – annealed |
| dsRNA-L1 | double stranded ribonucleic acid – long |
| dsRNA-S | double stranded ribonucleic acid - short |
| E.coli | Escherichia coli |
| EDTA | ethylene diamine tetra acetic acid |
| FGF | fibroblast growth factor |
| l | litre |
| LBroth | Luria Broth |
| kb | kilobases |
| kD | kilo Dalton |
| M | molar |
| MAP kinase | mitogen-activated protein kinase |
| MBT | midblastulatransition |
| mg | milligram |
| ml | millilitre |
| mM | millimolar |
| MMLV | moloneymurineleukaemiavirus |
| MO | Morpholino |
| MO1 | Xanx-4 morpholino 1 |
| MO2 | Xanx-4 morpholino 2 |
| mRNA | messengerribonucleicacid |
| ng | nanograms |

| | |
|--------------|--------------------------------------|
| nl | nanolitres |
| nM | nanomolar |
| NP-40 | nonidetP40 |
| nt | nucleiotides |
| PAGE | polyacrylamidegelelectrophoresis |
| PKR | protein kinase R |
| PMSF | phenylmethysulphonylfluoride |
| PCR | polymerasechainreaction |
| pM | picomolar |
| pmol | picomoles |
| PTGS | post-transcriptional gene silenceing |
| RNA | ribonucleicacid |
| RNAi | ribonucleic acid interference |
| RNase | ribonuclease |
| RT-PCR | reversetranscriptionPCR |
| SDS | sodiumdodecylsulphate |
| siRNA | short interfering ribonucleic acid |
| ssRNA | single stranded RNA |
| ssRNA-Asense | single stranded RNA antisense strand |
| ssRNA-NAnn | single stranded RNA not annealed |
| ssRNA-Sense | single stranded RNA sense strand |
| TGFβ | Transforming growth factor β |
| Tris | tris(hydroxymethyl)aminomethane |
| TGS | transcriptional gene silencing |
| UTR | untranslated region |
| UV | ultraviolet |
| V | volts |
| w/v | weight/volume |
| μg | microgram |
| μl | microlitre |
| μM | micromolar |

1 Introduction

1.1 The vertebrate kidney

Vertebrate kidney organogenesis is characterised by the successive formation of three temporally and spatially distinct organs; the pronephros, the mesonephros and the metanephros (Saxén, 1987). All three have a similar function and organisation and all arise from the intermediate mesoderm by an inductive process that is dependent for its formation on the previous temporal form. The pronephros is the first to form, it is the functional embryonic kidney of lower vertebrates and although it is vestigial in higher vertebrates, it is a necessary precursor for the other kidney types. The mesonephros is the adult kidney in amphibia and fish and is the functional embryonic kidney in higher vertebrates. The metanephros is the mature adult kidney in mammals and birds. Vertebrates require a series of more complex kidneys as they grow and develop. The pronephros consists of a single nephron (the basic functional unit of the kidney). The mesonephros contains 10-50 nephrons and the final, metanephric kidney contains over 1 million nephrons (figure 1.1). All three kidney forms function to control water balance and dispose of wastes (Saxén, 1987; Vize et al., 1997; Brändli, 1999; Dressler, 1999).

1.2 The pronephros

The simplicity of this organ, coupled with the fact that it displays the same basic organisation and function as the more complex mesonephros and metanephros, make this an attractive model to study the earliest events in vertebrate kidney morphogenesis. The development of the pronephros has been studied in a

Figure 1.1

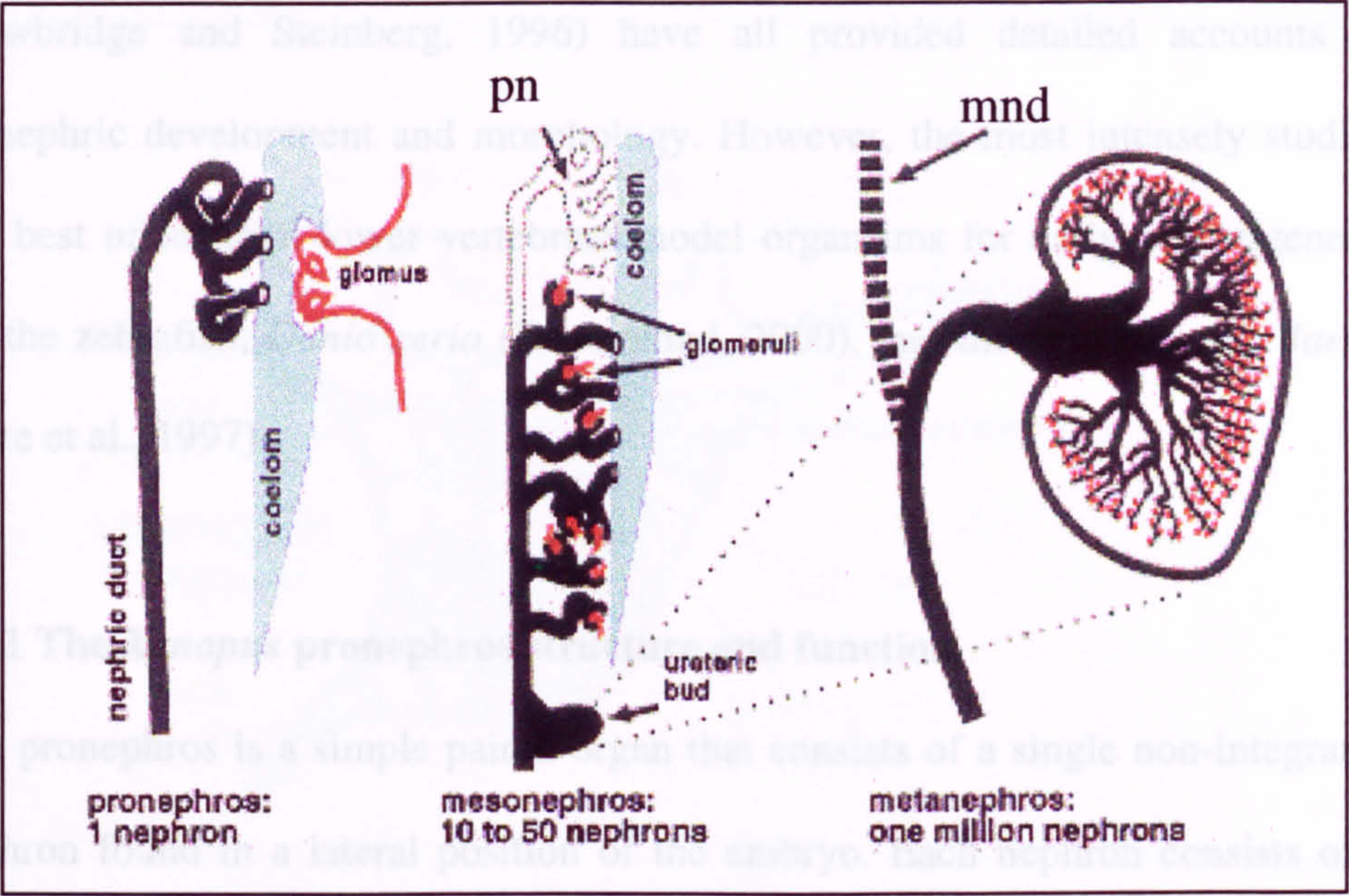


Figure 1.1: Organisation of the nephrons of the pronephros, mesonephros and metanephros. The pronephros is composed of a single nephron comprising of one set of tubules, a single duct and a capsule (coelom and glomus). As development progresses the pronephros regresses and the mesonephros forms in a more posterior position. The mesonephros is composed of 10-50 nephrons. The metanephros forms from a branch of the ureteric bud and on maturation, is composed of 1 million nephrons. pn: pronephros, mnd: mesonephric duct. (Reproduced from Vize et al., 1997).

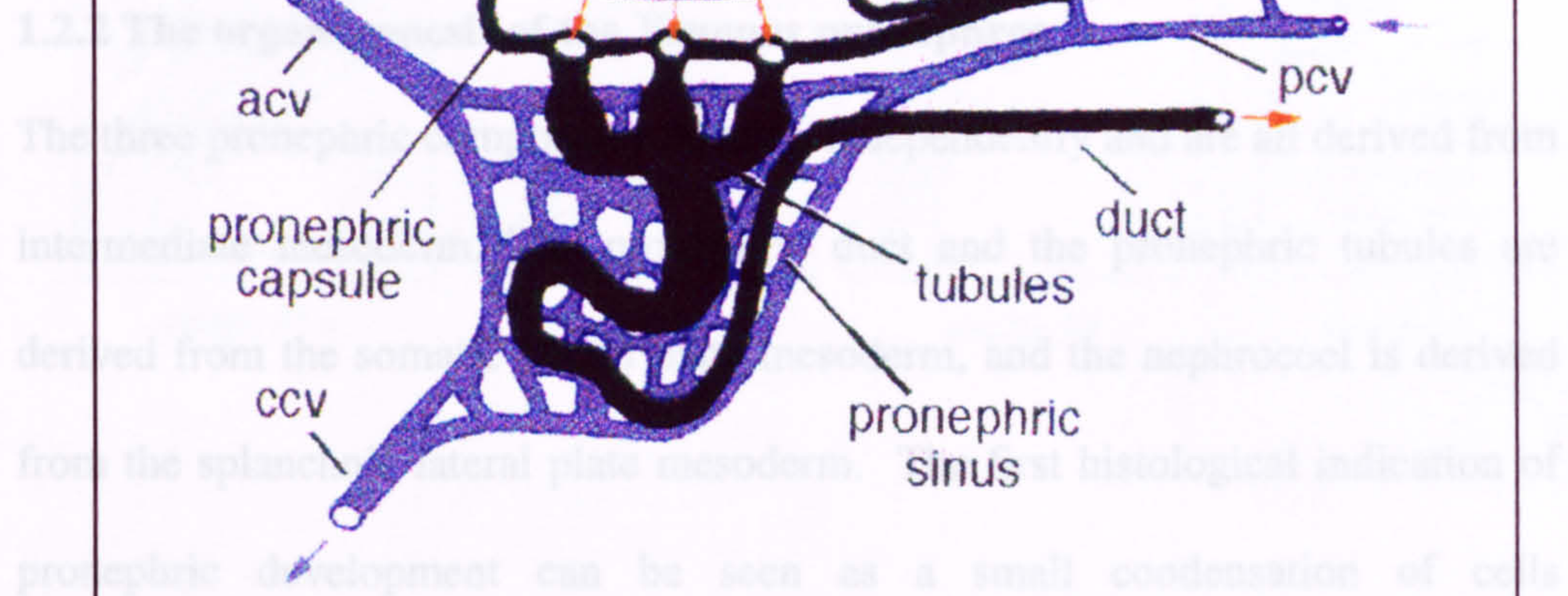
number of vertebrate model organisms. Studies conducted in lampreys, (*Lampetra fluviatilis* and *Petromyzon marinus*, Kluge and Fischer, 2000), in fish including mudskipper (*Periophthalmus koelreuteri*, Safer et al., 1982) and trout (*Salmo trutta*, Tytler, 1988) and several amphibians including, the green toad (*Bufo viridis*, Mobjerg et al., 2000), and the axolotl (*Ambystoma mexicanum*, Drawbridge and Steinberg, 1996) have all provided detailed accounts of pronephric development and morphology. However, the most intensely studied and best understood lower vertebrate model organisms for early nephrogenesis are the zebrafish, *Danio rerio* (Drummond, 2000), and the frog *Xenopus laevis* (Vize et al., 1997).

1.2.1 The *Xenopus* pronephros structure and function

The pronephros is a simple paired organ that consists of a single non-integrated nephron found in a lateral position of the embryo. Each nephron consists of a single fused pronephric corpuscle, one set of tubules and a single duct (figure 1.2). The pronephric corpuscle is composed of two parts, the nephrocoel and the glomus. The glomus is a capillary network formed from branches of the dorsal aorta, it filters waste from the blood by size-selective pressure filtration. The nephrocoel is the pronephric filtration chamber lined with visceral and parietal epithelium. The pronephric tubules are composed of the nephrostomes, the connecting tubules and the common tubule, which is connected to the pronephric duct. The tubules are composed of a single layer of polarised epithelial cells. The filtrate passes into the nephrocoel, where it is swept by ciliated funnels (nephrostomes) into the connecting tubules and subsequently into the common tubule. The sinus surrounding the tubules allows ions, water and other molecules

Figure 1.2 | Urine, formed in the nephron, flows along the proximal duct and is disposed of to

dorsal aorta



functional. At stage 37/38 the tubules resemble the Greek letter τ (figure 1.4A, 1.4B) at which time they begin to extend and coil and by stage 42 the tubules have lengthened and form a highly coiled, convoluted structure (figure 1.4C, 1.4D). At stage 54 the pronephric tubules undergo a process of atrophy and

to be recovered from the filtrate and returned to the blood via the common cardiac vein. Rostrally, the pronephric duct connects with the tubules. It then runs caudally along the length of the body, ventral to the somites, until it fuses with the rectal diverticulum outgrowth of the cloaca. Molecules that are not recovered from the filtrate, flow along the pronephric duct and are disposed of to the exterior, via the cloaca (Saxén, 1987; Vize et al., 1995; Vize et al., 1997; Brändli, 1999).

1.2.2 The organogenesis of the *Xenopus* pronephros

The three pronephric components develop independently and are all derived from intermediate mesoderm. The pronephric duct and the pronephric tubules are derived from the somatic lateral plate mesoderm, and the nephrocoel is derived from the splanchnic lateral plate mesoderm. The first histological indication of pronephric development can be seen as a small condensation of cells immediately below somites 3-5 at stage 21 (figure 1.3). This condensation is the primordia of both the tubules and duct which segregates into its two components by stage 24. The pronephric, or Wolffian, duct commences its extension posteriorly towards the cloaca. By stage 27, the pronephros has a distinct tubular organisation, branching of the tubules follows, and the nephrostomes form around stage 29/30. The glomus develops as a fold in the splanchnic lateral plate that extends into the coelom. At stage 37 the pronephros becomes fully functional. At stage 37/38 the tubules resemble the Greek letter τ (figure 1.4A, 1.4B) at which time they begin to extend and coil and by stage 42 the tubules have lengthened and form a highly coiled, convoluted structure (figure 1.4C, 1.4D). At stage 54 the pronephric tubules undergo a process of atrophy and

Figure 1.3

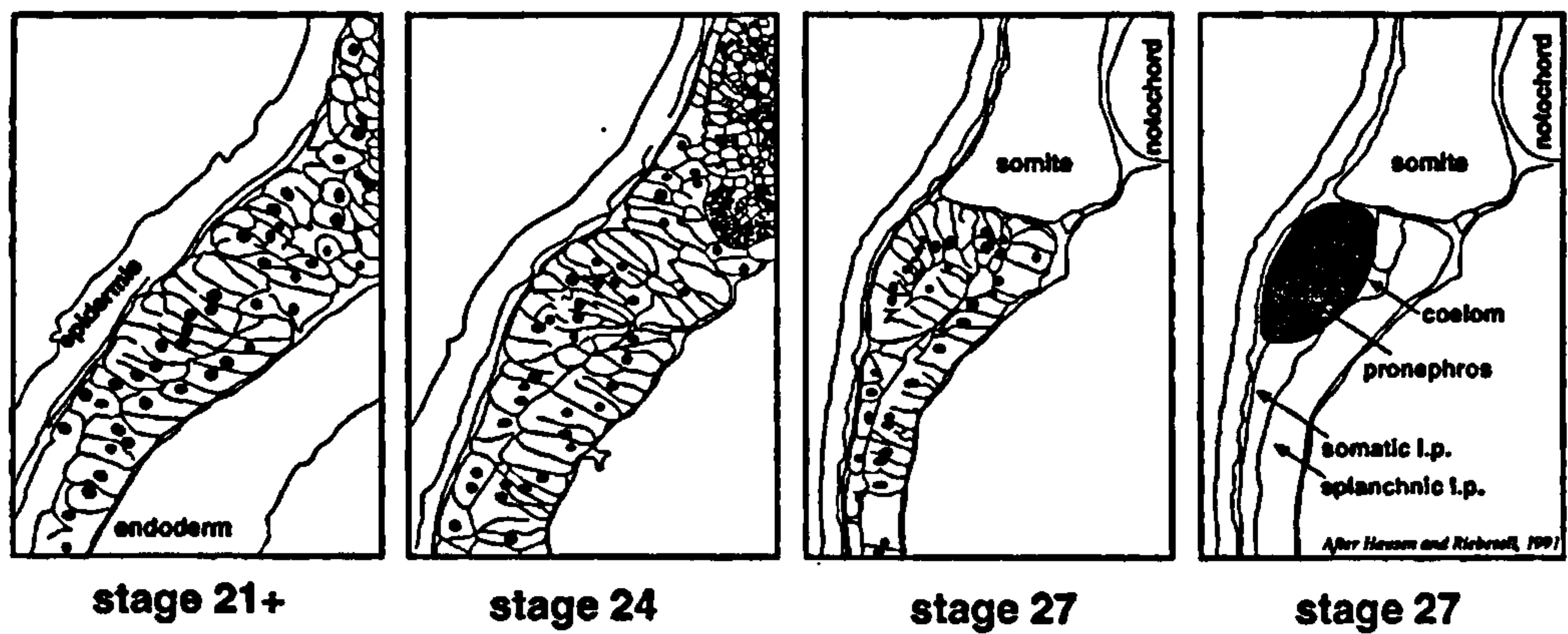


Figure 1.3: The segregation of the pronephric anlagen from the intermediate mesoderm. Transverse sections *Xenopus laevis* embryos at stage 21, 24 and 27. The pronephric anlagen is histologically distinct as a condensation of cells of the intermediate mesoderm by stage 21. At stage 24 the cells become columnar, this compact mass of cells distends the overlying ectoderm and can be seen as a swelling on the outside of the embryo. By stage 27 the cells display a tubular arrangement and a lumen forms in the centre by stage 28. l.p.: lateral plate. (Reproduced from Vize et al., 1997).

regression, with their function being replaced by the second amphibian kidney, the mesonephros (Nieuwkoop and Faber, 1994; Vize et al., 1995).

Figure 1.4

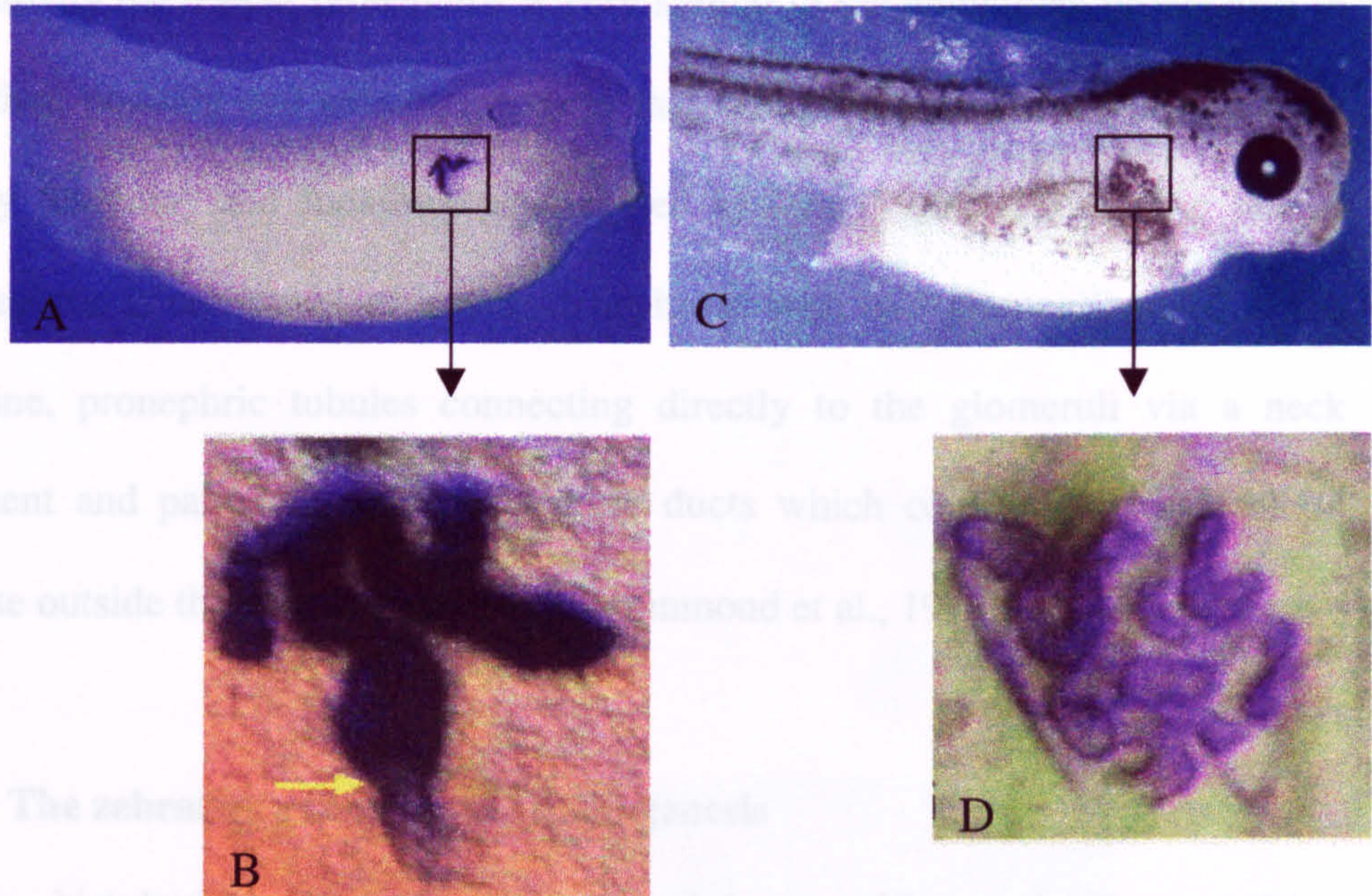


Figure 1.4: Pronephric tubule formation in *Xenopus laevis*. All embryos are stained with pronephric tubule specific monoclonal antibody 3G8. (A) Wholemount *Xenopus* embryo stage 35/36. Tubules can be seen in the characteristic Tor shape ventral to somites 3-5, the three nephrostomes are clearly visible (B), ventrally the tubules connect to the duct (arrowed). (C and D) By stage 40 the tubules have elongated and are tightly coiled. (A, B and D are reproduced from Vize et al., 1995).

regression, with their function being replaced by the second amphibian kidney, the mesonephros (Nieuwkoop and Faber, 1994; Vize et al., 1995).

1.2.3 The zebrafish pronephros structure and function

Essentially the teleost pronephros is very similar to the amphibian pronephros in function, position and structure, except that it has no connection with the body cavity (coelom) and functions as a closed system (Tytler, 1988). The teleost pronephros is composed of a pair of nephrons with two glomeruli fused at the midline, pronephric tubules connecting directly to the glomeruli via a neck segment and paired bilateral pronephric ducts which convey the waste blood filtrate outside the animal (figure 1.5. Drummond et al., 1998).

1.2.4 The zebrafish pronephros organogenesis

Using histological studies and pronephric specific molecular markers, Drummond et al., (1998) have described the development of the zebrafish pronephros to occur in 4 stages (figure 1.6). The first stage involves the establishment of the pronephric field, 10-13 hours post fertilisation (hpf), as demonstrated by the expression patterns of *pax2.1* and *lim-1*. In the second stage, pronephric duct development follows the onset of somitogenesis and is complete by 24 hpf. The primordium of the nephron (glomerulus and tubules) can be histologically detected as a coelomic fold ventral to the third somite, at 24 hpf. By the third stage, 32-33 hpf, this condensation of cells, now distinct from the coelom, forms a vesicle with a distinct lumen. The tips of the forming pronephric duct appear adjacent and lateral to the cellular condensate. The pronephric primordium appears to be partitioned into a lateral and a medial region; the

Figure 1.5

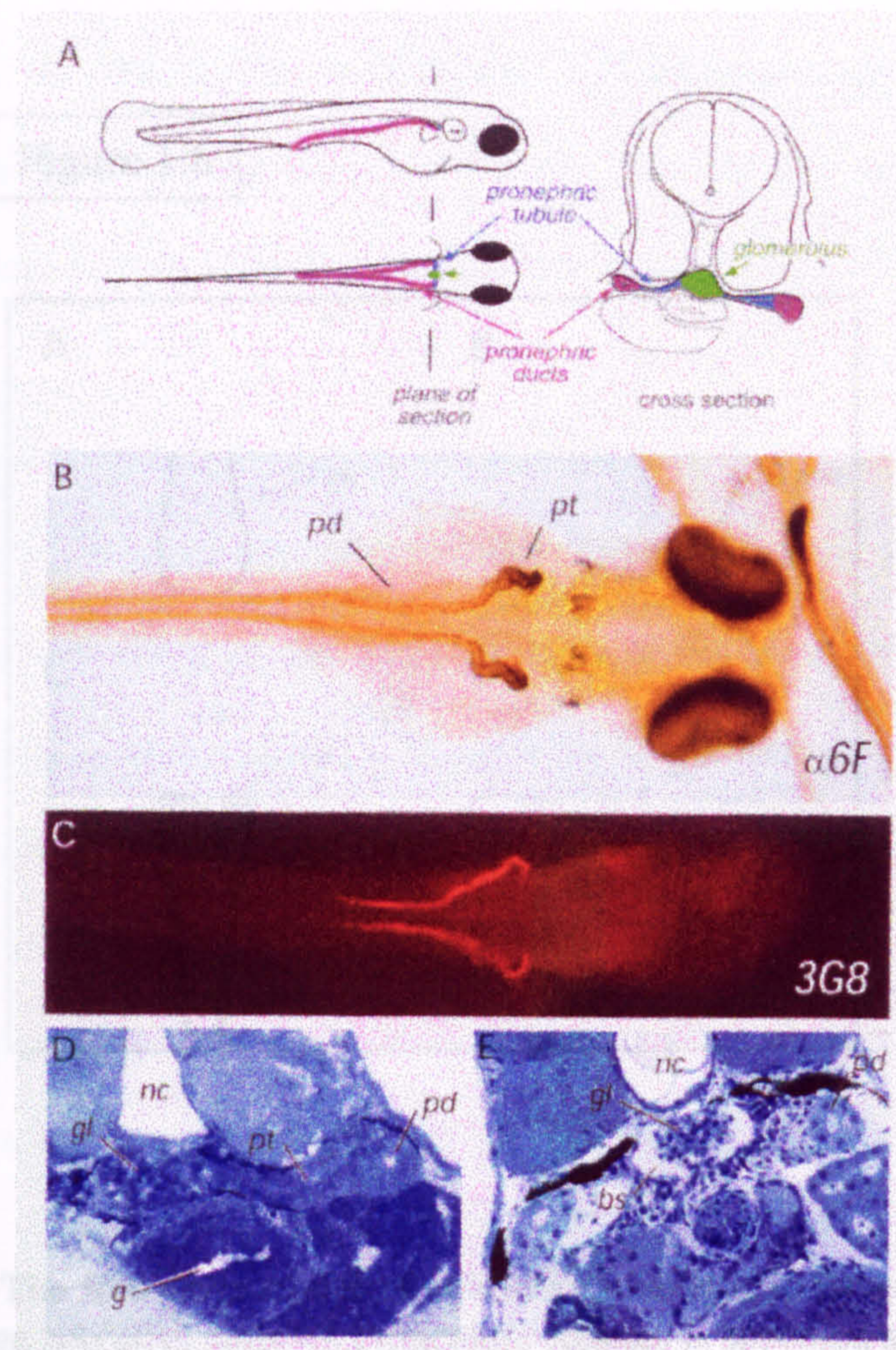


Figure 1.5: The zebrafish pronephros. (A) A schematic representation of the zebrafish pronephros, showing the position of the tubules, duct and glomerulus. (B) 84hpf zebrafish embryo stained with anti- Na^+/K^+ -ATPase alpha subunit monoclonal antibody ($\alpha 6F$). The pronephric tubules are just formed and will continue to elongate and coil to maturity. The duct can be seen running the length of the body either side of the mid-line. (C) Wholemount antibody 3G8 staining with rhodamine secondary. Although 3G8 is tubule specific in *Xenopus laevis*, in zebrafish it recognises the lateral pronephric tubules and the anterior of the pronephric duct. (D) Transverse section of a 72hpf zebrafish embryo, the pronephric components form between the gut (g) and the notochord (nc). (E) Transverse section of a 6.5 day zebrafish embryo, Bowman's space (bs) is observable. pt: pronephric tubules, pd: pronephric duct, gl: glomerulus. (Reproduced from Drummond et al., 1998).

Figure 1.6

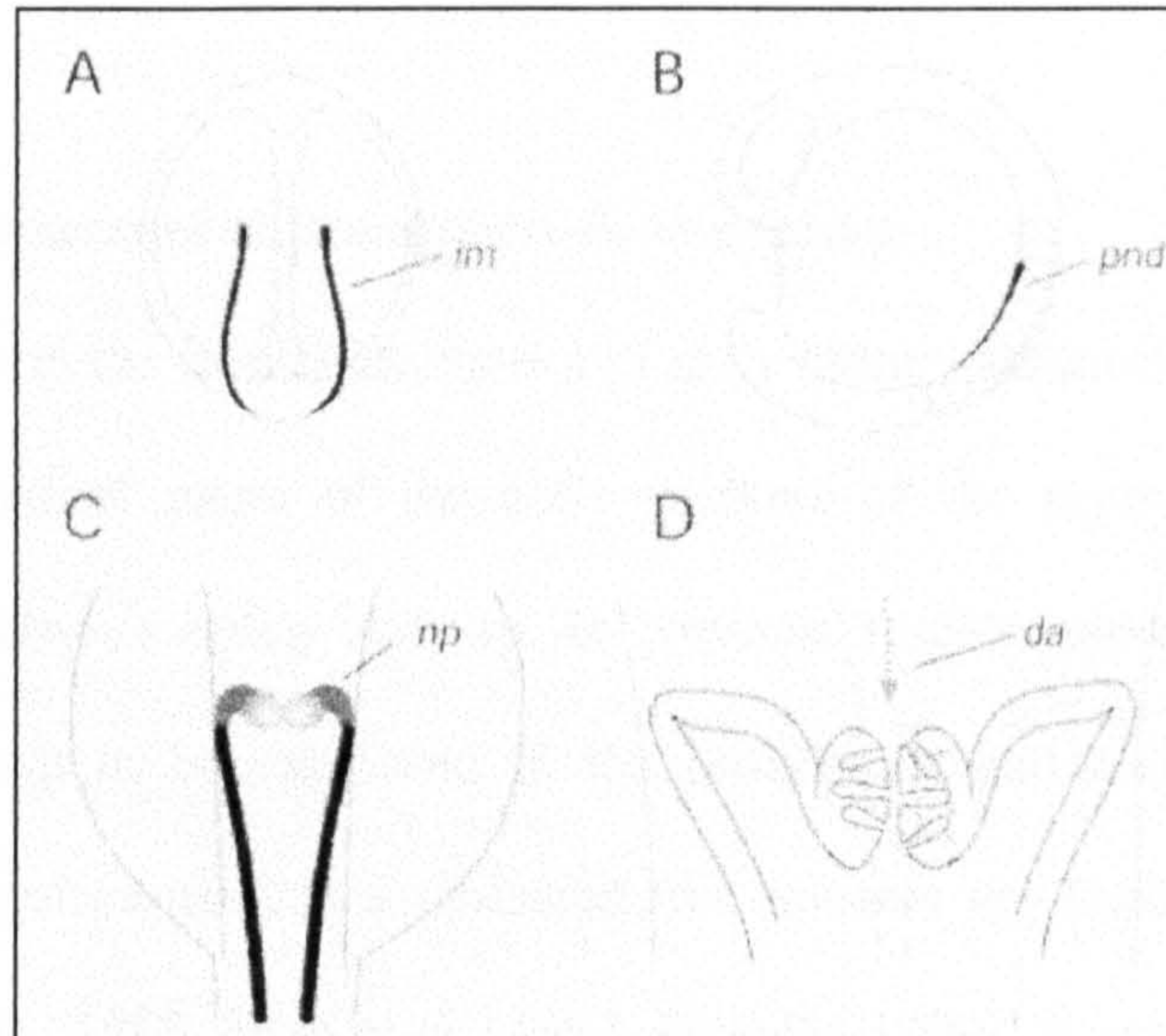


Figure 1.6: The four-step model of zebrafish pronephric development. (A) 8-somite stage zebrafish embryo. Pronephric anlagen is specified as detected by expression pattern of *pax2.1* and *lim-1* in the intermediate mesoderm (im). (B) At 12-24 hpf early somitogenesis the pronephric duct (pnd) grows posteriorly along the length of the embryo, ventral to the somites and the nephron forms at the anterior tip of the duct by 24hpf. (C) At 24-42 hpf the nephric primordia (np), below somite 3, segregates into tubules and glomerulus primordia. (D) At 42-48 hpf vascularisation occurs over the next 24hrs as does the onset of glomerular filtration. (Reproduced from Drummond et al., 1998).

presumptive tubules and glomerulus respectively. During the fourth stage, from 40 hpf, the medial region forms a capsule and the lateral region takes on a tubule appearance. The two glomeruli have fused at the midline by 50 hpf, the tubules and duct are connected and a lumen is visible. By 60 hpf the connection between the glomerulus and the tubules is apparent. As development progresses, the tubules become progressively more convoluted. The pronephros persists in position for at least 1 month after hatching (Drummond et al., 1998).

1.3 Molecular markers of pronephric development.

In order to unravel the molecular control of early kidney induction and patterning a molecular map of many of the early markers of the pronephric field and pronephric anlagen is being built up. In previous studies, more than 30 genes have been shown to be expressed in the pronephros and their temporal and spatial patterns of expression established (for reviews see Davies and Brändli, 1997, Vize et al., 1995, Vize et al., 1997, Brändli, 1999). A selection of *in situ* patterns for marker genes expressed in the pronephros, some of which are utilised in this thesis, are shown in figure 1.7. Interestingly, many of these pronephric genes are also expressed in mesonephric and metanephric kidneys in higher vertebrates.

1.3.1 LIM class transcription factors

The LIM class homeobox gene *lim-1* is required for anterior patterning and nephrogenesis in the mouse. Loss-of-function mutation in the mouse causes failure of development of head structures, mesonephros and metanephros (Shawlot and Behringer, 1995). The *Xenopus* ortholog *Xlim-1* is expressed in the

Splanchnopleuric mesoderm, notochord and central nervous system. The pronephric expression commences in lateral mesoderm at stage 13. At stage 14 a mesonephric duct encircling the embryo is observed and at stages 15-18

Figure 1.7

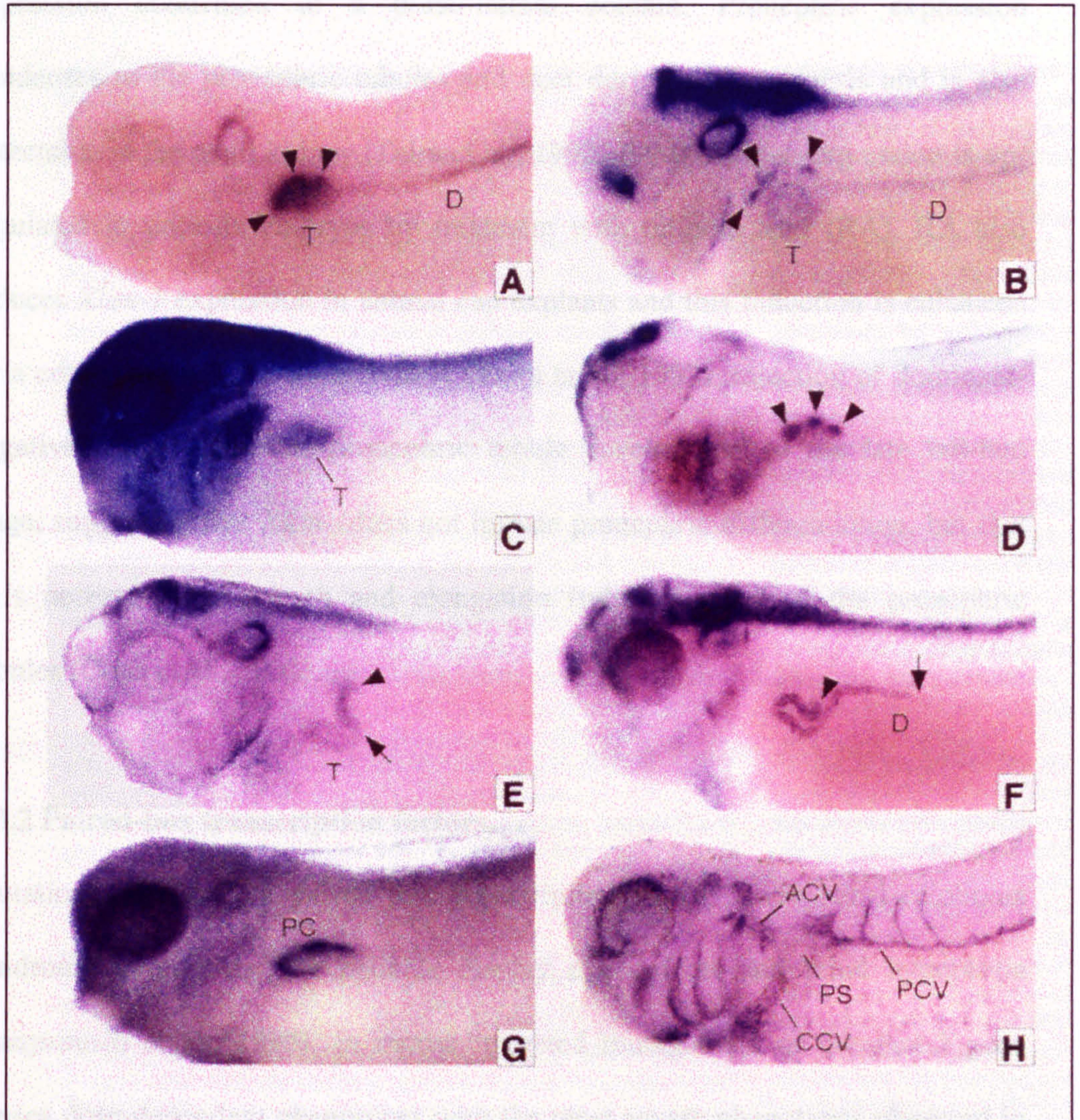


Figure 1.7: A selection of in situ patterns for marker genes of the pronephros in *Xenopus laevis*. (A) *XPax-8* stage 32, expression is detected in the pronephric tubules (arrowed) and at lower levels in the duct. (B) *XPax-2* stage 36, expression is detected in the nephrostomes (arrowed) and at lower levels in the developing tubules and duct. (C) *Delta-1* stage 30, expression is detected in the tubule primordia (T). (D) *xWnt-4* stage 32, expression strong in the nephrostomes and very weak in the tubules. (E) *Iro-3* stage 36, expression is detected in the common pronephric tubule. (F) *Sal-1* stage 38, expression is detected in the lower common tubule (arrowed) and the anterior pronephric duct (D). (G) *xWT1* stage 30 expression is detected exclusively in the developing pronephric capsule. (H) *Msr* stage 34, expression is restricted to the developing vasculature ACV: anterior cardinal vein, PCV: posterior cardinal vein, PS: pronephric sinus, CCV: common cardinal vein. T: tubules, D: duct (Reproduced from Brändli, 1999).

Spemann organiser, pronephros, notochord and central nervous system. The pronephric expression commences in lateral mesoderm at stage 13. At stage 14 a stripe of expression encircling the embryo is observed and at stages 15-18 expression condenses to a dorso-lateral domain. Pronephric expression condenses to the pronephric tubules and duct during nephrogenesis and is also detectable in the adult kidney (Taira et al., 1992, 1994). *Xlim-1* expression is up-regulated in gastrula embryos by treatment with retinoic acid (RA). RA also induces *Xlim-1* expression in animal cap explants and this induction is enhanced by a combination RA with activin A (Taira et al., 1992). Injection of dominant-negative *Xlim-1* inhibited pronephric tubule development at the late tail-bud stage, suggesting that *Xlim-1* does not initiate pronephric differentiation, but that it is necessary for growth and elongation (tubulogenesis) of the pronephric tubules (Chan et al., 2000).

1.3.2 Paired-box transcription factors.

Mutations in *Pax-2*, a paired box transcription factor, cause renal-coloboma syndrome in humans; the patients display eye defects and renal hypoplasia (Sanyanusin et al., 1995). In mouse, targeted mutagenesis of the *Pax-2* gene causes dose-dependent phenotypes with the most severe phenotypes observed in the homozygous mutants displaying a complete lack of the mesonephros and metanephros, ureters and genital tracts (Torres et al., 1995, Favor et al., 1996). Mutations in the *Pax-2* homologue in zebrafish (*pax2.1*), the *no isthmus* (*noi*) mutation, results in a lack of pronephric tubules and duct, combined with defects of the nervous system and sensory organs (Brand et al., 1996). This has been shown to be the result of a patterning defect during differentiation of the

pronephric primordium. It appears that *pax2.1* expression is required, in the lateral cells of the presumptive pronephros, to restrict the domains of *wt1* and *VEGF* expression to the podocytes of the future glomerulus (Majumdar et al., 2000). In *Xenopus* *XPax-2* is expressed in the tubule and duct primordium from stage 22, in the developing tubules and duct (figure 1.7B) to at least stage 42, with highest expression in nephrostomes (Heller and Brändli, 1997). Depletion of *XPax-2* in *Xenopus* has not been examined to date.

Another member of the paired box transcription factor family, *Pax-8*, is also expressed in the kidney in a number of species. In the mouse, although *Pax-8* is expressed in the mesonephros and metanephros, targeted ablation gives no aberrant kidney phenotype (Torres et al., 1995). In *Xenopus*, *XPax-8* is expressed in the intermediate mesoderm from stage 14. At stages 15-18, this expression condenses to a dorso-lateral domain. Duct and tubule expression can be observed as development continues (figure 1.7A) and at stage 36 expression is lost from duct but maintained in tubules (Carroll and Vize, 1999). Ectopic co-expression of either *XPax-2* or *XPax-8* with *Xlim-1* results in a synergistic effect producing increased pronephric tubule complexity, enlarged tubules and ectopic tubules. Ectopic expression of either *XPax-2* or *XPax-8* alone has a moderate effect. This suggests that *Xlim-1* is acting as a co-factor for *XPax-2* and *XPax-8* function (Carroll and Vize, 1999). In zebrafish *pax8* is expressed in the intermediate mesoderm at the 1-somite stage, but not in the pronephros as it is forming. It is suggested that *pax8* expression occurs too early to have a major role in zebrafish nephrogenesis (Pfeffer et al., 1998).

1.3.3 Hepatocyte nuclear factors (HNF).

Three members of the *hepatocyte nuclear factor (HNF)* family of tissue specific transcription factors are known to be expressed in the *Xenopus* pronephros, *HNF-1 β* , *HNF-1 α* and *HNF-4*. *HNF-1 β* is first detected in the pronephric anlagen from around stage 15 and in the tubules and duct as nephrogenesis proceeds (Demartis et al., 1994). *HNF-1 α* and *HNF-4* are both expressed from stage 20 onwards, and are expressed later in the pronephric tubules but not in the duct (Weber et al., 1996; Holewa et al., 1996). These *HNFs* are also expressed in the murine kidney. Loss-of-function studies have been hampered due to lethality upon gastrulation, thus preventing analysis of any kidney phenotype (Chen et al., 1994). *HNF-1 α* mutant mice have dysfunctional kidneys but appear morphologically normal, functional redundancies between family members are thought to be responsible for this. In a more recent study Pontoglio et al., (2000) have shown that the mutant mice are diabetic and the kidney dysfunction is due to reduced tubular glucose reabsorption. It appears that *HNF-1 α* controls expression of the glucose transporter SGLT2 gene. Mutations in *HNF-1 β* causes early on set diabetes and severe primary renal defects in humans. Expression of a mutated form of the human *HNF-1 β* in *Xenopus* embryos causes defective development and agenesis of the pronephros demonstrating a conserved role of *HNF-1 β* in renal development (Wild et al., 2000).

1.3.4 Wilms' Tumor

The Wilms' tumor suppressor gene, *WT1*, is a zinc finger transcription factor and was first identified in humans, where it is implicated in paediatric tumours of the

kidney and gonads (Call et al., 1990). The *WT1* knockout mouse has reduced mesonephric tubules and metanephros formation is completely blocked (Kreidberg et al., 1993). In *Xenopus* *xWT1* expression is detected in the splanchnic mesoderm, ventral to somites 3 and 4. From stage 20, *xWT1* is expressed in the glomus primordium and later in developing glomus (figure 1.7G). From stage 38 onwards, *xWT1* is also expressed in developing heart (Carroll and Vize, 1996). Overexpression of *xWT1* by injection of mRNA inhibited pronephric tubule development and represses expression of *XPax-2*. It was suggested that *xWT1* acts to repress tubule-specific gene expression in the portion of the pronephros fated to become the glomus (Wallingford et al., 1998). The zebrafish ortholog *wt1* is also expressed in the glomerulus of embryos commencing 30 hpf (Serluca and Fishman, 2001).

1.3.5 Helix-loop-helix transcription factors.

Tissue-specific bHLH proteins have been found to be essential transcription factors which control the fate of cells in the nervous system and in muscle formation (Murre et al., 1994). *Xenopus xId-2* is expressed in the pronephros throughout development (Wilson and Mohun, 1995). Another bHLH gene, *xArnt* has been cloned in *Xenopus* and shown to be expressed in the marginal zone at gastrula stages, and later in branchial arches, optical and otic vesicles and at a high level in the developing pronephros at tailbud stages (Bollerot et al., 2001). In zebrafish two homologs of the *arnt* genes have been cloned. *arnt2* and *arnt2A* are expressed in the developing pronephros and on overexpression cause severe defects in the sensory organs heart and gut (Hsu et al., 2001).

1.3.6 Vascular Endothelial Growth Factor (VEGF).

Vascular Endothelial Growth Factor (VEGF) is involved in neovascularisation and is expressed strongly in the glomerulus. Knockout mice die very early due to severe defects in the developing vasculature (Carmeliet, 1999), which does not allow the analysis of any glomerular phenotype. In *Xenopus* *VEGF* is expressed in the glomus from stage 28 onwards and it is suggested to have a role in populating the glomus with endothelial cells (Cleaver and Krieg, 1998).

1.3.7 Wingless family members (Wnt)

Three members of the Wnt family of secreted growth factors, *Wnt-4*, *Wnt-7b* and *Wnt-11*, have highly characteristic expression patterns during murine nephrogenesis (Parr and McMahon, 1994). Loss-of-function mutations in *wnt-4* result in severe defects in mesenchyme-to-epithelial transition during metanephric development, the kidneys are small and dysgenic (Stark et al., 1994). *Wnt-7b* expression is localised to the ureteric bud and collecting ducts late on in development and is unlikely to play a major role in metanephric kidney development. *Wnt-11* is expressed in the caudal end of the elongating nephric duct and upon ureteric bud formation, it is strongly expressed in the tips as branching occurs. Mutations causing loss-of-function of *wnt-11* in mouse results in the loss of branching of ureteric bud, however, *Wnt-11* is not sufficient to induce tubulogenesis *in vitro* (Kispert et al., 1998).

The *Wnt-4* *Xenopus* ortholog, *Xwnt-4* is weakly expressed throughout pronephric mesoderm at stage 18 and as development progresses, expression is seen in the tubule and duct anlagen. Expression is strong in the tips of the tubules

(nephrostomes) and weak in duct, figure 1.7D (Carroll et al., 1999). Ungar et al., (1995) have reported *wnt-4* expression in the zebrafish pronephros. Overexpression of *wnt-4* and *wnt-5A* in zebrafish caused cyclopia, mis-folding of the brain and notochord forking; the authors suggest wnts inhibit cell movements (Ungar et al., 1995). In *Xenopus*, although *Xwnt-11* is not expressed in the pronephros, it is expressed in the developing somites (Ku and Melton, 1993), the tissue that may be responsible for the pronephric inducing signals (Seufert et al., 1999).

1.3.8 Frizzled Receptors of Wnt family ligands

Members of the *Frizzled* family, of seven-pass transmembrane receptors, act as receptors of the wnt family ligands. *Xfrizzled-3* is expressed at high levels in the nervous system and at low levels optic and otic vesicles. Overexpression of *Xfz3* block neural tube closure and results in embryos with shortened antero-posterior axis, but does not effect the expression of organiser specific genes or gastrulation. Expression is also detected in the pronephros in overlapping domains with *Xwnt-4*, although it is not known if *Xwnt-4* is the ligand of *Xfz-3* (Shi et al., 1998). A related frizzled gene, *Xenopus Crescent* contains a frizzled-like domain and is expressed in the organiser, endomesoderm and later in the pronephros. In animal cap assays *crescent* gene expression was synergistically upregulated by coexpression of *Xlim-1*, *Ldb-1* and *Siamois* but not by activin A (Shibata et al., 2000).

1.3.9 Bone Morphogenetic Proteins (BMP).

In mouse, BMP-7 is expressed in the Wolffian duct, mesonephric tubules and condensing mesenchyme of the metanephros. It has been shown to induce tubulogenesis in isolated mesenchyme (Vukicevic et al., 1996). BMP-7 null mice possess dysplastic kidneys that appear arrested in development and die soon after birth (Dudley et al., 1995). The *Xenopus XBMP-7* and *XBMP-4* are expressed in a wide variety of domains including presumptive pronephric regions (Wang et al., 1997). Overexpression of *XBMP-7* causes ectopic alpha-globin expression (ventral) and suppression of dorsal anterior structures (dorsal). The authors suggest *XBMP-7* has a role in haematogenesis (Wang et al., 1997). In zebrafish *bmp2b*, 4 and 7 are expressed in discrete areas of otic epithelium and the authors suggest a role for bmp in the developing vertebrate ear (Mowbray et al., 2001).

1.3.10 Hedgehog family

Members of the hedgehog family of secreted glycoproteins are known for their essential morphogenic roles in early embryos (for review see Capdevila and Johnson, 2000; Chuong et al., 2000). A member of this family, *banded hedgehog*, is expressed in the developing pronephric tubules, although no function has yet been assigned to this observation (Ekker et al., 1995).

1.3.11 Glial-derived neurotrophic factor.

It has been suggested that guidance cues direct the migration of the developing pronephric duct from the pronephric anlagen to the rectal diverticula in the axolotl embryo (Drawbridge and Steinberg, 1996). The TGF β superfamily member GDNF and its receptor complex the GPI-linked GFR α -1 co-receptor and the Ret tyrosine kinase receptor, have expression patterns which suggest

their involvement in the development of the collecting ducts. Murine GDNF is expressed in the uncondensed metanephric mesenchyme and the receptor (c-ret) is expressed in the Wolffian duct and the tips of the branching collecting tubules. Mouse knockouts of GDNF and c-ret have severe renal agenesis (Sanchez et al., 1996; Schuchart et al., 1996). Interestingly, the *Xenopus* ortholog *X-ret* is expressed in the caudal tip of the migrating pronephric duct and at low levels in the tubules (Carroll et al., 1999). In zebrafish, although GDNF is expressed in the nervous system and the pronephros, depletion of GDNF causes major defects in the enteric nervous system but has no effect on kidney organogenesis (Shepherd et al., 2001). The zebrafish homolog of *c-ret*, *ret1*, is expressed in the developing pronephros and in the migrating pronephric duct (Marcos-Gutierrez, 1997). In axolotl, the work of Drawbridge et al., (2000) demonstrates that GDNF and the co-receptor GFR α -1 are required in the pathfinding behaviour of the axolotl pronephric duct primordium.

1.3.12 Fibroblast growth factor (FGF) pathway.

The FGF receptor (FGFR) signal transduction pathway regulates the posterior development of embryos in *Xenopus*. Using a dominant-negative approach, it was discovered that blocking activation of endogenous FGFR caused severe posterior truncations with only minimal anterior defects (Amaya et al., 1991). FGFR was shown to perform critical functions in the Spemann's organiser to induce formation of somitic muscle and the pronephros (Mitchell and Sheets, 2001).

1.3.13 The Notch and Delta family.

The notch signalling pathway is an evolutionarily conserved mechanism that is used by multicellular organisms to control cell fates through local cell interactions, the Notch transmembrane receptor is activated by its ligands Delta and Serrate (Artavanis-Tsakonas et al., 1999). In *Xenopus Notch-1* and *Delta-1* are expressed in the pronephric anlagen from stage 20. At later stages, *Notch-1* is restricted to tubules until stage 38, whereas *Delta-1* is restricted to the most dorso-anterior region (figure 1.7C) and is down regulated by stage 34. *Serrate-1* is expressed in the pronephric anlagen from stage 25-26 and later, during tailbud, is restricted to tubules and nephrostomes until stage 38. The expression of *Notch-1* is maintained in a pattern overlapping the domains of the two ligands; *Delta-1* is restricted to the margin between the tubules and the corpuscle, *Serrate-1* is also expressed in the dorsoanterior region of the tubules but more ventral than *Delta-1*. Expression in duct was not observed. The authors showed that activation of the *Notch* pathway altered or ablated the expression of duct markers (*Xlim-1*, *c-ret* and 4A6), and inhibition of *Notch* pathway appeared to recruit cells to the duct anlagen. Thus suggesting that *Notch-1* functions to repress duct cell differentiation in the region of pronephric tubule cell fate. In addition, *Notch-1* pathway activation increased the region of expression of tubule markers *XPax-8* and *XPax-2* in the ventroposterior region destined to become duct, and of the *xWT1* expression domain in the glomus. It seems likely that the Notch-1 signalling pathway is required for partitioning of the pronephric primordia destined for particular cellular fates (McLaughlin et al., 2000). Four homologs of the *Notch* ligands, *deltaA-D*, have been identified in zebrafish. All these homologs are expressed in the nervous system and sensory organs, but only *deltaC* is expressed in the pronephros (Smithers et al., 2000).

1.3.14 Integrins and cadherins.

Integrins are a family of enzyme-linked cell-surface receptors that bind to the extracellular matrix and mediate intracellular signalling events. In humans the *integrin $\alpha 6$* is expressed in the basal region of the cells of the glomerulus and tubules where it is thought to maintain cell polarity (for review see DeSimone, 1994). *Xenopus integrin $\alpha 6$* is expressed in the early nervous system and in the pronephros. Using antisense oligonucleotides, the authors produced embryos depleted in *integrin $\alpha 6$* that caused severe neural defects, but any pronephric abnormalities were not reported. It is suggested that *integrin $\alpha 6$* may be involved in the mesenchyme-to-epithelial transition during nephrogenesis (Lallier et al., 1996).

Cadherins are a family of calcium-dependent cell adhesion molecules implicated in the formation and development of epithelial tissues. Surprisingly, *Xenopus E-cadherin* is not expressed in the developing pronephros although it is present in tissues of the mesonephros (Levi et al., 1991). In contrast the *Xenopus* ortholog of *N-cadherin* is expressed at high levels in the pronephros, heart and brain (Simonneau et al., 1992).

1.3.15 Cold-inducible RNA binding protein (CIRP).

The *Xenopus* homolog of cold-inducible RNA-binding protein, *XCIRP*, is transiently expressed in the pronephros and nervous system. Expression was observed in the presumptive pronephros from early tail bud stages, and in the pronephric field through to stage 35 (Uochi and Asashima, 1998). A homolog of

XCIRP, *XCIRP-1* has been demonstrated to be required for kidney formation. Targeted suppression, using full-length antisense mRNA of *XCIRP-1* (C3), altered the morphogenetic lineage movement of the C3 cells and resulted in a defective pronephros at tailbud stages. Furthermore, animal caps dissected from embryos injected with antisense *XCIRP-1* mRNA and cultured in activin and RA (which normally results in the induction of pronephric tubules), were induced to form mesoderm but did not express pronephric markers (*Xlim-1* and *xWT1*). These effects could be rescued by coinjection of sense strand *XCIRP-1* mRNA. *XCIRP-1* is an RNA binding protein, it is suggested that *XCIRP-1* may be required for marking gene transcripts, perhaps by changing their conformation to establish competence for future differentiation programs (Peng et al., 2000).

1.3.16 Other useful markers of pronephric components.

Two antibodies, tubule specific 3G8 monoclonal and duct specific 4A6 monoclonal antibodies, are excellent pronephric markers, although the epitopes are unknown (Vize et al., 1995). *Xclaax-1*, although an unknown gene, is a useful marker for pronephros as it is located to the baso-lateral domain of the pronephric tubules (Cornish et al., 1992). There are numerous other genes which show expression patterns in the pronephros as well as other tissues. The review above is a representation of the most prominent players in pronephrogenesis at this time (for other markers see Davies and Brändli, 1997).

In summary, it appears that the different kidney forms express the same genes in analogous structures, and orthologous genes in the same kidney form in different species. This observation leads to the hypothesis that similar signalling cascades

are utilised by the different kidney types to form similar structures and perform similar functions. Genes that play significant roles or display partial redundancy in one form appear to do so in others. For induction, specification and subsequent development of the pronephros, cascades of molecular events are required to orchestrate the cellular and tissue events involved in these processes. A summary of the timing of onset of pronephric gene expression is shown in figure 1.8. Studies conducted in the various model organisms all contribute, in their own particular way, to create an overall picture of nephrogenesis.

1.4 Mutagenesis studies in the zebrafish pronephros

Xenopus laevis has limited usefulness as a genetic system due to its psuedo-tetraploidy and long life cycle. However, the zebrafish is a particularly useful model system as its diploid genome is amenable to genetic studies. Recently, a large scale ENU mutagenesis screen for zebrafish developmental mutants was carried out (Driever et al., 1996). Work by Drummond et al., (1998) has isolated eighteen independent recessive mutations affecting pronephric development (Table 1.1). A common theme for the phenotypes of these mutants was the appearance of fluid-filled cysts in the pronephric region followed by general oedema. Obstruction or extirpation of the pronephric duct has been shown to cause tubule dilation followed by general oedema (Fales 1935). On closer examination of the mutant phenotypes, duct obstruction and axis deformity were ruled out as possible explanations. The authors suggest that the phenotypes observed are the consequence of pronephric failure and altered osmoregulation.

Figure 1.8

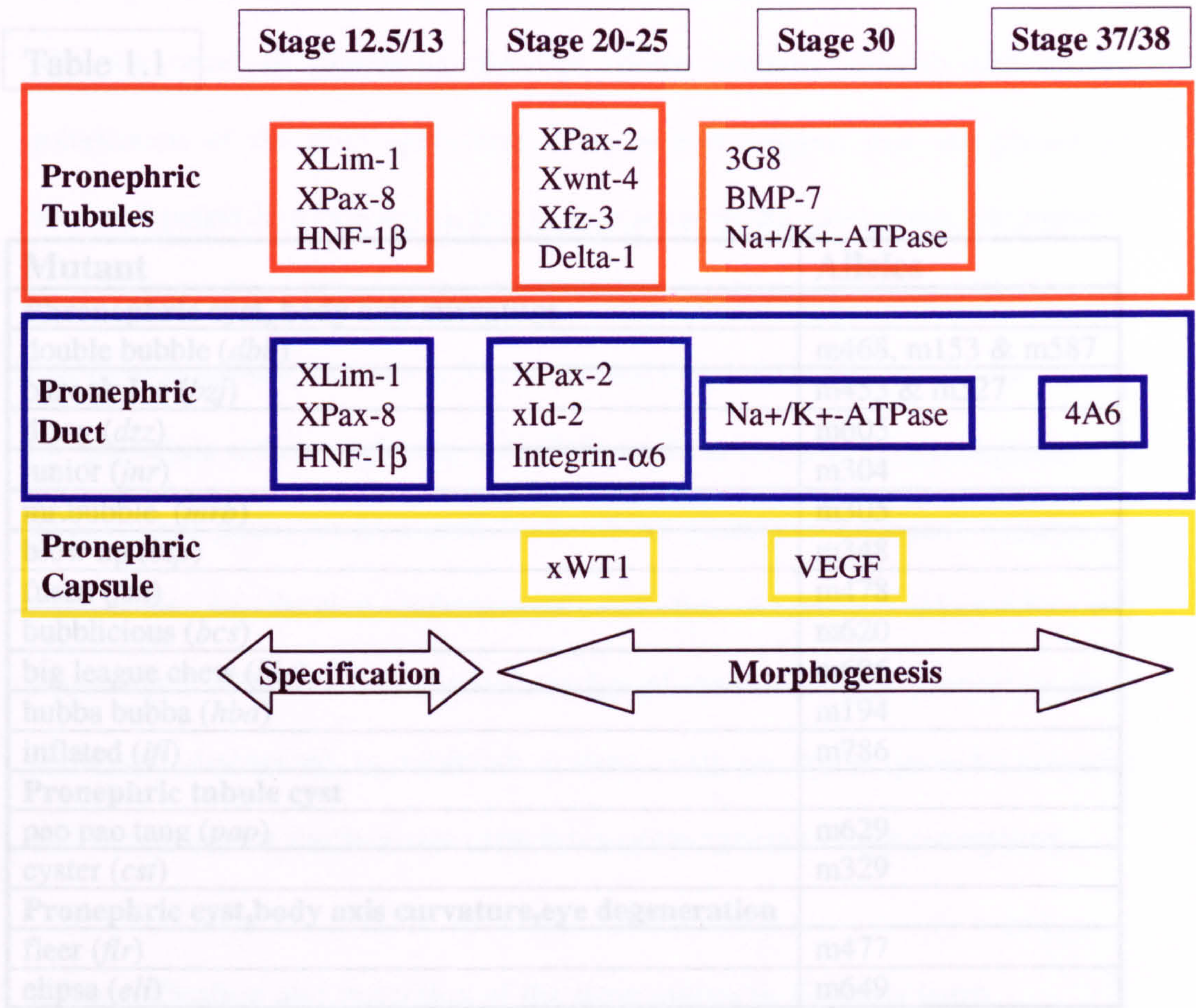


Figure 1.8: The onset of pronephric gene expression in *Xenopus laevis*. The coloured boxes indicate those genes expressed in the corresponding region, red: pronephric tubules, blue: pronephric duct, yellow: pronephric capsule. (Redrawn based on Brandli, 1999).

Table 1.1

| Mutant | Alleles |
|---|-------------------|
| Pronephric cyst, body axis curvature | |
| double bubble (<i>dbb</i>) | m468, m153 & m587 |
| bazook Joe (<i>bzj</i>) | m453 & m527 |
| dizzy (<i>dzz</i>) | m605 |
| junior (<i>jnr</i>) | m304 |
| mr.bubble (<i>mrb</i>) | m305 |
| blow up (<i>blp</i>) | m348 |
| fusen (<i>fsn</i>) | m478 |
| bubblicious (<i>bcs</i>) | m620 |
| big league chew (<i>blc</i>) | m696 |
| hubba bubba (<i>hba</i>) | m194 |
| inflated (<i>ifl</i>) | m786 |
| Pronephric tubule cyst | |
| pao pao tang (<i>pap</i>) | m629 |
| cyster (<i>cst</i>) | m329 |
| Pronephric cyst,body axis curvature,eye degeneration | |
| fleer (<i>flr</i>) | m477 |
| elipsa (<i>eli</i>) | m649 |

Table 1.1: Aberrant pronephric phenotypes isolated from a zebrafish mutant screen. Mutants shown were isolated from a large-scale zebrafish mutant screen. The best characterised thus far is the double bubble (*dbb*) which displays glomerula malformations leading to general oedema and cyst formation in the glomerula, tubules and later in the duct (Reproduced from Drummond, 2000).

The *double bubble* mutation, as a representative of the largest group, was analysed in detail. Histological analysis of the mutant shows that the glomerulus is loose and distorted, swelling is apparent and the cells appear flattened. The glomerulus overall architecture is disorganised and the basement membrane is severely distorted. The timing of the formation of the glomerula cysts coincides with the onset of glomerula filtration. Some mutants also showed altered polarisation of the duct epithelium. The authors suggest that the phenotype observed points to a primary defect in formation of the glomerulus (Drummond et al., 1998). The zebrafish mutants *floating head*, *sonic you* and *you-too* are defective in midline structures. It is suggested that notochord provides the signals for glomerula differentiation in zebrafish. In these mutants glomerulogenesis is blocked, but podocyte formation (cells of the glomerula basement membrane) was found to develop independently of the notochord (Majumdar and Drummond, 2000). Further detailed studies of these and other pronephric gene mutations, discovered in zebrafish screens, will no doubt, provide essential information on the mechanisms underlying organogenesis of the pronephros.

1.5 Specification and induction of the pronephros in *Xenopus laevis*

In the early *Xenopus* embryo, mesoderm is induced at the equator by signals from the endoderm converting overlying ectoderm cells to a mesodermal fate, thus creating the three primary germ layers (Nieuwkoop, 1969). Candidate molecules for mesoderm induction include FGF family members and vegetally localized members of the TGF- β superfamily. It is widely accepted that a maternal T-box transcription factor VegT activates zygotic *Derrière*, *Xnr-1*, -2, -4, -5 and -6. Dorso-ventral patterning of the mesoderm appears to involve

differential regulation of these downstream targets of VegT. *Xnr-1* and *Xnr-2* are expressed at higher levels in the dorsal side than the ventral side due to the action of the Wnt pathway effector β -catenin (Agius et al., 2000). *Xnr-1* and *Xnr-2* expression also requires TGF- β signalling probably in the form of maternal Vg1 and/or an autoregulatory loop, whereas *Xnr-4* and *Derrière* do not (Clements et al., 1999).

The pronephros is derived from tissues of the intermediate mesoderm. The inductive signals that specify and pattern the pronephric mesoderm *in vivo* remain elusive. It is thought that the initial signals occur during gastrulation and by early neurula the pronephros is specified (Saxén, 1987). The experiments of Fales (1935) demonstrate that the prospective pronephric region in urodeles is capable of self-differentiation by midneurula stages. More recently, the temporal specification of all three components of the kidney in *Xenopus laevis* have been established; the tubules and duct are specified at stages 12.5 and 14 respectively and the glomus is specified at stage 12.5 (Brennan et al., 1998, Brennan et al., 1999). Although a number of genes that are expressed early in this region have been cloned and characterised, their roles in pronephric induction and specification are as yet unknown. Studies of pronephric development in UV-ventralised and lithium-dorsalised embryos, demonstrated that dorsal tissues, especially anterior somites are responsible for the establishment of the intermediate mesoderm and induction of the embryonic kidney (Seufert et al., 1999). A model of pronephric organogenesis in *Xenopus* is shown in figure 1.9 (Brändli, 1999).

Figure 1.9

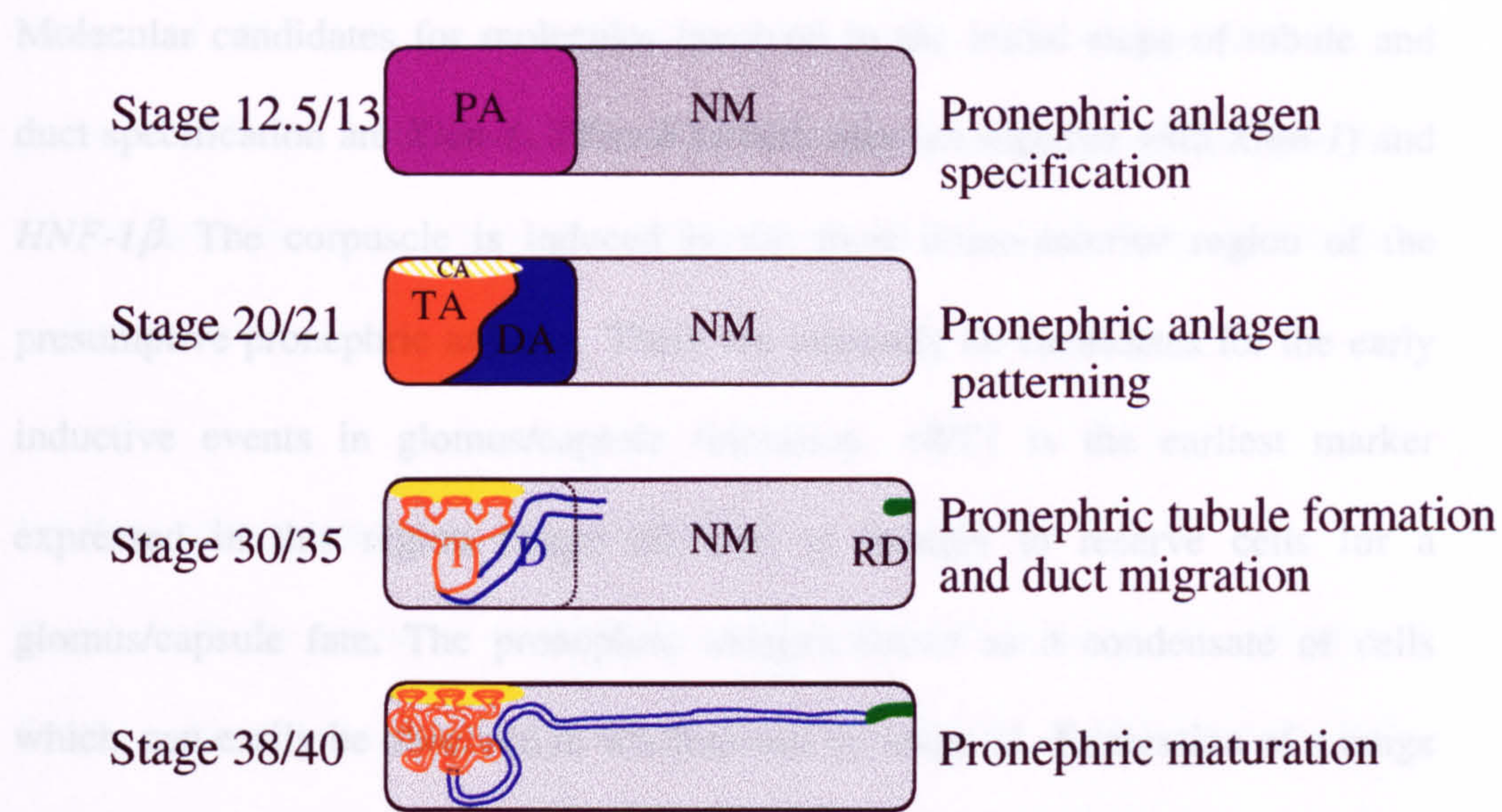


Figure 1.9: Specification and patterning of intermediate mesoderm forming the lineage of the pronephric components during pronephrogenesis. Pronephric anlagen specification (stage 12.5/13), the pronephric anlagen (PA) is specified in the anterior portion of the nephrogenic mesoderm (NM). Pronephric anlagen patterning (stage 20/21), tubule anlagen (TA) is specified in the dorso-anterior region and the duct anlagen (DA) in the more ventro-posterior region of the PA. Capsule anlagen (CA) is specified in the most dorso-anterior region of the PA, although no markers of this region are yet known (see figure 1.8). Pronephric tubule formation and duct migration (stage 30/35), the tubules form (T) and the duct (D) begins to migrate posteriorly and the rectal diverticulum (RD) begins to migrate anteriorly into the NM. Pronephric maturation (stage 38/40) the tubules extend and coil and the duct joins with the rectal diverticulum. (Redrawn based on Brandli, 1999).

The pronephric kidney components are specified by stage 12.5 and 14 (tubules, glomus and duct respectively) probably at least in part from signals produced by the anterior somites; *xwnt-11* may be a candidate signalling molecule. The tubules and duct are induced in the lateral mesoderm ventral to somites 3-5, with the tubules specified in the more anterior region as opposed to the duct. Molecular candidates for molecules involved in the initial steps of tubule and duct specification are *Xlim-1*, *XPax-8* (which may act together with *Xlim-1*) and *HNF-1 β* . The corpuscle is induced in the most dorso-anterior region of the presumptive pronephric anlagen. There are currently no candidates for the early inductive events in glomus/capsule formation. *xWT1* is the earliest marker expressed in this region (stage 20) and is thought to reserve cells for a glomus/capsule fate. The pronephric anlagen forms as a condensate of cells which, can easily be observed in wholemount by stage 21. Expression of a range of molecules commences at this stage in the pronephric anlagen. *Notch* and its ligands *Delta* and *Serrate*, commence expression at this time and have been suggested to have roles in the partitioning of the capsule and tubule anlagen. Little is known regarding the action of BMP-4 and -7 in the pronephros in *Xenopus*, but they may well serve to pattern the lateral mesoderm. In the tubules *Xwnt-4* and its proposed receptor *Xfz3* are expressed and at particularly high levels in the nephrostomes. The differentiation and onset of function of the various pronephric components coincides with the beginning of expression of genes with known tissue specific functions. From around stage 27 the lumen forms in the tubules. At this stage the expression of the Na⁺/K⁺-ATPase (sodium pump) commences, together with integrin as a marker of epithelial polarisation. The expression of VEGF in the glomus from around stage 30 is a signature of

podocyte differentiation. As development proceeds, most of the genes display continued, but more restricted, patterns of expression (e.g. *Xwnt-4* restricts to the nephrostomes) whereas some are replaced by family members (*XPax-8* is replaced by *XPax-2*). Duct differentiation and caudal migration probably involves GDNF signalling, as identified in the axolotl model system. The current picture of the molecular mechanisms underlying the development of the pronephros is far from complete, only further investigation of these molecules and the identification of new ones will provide a full picture of the principles of nephrogenesis.

1.6 Pronephric cell lineages in Zebrafish

In zebrafish the origin of the different cell types that make up the pronephric lineages have been mapped (figure 1.10). Serluca and Fishman (2001) discovered that by using laser GFP un-caging to label a subset of intermediate mesoderm cells (8-10 somite stage), they were able to track these cells through development and determine their fate. They also used *in situ* probes, shown to be good markers of pronephric rudiments in other species, *wt1* (glomus), *pax2.1* (tubules) and *sim1* (duct). The most anterior cells in the pronephric field gave rise to podocytes (glomus) and the *wt1* expressing region. The more posterior cells gave rise to the tubules and express both *wt1* and *pax2.1*. The most posterior cells contribute to the duct and express *pax2.1* and *sim1* but not *wt1*. Thus demonstrating that the intermediate mesoderm is pre-patterned and that this pattern corresponds to particular combinations of transcription factor gene expression. This data is in good agreement with the analysis of the pronephric lineages in *Xenopus* (Seufert et al., 1999).

Figure 1.10

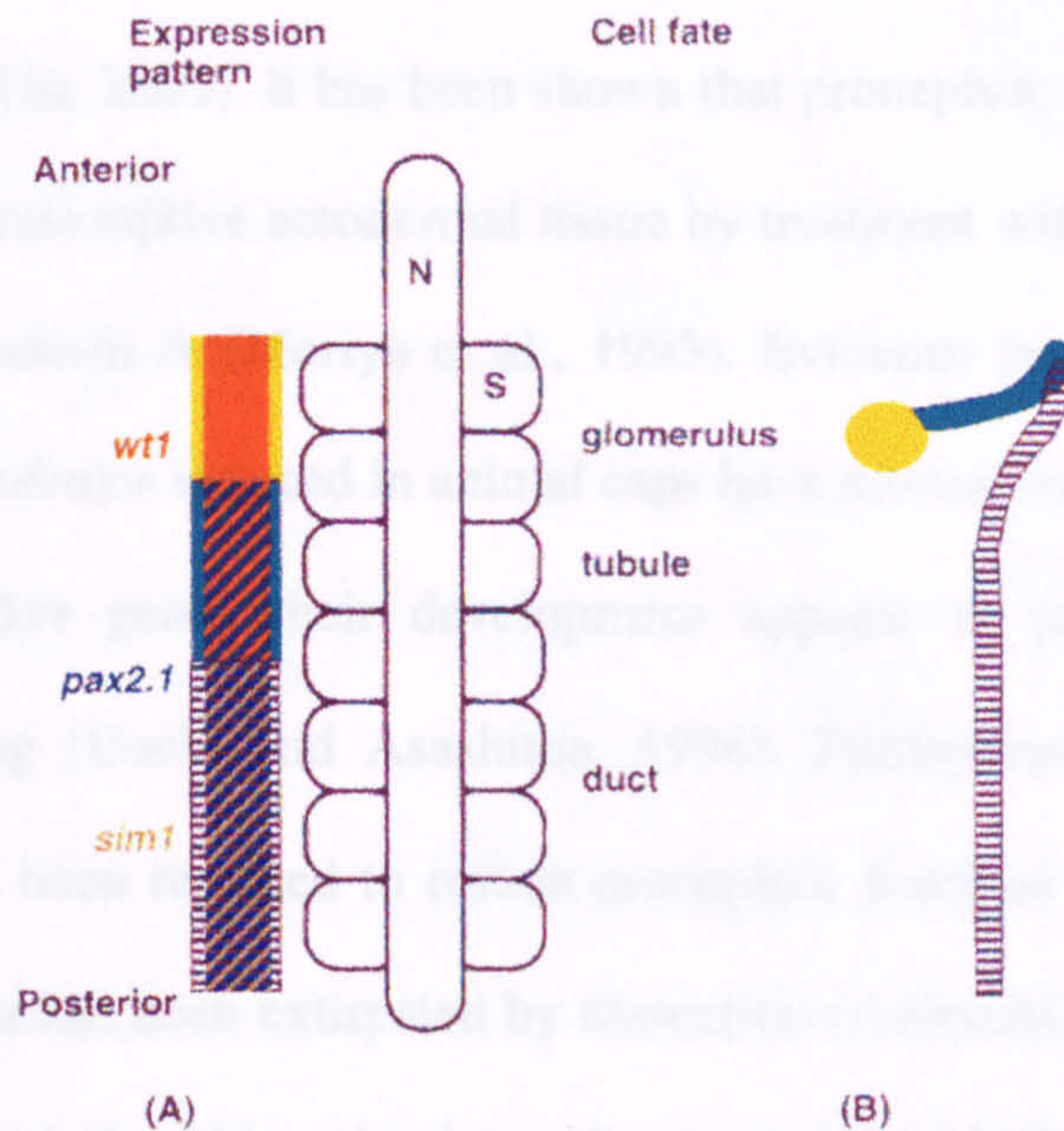


Figure 1.10: Patterning of the intermediate mesoderm giving rise to the components of the zebrafish pronephros. (A) Expression of *wt1* (orange), *pax2.1* (blue) and *sim1* (brown) at the 8-10 somite stage. Notochord (N) and somites (S) are shown for axial reference. The glomerula progenitors are in yellow, tubule in green and duct in horizontal lines. (B) Diagram of the mature pronephros including colours relating to the position (A-P) and gene expression patterns (Reproduced from Serluca and Fishman, 2001)

1.7 *In vitro* induction of pronephric tissues

Members of the FGF and TGF- β families of secreted growth factors can mimic the induction of mesoderm *in vitro* in ectodermal tissues (Green and Smith, 1990, Green et al., 1990, Gurdon et al., 1994). The explant can be induced to form different types of mesoderm in a dose dependent manner, with higher doses of activin inducing more dorso-anterior tissues (Figure 1.11) (Moriya et al., 2000; Ariizumi and Asashima, 2001). It has been shown that pronephric tubules can be induced to form in presumptive ectodermal tissue by treatment with retinoic acid (RA) (10^{-5} M) plus activin A (Moriya et al., 1993). Evidence from histological studies indicate that tubules induced in animal caps have normal morphology and by analysis of marker genes their development appears to parallel normal developmental timing (Uochi and Asashima, 1996). Furthermore, the kidney tubules formed have been reported to rescue pronephric function in tadpoles in which the pronephros has been extirpated by dissection (Ariizumi and Asashima 2001). Glomus can be induced in animal caps by treatment with RA (10^{-4} M) plus activin A or RA (10^{-4} M) plus bFGF (Brennan et al., 1999). No combination of RA, activin or bFGF has been found to induce pronephric duct at high frequency (EAJ unpublished).

1.8 Cloning of *Xenopus laevis* annexin IV (Xanx-4)

In order to identify novel genes that may be involved in pronephros development a subtractive hybridisation strategy was adopted that enriches for those genes expressed early in kidney development (Nijjar and Jones unpublished). This approach was based on the observations that animal caps treated with a combination of retinoic acid and activin develop *in vitro* into differentiated

Figure 1.11

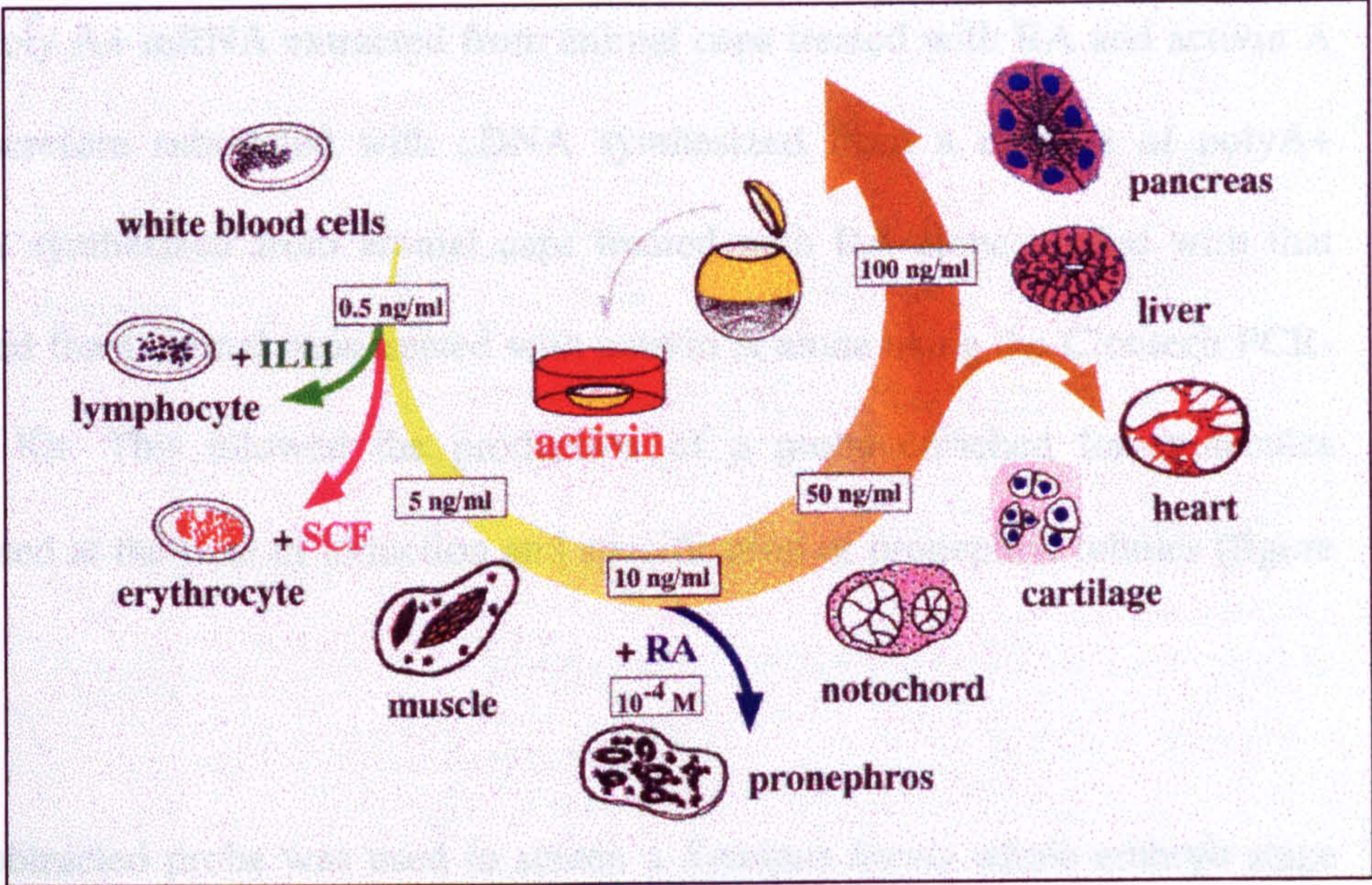


Figure 1.11: Tissue types induced by activin in *Xenopus* and newt animal caps. Treatment of animal caps with different concentrations of activin will induce different kinds of mesoderm. As concentration increases the type of mesoderm induced changes from ventral to more dorsal type (Reproduced from Ariizumi and Asashima, 2001).

kidney tubules (Moriya et al., 1993, Brennan and Jones unpublished observations). Treatment of animal cap ectoderm, dissected from blastula stage *Xenopus* embryos, with 5ng activin A and 10^{-5} M retinoic acid (RA) results in the formation of pronephric tubules at high frequency (figure 1.12), whereas, treatment of animal caps with activin A or RA alone does not. cDNA synthesized from poly A+ mRNA extracted from animal caps treated with RA and activin A was therefore subtracted with cDNA synthesized from a mixture of polyA+ mRNA synthesized from animal caps treated with RA alone pooled with that prepared from animal caps treated with activin A alone using the Clontech PCR-Select Kit. This allowed the production of a probe enriched for molecules expressed at the time of induction and specification of pronephric tubules (figure 1.13).

The subtracted probe was used to screen a *Xenopus laevis* whole embryo stage 13 λ gt 11 cDNA library (kindly provided by I.Dawid) in order to identify genes expressed early in pronephric organogenesis. A number of positive clones were identified and taken through four rounds of screening until the clones were plaque pure. One of the clones, K2, was a 1131bp cDNA insert and was subcloned into pGEM-T Easy (appendix 1). Partial sequencing revealed K2 to be the *Xenopus laevis* ortholog of Bovine annexin IV and preliminary *in situ* data showed it to be expressed in the pronephros.

During the course of this study a similar subtractive hybridisation strategy was used to successfully clone the pronephros specific genes *XCIRP* (Uochi and Asashima, 1998) and *XSMP-30* (Sato et al., 2000). *In vitro* induction followed by

Figure 1.13

Figure 1.12

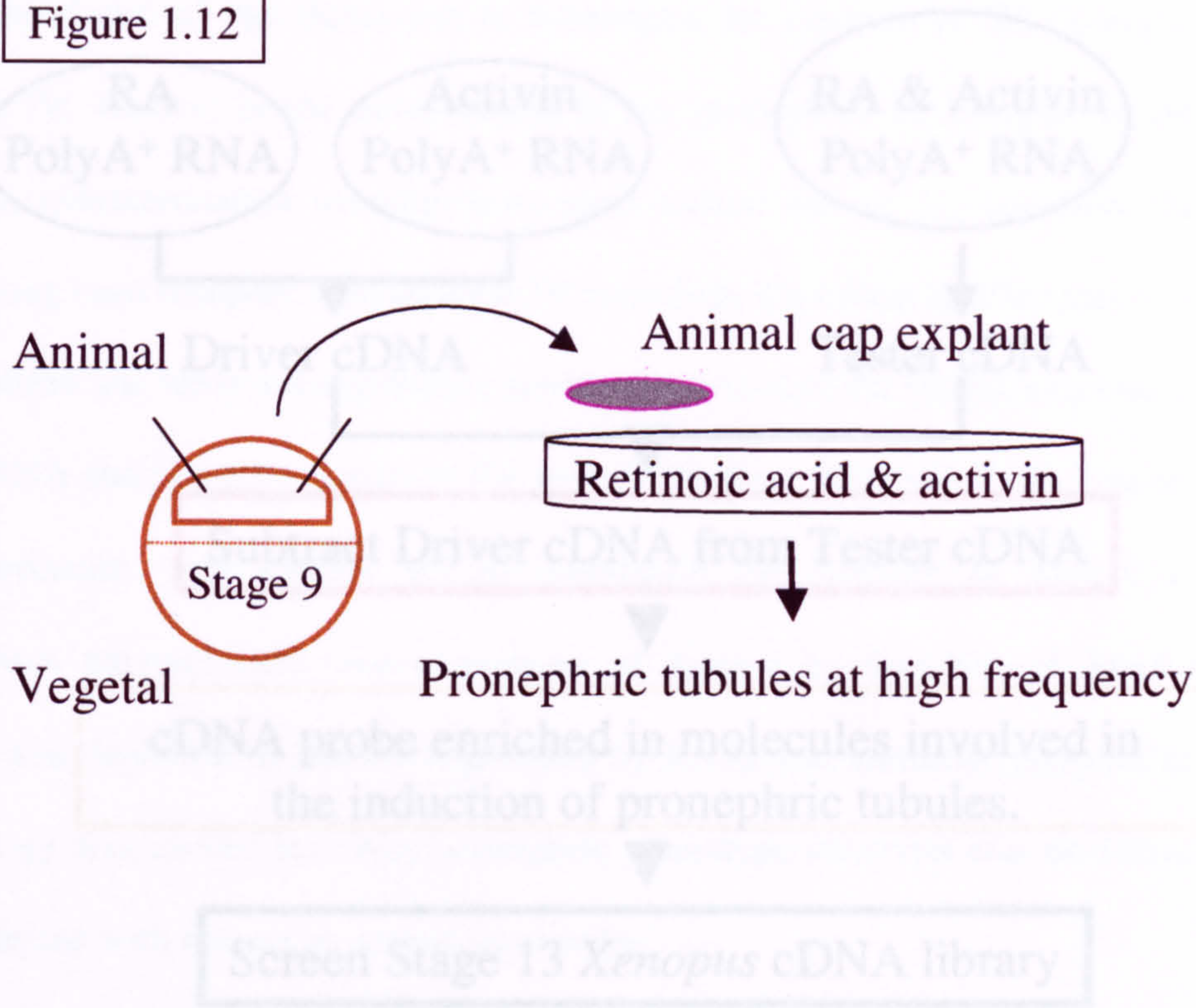


Figure 1.12: Induction of pronephric tubules in animal caps of *Xenopus laevis*. Animal caps taken from stage 9 embryos are cultured in Barth X containing retinoic acid and activin. Pronephric tubules are induced at high frequency. Incubation of animal caps in activin or retinoic acid alone does not.

Figure 1.13

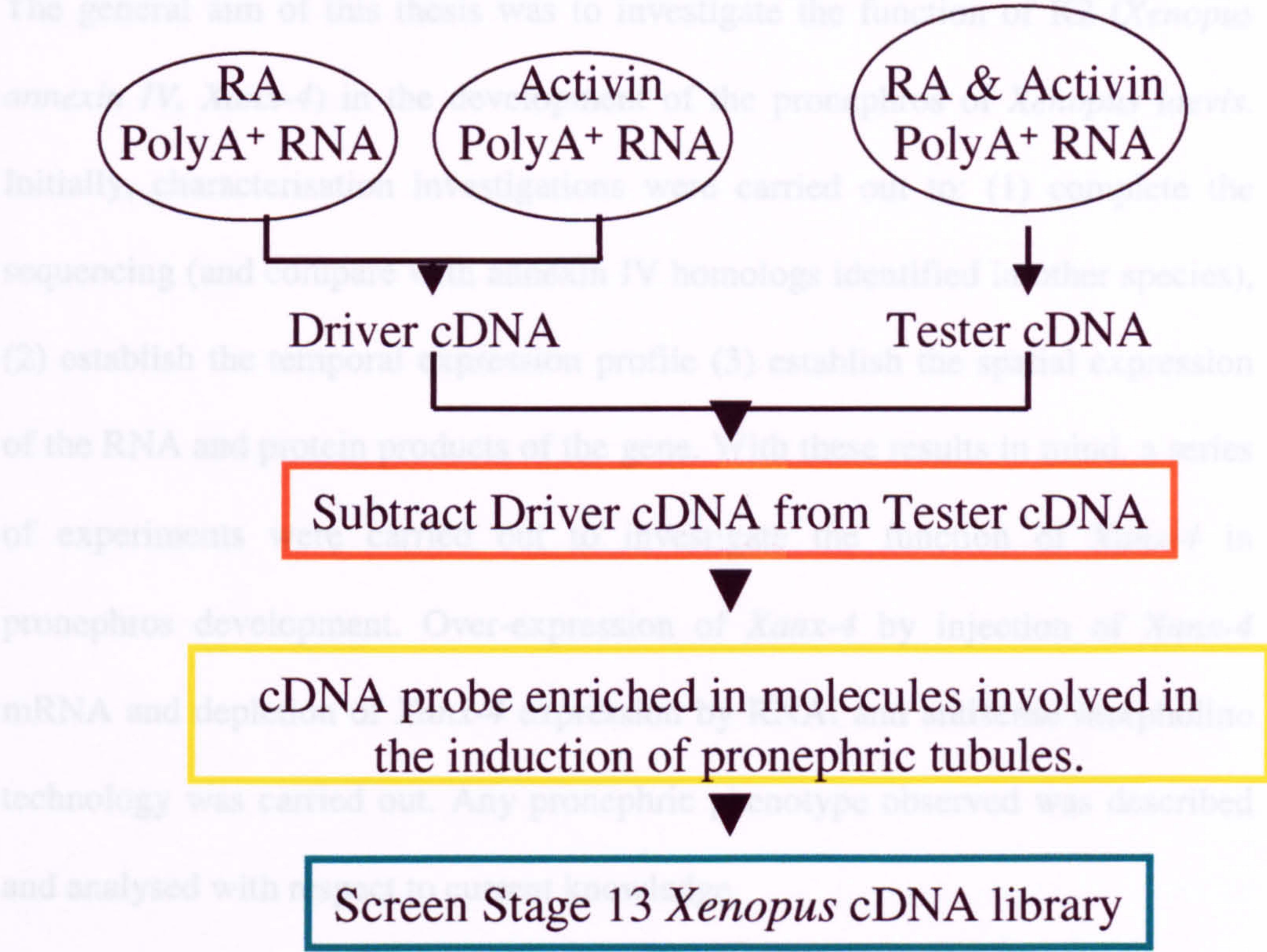


Figure 1.13: Preparation of the subtracted probe. Animal caps were incubated in retinoic acid (RA) alone and activin alone, polyA+ RNA and cDNA was prepared and the two samples pooled producing Driver cDNA. Animal caps were incubated in a combination of RA and activin (induces tubules), polyA+ RNA was prepared and cDNA producing the Tester cDNA. Subtraction of Driver from tester allowed the production of a probe enriched in molecules involved in the induction of pronephric tubules. This probe was then used to screen a stage 13 *Xenopus* cDNA library, which resulted in the cloning of Xanx-4.

differential display resulted in the isolation of *Xsal-3* that is also expressed in the pronephros (Onuma et al., 1999).

1.9 The aims of this thesis.

The general aim of this thesis was to investigate the function of K2 (*Xenopus* annexin IV, *Xanx-4*) in the development of the pronephros of *Xenopus laevis*. Initially, characterisation investigations were carried out to: (1) complete the sequencing (and compare with annexin IV homologs identified in other species), (2) establish the temporal expression profile (3) establish the spatial expression of the RNA and protein products of the gene. With these results in mind, a series of experiments were carried out to investigate the function of *Xanx-4* in pronephros development. Over-expression of *Xanx-4* by injection of *Xanx-4* mRNA and depletion of *Xanx-4* expression by RNAi and antisense morpholino technology was carried out. Any pronephric phenotype observed was described and analysed with respect to current knowledge.

During the course of this work, descriptions of a variety of techniques for interfering with gene expression were published. This provided an ideal opportunity for them to be assessed in the *Xenopus* system for their efficacy. At the time when our RNAi experiments were started (May 1999) there were no published examples of the RNAi technique having been used either with or without success in *Xenopus*. The utilisation of the siRNA approach has not yet been published in *Xenopus* and to our knowledge this thesis represents the first time it has been tested. Therefore this thesis describes a series of experiments which attempt to assess the usefulness of these technologies with a gene which

we have shown by morpholino studies provides a phenotype in pronephros development. In our view it reports studies which fail to support the usefulness of RNAi and siRNA in *Xenopus* embryos.

Chapter 2 Materials and Methods

2.1 Materials

Bench chemicals were supplied by Sigma, Merck or Melford. DNA oligonucleotides were synthesized by Life Technologies (Gibco BRL). RNA oligonucleotides were synthesized by MWG-Biotech UK Ltd. Morpholino oligonucleotides were synthesized by Gene Tools (Oregon USA). Enzymes were supplied by Life Technologies (Gibco BRL) except proteinase K which was supplied by Boehringer-Mannheim, T4 DNA Ligase was supplied by Fermentas and Roche supplied DNase I and calf intestinal phosphatase. ^{32}P -dGTP was supplied by Amersham Pharmacia Biotech and ^{35}S -methionine was supplied by NEN. Automated sequencing reagents by PE Applied Biosystems (Perkin-Elmer). Protein markers were from New England BioLabs and DNA marker from Life Technologies (Gibco BRL). *In situ* hybridisation reagents were supplied by Roche, except for the Fast Red TR/Naphthol AS/MX alkaline phosphatase colour substrate which was supplied by Sigma. Secondary antibodies were supplied by Sigma. Nylon membranes for blotting protocols were supplied by Amersham. Trizol for RNA isolation was supplied by Life Technologies (Gibco BRL). Chemiluminescent Protein detection kit was supplied by Bio-Rad. *In vitro* translation reticulocyte lysate system was supplied by Promega. Hoescht stain (33258) and FLDX was supplied by Sigma.

2.2 Media and stock solutions

All general media and stock solutions were prepared according to Sambrook et al, 1989.

2.3 Vectors

pGEM-T Easy (Promega) contained the original K2 (*Xanx-4*) clone from the library screen (appendix 1).

pBluescript RN3 (Kreig and Melton, 1984) was used as an expression vector. This vector contains a 5' *β-globin* UTR sequence 5' to the insert and a 3' *β-globin* UTR sequence 3' to the insert which stabilises the mRNA when expressed in the embryo or oocyte (appendix 2).

PCS3+MT (Vojtek 1995, FHCRC) was used as an expression vector, it contains CMV IE94 promoter and 6 myc epitope tags, which allows translation products from this vector to be detected using anti-myc antibody (appendix 3).

2.4 DNA techniques

2.4.1 Agarose gel electrophoresis

Agarose gels of between 1%-2% were prepared using 1x TBE with ethidium bromide added to give a final concentration of 0.5µg/ml. The DNA/RNA was separated by electrophoresis in 1x TBE at 80-150V and were then photographed under UV light. Where required, DNA was extracted from the gel using a Qiagen gel extraction kit according to the manufacturer's instructions.

2.4.2 Restriction enzyme digests

Restriction digests were carried out according to supplier's instructions. Following digestion of plasmids for ligation, the plasmid was treated with

phosphatase to prevent re-ligation. 1µl of calf intestinal alkaline phosphatase was added for each 10µl of reaction, and the reaction was incubated at 37°C for a further 20 minutes. The phosphatase was removed by phenol extraction, before ligation.

2.4.3 DNA minipreps

An overnight culture of 5mls was set up and was used with a Qiagen miniprep kit (27104) according to the instructions.

2.4.4 Ligation of DNA into plasmid vectors

For the ligation of *Xanx-4* into the pBluescriptRN3 (appendix 2) vector, the insert was first released from *Xanx-4*/pGEM-T Easy construct (appendix 1) by digestion with *EcoRI* restriction enzyme. The digested plasmid was then separated on an agarose gel and the insert extracted using the QIAquick kit (28704). The insert was added to plasmid vector previously digested with *EcoRI* with a 1-3 molar excess of insert to vector. Ligation reactions were made up to a final volume of 10µl including T4 DNA ligase and ligation buffer and incubated for 1 hour at RT.

2.4.5 Preparation of the *myc-Xanx-4* and *Xanx-4-MUT* inserts and their ligation into plasmid vectors.

This technique was used in the preparation of myc-tagged (myc-*Xanx-4*/pCS3+MT, appendix 3) and mutant (*Xanx-4-MUT*/RN3, appendix 4) *Xanx-4* constructs. The technique allows insertion of restriction enzyme sites and/or simple mutations. The PCR primers AN4-MYC1 and AN4-MYC2 (Table 2.2)

were used to amplify the *Xanx-4* coding region and produce the *myc-Xanx-4* insert, the restriction enzyme site is in bold. PCR was performed using pGEMTEasy/*Xanx-4* construct (appendix 1) as a template and the product phenol/choroform, choroform extracted and ethanol precipitated. The pellet was taken up in 10µl ddH₂O and digested with *Bam*HI. The digest was then separated on an agarose gel and the insert extracted using the QIAquick Gel Extraction Kit. The insert was added to pCS3+MT plasmid vector previously linearised with *Bam*HI with a 1-3 molar excess of insert to vector. Ligation reactions were made up to a final volume of 10µl including T4 DNA ligase and ligation buffer and incubated for 1 hour at RT.

The PCR primers AN4-MUT and T7 were used to amplify the *Xanx-4* coding region and produce the *Xanx-4-MUT* insert (see chapter 6.2.5 for details of mutations). Table 2.3 shows the primer sequences and conditions, the restriction enzyme sites are in bold and the mutations are underlined. PCR was performed using pGEMTEasy/*Xanx-4* construct (appendix 1) as a template and the product phenol/choroform, choroform extracted and ethanol precipitated. The pellet was taken up in 10µl ddH₂O and digested with *Eco*RI. The digest was then separated on an agarose gel and the insert extracted using the QIAquick Gel Extraction Kit (28704). The insert was added to pBluescript RN3 plasmid vector previously linearised with *Eco*RI, with a 1-3 molar excess of insert to vector. Ligation reactions were made up to a final volume of 10µl, including T4 DNA ligase and ligation buffer and incubated for 1 hour at RT.

Table 2.2 Primer pairs used for preparation of *myc-Xanx-4* and *Xanx-4*-MUT inserts.

| Primer name | Primer sequence (5'-3') | Annealing temperature, No. of cycles |
|--------------|--------------------------------|---|
| AN4-MYC1 | u-gccgggatcccatggcagcacctc | 50°C – 5 cycles |
| AN4-MYC2 | d-cggcggatccgtcttcccctccg | 60°C – 25 cycles |
| AN4-MUT | u-gccgggaattccatggcgcactgggaac | 50°C – 5 cycles |
| T7 (Promega) | d-taatacgactcactataggg | 60°C – 25 cycles |

Automated sequencing was carried out on all new constructs to ensure correct sequence and orientation.

2.4.6 Transformation of plasmid DNA into competent *E. coli* by heat shock.

E.coli strains DH5α or XL1B competent cells were prepared for heat shock transformation according to Sambrook et al., (1989). 10ng of ligation mix was mixed with 100µl of *E.coli* competent cells and incubated on ice for 15 minutes. The cells were then placed at 42°C for 1 minute and incubated on ice for 2 minutes. The cells were transferred to 1ml L-broth and incubated at 37°C for 1 hour. Following this incubation the cells were microcentrifuged for 5 minutes at 2,500g, resuspended in 50 µl L-broth and plated out on L-broth plates containing ampicillin at 100µg/ml. Plates were incubated overnight at 37°C.

2.4.7 DNA sequencing

Automated sequencing reactions were set up as follows. 500ng of plasmid DNA was added to 2.5pmol primer and 4µl sequencing buffer (200mM Tris pH9, 50mM MgCl₂) and made up to a total volume of 16µl with H₂O. 4µl sequencing reaction mix was added and the reactions were subjected to PCR on the following program: 94°C 10 seconds, 50°C 5 seconds, 60°C 4 minutes – 30 cycles. The samples were then precipitated with 50µl ethanol and 2µl 3M NaOAc pH4.6 at room temperature for 30 minutes. Samples were then microcentrifuged at 10,000g for 20 minutes, washed with 70% ethanol and the pellet was provided to the departmental automated sequencing for gel loading and running.

2.5 RNA techniques

2.5.1 RNA extraction from embryos and animal caps

Volumes given below are for extraction of RNA from five whole embryos, for different numbers of embryos the volumes were adjusted accordingly. Five embryos were homogenised in 450µl extraction buffer (300mM NaCl, 20mM Tris pH7.5, 1mM EDTA pH8, 1% SDS) with 6µl proteinase K (15mg/ml) and incubated at 37°C for 15 minutes. The homogenate was phenol extracted with an equal volume of phenol and 5µg of glycogen was added to the upper phase. The RNA was precipitated with two volumes of ethanol at –20°C for at least 30

minutes. Following precipitation the sample was microcentrifuged at 10,000g for 20 minutes and the pellet was resuspended in 90µl DNase buffer (20mM Tris pH8.3, 30mM NaCl, 2.5mM MgCl₂) containing 2µl DNaseI (40U) and 2µl placental RNase inhibitor (40U) and incubated at 37°C for 15 minutes. 360µl extraction buffer and 6 µl proteinase K were added and the sample was incubated for a further 20 minutes at 37°C. The samples were phenol extracted and then phenol/chloroform extracted before precipitation with 2 volumes ethanol at room temperature for no longer than 30 minutes. The samples were microcentrifuged as before and the RNA pellet was resuspended in 30µl H₂O. 1µl RNA was loaded on a 1% agarose gel to determine purity and yield.

2.5.2 Reverse transcription PCR

RT-PCR was performed as described by Barnett et al., (1998). RNA extracted from animal caps or whole embryos was mixed with water to give a final volume of 21.1 µl, heated to 75°C for 5 minutes and placed on ice. Volumes of RNA used were adjusted according to concentration of the RNA as determined by separation on an agarose gel. 7.9µl of reaction mix (3.3µM random hexamers, 1x PCR buffer, 3mM MgCl₂, 500µM dNTPs, 1U/µl RNase inhibitor) was added to each sample and the reactions were incubated at 37°C for 5 minutes. 2µl MMLV reverse transcriptase was added to each sample and the reactions were incubated for a further 1 hour at 37°C. After this time the samples were heated to 95°C for 5 minutes and then cooled on ice and stored at -20°C. The resulting cDNA was used in PCR analysis. 1µl each cDNA was made up to a final volume of 25µl with reaction mix: 1x PCR buffer, 1.5mM MgCl₂, 200µM dNTPs, 1µM each

primer, 1 μ Ci α^{32} P-dGTP and 1U Taq polymerase. The samples were overlaid with oil. The number of cycles and standard PCR conditions were:

Step 1. 94°C 3 minutes, 55°C 1 minute, 72°C 1 minute – 1 cycle

Step 2. 94°C 30 seconds, 55°C 1 minute, 72°C 1 minute – 18 cycles

Step 3. 72°C 5 minutes – 1 cycle

Amplifications were as above for EF1 α primers or ODC primers and the volumes of cDNA were adjusted to ensure equal loading. These adjusted volumes were then used in all subsequent PCR reactions. Primers used, cycles and annealing temperatures for different genes are shown in table 2.1.

7.5 μ l of each PCR reaction was mixed with 7.5 μ l loading buffer (95% deionised formamide, 10mM EDTA pH8, 0.1% xylene cyanol, 0.1% bromophenol blue) and heated to 95°C for 5 minutes before being loaded on a 6% denaturing acrylamide gel and separated at 650V for approximately 1 hour. The gel was dried and exposed to X-ray film or a phosphorimager screen.

Table 2.1 Sequences of primers and conditions used for RT-PCR analysis of RNA samples (u-upstream, d-downstream)

| Gene | Primer sequence (5' to 3') | Annealing temperature, No. of cycles | Reference |
|----------------|---|--------------------------------------|---|
| <i>Xanx-4</i> | u-agcaggcacgatgaagatg d-tcattcacggtgctgctctg | 57°C 27 | This work |
| <i>Xlim-1</i> | u-gaaggatgagaccactggtgg d-cactgccgtttcgttcatttc | 55°C 25 | Witta & Sato, 1997 |
| <i>XPax-2</i> | u-tcggaagaagagtgggtctac d-ggtattcatattccgcattc | 60°C 24 | This work |
| <i>XPax-8</i> | u-ccaacagcagcatcagatc d-caatgacacctggccggata | 53°C 24 | This work |
| <i>Xwnt-4</i> | u-gagtggaatgcaagtgtc d-tacactgccgaccagttg | 57°C 25 | This work Accession No.U13183 |
| <i>Xwnt-11</i> | u-gaagtcaagcaagtctgctgg d-gcagtagtcaggggaactaaccag | 55°C 25 | http://www.lifesci.ucla.edu/hhmi/derobertis/index.html |
| <i>XWT1</i> | u-cacacgcacgggggtct d-tgcatgttgatgatgacg | 55°C 27 | Carroll & Vize, 1996 |
| <i>ODC</i> | u-ggagctgcaagtttggaga d-tcagttgccagtgtggtc | 55°C 18 | Bassez <i>et al.</i> , 1990 |
| <i>EF1α</i> | u-cagattggtgctggatatgc d-cactgccttgatgactccta | 55°C 18 | Mohun <i>et al.</i> , 1989 |

2.5.3 *In vitro* transcription of mRNA

Plasmid template was linearized with the appropriate restriction enzyme and purified using a Qiagen gel extraction column. The template was eluted in 30 µl H₂O and 6 µl used as a template for transcription with mMESSAGE mMACHINE kit from Ambion. Transcriptions were incubated for 1 hour with T7 or T3 polymerase or 2 hours with SP6 polymerase. The RNA concentration was quantified by agarose gel electrophoresis and UV absorbance.

Xmad2 mRNA was prepared from pSP64TNE-*Xmad2* construct (gift from D.Melton, Harvard MA) linearised with *XbaI* and transcribed with SP6 RNA polymerase. *Xsox17β* mRNA was prepared from pSPXsox17β construct (gift from D.Clements, Warwick) linearised with *XhoI* and transcribed with SP6 RNA polymerase. Truncated activin receptor (Δ 1XAR1) mRNA was prepared from p64T-DMNI/Stop construct (gift from A. Hemmati-Brivanlou, Harvard MA) linearised with *EcoRI* and transcribed with SP6 RNA polymerase.

2.5.4 Wholemount *in situ* hybridization

Wholemount *in situ* hybridization was carried out as described in Harland, 1991. The embryos were fixed in MEMFA (0.5M MOPS, pH7.4, 100mM EGTA, 1mM MgSO₄, 4% formaldehyde) and hybridised with RNA probes produced from cDNA clones.

The *Xanx-4* antisense probe was transcribed from the pGEM-T Easy/*Xanx-4* construct (appendix 1) previously linearised with *NcoI*, with SP6 RNA polymerase. The sense control probe was linearised with *Sall* and transcribed with T7 RNA polymerase. Probes were synthesised and labelled using a DIG

labelling kit (Boehringer) and visualised using anti-DIG-alkaline phosphatase secondary and NBT/BCIP for the colour reaction according to manufacturer's recommendations (Boehringer).

Xlim-1 antisense probe was prepared from construct pBlueKS-lim-1 (gift from T.Carroll, Texas) linearised with *XhoI* and transcribed with T7 RNA polymerase. *xWT-1* antisense probe was prepared from construct pGEM7-WT1 (gift from T.Carroll, Texas) linearised with *EcoRI* and transcribed with T7 RNA polymerase. *XPax-8* antisense probe was prepared from construct pSP64T-Pax8 (gift from T.Carroll, Texas) linearised with *XhoI* and transcribed with T3 RNA polymerase.

2.5.5 Northern blot analysis

Total RNA was extracted from different adult tissues using Trizol (Gibco-BRL Life Technologies) following the manufacturer's protocol. Samples of denatured RNA (30 µg per lane) were fractionated by electrophoresis through 1.2% agarose, 2.2M formaldehyde gels in MOPS buffer (50mM MOPS pH7; 1mM EDTA; 20mM sodium acetate), blotted for 48 hours in 10X SSC onto a Hybond-N membrane (Amersham) and fixed by baking for 2 hours at 80°C. The filters were hybridized overnight at 42°C with ³²P-labelled *Xanx-4* specific probe in 0.5M phosphate buffer pH 7.2 in the presence of 7% SDS and 5mM EDTA. The probe was prepared from 3' specific fragment, by PCR amplification (Primers 5'-3', u-gcataaagagcaggccagcc, d-cgattggttatgtgttcaat). After hybridization, the filters were washed at room temperature in 2XSSC, 0.1%SDS, twice for 15min at 42°C, and then for 15 min at 65°C in 1XSSC, 0.1%SDS. Autoradiographs

were obtained by exposing Fuji super RX films with intensifying screens at – 80°C.

2.6 Protein techniques

2.6.1 Protein expression in oocytes

Oocytes were injected with 10 ng of mRNA. Two hours after injection they were transferred to a dish of Barth's medium containing 10 µCi ³⁵S-methionine. The oocytes were then incubated overnight at 18°C before being harvested for protein extraction.

2.6.2 Protein extraction from oocytes and embryos

Oocytes or embryos were washed in Barth's medium then homogenised in groups of 5 oocytes in 50µl cell-lysis buffer (150 mM NaCl, 1% NP-40, 50 mM Tris-Cl pH8) and 1 mM PMSF. The samples were microcentrifuged at 10,000g for 5 minutes and the middle layer of supernatant was removed. 5µl of supernatant was mixed with 5 µl of protein loading buffer and heated to 95°C for 3 minutes before loading. Samples were stacked at 100V through a 5% acrylamide stacking gel and separated at 200V through a 12% acrylamide resolving gel in tris/glycine running buffer using the BioRad Mini Protean II system. The gel was then either dried and exposed to x-ray film or subjected to western immunoblot analysis.

2.6.3 Sucrose gradient fractionation of oocytes

Oocytes injected with 10ng of mRNA, were allowed to recover for 2 hours at 18°C. Groups of five oocytes were transferred into 50µl Barth's medium

containing 10 μ Ci 35 S-methionine in a microtitre well and incubated overnight at 18°C. Oocytes were enucleated and groups of five nuclei were homogenised in 50 μ l cell lysis buffer at 4°C. The following protocol was conducted at 4°C. The enucleated oocytes were homogenised in groups of five in 50 μ l sucrose T buffer (10% sucrose 150mM NaCl, 1%NP-40, 1mM PMSF) and loaded onto a 3ml 50-20-10% sucrose column. The column was then centrifuged for 30 minutes at 15,000g. The appropriate fractions were removed using a Pasteur pipette; the cytosolic fraction within top 10% layer and the membrane fraction at the 20-50% border. 10 μ l of each sample was mixed with 10 μ l of protein loading buffer and heated to 95°C for 3 minutes before being separated on a 12% acrylamide gel as for oocyte protein extracts. The gel was dried and exposed to X-ray film.

2.6.4 *In vitro* translation

In vitro translation of mRNA was carried out using the Promega rabbit reticulocyte lysate system. Reactions were incubated for 90 minutes at 30°C. 5 μ l of product was mixed with 5 μ l of protein loading buffer and heated to 95°C for 3 minutes before being separated on a 5%-12% acrylamide gel as for oocyte protein extracts.

2.6.5 Western immunoblot analysis.

SDS-PAGE was performed on 5%-12% (w/v) resolving gel using a vertical BioRad minigel apparatus for 1 hour at 20mA. The proteins were transferred to nitrocellulose membrane (Amersham) according to Harlow and Lane, (1988) for

2 hours at 350mA or overnight at 50mA. After transfer the nitrocellulose was incubated for 1 hour at room temperature in TBS-Tween (0.15M NaCl, 10mM Tris-Cl, pH7.4, 0.1% Tween-20) containing 3% (w/v) powdered milk. The blots were then incubated in 1:1000 anti-myc monoclonal antibody (gift from D.Stott, Warwick) in TBS-Tween overnight at room temperature. After washing the blots were incubated in 1:2,000 alkaline phosphatase-conjugated goat anti-mouse (Sigma) in TBS-Tween for 1 hour at room temperature. Immuno-star Detection Kit (BioRad) was used for detection according to manufacturer's recommendations.

2.7 Wholemout immunohistochemistry

Wholemout immunohistochemistry was performed by standard methods (Sambrook et al., 1989, Sive et al., 2000) on MEMFA (0.5M MOPS, pH7.4, 100mM EGTA, 1mM MgSO₄, 4% formaldehyde) fixed embryos. The primary antibodies used were as follows and the concentrations are in brackets. Pronephric tubule specific monoclonal antibody 3G8 (1:1), pronephric duct specific monoclonal antibody 4A6 (1:1) (Vize *et al.*, 1995) and anti-annexin IV monoclonal antibodies BL7B1 (1:1) (Massey et al., 1991a) and AS17 (1:500) (Sato et al., 1997). The secondary antibodies were alkaline phosphatase-conjugated goat anti-mouse (Sigma S-3635) (1:500) and FITC-conjugated goat anti-mouse (Sigma F-2012) (1:100) for 3G8, 4A6 and AS17. For BL7B1 the secondary antibodies used were alkaline phosphatase-conjugated goat anti-rat (Sigma S-3656) (1:500) and FITC-conjugated goat anti-rat (Sigma F-7546) (1:100). BCIP/NBT (Boehringer) or Fast Red TR/Naphthol AS/MX (Sigma) was used for the colour reaction according to manufacturer's recommendations.

2.8 Histology

2.8.1 Acrylamide embedding and cryostat sectioning

Embryos were fixed in MEMFA overnight at 4°C, rinsed in PBS and incubated at 4°C for 5 hours in embedding acrylamide (8.4g acrylamide, 13.4mg bis-acrylamide, 700µl TEMED to 100mls in PBS). The embryos were embedded in acrylamide using 5µl/ml 10% ammonium persulphate to polymerise overnight at 4°C. The acrylamide blocks were frozen in iso-pentane over liquid nitrogen for 5 minutes. The blocks were then allowed to warm to -20°C and sectioned on a cryostat at 12µm. The sections were lifted onto 0.1% gelatin subbed slides (300 bloom), fixed in acetone and mounted in 50% PBS/50% glycerol.

2.8.2 Histological staining

Nuclear staining was carried out using Hoescht stain (33258) at a concentration of 1µg/ml on acrylamide embedded sections for 10 mins at RT. The slides were washed twice in PBS, mounted in glycerol and viewed on a Nikon microscope using a UV filter.

2.9 Embryo manipulations

2.9.1 *In vitro* fertilization of *Xenopus* eggs

Eggs were laid into Barth X (88mM NaCl; 1mM KCl; 24mM NaHCO₃; 15mM Tris-HCl; 0.33mM Ca(NO₃)₂; 0.41mM CaCl₂; 0.8mM MgSO₄ pH7.5) and were

removed into a petri dish for fertilisation. The Barth X was removed from the dish and a testis that had been broken open a little was used to brush over the eggs. 1-2 mls H₂O was then added to the dish and the eggs left to fertilise. After 30-40 minutes embryos were dejellied by removal of the water and addition of 2% (w/v) cysteine pH8. The cysteine was removed after 5-10 minutes and the embryos were washed several times with 1/10 Barth X solution. Embryos were cultured in 1/10 Barth X solution with 10 µg/ml gentamycin at 12-24°C to the required stage.

2.9.2 Micro-injection of embryos

Embryos were microinjected at either the 1-cell stage or into one cell of two at the two-cell stage (left vs right comparisons) or 1-cell of the 32-cell stage embryos (targeted lineage labelling). Injections were performed in 4% Ficoll in Barth X. Quantities of mRNA injected are described for individual mRNAs. Lineage label, when used, was FLDX (Fluorescein Lysine Dextran) at a final concentration of 50ng per embryo. Embryos were allowed to recover overnight and then cultured to the required stage in 1/10 Barth X solution with 10 µg/ml gentamycin.

2.10 Bespoke oligonucleotides for gene expression perturbation

Only technical data is contained in the following methods section. The scheme used to prepare all the constructs in this section are detailed within the introduction to chapter 5.

2.10.1 dsRNA constructs

PCR was performed as follows: 1ng plasmid template DNA was made up to a final volume of 25 µl with reaction mix: 1x PCR buffer, 1.5 mM MgCl₂, 200 µM dNTPs, 1 µM each primer (Table 2.3) and 1 U Taq polymerase. The samples were overlaid with oil. The number of cycles and PCR conditions were:

Step 1. 94°C 20 seconds, 50°C 20 seconds, 72°C 20 seconds – 5 cycles

Step 2. 94°C 20 seconds, 60°C 20 seconds, 72°C 30 seconds – 25 cycles

Step 3. 72°C 5 minutes – 1 cycle

Table 2.3: Primers used for preparation of dsRNA.

| Primer Name | Sequence (5'-3') | Modification & Position |
|-------------|---|-------------------------|
| S1 (T7) | taatacgactcactataggggagcagcaccgtgaatgaag | T7, 491 |
| S2 (T7) | taatacgactcactatagggcccacttcttctcaccggcttc | T7, 616 (complement) |
| L1 (T7) | taatacgactcactataggggatggcagcactcggaactaagg | T7, 1 |
| L2 (T7) | taatacgactcactatagggctcctctgcgctgcgagatg | T7, 365 (complement) |
| L2 (T3) | attaaccctcactaaagggactcctctgcgctgcgagatg | T3, 365 (complement) |
| XEZR1 | taatacgactcactatagggcgtagctaggctagcttagc | T7 |
| XEZR2 | taatacgactcactatagggtagtctagcctagtgtgaag | T7 (complement) |

In vitro transcription was performed with an input of 6µl of PCR reaction using T7 mMESSAGE mMACHINE Kit (Ambion) according to manufacturer's recommendations, using termination and recovery method 1 and resuspending the precipitate in 10µl ddH₂O. The mixture is then treated with 0.5µg/ml RNase A in 300mM NaCl for 30 minutes at 37°C to remove single stranded RNA. The

product was separated on an agarose gel and extracted using Qiagen gel extraction kit. The concentration was determined on an agarose gel and by UV absorbance.

For the single stranded RNA constructs, the PCR was performed using a combination of *Xanx-4/T7* and *Xanx-4/T3* primers. For the *in vitro* transcription T7 RNA polymerase or T3 RNA polymerase was used to transcribe only *Xanx-4/T7* sense or *Xanx-4/T3* antisense RNA. For the sense and antisense not-annealed samples equal amounts of sense and antisense single stranded RNA molecules were mixed thoroughly and snap frozen on dry ice.

For the sense and antisense annealed, equal amounts of single stranded sense and antisense RNA molecules were mixed in annealing buffer (10mM Tris-HCl pH7.4, 0.1mM EDTA) incubated for 10 minutes at 68°C and 37°C for 3-4 hours. The mixture is then treated with 0.5µg/ml RNase A in 300mM NaCl for 30 minutes at 37°C to remove single stranded RNA. The product was separated on an agarose gel and extracted using QIAquick Gel Extraction Kit. Following gel extraction the concentration of the resultant product was determined on an agarose gel and by UV absorbance.

2.10.2 siRNA constructs

The siRNA oligos synthesised by MWG Biotech. (0.2µM synthesis) were deprotected using RNA Deblocking Kit supplied by Cruachem Ltd (Glasgow) according to manufacturer's recommendations. All steps were conducted under ribonuclease free conditions, according to Sambrook et al., 1989. The

oligonucleotide pellet was resuspended in 0.5ml aqueous ammonia (SG 0.88) by vortexing and incubated at 55°C overnight. The sample was cooled, centrifuged at 10,000g for 2 minutes and pelleted by vacuum centrifugation. 500µl acidic buffer (Cruachem Ltd) was added and the pellet was resuspended by sonication in an ultrasonic water bath for 2 minutes and incubated at 25-30°C for 36 hours. To the 500µl acidic solution, 100µl of the neutralising buffer was added, the mixture vortexed for 1 minute and centrifuged at 8000g for 3 minutes. The supernatant was transferred to a fresh microfuge tube and vortexed for 1 minute. Precipitation of the RNA oligo was carried out in 3x analytical grade ethanol at -20°C for 30 minutes and pelleted by centrifugation for 5 minutes at 8,000g. The supernatant was discarded and the pellet dried by vacuum centrifugation. The pellet was then resuspended in ddH₂O and the concentration determined by UV absorbance.

For the double stranded siRNA, equal amounts of single stranded sense and antisense RNA molecules were mixed in annealing buffer (10mM Tris-HCl pH7.4, 0.1mM EDTA), incubated for 10 minutes at 68°C and then 37°C for 3-4 hours. The mixture was then treated with 0.5µg/ml RNase A in 300mM NaCl for 30 minutes at 37°C to remove single stranded RNA. Following phenol/chloroform extraction and ethanol precipitation the concentration of the resultant product was determined by UV absorbance.

2.10.3 Morpholinos

Xanx-4 MO1, *Xanx-4* MO2, *Xsox17 β* (gift from D.Clements) and control Morpholinos were designed and supplied by GeneTools, LLC (Corrallis, OR) (*Xanx-4* MO1: 5'-acccttagttccgagtgtgcatg-3', *Xanx-4* MO2: 5'-tccgagtgtgcatgatgtccacc-3', control MO: 5'-cctcttacctcagttacaattata-3'). The morpholinos were dissolved in ddH₂O to a stock concentration of 10 μ g/ml. 5, 10 or 20ng was injected into one cell stage embryos alone or in combination with mRNA as specified in the text.

Chapter 3: Characterisation of the clone K2

3.1 Introduction

Initial events in kidney organogenesis are not yet fully understood and *Xenopus* provides an ideal vertebrate system to identify and establish the functional role of genes involved in early kidney development. The simplicity of the pronephros coupled with the fact that it displays the same basic organisation and function as the more complex mesonephros and metanephros make this an attractive model to study the earliest events in vertebrate kidney morphogenesis (Vize et al., 1997).

Some of the biological parameters that control pronephros formation have already been established. The temporal specification of all three components of the kidney have been established and all occur between stages 12.5 and 14 (Brennan et al., 1998; Brennan et al., 1999). A molecular map of many of the early markers of the pronephric field and pronephric anlagen is also being built up in order to unravel the molecular control of early kidney induction and patterning. Using a variety of strategies, previous studies have identified more than 30 genes that are expressed in the pronephros (section 1.3). Many of these genes are also expressed in mesonephric and metanephric kidneys in higher vertebrates.

In order to identify novel genes that may be involved in pronephros development, previous members of the research group adopted a subtractive hybridisation strategy that enriches for those genes expressed early in kidney

development (section 1.4). The strategy adopted led to the cloning of K2 cDNA and the analysis of this clone formed the main area of interest of my three-year research work and the basis of my thesis.

A full characterisation is the first fundamental step in the explorational analysis of a novel gene. Certain basic information is required which provides a foundation upon which one can design approaches that will eventually lead to the establishment of the function of the gene in question. Initially nucleic acid sequence information allows database searching and can place a gene within a family whose functions maybe known. Amino acid sequence can then be deduced and by comparison with information collected on databases, protein structure and motif analysis can be derived. To developmental biologists when and where a gene is expressed is the fundamental basis on which further exploration can be based. The normal expression pattern, timing and localisation can often lead to insights into the function of a gene.

The central questions addressed in the following chapter are:

- (1) What is the sequence of the clone K2?
- (2) What is the temporal expression profile during embryonic development?
- (3) What is the spatial expression profile during embryonic development?
- (4) What is the spatial expression profile of the gene in the adult organism?
- (5) What does this information tell us about the gene?

In the course of this study, nucleic acid sequencing was carried out and the deduced amino acid sequence was confirmed. The temporal and spatial

expression patterns both of mRNA and protein in embryos and the mRNA expression pattern by Northern analysis in the adult organism, was established. Finally, this information was analysed in the context of current scientific knowledge and understanding.

3.2 Results

3.2.1 The cDNA clone K2 was identified as *Xenopus laevis annexin IV*

The first step in the analysis of a novel clone is sequencing and database comparisons. Sequencing revealed K2 to be a clone of 1131 nucleotides, containing an in-frame coding sequence confirming identification as *Xenopus laevis annexin IV* (*Xanx-4*), including 50 bases 5'UTR and 118 bases 3'UTR. Conceptual translation of *Xanx-4* yielded a predicted amino acid sequence of 321 amino acids (figure 3.1). Annexin IV (*anx-4*) has been cloned and sequenced in a number of species including plants, fungi, invertebrates and higher and lower vertebrates (section 7.1). Figure 3.2 shows an alignment using DNA Star software of the predicted amino acid sequence of *Xanx-4* against a selection of vertebrate *Anx-4* predicted amino acid sequences available on the database (NCBI GenBank). The alignment shows that *Xanx-4* displays identity with *Anx-4* in other vertebrate species of between 67-74%, with Medaka killifish being the least similar at 67% and bovine annexin IV being the most similar at 74%. Analysis of the predicted amino acid (aa) sequence using motif analysis software (Prosite) confirmed that *Xanx-4* contained the archetypal conserved C-terminal annexin domain (figure 3.3) previously identified (Raynal and Pollard, 1994). The N-terminal region (aa 1-32) contains the protein kinase C phosphorylation

Figure 3.1

Xenopus laevis annexin 4 nucleotide sequence and deduced amino acid sequence.

| | | | | | | | | | | | | | | | | | | | |
|---|-----|-----|-----|-----|-----|-----|-----|-----|-----|-----|-----|-----|-----|-----|-----|-----|-----|------|----|
| CCGCAGCCGACATCTGCTTAGAAATTCTCTGCTTCACAGTTGGTGGACATC | | | | | | | | | | | | | | ATG | GCA | GCA | CTC | GGA | 66 |
| | | | | | | | | | | | | | | M | A | A | L | G | 5 |
| ACT | AAG | GGT | ACA | ATT | AAA | CCC | TAC | CCC | AAT | TTC | AAT | GCA | GCA | GAT | GAT | GTG | CAG | 120 | |
| T | K | G | T | I | K | P | Y | P | N | F | N | A | A | D | D | V | Q | 23 | |
| AAG | CTG | AGG | AAC | GCC | ATG | AAA | GGA | GCA | GGC | ACC | GAT | GAA | GAT | GCT | GTC | ATT | GAC | 174 | |
| K | L | R | N | A | M | K | G | A | G | T | D | E | D | A | V | I | D | 41 | |
| GTC | ATT | GCA | AAC | AGG | ACT | CTT | TCT | CAG | CGC | CAG | GAA | ATC | AAG | ACT | GCT | TAT | AAA | 228 | |
| V | I | A | N | R | T | L | S | Q | R | Q | E | I | K | T | A | Y | K | 59 | |
| ACC | ACT | GTT | GGA | AAA | GAT | CTT | GAT | GAT | GAT | TTA | AAA | TCC | GAA | CTG | ACA | GGG | AAC | 282 | |
| T | T | V | G | K | D | L | D | D | D | L | K | S | E | L | T | G | N | 77 | |
| TTT | GAA | AAA | GTC | ATC | CTG | GGA | CTT | ATA | ACC | TCA | TCC | ACT | CTC | TAT | GAT | GTG | GAG | 336 | |
| F | E | K | V | I | L | G | L | I | T | S | S | T | L | Y | D | V | E | 95 | |
| GAA | CTG | AAA | AAA | GCC | ATG | AAG | GGT | GCA | GGG | ACA | GAC | GAG | GGC | TGT | TTG | ATT | GAG | 390 | |
| E | L | K | K | A | M | K | G | A | G | T | D | E | G | C | L | I | E | 113 | |
| ATT | TTG | GCA | TCT | CGC | AGC | GCA | GAG | GAG | ATC | AAG | AAC | ATA | AAT | ATC | ACC | TAC | AAA | 444 | |
| I | L | A | S | R | S | A | E | E | I | K | N | I | N | I | T | Y | K | 131 | |
| ATA | AAA | TAT | GGT | AAA | TCT | CTG | GAG | GAC | GAT | ATT | TGC | TCA | GAC | ACG | TCT | TTC | ATG | 498 | |
| I | K | Y | G | K | S | L | E | D | D | I | C | S | D | T | S | F | M | 149 | |
| TTC | CAG | AGA | GTT | CTG | GTA | TCT | TTG | GCT | GCT | GGT | GGG | AGA | GAC | CAG | AGC | AGC | ACC | 552 | |
| F | Q | R | V | L | V | S | L | A | A | G | G | R | D | Q | S | S | T | 167 | |
| GTG | AAT | GAA | GAC | CTT | GCA | AAA | CAA | GAT | GCC | AAT | GAC | CTA | TAT | GAA | GCC | GGT | GAG | 606 | |
| V | N | E | D | L | A | K | Q | D | A | N | D | L | Y | E | A | G | E | 185 | |
| AAG | AAG | TGG | GGG | ACC | GAT | GAG | GTG | AAA | TTC | CTG | ACT | ATC | CTT | TGC | AGC | AGA | AAC | 660 | |
| K | K | W | G | T | D | E | V | K | F | L | T | I | L | C | S | R | N | 203 | |
| CGG | AAC | CAC | TTA | CTG | AAA | GTT | TTT | GAA | GAG | TAC | AAA | AAG | ATT | GCA | AAG | AAA | GAT | 714 | |
| R | N | H | L | L | K | V | F | E | E | Y | K | K | I | A | K | K | D | 221 | |
| CTT | GAG | GCC | AGT | ATA | AAA | TCT | GAA | ATG | TCG | GGA | CAC | TTA | GAA | GAT | TCT | CTT | TTG | 768 | |
| L | E | A | S | I | K | S | E | M | S | G | H | L | E | D | S | L | L | 239 | |
| GCA | ATC | GTG | AAA | TGC | ATA | AAG | AGC | AGG | CCA | GCC | TAC | TTT | GCA | GAA | CGA | TTG | TAT | 822 | |
| A | I | V | K | C | I | K | S | R | P | A | Y | F | A | E | R | L | Y | 257 | |
| AAA | TCT | ATG | AAG | GGT | CTG | GGG | ACA | GAC | GAT | AAA | ACT | CTG | ATC | AGA | GTT | ATG | GTT | 876 | |
| K | S | M | K | G | L | G | T | D | D | K | T | L | I | R | V | M | V | 275 | |
| TCT | CGT | TGT | GAA | ATT | GAC | ATG | CTG | GAA | ATC | CGC | TGC | GAG | TTC | AAG | AAG | ATG | TAT | 930 | |
| S | R | C | E | I | D | M | L | E | I | R | C | E | F | K | K | M | Y | 293 | |
| GGC | AAA | TCT | CTG | CAT | TCA | TTT | ATT | AAG | GGT | GAC | TGC | TCG | GGA | GAT | TAC | AGG | AAG | 984 | |
| G | K | S | L | H | S | F | I | K | G | D | C | S | G | D | Y | R | K | 311 | |
| GTG | CTC | TTG | AAA | CTT | TGC | GGA | GGG | GAA | GAC | TAA | GTA | ACA | TAG | CCT | TTC | TGT | GTG | 1038 | |
| V | L | L | K | L | C | G | G | E | D | * | | | | | | | | 321 | |
| TCC | AAG | AAA | AGT | CTG | TTG | TGT | CTA | ATT | GAA | CAC | ATA | ACC | AAT | GCA | AAA | TAA | AAA | 1092 | |
| CCT | TCT | GAT | GCC | TTT | TTT | AAA | AAA | AAA | AAA | AAA | AAA | A | | | | | | 1129 | |

Figure 3.1: *Xenopus laevis* annexin 4 nucleotide sequence and deduced amino acid sequence. Nucleotide sequence of *Xanx-4* (1131 nucleotides) including 50 bases 5'UTR and 118 bases 3'UTR and below the predicted amino acid sequence (321 aa) performed using DNA Star software.

Figure 3.2

| Xanx-4 | 1 - 321 | (321 aa) | Homology |
|--------|---------|----------|----------|
| Human | 1 - 321 | (321 aa) | 72% |
| Rat | 1 - 319 | (319 aa) | 72% |
| Mouse | 1 - 319 | (319 aa) | 71% |
| Cow | 1 - 319 | (319 aa) | 74% |
| Medaka | 1 - 320 | (320 aa) | 67% |

Xenopus 1) maalgtkgtikpypnfnaaddvqklrnamkgagtdedavidvianrtlsqrqeiktaykt
Human 1) ..matkg..v.aasg...me.a.t..k....l.....i.s.l.y.nta.....r....s
Rat 1) .etk.--..v.aasg...te.a.v..k....l.....i.g.l.c.nta.....r....s
Mouse 1) .e.k.--..v.aasg...te.a.t..k....l.....i.gil.y.nta.....rs...s
Cow 1) ...k.--..v.aasg....e.a.t..k....l.....i.n.l.y.sta.....r.....
Medaka 1) ...i.nr..vteasg..pd..a....e.....a.i.k.l.h..ia...r..l...q

(61) tvgkdldddlkseItgnfekvilglitsstlydveelkkamkgagtddegclieilasrsa
(61) .i.r..i.....s....q..v.mm.ptv....q..rr.....tp
(59) .i.r..le.....ss...q....mm.ptv....q..rr.....np
(59) .i.r..ie.....ss...q....m.ptv....q..rr.....tp
(59) .i.r..m.....s....q....mm.ptv....q.vr.....tp
(61) s.....ae..s...s.h.qs.v...lmpapv..ay...a.....e.a...d.....n

(121) eeikninitykikygksleddicsdtsfmfqrvlvslaaggrdqsstvnedlakqdandl
(121) ...rr.sq..qqq..r.....r.....s.....egnyllda.vr...q..
(119) ...rr..q..qqq..r...e.....t.....egnyllda.vr...q..
(119) ...rr..q..qqq..r...e.....f.s.a...egnyllda.m....qe..
(119) ...rr..q..qlq..r.....r.....s.....e.nyllda.mr...q..
(121) s.mna..ev..ke...t...av.g...g.....lta...e.dk.d.aq.vk..k.i

(181) yeagekkwgtdevkfltilcsrnrrnhllkvfeeykkiakkdleasiksemsglhedslla
(181)v.....h..d...r.sq..i.q.....t..sf..a...
(179)r.....s.....h..d...r.sq..i.q.....t..sf..a...
(179)r.....s.....h..d...r.sq..i.q.....t..sf..a...
(179)v.....h..dk..r..q..i.q.....t..sf..a...
(181) f....ar.....v..v.....r..d.....s.r.i.d...r....s...vf..

(241) ivkciksrpayfaerlyksmkglgtddktlirvmvsrceidmleircefkkmygkslhsf
(241)mrnks.....k.....n.....a.....d..ah..rl....y..
(239)mrnk.....s.....p.....d.pan..rv....y..
(239)mr.k.s.....n.....a.....d..as..rl....y..
(239)mrnks.....d.....a.....d..an..rl....y..
(241)lr.k..f.....t.sv...i....a.....d.keh.l.t.....

(301) ikgdcsgdyrkvlklcgged
(301)t.....v....d.
(299)t.....i....d.
(299)t.....i....d.
(299)t.....i....d.
(301)t.....i.e.....-

Figure 3.2: Predicted amino acid sequence for *Xenopus laevis* annexin IV aligned against deduced amino acid sequences of annexin IV proteins identified in other vertebrate species. The alignment was performed using DNA Star software with sequences retrieved from NCBI Genbank database. Stops indicate identity or conserved substitutions, hyphens indicate missing residues.

Figure 3.3

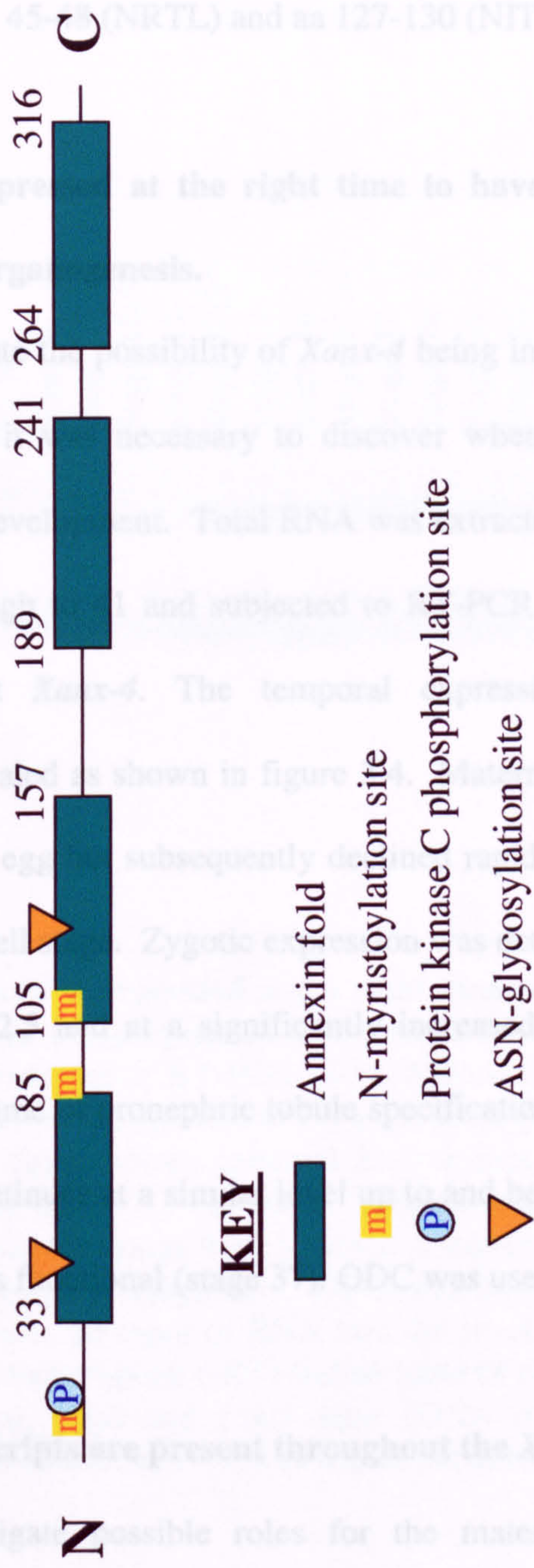


Figure 3.3: Motif diagram for *Xenopus laevis* annexin 4. Using Prosite analysis software the deduced amino acid sequence of *Xenopus laevis* annexin 4 was analysed for conserved motifs. The N-terminal domain contained protein kinase C phosphorylation site and N-myristoylation site. The C-terminal was found to comprise of a four-fold repeat annexin fold region, including ASN-glycosylation and N-myristoylation sites.

site threonine 9 (TIK) and an N-myristoylation site at Gly5 (GTKGTI). The C-terminal annexin fold region (aa 33-316) is composed of four highly conserved 70 amino acid repeats (aa 33-85, 105-157, 189-241, 264-316), containing the Ca²⁺ and phospholipid-binding sites. N-myristoylation sites were identified at aa 84-89 (GLITSS) and aa 105-110 (GTDEGC) and ASN-glycosylation sites were identified at aa 45-48 (NRTL) and aa 127-130 (NITY).

3.2.2 *Xanx-4* is expressed at the right time to have a role in pronephric specification and organogenesis.

In order to investigate the possibility of *Xanx-4* being involved in organogenesis of the pronephros, it was necessary to discover when the gene is expressed during embryonic development. Total RNA was extracted from egg and embryo stages 32 cell through to 41 and subjected to RT-PCR using primers designed specifically against *Xanx-4*. The temporal expression profile of *Xanx-4* transcripts was revealed as shown in figure 3.4. Maternal expression of *Xanx-4* was detected in the egg but subsequently declined rapidly and was substantially reduced by the 32-cell stage. Zygotic expression was detected at a very low level between stages 9-12.5 and at a significantly increased level at stage 13. This coincides with the time of pronephric tubule specification (Brennan *et al.*, 1998). Expression then continues at a similar level up to and beyond the stage when the pronephros becomes functional (stage 37). ODC was used as a loading control.

3.2.3 *Xanx-4* transcripts are present throughout the *Xenopus laevis* oocyte.

In order to investigate possible roles for the maternal *Xanx-4* transcripts, localisation of *Xanx-4* transcripts in oocytes was determined. Oocytes were snap

Figure 3.4

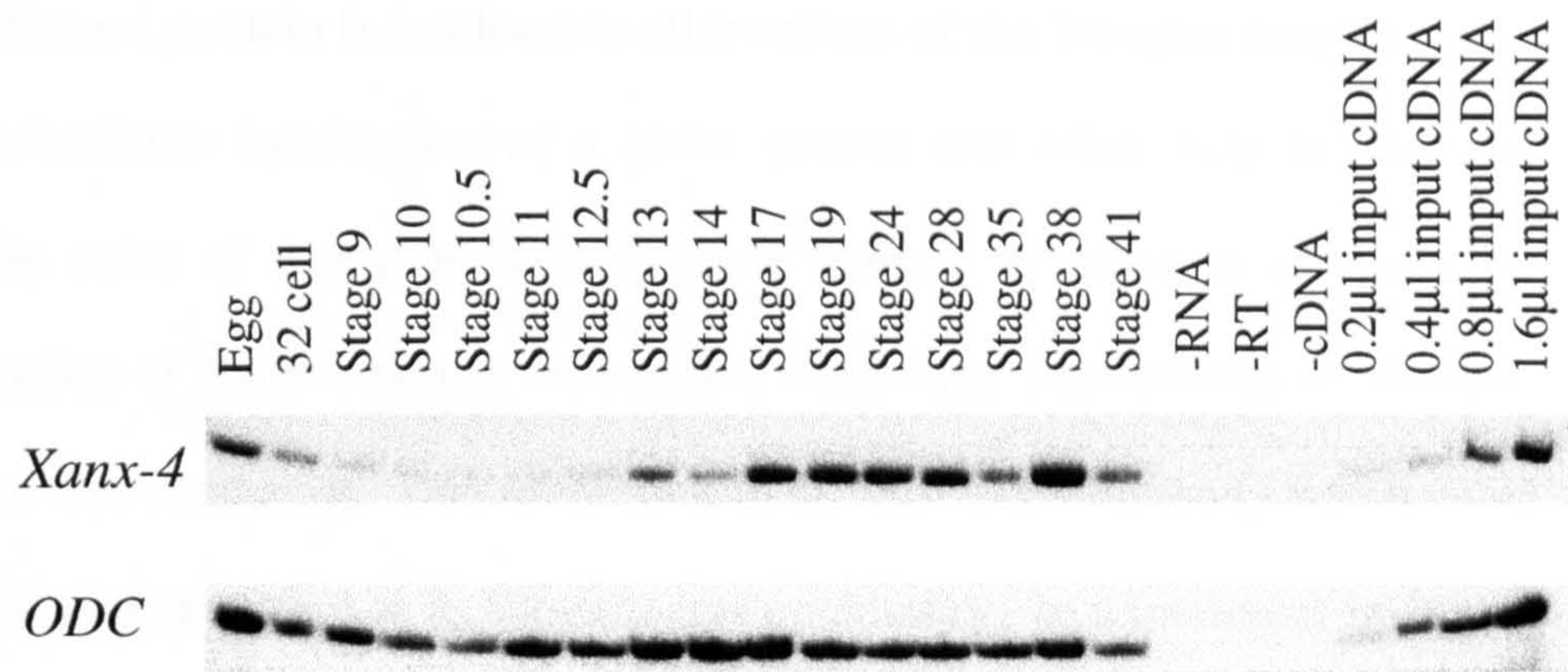


Figure 3.4: *Xanx-4* is expressed at the right time to have a role in pronephric specification and organogenesis. The temporal expression profile of *Xanx-4* transcripts was revealed by RT-PCR. Total RNA extracts from egg and stages 32 cell through to 41 were subjected to RT-PCR using primers designed specifically to *Xanx-4*. The figure shows maternal *Xanx-4* expression in the egg, which is barely detectable by the 32 cell stage. Zygotic transcription was detected at a very low level between stage 9-12.5, which is substantially increased by stage 13 and persists through to stage 41. *ODC* was used as a loading control. The controls used were, no input of RNA into the reverse transcription (-RNA), no input of reverse transcriptase (-RT) and no input of cDNA into the PCR reaction. The 0.2μl, 0.4μl, 0.8μl and 1.6μl input cDNA into the PCR reaction were included so as to ensure the PCR was within the linear range.

frozen on dry ice and manually dissected into animal and vegetal poles. Groups of five poles and whole oocytes (in duplicate) were subjected to RT-PCR using *Xanx-4* specific primers (figure 3.5). It was found that *Xanx-4* transcripts are present in virtually equal amounts in the animal and vegetal poles of the *Xenopus* oocyte. No specific localisation of *Xanx-4* transcripts in the oocyte was therefore observed. ODC was used as a loading control.

3.2.4 *Xanx-4* protein is localised to all fractions of the *Xenopus* oocytes.

The subcellular localisation of a given protein can often help to elucidate possible roles of that protein in a given tissue. In order to ascertain the localisation of *Xanx-4* protein in oocytes, subcellular fractionation of *Xenopus* oocytes was conducted. Due to the lack of an anti-Anx-4 antibody which could be used to detect *Xanx-4* in Western immunoblotting, an experiment involving labelling protein translated from exogenous injected *Xanx-4* mRNA was designed.

Oocytes were injected with *Xanx-4* mRNA, incubated overnight in 35S-methionine. Groups of five oocytes were enucleated, and the remaining tissues subjected to sucrose gradient fractionation. The sucrose layers were selected so as to allow clean separation of cytosolic and membrane fractions. Samples taken from the sucrose gradient along with the appropriate nuclear fraction (equal relative amounts) and a sample of incubation medium, were denatured at 95°C and subjected to SDS-PAGE and autoradiography. Notwithstanding the assumption that protein translated from exogenous injected mRNA will localise to the same region as endogenous protein, the experiment included carefully

Figure 3.5

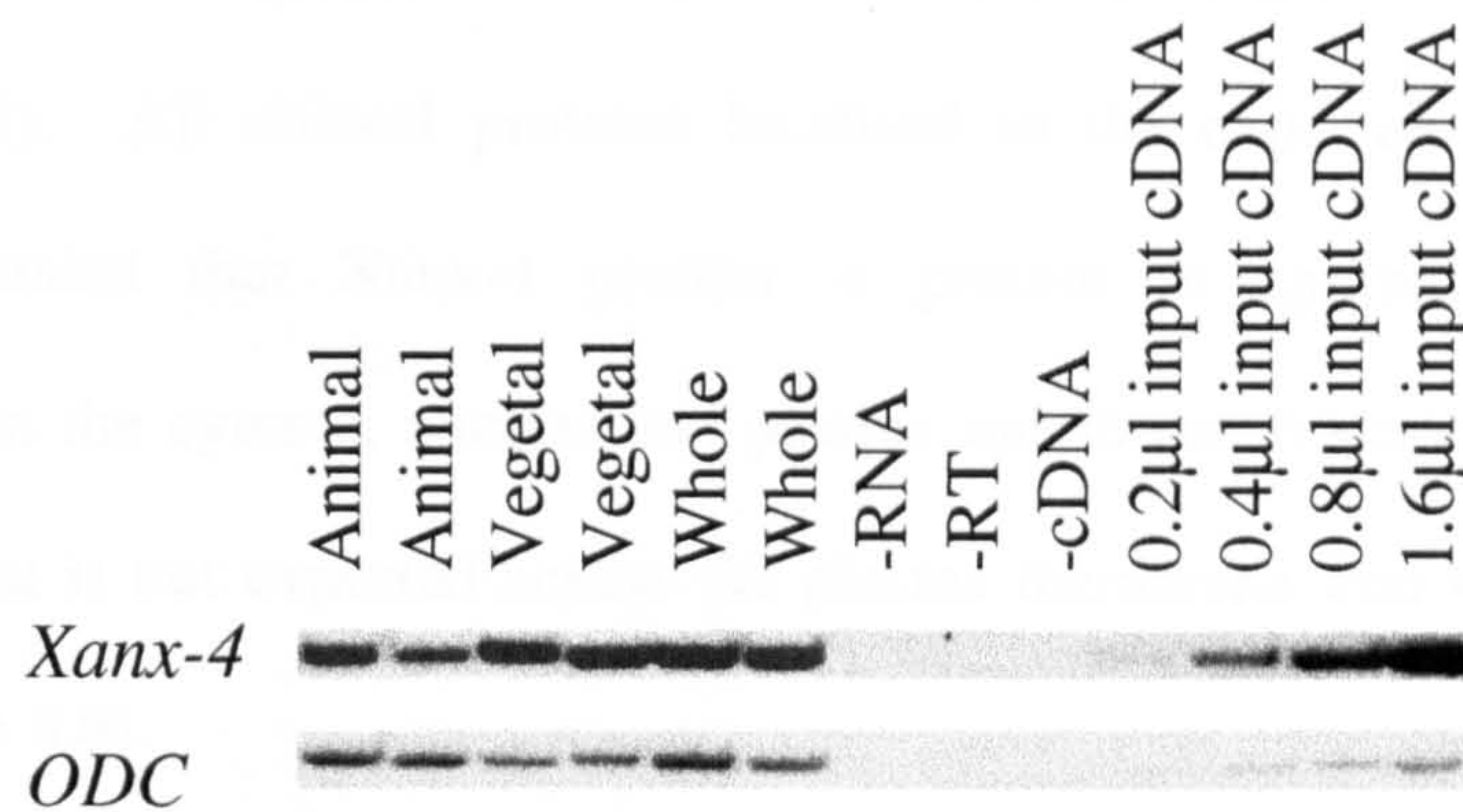


Figure 3.5: *Xanx-4* transcripts are present throughout the *Xenopus laevis* oocyte. Oocytes were manually dissected into animal and vegetal poles and duplicate samples were subjected to RT-PCR using *Xanx-4* specific primers. ODC was used as a loading control. *Xanx-4* transcripts were detected at equal levels in both the animal and vegetal pole samples. The controls used were, no input of RNA into the reverse transcription (-RNA), no input of reverse transcriptase (-RT) and no input of cDNA into the PCR reaction. The 0.2µl, 0.4µl, 0.8µl and 1.6µl input cDNA into the PCR reaction were included so as to ensure the PCR was within the linear range.

chosen controls. mRNA, prepared from a range of clones with known protein size and specific localisation in oocytes, was injected into oocytes which were then analysed in the same way. The controls used were as follows; Xmad2, 58kDa, predominantly cytosolic, small amount nuclear membrane (Graff et al., 1996); Xsox17 β , doublet 50-54kDa, nuclear (Hudson et al., 1997); Δ 1XAR1 (truncated activin receptor), 30kDa, plasma membrane (Hemmati-Brivanlou & Melton 1992). All control proteins localised to the expected fraction. The analysis revealed that Xanx-4 protein is present in approximately equal proportions in the cytosol, nuclear and plasma membrane fractions, throughout the oocyte but is not exported across the plasma membrane into the incubation media (figure 3.6).

3.2.5 Expression of *Xanx4* transcripts is restricted to the otic vesicle and to the pronephric tubules in *Xenopus laevis* embryos

To test whether the active transcription detected in the stage series RT-PCR experiment (figure 3.4) was localised to particular tissues in the developing embryo, wholemount *in situ* hybridisation was carried out on a range of stages of albino *Xenopus laevis* embryos. The protocol was performed using a DIG labelled *Xanx-4* antisense probe prepared from full-length cDNA clone in pGEM-T Easy (Appendix 1). For the antisense probe the construct was linearised with *NcoI* and transcribed with Sp6 RNA polymerase and for sense control probe the construct was linearised with *Sall* and transcribed with T7 RNA polymerase. *Xanx-4* transcripts were detected in the pronephric anlagen throughout organogenesis.

Figure 3.6

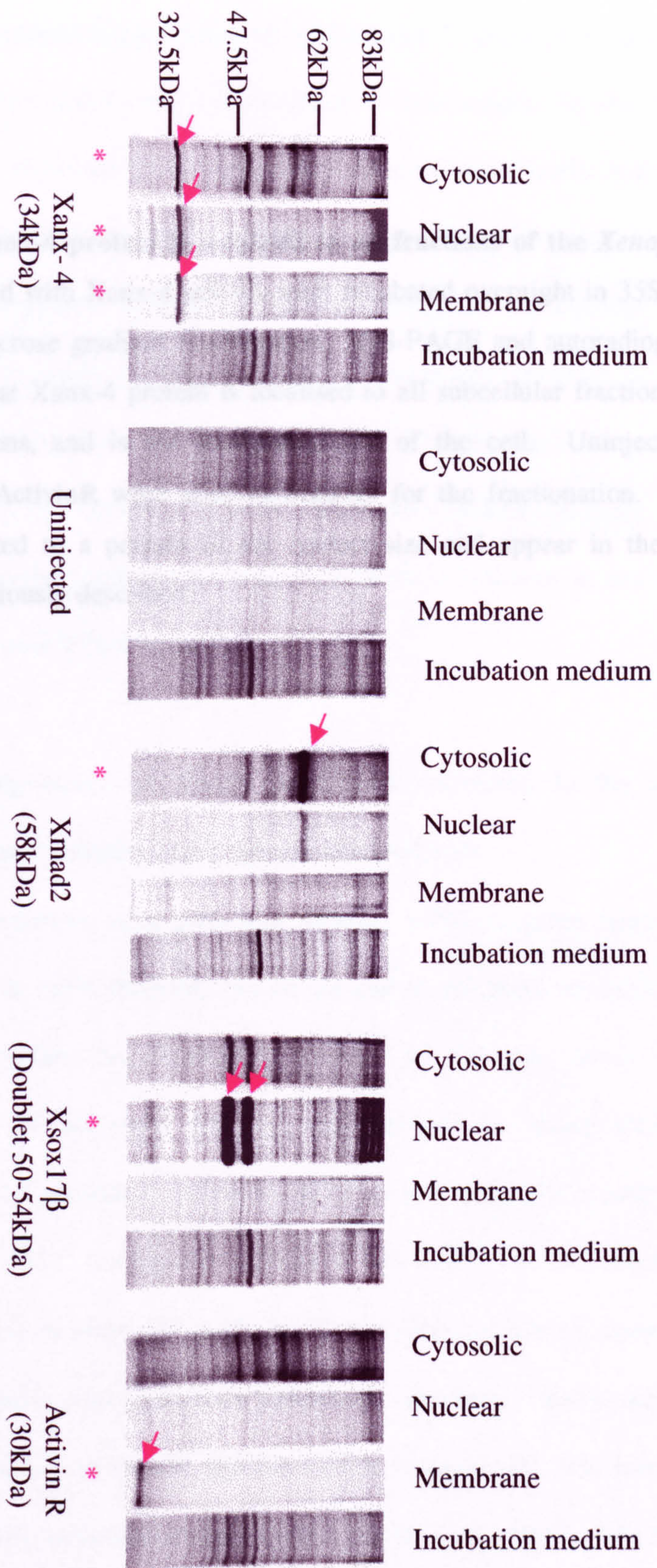


Figure 3.6: Xanx-4 protein is localised to all fractions of the *Xenopus* oocytes. Oocytes injected with Xanx-4 mRNA were incubated overnight in 35S-methionine, subjected to sucrose gradient fractionation, SDS-PAGE and autoradiography. The results show that Xanx-4 protein is localised to all subcellular fractions isolated in equal proportions, and is not transported out of the cell. Uninjected, Xmad2, Xsox17 β and ActivinR were used as controls for the fractionation. The control mRNA translated to a protein of the correct size and appear in the appropriate fraction as previously described.

At stage 26, *Xanx-4* transcripts were detected in the pronephric anlagen and in the otic vesicle (figure 3.7A, O: otic vesicle, P: pronephric anlagen). Expression in the otic vesicle was not detected in later stages. As the pronephric tubules continue to develop transcripts were detected specifically in the tubules, at stage 36/37 (figure 3.7C) around the time when the pronephros becomes functional, and through and beyond maturation (elongation and coiling) of the pronephric tubules to stage 42 (Figure 3.7D). Transverse sections of stage 26 embryo (figure 3.7F) shows otic vesicle staining (O: otic vesicle), and stage 42 embryo (figure 3.7G) revealed specific pronephric tubule staining. A sense *Xanx-4* control probe produced no staining pattern in embryos at any stage (figure 3.7B stage 26 and 3.7E stage 42).

3.2.6 Expression of *Xanx4* protein is restricted to the apical surface of pronephric tubules in *Xenopus laevis* embryos

The distribution of a particular protein, within a given tissue, will often give insights as to its function. In an attempt to establish the localisation of *Xanx-4* protein within the developing embryo of *Xenopus laevis* wholemount anti-annexin IV antibody staining was carried out using alkaline phosphatase conjugated secondary and NBT-BCIP substrate for the colour reaction. For the sections FITC conjugated secondary was used. In the absence of a *Xenopus laevis* anti-annexin IV antibody, two antibodies raised against annexin IV in other species, and previously published, were used. Firstly, monoclonal antibody AS17, raised in mouse against human annexin IV, has been shown to react specifically with human annexin IV (Sato et al., 1997). AS17 cross reacts with *Xanx-4* and was used in wholemount immunohistology on *Xenopus laevis*

Figure 3.7

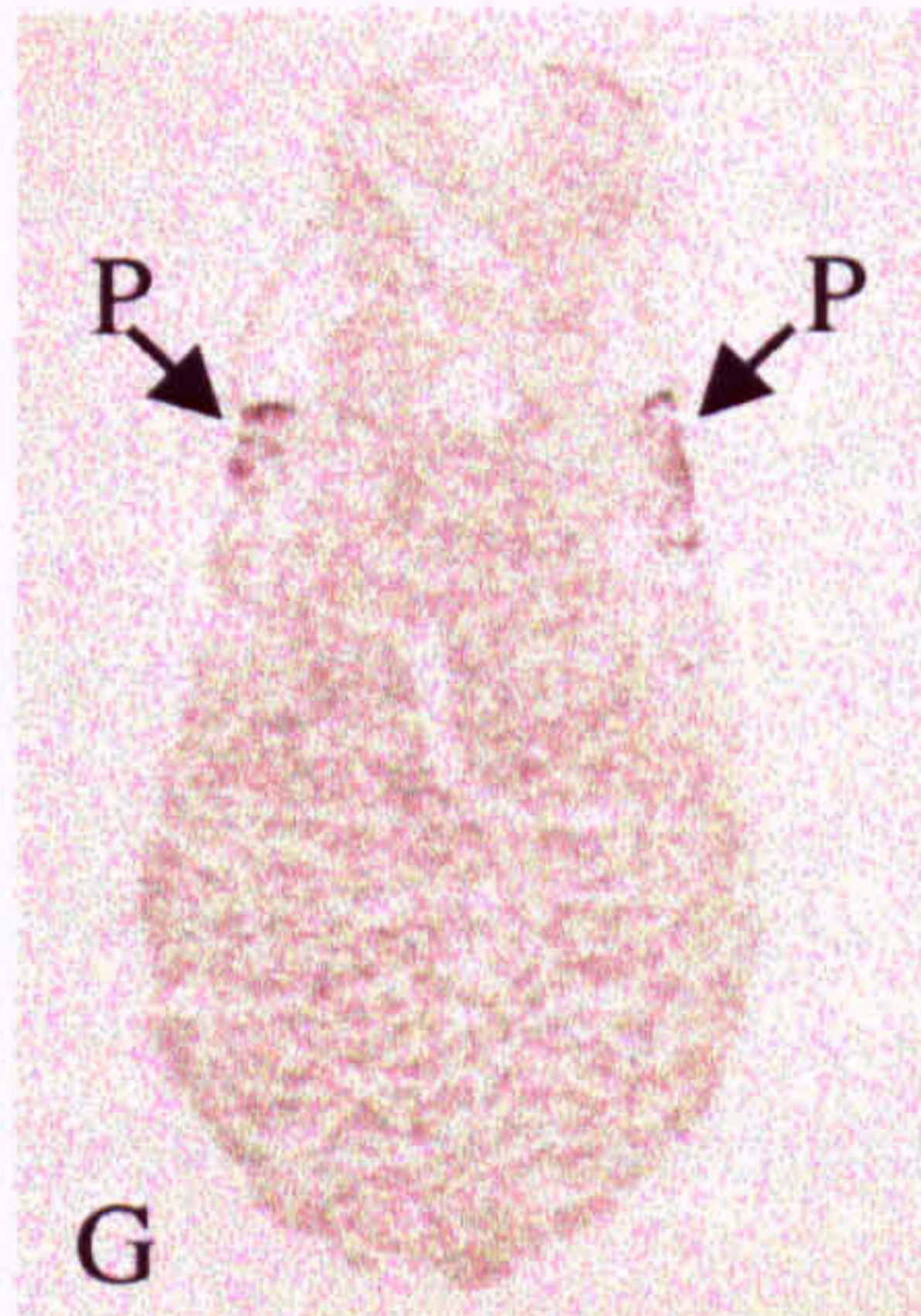
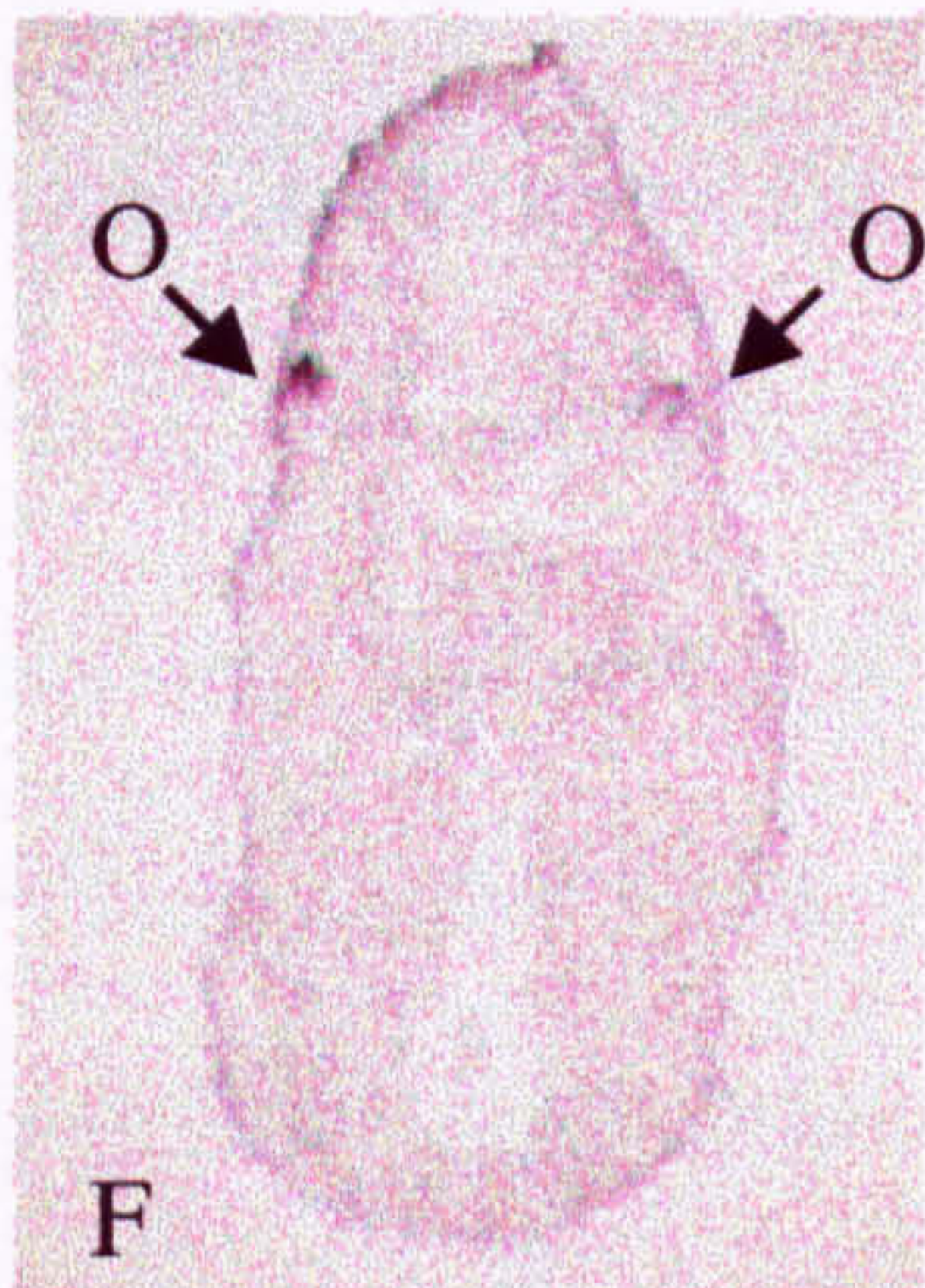
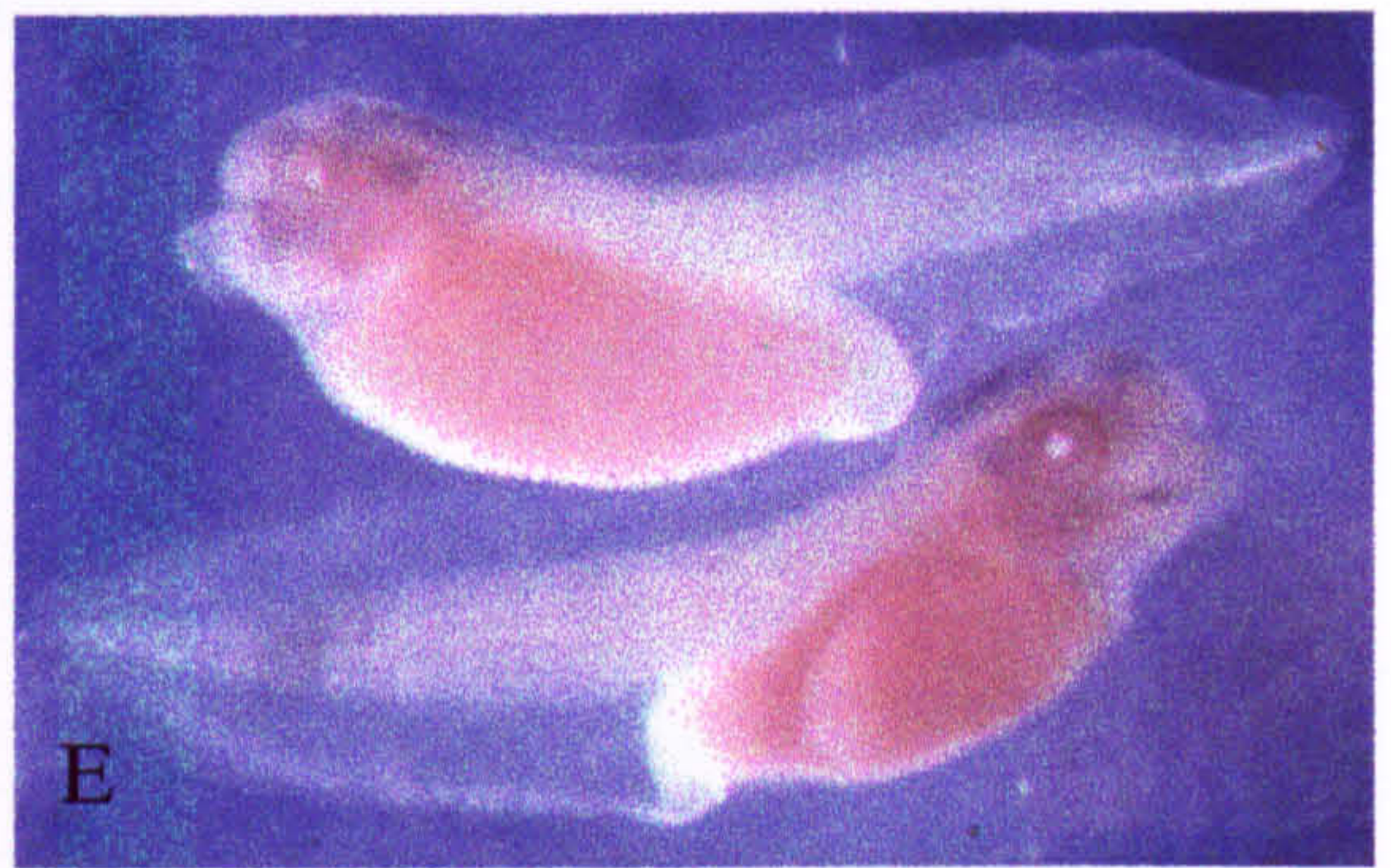
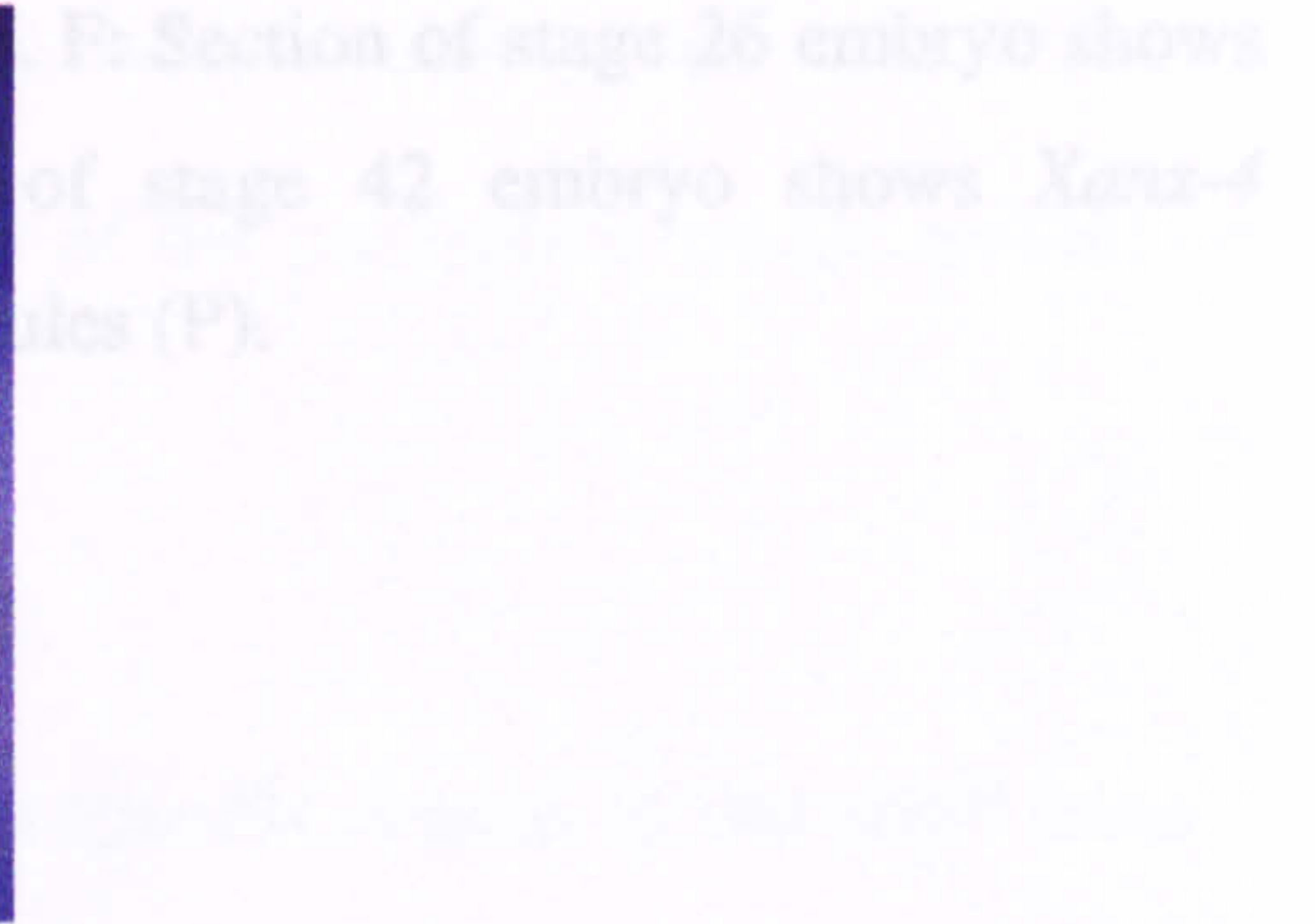
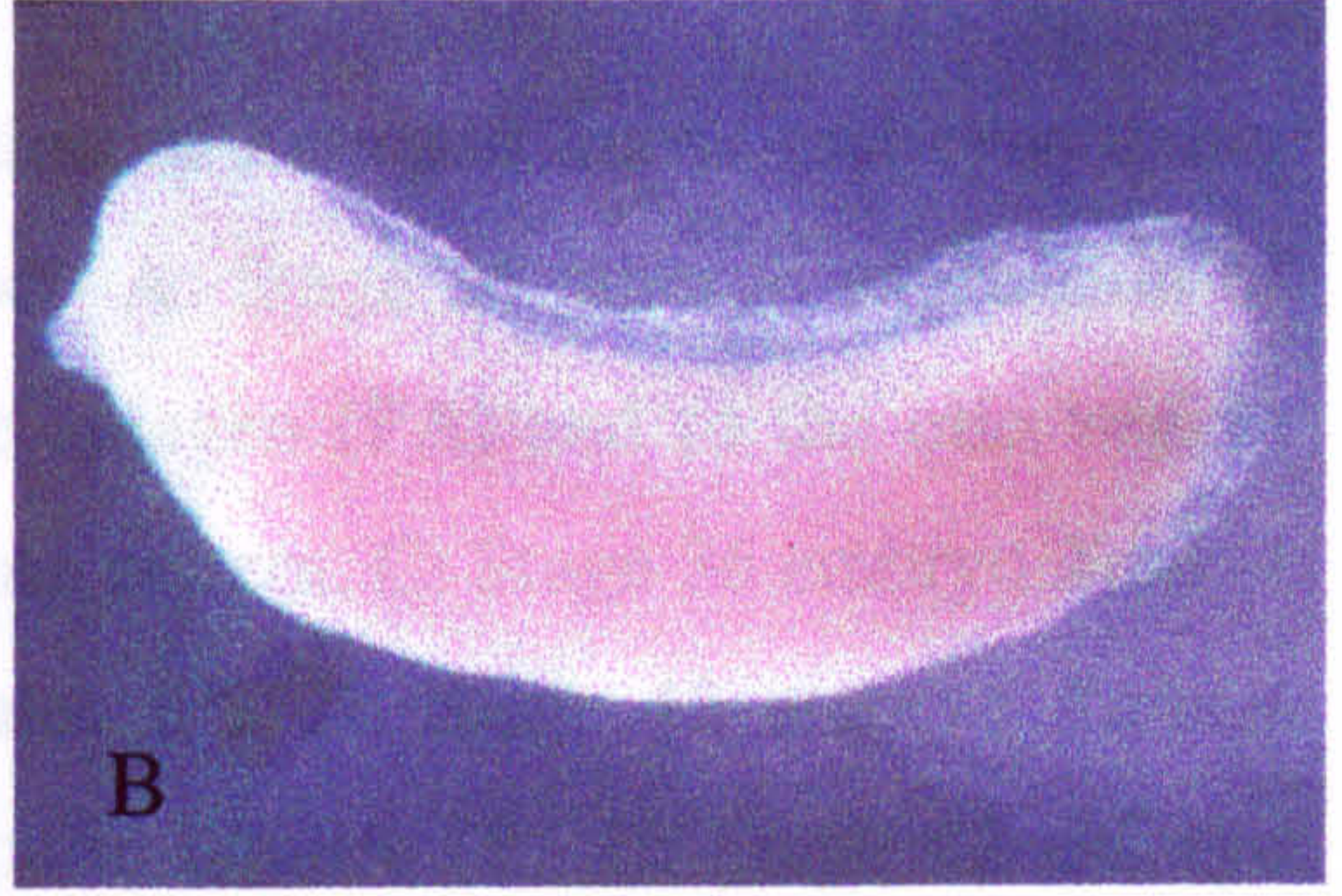
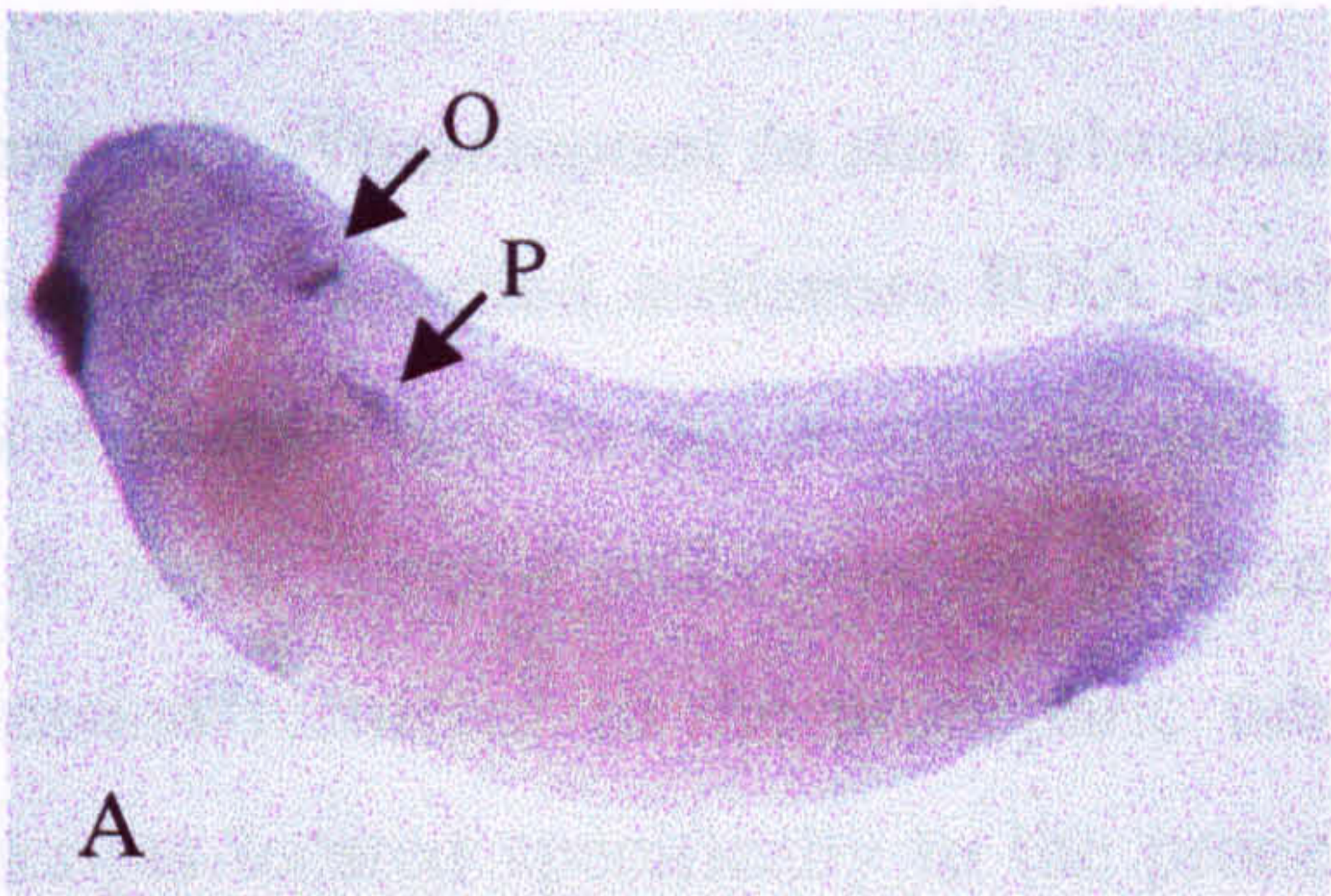


Figure 3.7: Wholemount *in situ* hybridisation of *Xenopus laevis* embryos using *Xanx-4* DIG labelled antisense RNA probe. A: Stage 26 embryo expression of *Xanx-4* is restricted to the pronephric tubule anlagen (PA) and to the otic vesicle (O). B: Sense *Xanx-4* probe control, no staining pattern. C: Stage 36 embryo *Xanx-4* expression restricted to the pronephric tubules (P). D: Stage 42 embryo *Xanx-4* transcripts located specifically to the pronephric tubules (P). E: Stage 42 embryo sense probe control shows no staining pattern. F: Section of stage 26 embryo shows otic vesicle staining (O) and G: Section of stage 42 embryo shows *Xanx-4* transcripts are restricted to the pronephric tubules (P).

embryos. The staining pattern shows Xanx-4 localisation to the pronephric tubules from stage 38 (figure 3.8A) and at stage 40 (figure 3.9B & 3.8C). Some staining is also seen in the proctodeum at these stages with the AS17 antibody. Secondly, monoclonal anti-annexin IV antibody BL7B1, raised in rat against rabbit annexin-4 has been shown to react specifically with rabbit annexin IV (Massey et al., 1991a), and cross-reacts with the Xanx-4 protein. The staining pattern observed, with BL7B1 antibody, indicates that Xanx-4 protein is specifically localised to the pronephric tubules of *Xenopus laevis* embryos at stage 40 (Figure 3.8D & 3.8E). BL7B1 staining of transverse sections of stage 40 embryos reveals Xanx-4 is located on the luminal side of the tubule and is probably confined to the apical membrane of the pronephric tubule epithelium (Figure 3.8F).

3.2.7 Expression of *Xanx-4* is restricted to specific organs in the adult frog.

To further investigate the dynamic developmental expression profile of *Xanx-4*, northern blot analysis of RNA isolated from dissected adult organs was carried out (Figure 3.9). RNA was isolated from dissected adult organs using Trizol reagent. Approximately 30µg of RNA was loaded onto a formamide/agarose gel and separated according to manufacturer's recommendations (figure 3.9A). The RNA was transferred onto nitrocellulose membrane by capillary action in 10x SSC buffer over 48 hrs. After baking the membranes were probed using a ³²PαGTP labelled 3' *Xanx-4* probe. The membranes were washed and exposed to X-ray film. Transcripts of approximately 1600 bases were detected at the highest level in the gall bladder, duodenum and ileum. Lower levels were detected in the lung, kidney, ovary, testis, stomach, rectum, bladder, spleen and pancreas

Figure 3.8

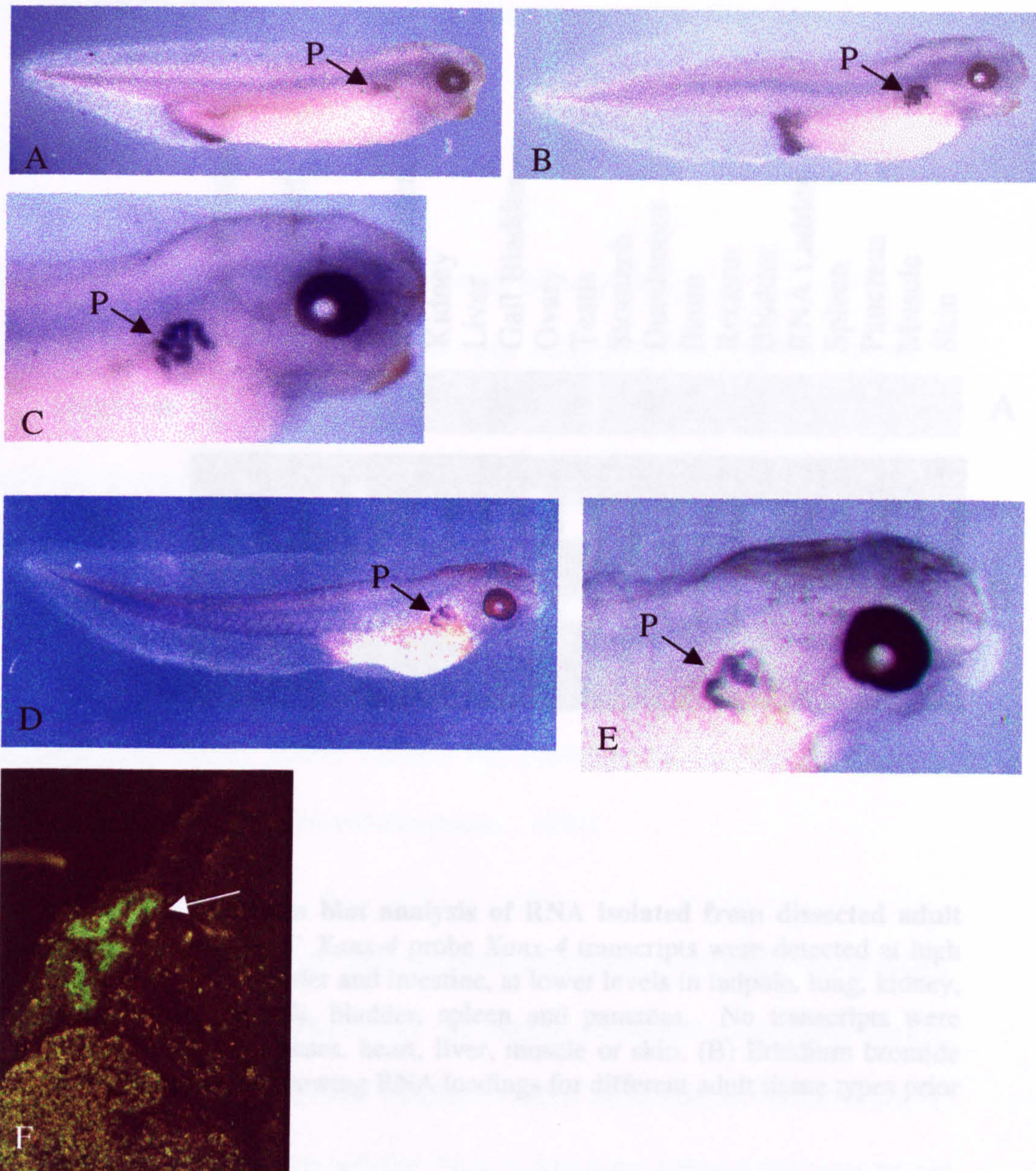


Figure 3.8: Wholemount anti-annexin IV antibody staining on *Xenopus laevis* embryos. Using anti-annexin IV antibody AS17, Xanx-4 protein is localised to the pronephric tubules (P) and the proctodeum at stage 37 (figure 3.8A) and stage 40 (figure 3.8B & 3.8C). Wholemount immunohistochemistry using anti-annexin IV antibody BL7B1 localises Xanx-4 protein specifically to the pronephric tubules (P) at stage 42 (figure 3.8D & 3.8E). Cryostat section of stage 42 *Xenopus laevis* embryo using antibody BL7B1 and FITC secondary localises Xanx-4 protein to the luminal surface of the pronephric tubule epithelium (figure 3.8F).

Figure 3.9

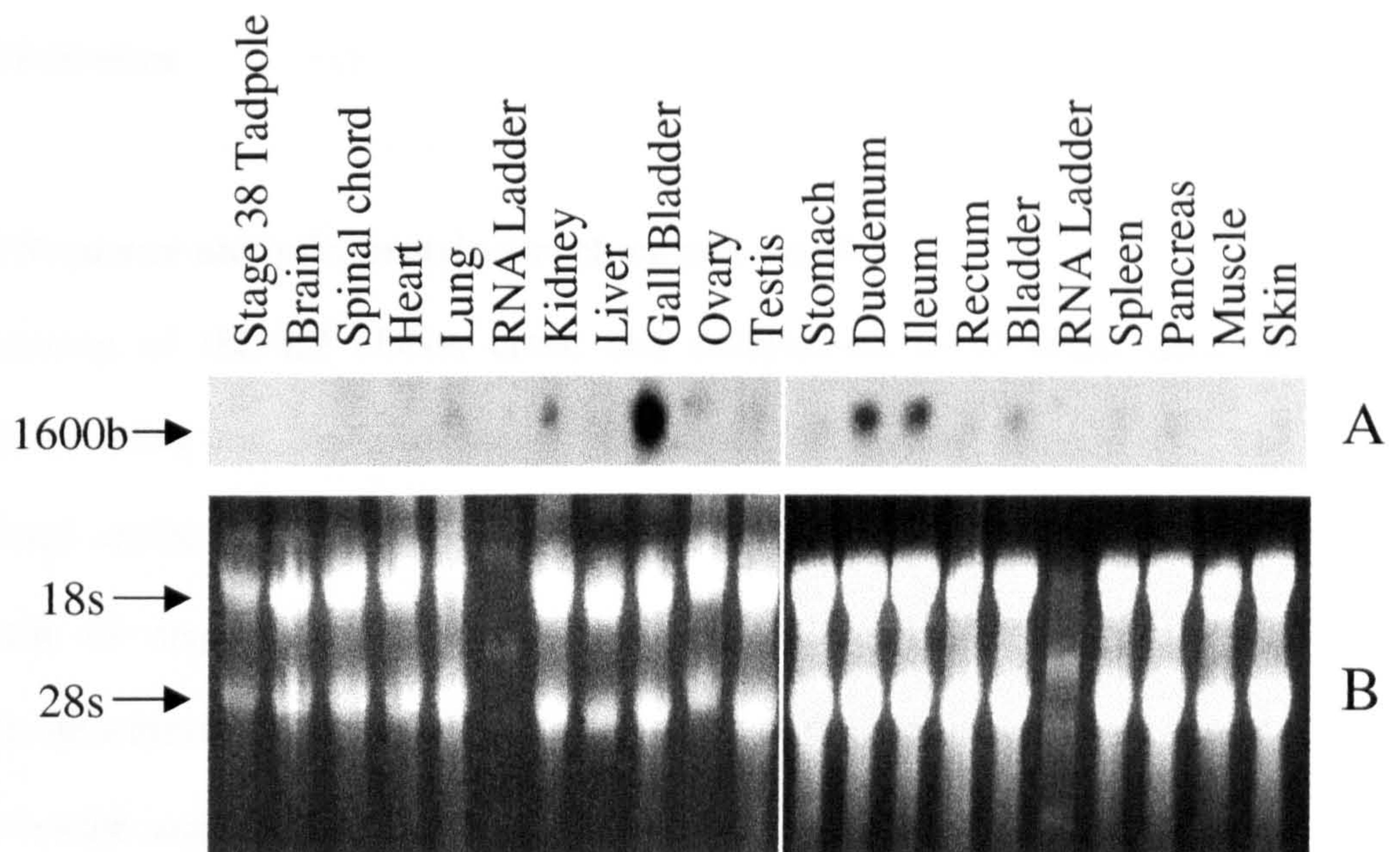


Figure 3.9. Northern blot analysis of RNA isolated from dissected adult organs. (A) Using 3' *Xanx-4* probe *Xanx-4* transcripts were detected at high levels in the gall bladder and intestine, at lower levels in tadpole, lung, kidney, ovary, testis, stomach, bladder, spleen and pancreas. No transcripts were detected in neural tissues, heart, liver, muscle or skin. (B) Ethidium bromide stained agarose gel showing RNA loadings for different adult tissue types prior to transfer.

(figure 3.9A). No *Xanx-4* transcripts were detected in the brain, spinal chord, heart, liver, muscle or skin. All the organs in which transcripts were detected contain significant quantities of polarised epithelial tissues, thus correlating with the observed polarised expression of the *Xanx-4* protein (section 3.2.6).

3.3 Discussion

3.3.1 Sequence analysis, protein structure and motifs

Sequencing of the K2 cDNA clone and comparison to Genbank database identified it as the *Xenopus laevis* orthologue of human annexin IV. The predicted amino acid sequence shows that *Xanx-4* has 69-74% identity with annexin IV sequenced in other vertebrate species. Surprisingly, of those vertebrate annexin IV sequenced so far, *Xanx-4* has the highest sequence identity with bovine annexin IV (74%) and lowest sequence identity with the more phylogenically closely related medaka fish (69%). This may be indicative of divergent evolution (Morgan and Fernandez., 1997).

Annexins have a common primary structure constituted of two different regions, the unique N-terminal domain and the highly conserved C-terminal domain (Raynal & Pollard et al., 1994). Through a motif search on the deduced amino acid sequence it was discovered that *Xanx-4* contained a four fold repeat of the 70 amino acid domain signature that identifies it as an annexin family member. The annexins possess a novel conserved type II Ca^{2+} binding motif that contains the sequence [(Leu/Met)-Lys-Gly-X-Gly-Thr-40X-acidic residue]. *Xanx-4* contains two of these active calcium-binding sites that are located in the first and

forth loops of the annexin core domain. These sites are thought to mediate the association of annexins with phospholipid membranes (Raynal and Pollard, 1994).

In contrast with the C-terminal domain, the sequence and length of the N-terminal domain is extremely variable amongst annexin family members (Morgan and Fernandez, 1997). It is this region which is thought to confer the particular specificity of a given annexin. On examination of the Xanx-4 N-terminal domain a number of motifs, common to annexin family members, were discovered. Both protein kinase C (PKC) and casein kinase 2 (CK2) sites, which suggest that Xanx-4 exists in activated and deactivated states. Two N-myristoylation sites and two ASN-glycosylation sites were also identified in Xanx-4. These sites are known to be present in molecules involved in membrane-cytoskeletal events including membrane-trafficking (Stryer, 1995).

3.3.2 Maternal Expression of Xanx-4

Xanx-4 transcripts are present in the oocyte as a maternal pool that is much reduced by 32-cell stage and by stage 9 is barely detectable (figure 3.4). It has been shown that these transcripts are present evenly throughout the oocyte (ie. not specifically localised) (figure 3.5). Although it is not certain whether these transcripts are translated, the result in figure 3.6 shows that injected exogenous mRNA is translated. Therefore, Xanx-4 is not specifically localised to one region of the oocyte but spread throughout the subcellular compartments in approximately equal amounts.

Annexins of lower vertebrates cloned thus far display maternal expression. Both *Xenopus annexin II* and *annexin VII* have two phases of expression one maternal and one zygotic (Izant & Bryson 1991, Srivastava *et al.*, 1996). Additionally, the *max1-4* medaka annexins are expressed maternally and zygotically (Osterloh *et al.*, 1998), as are *M.fossilis annexin I-V* (Ivanenkov *et al.*, 1994).

The presence of maternal pool of annexins in the oocyte/egg has suggested their involvement in events occurring during fertilisation. It has been suggested that annexins may be involved in cortical granule exocytosis (Ivanenkov *et al.*, 1994).

3.3.3 Zygotic embryonic Expression of *Xanx-4*

RT-PCR stage series (figure 3.4) demonstrates that upregulation of zygotic *Xanx-4* occurs from stage 13 and continues at a similar level through embryonic development to stage 41. Stages beyond this point were not analysed.

By *in situ* hybridization *Xanx-4* transcripts are first detected in the pronephric anlagen from stage 26 (figure 3.7). Interestingly, this coincides with the time of lumen formation in the pronephric tubules. This may reflect a condensation and polarisation of the tubule epithelium. Transcripts are detected in the pronephric tubules at all stages of organogenesis. *Xanx-4* is specific to the tor-shaped pronephric tubules (stages 35-38) and during later stages of elongation and coiling (stages 40+). The highly specific expression profile of *Xanx-4* during embryonic development suggests a role for *Xanx-4* in the formation and maturation of the pronephric tubules.

Xanx-4 protein is detected specifically in the apical domain of the functional pronephric tubules, which is in agreement with studies on annexin IV in other species (Kaetzel et al., 1989; Kaetzel et al., 1994; Mayran et al., 1996). This may reflect a role for Xanx-4 in the function of the pronephros.

Expression of *Xanx-4* transcripts in the otic vesicle is not surprising as almost all genes expressed in the pronephros identified so far display otic vesicle staining (Brändli, 1999). This may reflect the common anlagen of the two structures. It is also interesting to note that a number of human disorders with kidney phenotypes also involve ear abnormalities (Abdelhak et al., 1997, Kohlhase et al., 1998, Favor et al., 1996).

The expression pattern of the two other annexin family members characterized in *Xenopus* embryos is less specific. *Xenopus annexin II* is expressed in tailbud embryos at low levels in the brain and muscle, at higher levels in the heart, liver and kidney and highest in the skin (Izant and Bryson., 1991). Studies conducted on *Xenopus annexin VII* have shown that it is expressed in muscle, heart and brain in tailbud stage embryos (Srivastava et al., 1996).

The expression pattern of *annexin IV* in a number of fish species is far less specific than *Xanx-4*. Four annexins *max1-4* have been cloned from *Oryzias latipes* Killifish Medaka. *Max2* is assumed to be the fish homologue of *annexin IV* (59% identity). The expression pattern of *max2* by *in situ* hybridization showed transcripts are present in the primordial stomach and in the floor plate during stages 26-28 and from stage 30-33 transcripts were detected in the cloaca

and in the floor plate (Osterloh et al., 1998). Five annexins have been cloned from *Misgurnus fossilis* eggs (Ivanenkov et al., 1994).

Interestingly, the expression pattern of *annexin IV* mouse and rat embryos is restricted to neural tissues. Murine *annexin IV* is expressed in the notochord from E8.5, in the floor plate at E9.5 and in the roof plate at E10.5. *Annexin IV* is detected from caudal spinal cord, through the brain stem up to the diencephalon and lamina terminalis, in glial cells, sensory neurons and their axons, and ventral motor neurons in the spinal chord (Hamre et al., 1996). The expression pattern in rat embryos follows an almost identical pattern (Naciff et al., 1996).

The expression of *Xanx-4* is highly specific to the pronephric tubules during organogenesis. The temporal expression pattern of *Xanx-4* coincides with the specification, development and function of the pronephric tubules during embryogenesis of *Xenopus laevis*. Together, these observations implicate *Xanx-4* in the development of the pronephric tubules. It is expressed in the right place at the right time. Expression continues up to and beyond the time when the pronephros becomes functional, its location at the luminal surface implies *Xanx-4* may have a role in the development and also in the function of the pronephric tubules.

3.3.4 Expression of *Xanx-4* in the adult frog

The expression pattern of *Xanx-4* in adult tissues by northern blot analysis, using a highly specific 3'UTR probe shows *Xanx-4* to have tissue specificity. Although transcripts are present in the metanephros, the highest level of *Xanx-4*

expression is seen in the gall bladder and intestine. Low level expression is also seen in other epithelial tissues.

In agreement with this result *annexin IV* has been found in adult epithelial tissues of other animal species; lungs (Sohma et al., 1995), intestines and pancreas (Massey et al., 1991b), liver (Boustead et al., 1993) and kidney. Interestingly Bovine *annexin IV* is located in the apical membranes of the proximal tubules in adult kidney (Kojima et al., 1994), but basolaterally in the rabbit adult kidney (Massey-Harroche *et al.*, 1995). The common theme for annexin IV expression in adult tissues seems to be that of polarised epithelial tissue (Massey-Harroche et al., 1998). In many cases the pattern appears to be apical (Kaetzel et al., 1989, Kaetzel et al 1994, Mayran et al 1996).

3.3.5 In conclusion

All types of epithelia have one important function in common: they serve as selective permeability barriers, separating fluids on each side that have different chemical compositions. The fact that Xanx-4 is specifically located to the apical membrane of the pronephric tubule epithelia suggests an involvement in transcellular transport. This could involve transmembrane or membrane bound receptors and/or signalling their pathways; channels or pores and/or their regulation; endocytosis or exocytosis; protein chaperoning or cytoskeletal architecture. Current literature suggests an annexin family member candidate for each of these functions *in vitro* (Raynal and Pollard, 1994). The results achieved in this chapter provided a platform on which to mount the search for a function of Xanx-4 in the pronephric tubules in *Xenopus laevis*.

Chapter 4 The effect of overexpression of *Xanx-4* on pronephric structure in *Xenopus laevis*.

4.1 Introduction

Injection of mRNA into cleavage stage *Xenopus* embryos (overexpression) is often used to assess the developmental consequences of elevation of activity of a gene (Kreig and Melton, 1987). Increased activity can be used to determine the function of a particular protein during development. If the elevated expression causes specific reproducible developmental changes, this may indicate the normal function of the gene. The mRNA is translated immediately after its injection and depending on the longevity of the mRNA, can continue to exert an effect up to swimming tadpole stages. This results in expression, inconsistent with the normal timing of expression of the gene. Methods of temporal control include injection of inducible plasmid constructs (Kreig and Melton, 1987). However, this results in non-uniform expression (mosaicism) throughout a given tissue, since the DNA is episomal and the genes are not expressed from a stable position. This problem can be avoided by transgenic approaches that integrate multiple copies of a given gene into the host genome (Kroll and Amaya, 1996). Genes integrated under the control of a tissue specific promoter can allow expression of that gene at the right time and place. Constitutive promoters can also be used providing elevated expression of a gene in the wrong place at the wrong time, or the right place at the wrong time, which can also be extremely informative.

Overexpression of a number of pronephric genes in *Xenopus laevis* embryos has been used in previous studies to provide information on their function in pronephric organogenesis.

XPax-2/XPax-8 and Xlim-1

One such study involves the transcription factors XPax-2 and XPax-8 and their requirement for a co-factor Xlim-1. Ectopic co-expression of either XPax-2 or XPax-8 with Xlim-1 results in a synergistic effect producing increased pronephric tubule complexity, enlarged tubules and ectopic tubules while expression of either XPax-2 or XPax-8 alone has a moderate effect (Carroll and Vize, 1999).

xWT1

In this study the authors showed that ectopic expression of *xWT-1* inhibits pronephric tubule development, probably by repressing tubule specific gene expression in the portion of the pronephros fated to become tubules (Wallingford et al., 1998).

Notch

Targeted overexpression of notch signalling in the pronephric anlage both perturbed the characteristic pattern of the differentiated tubule network and increased the expression of early markers of pronephric cells, *XPax-2* and *xWT1*. Inducible constructs of active or dominant negative *Su(H)* were used to misactivate Notch signalling. The authors propose that Notch signalling plays a role in the early selection of duct and tubule cell fates as well as functioning

subsequently to control tubule patterning and development (McLaughlin et al., 2000).

The analysis of perturbed development generally includes inspection of the overall anatomy of the embryo and analysis using molecular markers and/or histology. Overexpression of some genes can lead to obvious changes in morphology that can be scored. Inclusion of a lineage tracer aids analysis of the phenotype by marking those cells or tissues carrying the injected protein especially in left versus right side comparisons. Persistence of a lineage tracer in the embryo also demonstrates how well the injected cells survive and contribute to a differentiated organ and controls for any altered fate in injected cells.

Previous work has demonstrated that the dorsal and ventral C-tier blastomeres of a 32-cell stage embryo are fated to become the lateral plate mesoderm and pronephric anlagen (figure 4.1) (Dale and Slack, 1987; Moody, 1987). Injecting into one of the two C2/C3 blastomeres allows internal control left vs. right.

The aim of the research contained in this chapter was to perform targeted overexpression of *Xanx-4* in *Xenopus laevis* embryos and to analyse any changes in morphology of the pronephros, as indicated by wholemount immunohistochemical staining with the monoclonal antibodies 3G8 and 4A6.

Figure 4.1

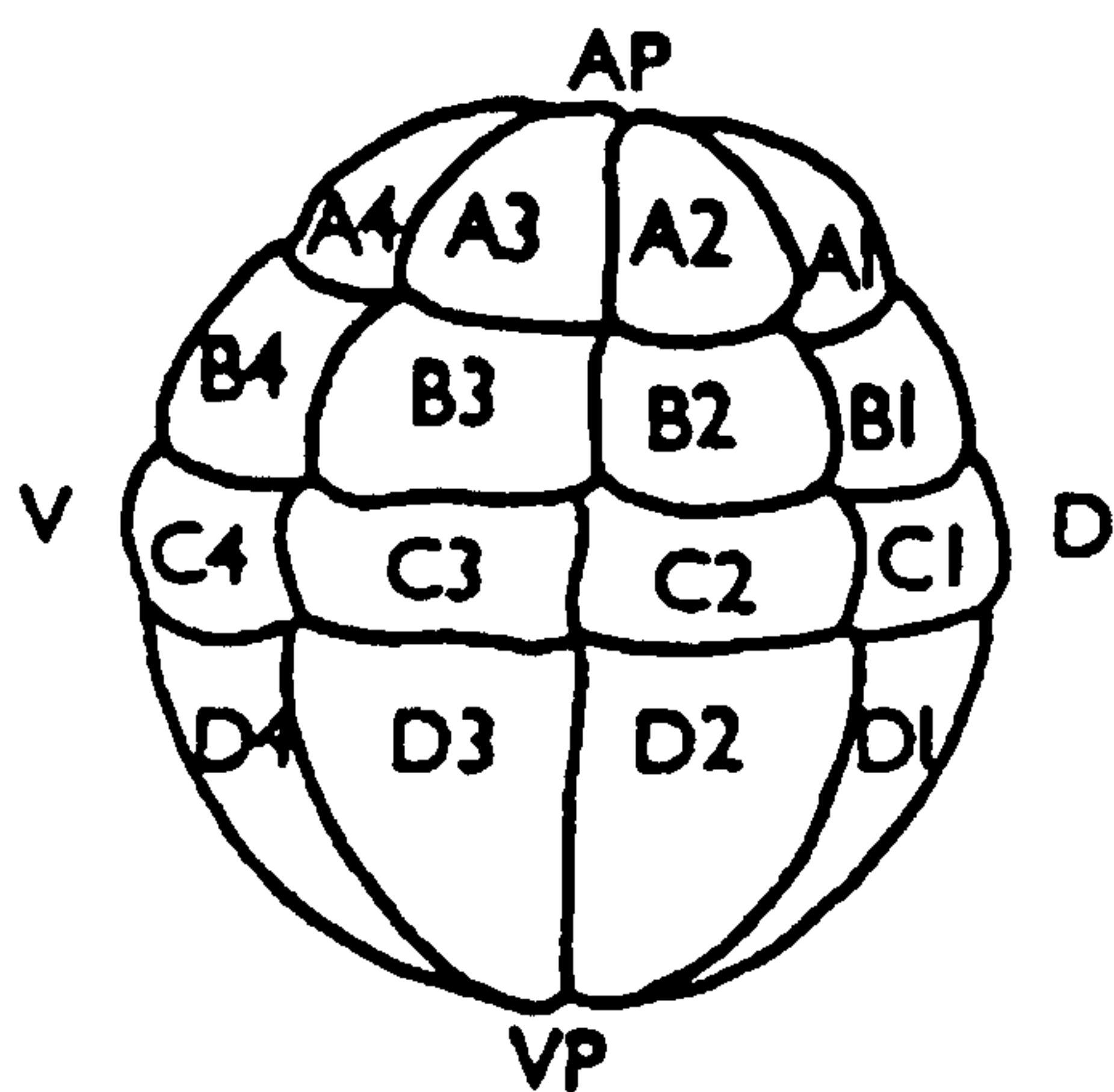


Figure 4.1: Nomenclature of blastomeres at 32-cell stage *Xenopus laevis* blastula embryo (reproduced from Dale and Slack, 1987). C2 and C3 blastomeres are fated to become pronephric anlagen (Moody, 1987).

4.2 Injected Xanx-4 mRNA translates into a 34 kDa protein at high level in oocytes.

It was firstly important to ensure that the *Xanx-4* mRNA would translate efficiently when injected. *Xanx-4* mRNA was prepared from the *Xanx-4*/RN3 construct (appendix 2) linearised with *SfiI* and transcribed with T3 RNA polymerase using the mMessage mMachine kit (Ambion) and diluted to 250µg/ml. 10ng (36nl) was injected into each oocyte which were cultured overnight in BarthX and ³⁵S methionine. The oocytes were homogenised and the equivalent of 0.5 of an oocyte was subjected to SDS-PAGE and autoradiography. Figure 4.2 shows the *Xanx-4* mRNA was successfully translated into a protein of approximately 34kDa at a high level (arrow).

4.3 Targeting of the Xanx-4 mRNA to the presumptive pronephric anlagen.

To ensure that the mRNA injected was targeted to the right place (i.e. the pronephric anlagen), the blastomeres were co-injected with mRNA plus FLDX as a lineage label. 18nl of the *Xanx-4*/FLDX mixture (0.5ng *Xanx-4* mRNA/10ng FLDX) was injected into the C2 or C3 blastomere of 32-cell stage *Xenopus laevis* embryos, cultured to stage 42 and fixed in MEMFA. After fixation, the embryos were immediately sorted for presence of FLDX (Figure 4.3A). Embryos with expression in the pronephros were sorted into those showing fluorescence in either the left or the right sides using an UV filter on a Nikon microscope (e.g. figure 4C left side FLDX is present and 4D right side of same embryo, no FLDX present). Those without FLDX in the pronephric field were discarded. FLDX was also injected into the A1/A2 blastomeres (neural

Figure 4.2

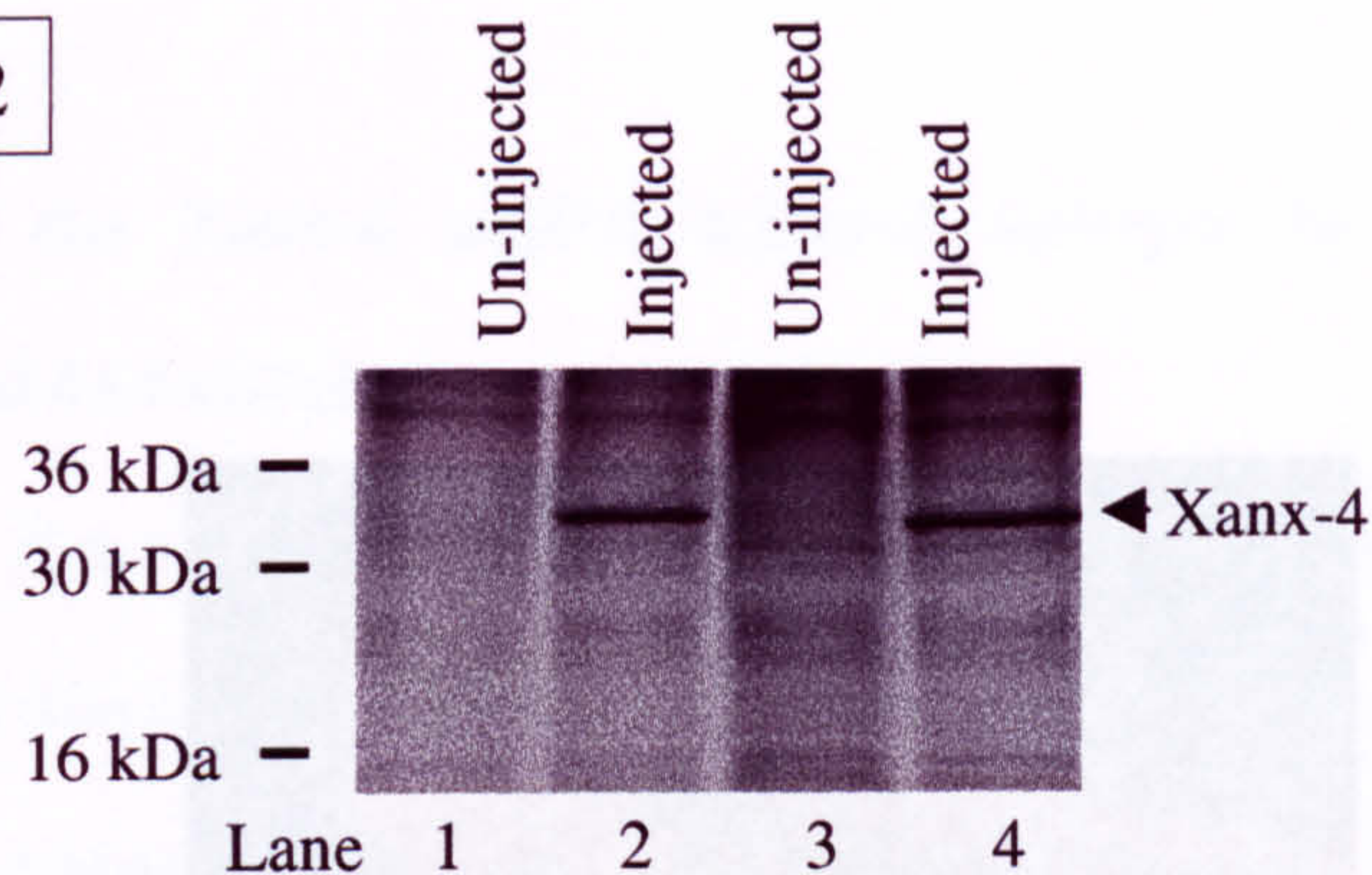


Figure 4.2 : Expression of *Xanx-4* in oocytes. *Xenopus laevis* oocytes were injected with *Xanx-4* mRNA and cultured overnight at 18°C in BarthX with ³⁵S methionine. The oocytes were homogenised and subjected to SDS-PAGE and autoradiography. Lanes 2 and 4: *Xanx-4* mRNA translates at a high level in oocytes, resulting in a protein product of approximately 34kDa. Lanes 1 and 3: Uninjected control oocytes.

Figure 4.3

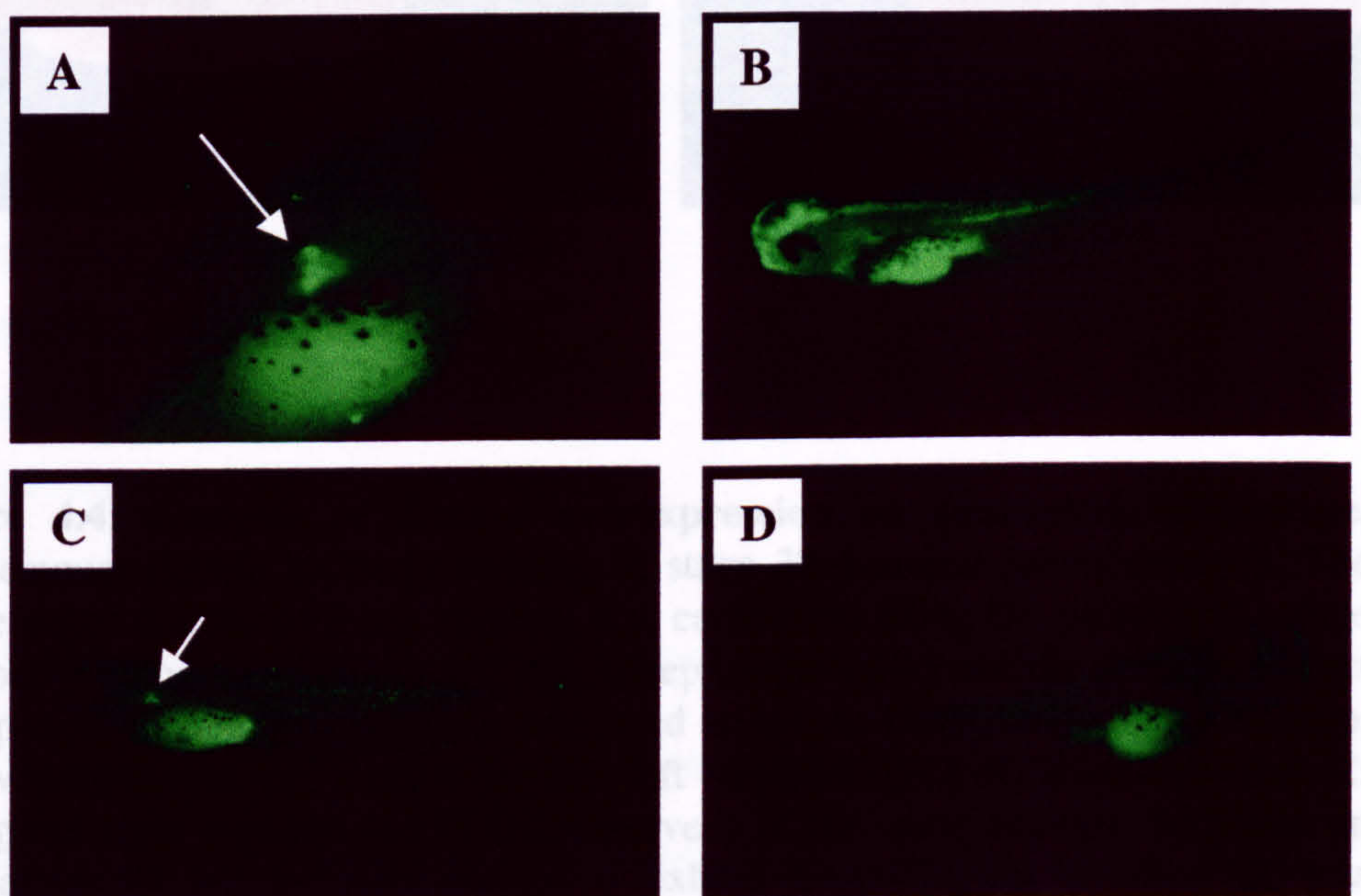


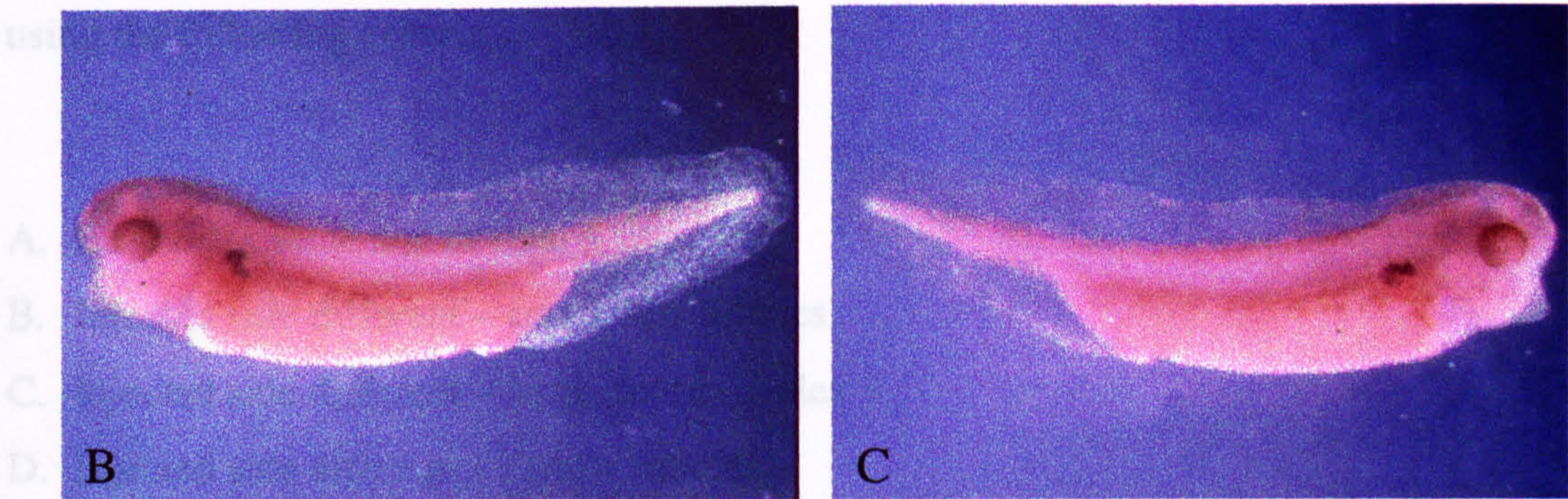
Figure 4.3: Targeted injections of *Xanx-4* to the pronephros. Embryos were injected with FLDX and *Xanx-4* mRNA at the 32-cell stage, cultured to stage 42, fixed and visualised under a microscope with UV filter. A: C2 blastomere injected, FLDX can be seen in the pronephros. B: Control, A1 blastomere targeted, shows FLDX in the brain and spinal chord. C: C2 blastomere targeted, FLDX only seen in the left nephron and D: Right hand view of C, no FLDX observed, this provides the uninjected control nephron.

anlagen) as a small control group for the injection targeting (figure 4.3B); these were not included in the phenotype analysis.

Figure 4.4

4.4.1. Analysis of the *Xanx-4* mRNA injected embryos by wholemount antibody 3G8 and 4A6 staining.

In order to assess if any overexpression of *Xanx-4* in the pronephros could affect the pronephric tubule staining using the tubule specific monoclonal antibody 4A6, wholemount double antibody staining for differences in morphology between injected side



A. Uninjected control embryo,
B. overexpression of *Xanx-4* in the left nephron (FLDX observed) and C: untargeted right nephron (no FLDX observed) of the same embryo. Although on comparison the left and right pronephroi exhibit morphological variation this was deemed to be within normal variation.

Figure 4.4: Analysis of *Xanx-4* overexpression on pronephric phenotype. Wholemount double antibody staining of stage 38 *Xenopus laevis* embryos. The wholemount double antibody staining was carried out using the pronephric tubule (T) specific monoclonal antibody 3G8, (deep purple stain) and the pronephric duct (D) specific monoclonal antibody 4A6, (red stain). A: Uninjected control embryo, B: overexpression of *Xanx-4* in the left nephron (FLDX observed) and C: untargeted right nephron (no FLDX observed) of the same embryo. Although on comparison the left and right pronephroi exhibit morphological variation this was deemed to be within normal variation.

4A6. ii and 4B6. ii). The summary of the scoring data for each experiment is shown in figures 4.5A and B. Although some pronephroi were considered abnormal, the trend (as shown in the graphs 4.5 A and B) is the same between

anlagen) as a small control group for the injection targeting (figure 4.3B); these were not included in the phenotype analysis.

4.4 Analysis of the *Xanx-4* mRNA injected embryos by wholemount antibody 3G8 and 4A6 staining.

In order to assess if any morphological changes had occurred to the embryos on overexpression of *Xanx-4*, the embryos were subjected to wholemount antibody staining using the tubule specific monoclonal antibody 3G8, and the duct specific monoclonal antibody 4A6 (figure 4.4). The embryos were scored for differences in morphology between the pronephroi on the uninjected side and injected side using the following criteria.

- A. Both sides same and normal
- B. Injected side different – small, less tubules
- C. Injected side different – large, more tubules
- D. Injected side different - narrow tubules
- E. Injected side different - wide tubules
- F. Injected side different - no tubules
- G. Gross phenotype abnormal
- H. Injected side: duct phenotype abnormal

The control injected embryos were scored as left versus right to indicate the level of natural variation within an embryo. Two independent experiments were carried out to control for individual genetic differences in the frog colony (Figure 4Ai, ii and 4Bi, ii). The summary of the scoring data for each experiment is shown in figures 4.5A and B. Although some pronephroi were considered abnormal, the trend (as shown in the graphs 4.5 A and B) is the same between

Figure 4.5A

Experiment 1: *Xanx-4* Overexpression

(i) Table shows phenotype scoring analysis of overexpression of *Xanx-4* : Experiment 1

| Scoring categories | A | B | C | D | E | F | Total | G | H |
|------------------------------------|-----|----|----|----|----|----|-------|-----|-----|
| <i>Xanx-4</i> side vs uninjected L | 31 | 1 | 1 | 0 | 2 | 4 | 37 | 5 | 6 |
| <i>Xanx-4</i> side vs uninjected R | 38 | 1 | 2 | 0 | 0 | 3 | 45 | 6 | 3 |
| Total | 69 | 2 | 3 | 0 | 2 | 7 | 82 | 11 | 9 |
| No. as a percentage of total | 84% | 2% | 3% | 0% | 2% | 9% | | 13% | 11% |
| Controls | 54 | 2 | 2 | 0 | 3 | 1 | 61 | 8 | 8 |
| No. as a percentage of total | 88% | 3% | 3% | 0% | 4% | 2% | | 13% | 13% |

(ii) Graph represents phenotype scoring analysis of overexpression of *Xanx-4* : Experiment 1

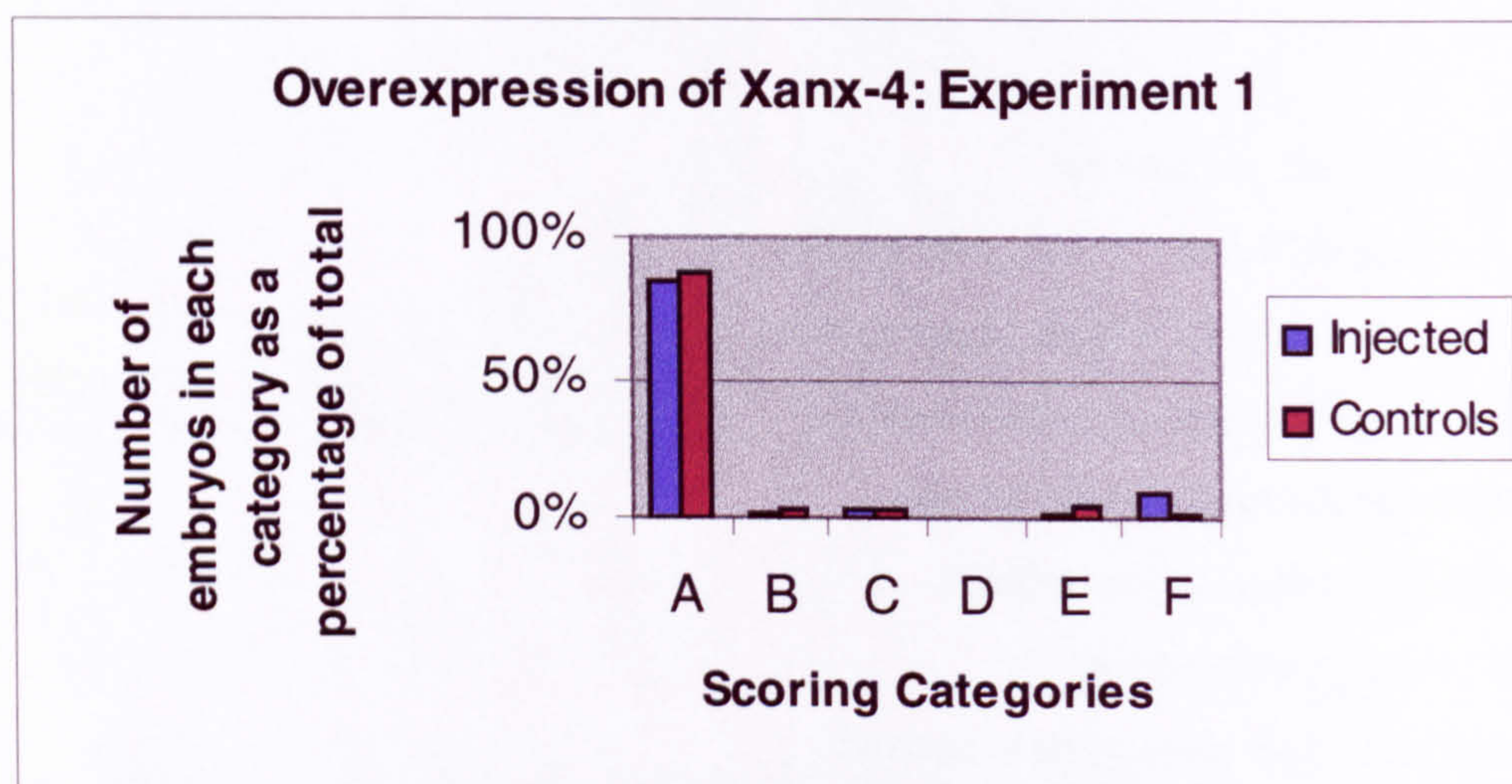


Figure 4.5: Morphogenic analysis of *Xanx-4* overexpressing embryos. The C2/C3 blastomeres of 32-cell stage embryos were co-injected unilaterally with *Xanx-4* mRNA and FLDX, cultured to stage 38 and sorted for the presence of FLDX marking left or right nephron. Those with no FLDX or FLDX not in the pronephros were discarded. The embryos were fixed and subjected to wholemount double antibody staining using 3G8 (tubules) and 4A6 (duct). Two independent experiments, using two different frogs were carried out. The embryos were then scored according to the categories listed in C, *Xanx-4* injected side versus uninjected side. The results of the scoring data for experiment 1 is shown in figure 4.5A: table (i) and graph (ii). The results of the scoring data for experiment 2 (a repeat experiment) is shown in figure 4.5B: table (i) and graph (ii). Small numbers of embryos were considered to have abnormal phenotypes, but these also appeared in the control category and were accepted as within the normal level of variation.

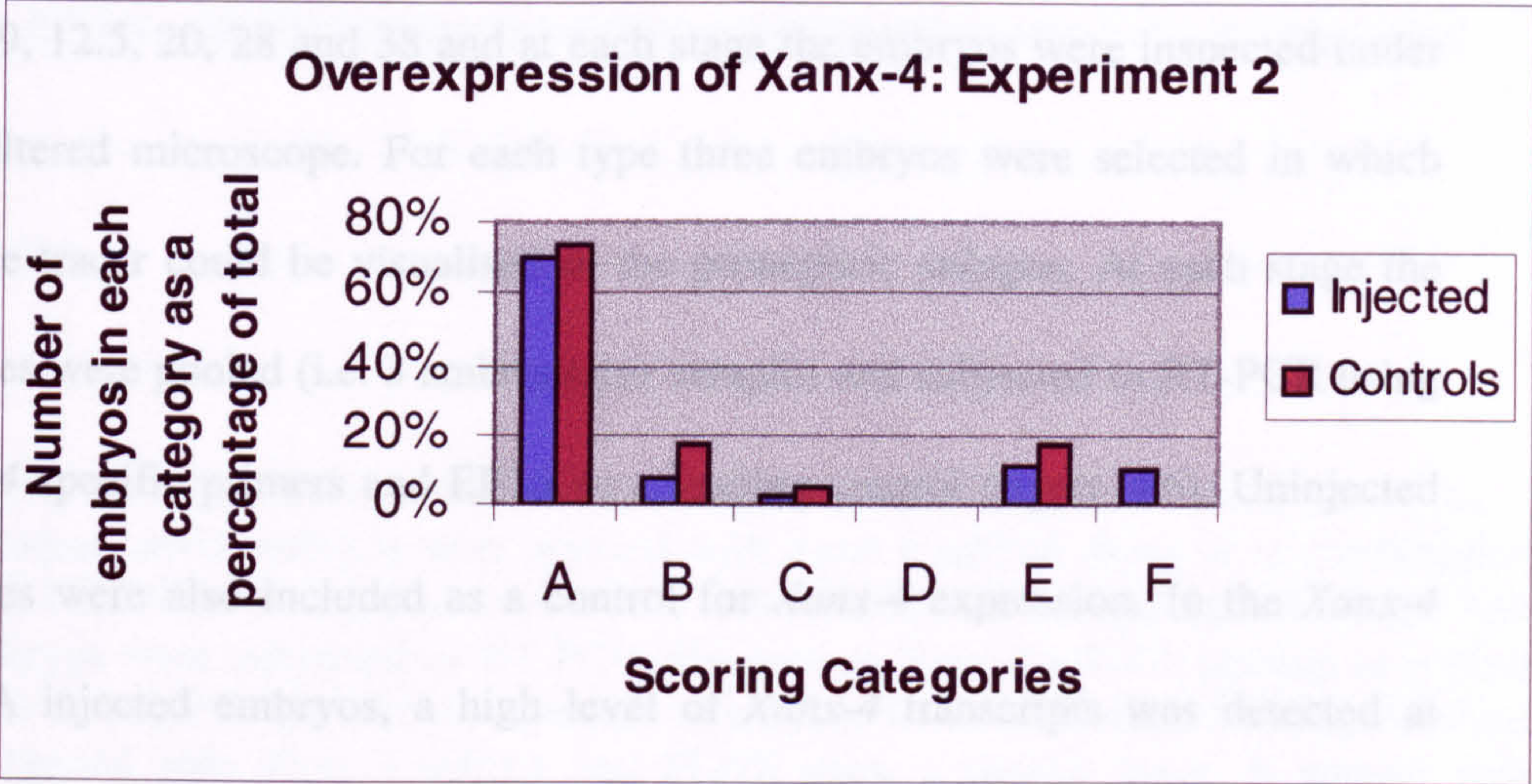
Figure 4.5B

Experiment 2: *Xanx-4* Overexpression

(i) Table shows phenotype scoring analysis of overexpression of *Xanx-4* : Experiment 2

| Scoring categories | A | B | C | D | E | F | Total | G | H |
|------------------------------------|-----|-----|----|----|-----|-----|-------|-----|-----|
| <i>Xanx-4</i> side vs uninjected L | 24 | 2 | 1 | 0 | 2 | 4 | 33 | 13 | 3 |
| <i>Xanx-4</i> side vs uninjected R | 19 | 2 | 0 | 0 | 5 | 2 | 28 | 4 | 4 |
| Total | 43 | 4 | 1 | 0 | 7 | 6 | 61 | 17 | 7 |
| No. as a percentage of total | 70% | 7% | 2% | 0% | 11% | 10% | | 28% | 11% |
| Controls | 31 | 3 | 1 | 0 | 7 | 0 | 42 | 5 | 2 |
| No. as a percentage of total | 74% | 17% | 5% | 0% | 17% | 0% | | 12% | 5% |

(ii) Graph represents phenotype scoring analysis of overexpression of *Xanx-4* : Experiment 2



| | | |
|--|-----|---|
| C | Key | Scoring Categories |
| A. Both sides same & normal | | E. Injected side different - wide tubules |
| B. Injected side different – small, less tubules | | F. Injected side different - no tubules |
| C. Injected side different – large, more tubules | | G. Gross phenotype abnormal |
| D. Injected side different - narrow tubules | | H. Injected side duct phenotype abnormal |

those with elevated *Xanx-4* expression and controls. Therefore the aberrant phenotypes observed are considered to be within normal range. No gross morphological differences were seen between left and right *Xanx-4* injected versus left and right control embryos.

4.5 Longevity of injected message

Injection of synthetic mRNA into *Xenopus* embryos allows the elevated expression of that gene, this will continue until the message is degraded. To test the longevity of the injected message and whether FLDX had any effect on this longevity, embryos were injected with *Xanx-4* mRNA alone or FLDX plus *Xanx-4* mRNA into C2/C3 of the 32-cell stage blastula. The embryos were cultured to stage 9, 12.5, 20, 28 and 38 and at each stage the embryos were inspected under UV filtered microscope. For each type three embryos were selected in which lineage tracer could be visualised in the pronephric anlagen. At each stage the samples were pooled (i.e. 3 embryos per sample) and subjected to RT-PCR using *Xanx-4* specific primers and EF1 α as a loading control (figure 4.6). Uninjected samples were also included as a control for *Xanx-4* expression. In the *Xanx-4* mRNA injected embryos, a high level of *Xanx-4* transcripts was detected at stages 9 and 12.5 but was much reduced by stage 20 and at normal levels (endogenous) at stage 28 and 38. This implies that a high level of exogenous message was present for translation between 32-cell stage and stage 20. The same result was seen in the *Xanx-4* mRNA plus FLDX samples, confirming that FLDX had no effect on the level or longevity of the injected message. In the uninjected samples the endogenous level of *Xanx-4* was detected. A phenotype

Figure 4.6

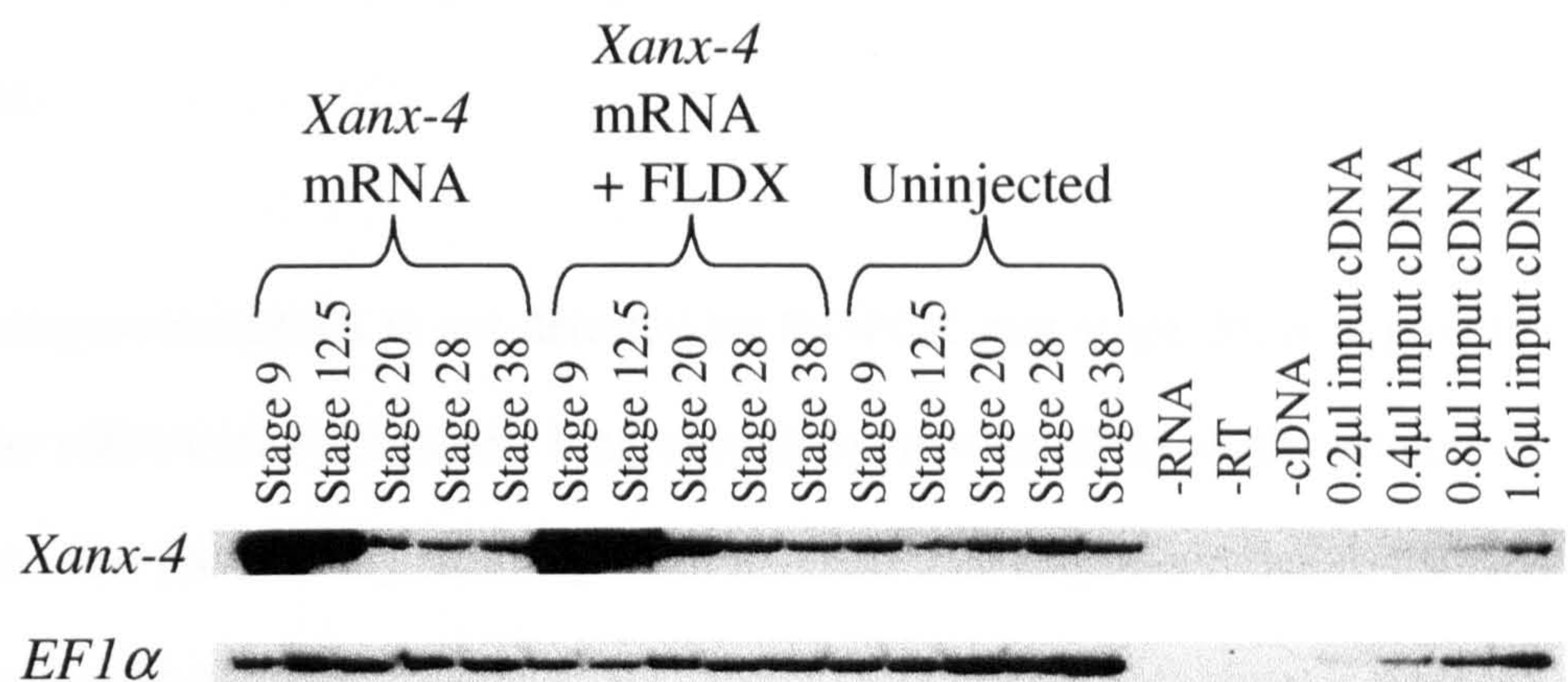


Figure 4.6: RT-PCR stage series showing longevity of injected *Xanx-4* mRNA.

Xenopus laevis embryos were injected with *Xanx-4* mRNA alone or in combination with FLDX or un-injected as controls and cultured to the appropriate stage. The embryos were subjected to RT-PCR. Exogenous *Xanx-4* mRNA persists at a high level to stage 9 and 12.5 and persists at a lower level until stage 20. The embryos coinjected with *Xanx-4* mRNA and FLDX show a similar result. It appears that FLDX has no effect on the persistence of the message. *EF1α* was used as a loading control. The controls used were, (-RNA) no input of RNA into the reverse transcription, no input of reverse transcriptase (-RT) and no input of cDNA into the PCR reaction. The 0.2μl, 0.4μl, 0.8μl and 1.6μl input cDNA into the PCR reaction were included so as to ensure the PCR was within the linear range.

would therefore only be expected to occur if *Xanx-4* functions prior to stage 20 in the presumptive pronephric anlagen.

4.6 Discussion

The exogenous *Xanx-4* mRNA injected into the oocyte translated into a 34kDa protein the size of which is in agreement with annexin IV proteins in other species.

The exogenous mRNA is not detected by RT-PCR past stage 20, it is possible that the mRNA may not persist long enough to have an effect on the pronephric tissues. The protein may still be present at much later stages, but due to the lack of an effective antibody to analyse this protein persistence, experiments were not carried out to analyse this. The *Xanx-4* protein may require a binding partner or other factors to exert a full overexpression effect, as is the case with other *Xenopus* genes (Carroll and Vize, 1999). It is also possible that an early elevated expression (32-cell to stage 20) of *Xanx-4* may not yield an aberrant phenotype as it is well tolerated at these stages and is not overexpressed at the right time and in the right place to have an effect. For example, *xWnt-4* dorsally targeted overexpression can cause shortened body axis whereas vegetally targeted overexpression has no effect (Du et al., 1995, Ungar et al., 1995).

In summary, overexpression of *Xanx-4* mRNA in embryos showed that *Xanx-4* does not affect the phenotype of the embryos. The majority of the pronephroi were of normal phenotype and it was concluded that the overexpression of *Xanx-4* in *Xenopus* embryos does not cause an aberrant phenotype. As shown by RT-

PCR, the use of FLDX as a lineage label did not seem to effect the longevity of the *Xanx-4* mRNA, although it is possible that FLDX could effect the translation of this message. This was not tested but a further experiment could be conducted by co-injection of FLDX and *Xanx-4* mRNA and western blot analysis using a suitable anti-*Xanx-4* antibody. Annexins are known to bind with a variety of proteins *in vitro*, for example S100 family (Raynal and Pollard, 1994), although this has not been studied *in vivo* in the kidney. Overexpression of *Xanx-4* in conjunction with other pronephric genes may reveal *Xanx-4* binding partners or synergistic effects. To test whether *Xanx-4* is required at a later stage in order to exert morphological effects, a hormone inducible *Xanx-4* construct could be prepared (for review see Mattioni et al., 1994) which would allow expression of *Xanx-4* to be induced at later stages of development.

Chapter 5: Perturbation of *Xanx-4* expression in *Xenopus laevis* by double stranded RNA.

5.1 Introduction

5.1.1 Studying gene activity in *Xenopus* by loss-of-function experiments.

As outlined in the previous chapter, successful perturbation of gene expression in *Xenopus* is often carried out using gain-of-function assays. These include injection of mRNA, inducible DNA constructs and production of transgenic tadpoles and frogs. This type of experiment can demonstrate that a gene is sufficient to carry out a particular function but not whether it is required *in vivo*. In contrast, loss-of-function studies can provide evidence for a specific requirement in normal development. The classic approach for knockout, homologous recombination, is not open to researchers in *Xenopus* due to its pseudo-tetraploid genome and long breeding cycles (Graf and Kobel, 1991). However, a number of other approaches have been attempted, and although some have proved very informative, in many, the results are often difficult to achieve and analyse. Many of these studies often require a good basic knowledge of the gene and protein product in question.

5.1.1.1 The dominant-negative approach

The use of dominant-negative proteins has been shown to be particularly useful in *Xenopus*. Dominant-negative ligands (Hoppler et al., 1996), receptors (Hemmati-Brivanlou and Melton 1992), transcription factors (Mead et al., 1996) and signal transduction pathway components (Pierce and Kimelman 1995) have

all allowed the elucidation of activity of the particular proteins. Injection of specific antibodies, which bind to and block the function of a protein, has also been used to assess the requirement of particular proteins (Ruiz I Altaba et al., 1991).

5.1.1.2 Antisense DNA and RNA

The injection of DNA expression constructs producing antisense RNA (Latinkic and Smith, 1999) or direct injection of antisense RNA into *Xenopus* embryos has been successful in reducing the amount of native protein synthesised, and led to phenotypes consistent with other signal reducing manipulations (Steinbeisser et al., 1995). There are, however, limitations to the former strategy due to the mosaic pattern of transcript expression obtained from injected plasmid vectors (Vize et al., 1991). Current opinion suggests that exogenous antisense RNA acts by blocking translation by binding to endogenous mRNA. Unfortunately, it seems that the results of antisense experiments in *Xenopus* can be inconsistent, and the outcomes are often difficult to interpret. Rebagliati and Melton, (1987) and Bass and Weintraub, (1987), have identified an 'unwindase' activity that unwinds RNA:RNA duplexes. The activity is present at low levels in oocytes, increasing during oocyte maturation, and is present at high levels in early embryos, decreasing by late blastula stage. It is thought that this might explain why antisense RNA strategies sometimes fail to ablate gene expression in embryos. A novel application of antisense RNA technology has used hammerhead RNA structures, the authors suggest that both degradation and translation arrest of *Histone H1* RNA occurs in the presence of this specialised

RNA. Although this phenomenon has yet to be demonstrated using mRNA other than *Histone H1* (Steinbach et al., 1997).

The most successful antisense experiments carried out so far are those that involve the depletion of maternal mRNAs in oocytes. The technique involves injection of short (~17mer) oligodeoxynucleotides (ODN) into oocytes, targeted to specific maternal mRNAs. These single stranded DNA molecules hybridise to their target mRNA and Ribonuclease H degrades the RNA strand of the heteroduplex. The oocytes are allowed to recover, implanted into a primed female and are then laid and fertilised in the normal way. Depletion of maternal *β-catenin* mRNA by sequence-specific ODN resulted in embryos with a loss of axial structures, which could be rescued by injection of mRNA (Heasman et al., 1994).

5.1.1.3 Rescue of dominant-negative, antisense and antibody induced phenotypes

Probably the most essential feature of analysing the specificity of dominant-negative, antisense and antibody experiments is the question of whether rescue of a resultant phenotype can be achieved. In the case of dominant-negative experiments, rescue may involve titrating in the wild-type gene product or activating the pathway downstream as a by-pass to the inhibition being exerted. Unless the phenotype observed can be successfully rescued by addition of sense mRNA in antisense experiments or protein in antibody depletion experiments, the results are difficult to interpret since the specificity of the effect is doubted. Until recently a simple method for specific and reproducible interference of gene

function was lacking for researchers using *Xenopus laevis* as a model vertebrate organism in developmental biology.

5.1.2 Transgene induced gene silencing.

With the widespread use of transgenesis, it was inadvertently discovered in a number of organisms that transgenes are able to elicit specific gene-silencing effects on the endogenous copies of the gene. This gene silencing has been termed co-suppression in plants and quelling in fungi (Napoli et al., 1990; Romano and Macino, 1992).

Epigenic gene silencing has also been observed and is associated with X-chromosome inactivation in mammals (Lyon, 1961), the yeast mating locus, paramutation (Brink, 1956), Position Effect Variegation and telomeric regions (reviewed by Karpen, 1994).

5.1.3 Transgene silencing in plants (co-suppression).

Transgene-induced gene silencing, or co-suppression has been well studied in plants (for reviews see Vaucheret et al., 1998, Gura, 2000). The silencing can occur at the level of DNA as in transcriptional gene silencing (TGS) or at the post-transcriptional level (PTGS). In TGS, transcription does not occur, it is meiotically heritable (Assaad., 1993) and thus far, it has only been reported in plants. TGS occurs when multiple copies of a transgene are inserted into a plant genome. Specific DNA methylation and condensation follows, resulting in the silencing of the endogenous copies of the gene (Wassenegger et al., 1994). This silencing can occur not only locally but can transfer from one locus to another,

suggesting that different parts of the genome can communicate. It has been suggested that DNA-DNA interactions may be responsible, or that diffusable RNA from one locus can result in RNA-DNA interactions at another (Park et al., 1996). Since epigenetic alterations in DNA methylation and condensation can block recombination, it is probable that the function of this phenomenon is a genome protection against harmful deletions during recombination events. This may also explain TGS in wild-type plants with large numbers of transposable elements.

In contrast to TGS, PTGS involves high levels of transcription although mRNA does not accumulate. It is thought that PTGS is a natural post-transcriptional antiviral defence mechanism. PTGS generally occurs when a strong promoter of either a transgene or virus produces a high level of mRNA (Napoli et al., 1990). It appears that the cellular machinery recognises this abnormally high level of transcription and triggers a cascade of events resulting in the degradation of both the endogenous and transgene or viral RNA (Lindbo & Dougherty 1992). Due to the fact that transcriptional activity of the transgene is required, it is suggested that a diffusable RNA is the messenger of this silencing action. Grafting experiments have shown that silencing factors can spread systemically and can trigger silencing in other tissues (Palauqui et al., 1997; Voinnet et al., 1998). However, silencing of endogenous genes by PTGS has also been shown to occur on insertion of promoterless or weakly transcribed genes (Van Blokland et al 1994), which may involve a different mechanism.

In *Arabidopsis*, an RNA-dependent RNA polymerase, Silencing Defective-1, (SDE1), has been found to be essential for the PTGS mediated by transgenes (Dalmay et al., 2000). Mourain et al., (2000) have shown that SGS2, an RNA-dependent RNA polymerase, and SGS3 are required for PTGS and natural virus resistance in *Arabidopsis*. It is current opinion that most cases of co-suppression in plants are due to genetic interference by double stranded RNA.

5.1.4 Gene silencing in fungi (Quelling)

A phenomenon, termed quelling, which is essentially similar to co-suppression in plants has been observed in fungi (Cogoni et al., 1996). It involves transgene-induced gene silencing. An elegant experiment in *Phytophthora* showed that on introduction of a transgenically silenced nucleus to a normal cell (creating a heterokaryon), the silencing was transferred to the wild-type nucleus and the endogenous gene was also silenced (van West et al., 1999). In *Neurospora crassa*, *qde-1*, 2 & 3 mutants are defective for quelling and are therefore implicated in the quelling process (Cogni & Macino, 1997). The QDE-1 protein is highly homologous to an RNA-dependent RNA polymerase (Cogoni & Macino, 1999) characterised in tomato (Schiebel et al., 1998). QDE-1 also shares homology with proteins from several different organisms *C.elegans* (ELEG1), *S.pombe* (POM) and *A.thaliana* (ARAB), indicating that gene silencing mechanisms may be conserved across species.

5.1.5 RNA interference (RNAi).

RNA interference (RNAi) is a recently discovered phenomenon that has been shown to actively and specifically silence gene expression in a range of

eukaryotic organisms, from trypanosomes to mouse. The silencing occurs in the presence of double-stranded RNA (dsRNA) and results in homologous mRNA being targeted for degradation. This RNA-triggered genetic-control mechanism of RNAi is currently of great interest and is thought to be related mechanistically to transgene silencing and transposition (for review see Plasterk and Ketting, 2000, Bosher and Labouesse, 2000).

5.1.5.1 *Caenorhabditis elegans*

The efficacy of RNAi as a means of interfering with gene expression was originally discovered in *C.elegans* and since then, has become of great interest as it provides a potent and specific method of mRNA ablation (Fire et al., 1998).

Since RNAi can provide a method of interfering with gene expression and thereby help elucidate the function of a gene, it has been used to systematically examine the function of genes on virtually whole chromosomes of *C.elegans*. Gonczy et al., (2000) synthesised dsRNA for 2232 genes (96%) encoded by chromosome III, and injected them into germline of *C.elegans* worms. Time-lapse DIC (differential interference contrast) microscopy was used to score for those dsRNAs that caused abnormalities in the first two cell divisions. 133 (6%) of the genes test produced such phenotypes. Of the 7 known genes on chromosome II with early cell division phenotypes, all showed RNAi phenotypes which matched the genuine mutant phenotype. 104 had no previous function identified in *C.elegans*, but have homologies to other species. 11 of the 133 were previously identified with a function in *C.elegans*. 18 of the 133 could not be ascribed a function on the basis of sequence homology and therefore this

approach has currently provided the best functional data available on these *C.elegans* genes.

Fraser et al., (2000) constructed a library of bacteria expressing dsRNA for 2416 of the genes on *C.elegans* chromosome I (87%); these dsRNAs were fed to the worms and RNAi induced phenotypes were scored under a dissecting microscope. 13% of the genes tested provided RNAi-induced phenotypes. This information increased the number of genes on chromosome I with known phenotypes from 70 to 378. Both of these studies validate the use of RNAi as a means to functionally analyse genome wide searches.

Considerable work has been carried out in *C.elegans* to try to elucidate the mechanism by which RNAi works, and the genes involved in the pathway. In *ego-1* mutants the worms are defective for germline RNAi effects (Smardon et al., 2000), *ego-1* encodes an RNA dependent RNA polymerase and is the homologue of *qde-1* in *N.crassa*. *rde-1* and *rde-4* mutants are also defective in RNAi but display no other aberrant phenotype (Tabara et al., 1999). The *Drosophila* homologues of *rde-1* are *piwi* and *sting*. *piwi* is required for maintenance of germ cell populations whilst mutations in *sting* cause de-repression of a normally silent repetitive locus (Schmidt et al., 1999). In *A.thaliana* the *rde-1* family members *zwillie* and *argonaute-1* are required for the maintenance of stem cell populations, possibly through repression of transcript processing (Lynn et al., 1999). Mutations in *rde-2*, *rde-3*, *mut-2* and *mut-7* display reduced RNAi response and an increase in transposon mobilisation, providing evidence for a connection between transposon silencing and RNAi in

C.elegans (Tabara et al., 1999). Mutations in *mut-2*, *mut-7*, *mut-8* and *mut-9* are defective in transposon silencing, co-suppression and RNAi, suggesting mechanistic similarities between these three phenomena (Ketting and Plasterk, 2000). Mut-7 protein has homology with RNaseD (3'-5' exoribonuclease) and a helicase, supporting the theory that RNAi works by dsRNA directed, enzymatic RNA degradation (Ketting et al., 1999).

5.1.5.2 *Drosophila melanogaster*

It has been shown that RNAi is a potent and specific inhibitor of gene activity in *Drosophila melanogaster* (Kennerdell & Carthew 1998). The authors injected into syncytial blastoderm embryos, dsRNAs designed to seven different genes, all of which generated loss-of-function phenotypes. Some generated null-phenotypes whereas others produced mosaicism close to the site of injection. In *Drosophila*, as with *C.elegans*, sub-stoichiometric levels of dsRNA are required to cause interference, dsRNA is more potent than ssRNA of either sense or antisense strands and a particular dsRNA may interfere with expression of highly related gene family members. By co-injection of two specific dsRNAs, this study demonstrates the use of RNAi as a method to overcome problems of redundancy amongst gene family members. Kennerdell and Carthew (1998) showed that *Frizzled* and *Drosophila Frizzled-2* function redundantly upstream of *zeste-white3* and downstream of *wingless* in the Wingless pathway. A number of other studies have also successfully used RNAi in *Drosophila* to inhibit gene expression and dissect signal transduction pathways (Clemens et al., 2000), providing phenotypic information on previously elusive mutants (Misquitta and Patternson, 1999).

In an attempt to unravel the mechanism underlying the effectiveness of RNAi, a cell free system using syncytial blastoderm extracts was developed (Tuschl et al., 1999). The study demonstrated that RNAi in *Drosophila* involves the specific degradation of target mRNA by dsRNA, and not by ssRNA. The fact that pre-incubation of the dsRNA potentiated the interference and that the interference could be competed out, [although it did not effect translation of other (untargeted) mRNAs so the factors required are not part of the translation machinery] suggests that other factors are required to associate with the dsRNA. Zamore et al., (2000) used this *in vitro* system to find that RNAi mediated degradation is ATP dependent but uncoupled from mRNA translation. During the RNAi reaction the dsRNAs are processed into 21-23 length nucleotides, a process which does not require target mRNA. But when the target is present, it too is cleaved into 21-23mers, suggesting that the cleaved dsRNAs are acting as templates or guides.

A tissue culture system set up to test RNAi in the *Drosophila* Schneider-2 (S2) cell line, used transient GFP expression and stable chloramphenicol acetyltransferase (CAT) expressing S2 models to show a dose-dependent response using a 78bp dsRNA (Caplen et al., 2000). The 78bp dsRNA was a chemically synthesised oligomer rather than an *in vitro* produced gel-purified transcript.

One study was set up to establish a biochemically tractable model in which the RNAi mechanism could be investigated. Hammond et al., (2000) showed that a

dsRNA-mediated response could interfere with transient lacZ and endogenous *cyclin E* expression. The result was potent and sequence specific, but required the dsRNA to be a minimum length of 300bp. Transfection with a 540bp dsRNA to *cyclin E* caused G1-phase cell-cycle arrest, thereby confirming inhibition of *cyclin E* expression and demonstrating a functional effect since cyclin E protein is required for cells to progress into S-phase of the cell cycle. dsRNAs of 540bp and 400bp were found to be effective whereas 300bp and 200bp were less potent and 50bp and 100bp were impotent. Using cell lysates from S2 cells, Hammond et al., (2000) identified an RNA-dependent nuclease, RISC (RNA-induced silencing complex), that specifically degrades exogenous transcripts homologous to the dsRNA into RNAs of approximately 25nt. Partial purification of the nuclease fraction of the cell lysates revealed that the lysates contained 25nt length RNA oligomers homologous to the target transcript.

Hammond et al., (2000) suggest that RISC is capable of ablating target mRNAs through the generation of sequence-specific nuclease activity. Occasionally observing putative intermediates in this process, the absence of stable cleavage end-products indicated the activity of an exonuclease (perhaps coupled to an endonuclease). Hammond et al., (2000) speculate that the RNA nuclease may make an initial endonucleolytic cut and then non-specific exonucleases may complete the degradation process (Shuttleworth and Colman, 1988). Furthermore, the fact that LacZ and GFP can be successfully targeted demonstrates that an endogenous copy of the target gene is not required.

Elbashir et al., (2001a) have demonstrated that 21 and 22nt RNA fragments are the sequence specific mediators of RNAi. These duplexes, short interfering RNAs (siRNA), are generated by RNase III-like processing from the initial dsRNA input. Using chemically synthesised siRNAs with 1-5nt 3' overhangs to mimic this process, targeted degradation of the mRNA occurs, at or near the centre of the sequence in the mRNA identical to the siRNAs. These results are in good agreement with previous studies. Hamilton and Baulcombe (1999) observed a population of small 25nt RNAs associated with PTGS in plants. Zamore et al., (2000) demonstrated *in vitro* in *Drosophila* blastoderm lysates that target mRNA is cleaved into 21-23nt by a process that requires ATP. They suggest that the cleavage sites are determined by a process that is able to measure the 21-23nt intervals.

Recent studies have shown that the product of the *Drosophila Dicer* gene is an RNase III enzyme and when purified from syncytial blastoderm lysates is capable of cleaving dsRNA into 22bp fragments (Bernstein et al., 2001). The authors suggest that Dicer protein is involved in the initiation of RNAi. Several classes of RNase III enzymes have been identified, the first is the canonical RNase III which contains a single RNase III signature motif and a dsRNA binding domain. The second class, contains two RNase domains and one dsRNA domain with homologues in *Drosophila* (*Drosha*), *C.elegans* (*CeDrosha*) and human (Filippov et al., 2000, Wu et al., 2000). The third class is represented by the *C.elegans* gene *K12H4.8*, the protein product of which has an amino-terminal RNA helicase motif, two RNase II catalytic domains and a dsRNA-binding motif (Bass 2000, Cerutti et al., 2000).

5.1.5.3 Zebrafish

Microinjection of RNAi to target specific genes with defined mutant phenotypes in zebrafish embryos induced specific embryonic defects that recapitulate those mutant phenotypes. The efficiency of producing defects was 20-30% with dsRNA compared to 2-3% with antisense RNA. The level of the targeted endogenous mRNA was significantly reduced and the effects were dose dependent (Wargelius et al., 1999).

Li et al., (2000) showed that null phenotypes for *Zf-1* (no tail) and *Pax6.1* (greatly reduced eye and forebrain development) could be recapitulated by injection of dsRNA. These specific phenotypes were the result of a 75% reduction in mRNA levels as detected by RT-PCR and the reduction rendered the expression of mRNA too low to be detected by *in situ* hybridization. Co-injection of *Pax6.1* and *Zf-1* dsRNA resulted in a phenotype equivalent to the combination null phenotypes. They also showed that transient GFP expression can be quenched by dsRNA directed to GFP. In a more recent study, despite the findings of Li et al., (2000), Oates et al., (2000) discovered that they were unable to reproduce specific effects on endogenous mRNA or to generate mutant phenocopies using dsRNA. They showed that injection of dsRNA causes non-specific effects on phenotype and non-specific depletion of numerous mRNA species, irrespective of the sequence of the dsRNA. This study brings into question the validity of the use of RNAi in the zebrafish model and the general applicability of this method of mRNA depletion.

5.1.5.4 Mouse

It appears that a pathway, induced by dsRNA, can also specifically cause the suppression of gene expression in mammals. Potent and specific RNAi in mouse oocytes and embryos has been reported (Wianny and Zernicka-Goetz, 2000; Svoboda et al., 2000). Wianny and Zernicka-Goetz (2000) showed that dsRNA is a specific inhibitor of maternal *c-mos* in the oocyte and zygotic *E-cadherin* and *GFP* (transgenic) in the preimplantation embryo. The phenotypes observed were consistent with those reported for the null mutants of the endogenous genes. They showed by western blot that the protein levels of the target gene were also much reduced. The embryos subjected to RNAi mediated interference of *GFP* developed normally showing that RNAi does not interfere with normal development.

5.1.5.5 Mammalian cell line studies

Studies on RNAi in mammalian cell culture systems have demonstrated a prevalent and non-specific response to dsRNA using 3.8-1.6kb dsRNAs (Caplen et al., 2000, Ui-Tei et al., 2000). This result was somewhat surprising as dsRNA has been shown to cause PTGS in Rat-1 fibroblasts (Bahramiam and Zarbl, 1999) and Elbashir et al., (2001b) showed that 21nt siRNA (short interfering RNA) duplexes specifically suppress expression of endogenous genes in different mammalian cell lines including one derived from human embryonic kidney. Current opinion suggests that RNAi involves initial input dsRNA (>100bp) being cleaved into siRNAs which are thought to be the mediators for targeting mRNA degradation. Therefore, there are currently conflicting views

concerning the efficacy or generality of RNAi and/or siRNA; only time and carefully controlled experiments will display the true picture.

A possible explanation for non-specific effects of dsRNA is suggested to involve the interferon response. One component of the response to dsRNA in mammalian cells is mediated by the dsRNA-dependent protein kinase (PKR) which phosphorylates and inactivates the translation factor eIF2 α , leading to a generalised suppression of protein synthesis and in some cases apoptosis (Meurs et al., 1990, Zhou et al., 1999). Additionally, Tuschl et al., (1999) tested dsRNA *in vitro* in rabbit reticulocyte lysate and wheat-germ extract translation system. They found that dsRNA caused a profound, rapid and non-specific degradation of mRNA when using the rabbit reticulocyte lysate and that this was not apparent when using the wheat-germ extract. Furthermore, in Zebrafish, specific RNAi interference is probably obscured by the rapid induction of non-specific antiviral responses by dsRNA (Zhou et al., 1999).

5.1.5.6 *Xenopus*

In *Xenopus* it has been reported that dsRNA can cause knock down of specific, exogenous and endogenous, gene expression by RNAi. Oelgeschläger et al., 2000 showed that injection of *Xenopus Twisted gastrulation (xTsg)* dsRNA into *Xenopus* embryos specifically inhibited expression of secreted xTsg protein. xTsg ventralizes embryos by competing with CR1 (a product of chordin cleavage generated by Xolloid) for binding to BMP. Microinjection of xTsg dsRNA resulted in abnormal development of the postanal region, in particular loss of the ventral fin, an identical phenotype to that produced by injection of dominant-

negative *xTsg* (*dn-xTsg*) mRNA; it was not reported whether this phenotype could be rescued by co-injection of *xTsg* mRNA. Both *xTsg* RNAi and *dn-xTsg* greatly potentiated the dorsalizing effects of injection of CR1; it was reported that these effects could be partially rescued by co-injection of *xTsg* mRNA but that the rescue was more efficient for *dn-Tsg*.

Nakano et al., (2000) showed in embryos that expression of exogenous luciferase reporter under the control of a CMV promoter was reduced by around 40% on injection of luciferase specific dsRNA. They also showed that *Xlim-1* dsRNA injected into embryos resulted in embryonic phenotypes which included reduced eyes or anterior truncations. Embryos injected with *Xlim-1* antisense RNA also produced very similar phenotypes. Other defects were also seen including gastrulation defects, bent body or shortened A-P axis. These phenotypes were also present in the embryos injected with control dsRNA; the authors suggest that these may be non-specific dsRNA injection phenotypes. The level of endogenous *Xlim-1* mRNA was shown to be reduced by 30-40%, as shown by RT-PCR.

5.1.5.7 *Trypanosoma brucei*

In *Trypanosoma brucei*, Ngo et al., (1998) found that transient introduction of gene-specific dsRNAs resulted in selective degradation of the corresponding mRNAs.

5.1.5.8 *Planarians*

RNAi has been shown to have great potential for genetic analysis in organisms conventionally difficult to produce knockouts. In metazoan regeneration

research, the planarian is a classic model; one group have shown dsRNA knockouts for known genes involved in regeneration (Sanchez Alvarado and Newmark, 1999).

5.1.5.9 *Hydra magnipapillata*

RNAi has been shown to work well in *Hydra magnipapillata* and has allowed functional genetic tests to decipher known developmental gene functions (Lohmann et al., 1999).

5.1.6 The specificity, length, localisation, delivery and heritability of dsRNA for RNAi.

Evidence from numerous studies demonstrates that RNAi is sequence specific and the sequences must be carefully selected to avoid cross-interference (Fire et al., 1998). Although there is an example in *C.elegans* of RNAi induced by operon sequences, it is necessary for the sequences of RNAi to be exonic and not intronic (Bosher et al., 1999). Generally, the dsRNAs that have been shown to potently initiate RNAi are several hundred base pairs (bp) long.

Work conducted by Parrish et al., (2000) analysed the specificity, length and location of dsRNAs required for RNAi in *C.elegans*. The homology of the dsRNA versus the target mRNA was tested; 96% identity sufficed but when the identity was less than 80%, the effects were much reduced. The positional specificity of dsRNA sequences along the target mRNA was assessed using 5 non-overlapping dsRNAs and all but one gave the expected phenotype. The dsRNA that did not give the expected phenotype may have been directed to an

inaccessible region, possibly containing secondary structure in the mRNA. The length of dsRNAs required to trigger RNAi was tested. Double stranded RNAs between 26bp and 81bp were observed to trigger RNAi and cause the predicted phenotype although the 26bp dsRNA was required at 250 fold higher concentration than that of 81bp dsRNA (Parrish et al., 2000).

In contrast, *Hydra* RNAi requires a minimum length of 100 bp dsRNA, less than 100bp was ineffective, increasing from 100-450bp significantly increased the degradation of the corresponding mRNAs (Ngo et al., 1998). Tuschl et al., (1999) demonstrated that in *Drosophila* lysates, dsRNA of 49bp was ineffective whereas 149bp was enhanced and both 505bp and 997bp caused robust mRNA degradation. Another study in *Drosophila* analysed the mRNA substrate requirements, they found that substrates of 600bp and 1kb were degraded, reduced activity was detected with 220 and 300bp, and 100bp was resistant (Hammond et al., 2000).

Evidence from a number of studies suggest that the site of RNAi activity within the cell is cytoplasmic (Tuschl et al., 1999) and not nuclear. Work by Ngo et al., (1998) showed that levels of pre-mRNA are not affected (Northern blotting), so they suggested that either enzymes responsible for RNAi are not present in the nucleus or RNAi factors cannot act on pre-mRNA.

The delivery method of choice for the dsRNA is generally microinjection directly into the cell (Trypanosomes, *Hydra*), syncitial blastoderm (*Drosophila*), blastula stage embryos and oocytes (Zebrafish, *Xenopus* and mouse) or liposome

transfection (cell lines). In *C.elegans* experiments the dsRNA is delivered by injection into the germline, but injection into the intestines is just as potent. It is suggested that the dsRNA is transported along with yolk proteins, which are made in the gut, to the gonads through pores in the sheath cells surrounding the germline. It has been shown that feeding *C.elegans* with bacteria expressing the target gene dsRNA targeting construct (Timmons & Fire, 1998, Kamath et al 2000) or just soaking the worms in a solution containing dsRNA (Tabara et al., 1998) is effective.

Injection of dsRNA into the gonad of *C.elegans* results in RNAi in 100% of the F1 progeny but no inheritance beyond that generation. Methods of penetrance have been devised to overcome this problem in *C.elegans* (Tavernarakis et al., 2000).

Plasmids carrying inducible hairpin target gene constructs have been developed. The target sequence is organised as an inverted repeat and is injected into the gonad. Using a strong heat-shock promoter the RNAi phenotype is produced. Transgenic lines are easy to produce and the transgene is inherited by future generations. Large numbers of transgenic animals can be produced, and because it is inducible it allows stage specific gene analysis. Genes which have essential early function, especially those which are early mutant-lethal, can be studied at a later time point (Tavernarakis et al., 2000). This method has also been successfully applied to *Drosophila* (Kennerdall and Carthew, 2000).

5.1.7 The current model of RNAi induced mRNA degradation

All studies conducted thus far agree that RNAi is mediated by sequence specific dsRNA, which is more potent than antisense or sense strands alone. The response to dsRNA is the degradation of its specific cognate mRNA which leads to the repression of target gene expression. Permanent gene modification or disruption of transcription have been experimentally eliminated as the mechanism of RNAi (Montgomery et al., 1998).

The current accepted model of RNAi is as follows (figure 5.1):

Step 1: Recognition and cleavage of dsRNA

The process begins with the binding of a dsRNA-processing protein complex to the dsRNA (blue, sense and green, antisense ovals). The dsRNA is cleaved into 21-23nt fragments with staggered 3' ends (siRNA) in a process likely to involve RNase III-like activity (Nicholson, 1999; Bass, 2000). Recently, an RNase III encoded by *Drosophila Dicer*, has been shown to be capable of cleaving dsRNA into 22bp fragments and is suggested to be involved in the initiation of RNAi (Bernstein et al., 2001). Interestingly, the Dicer protein also contains a PAZ motif restricted to gene families already known to be involved in RNAi induced mRNA degradation (*qde-2* and *rde-1*).

Step 2: Dissociation

The resulting short interfering RNAs (siRNAs) remain associated with the RNA-specific proteins (blue and green ovals) and is termed the small interfering ribonucleo-protein complex (siRNP). The separation of the two strands of the dsRNA following cleavage may require an ATP-dependent RNA helicase, the

protein encoded by the *mut-7* gene may be a candidate for this activity (Ketting, 1999).

Figure 5.1

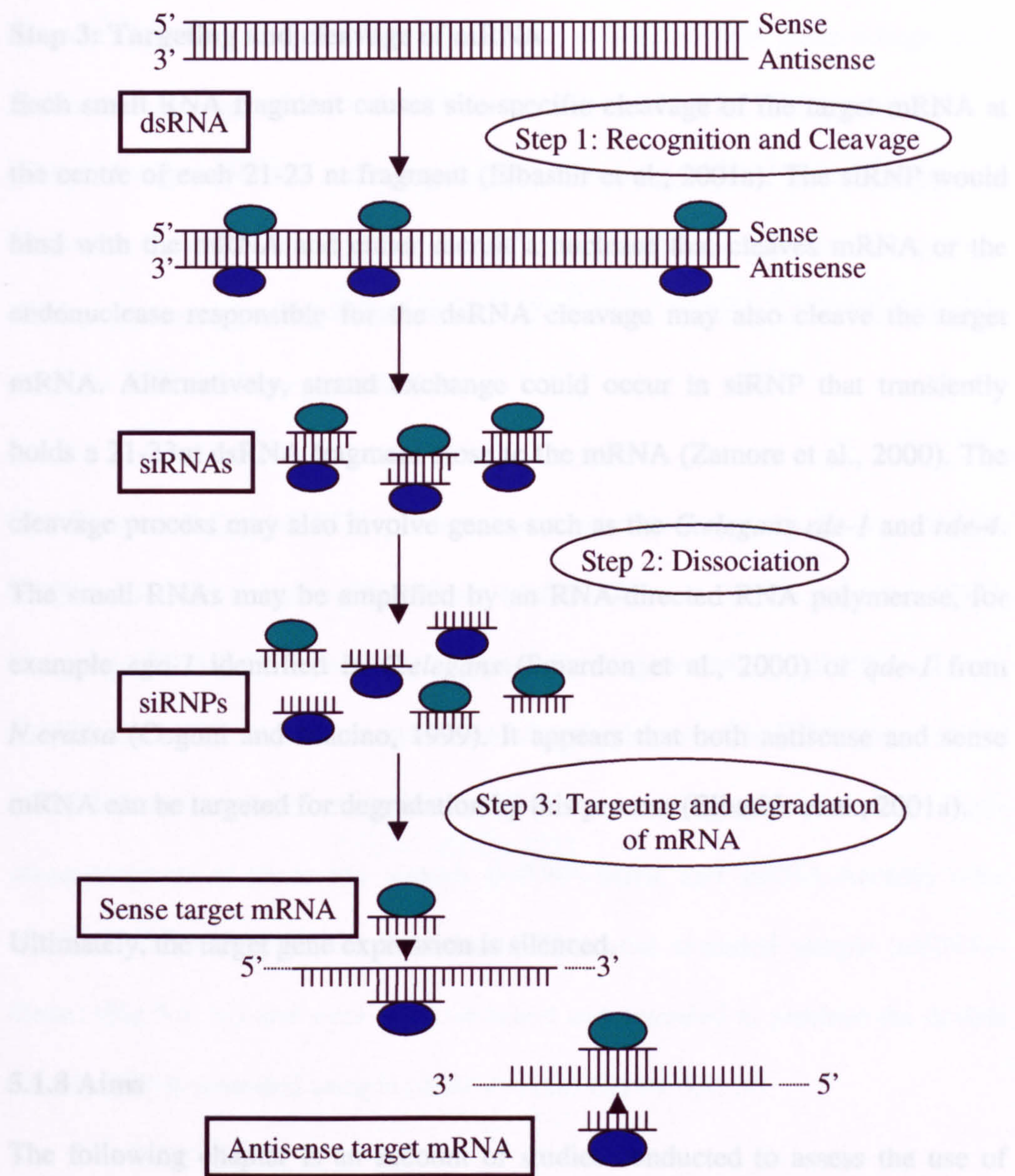


Figure 5.1: A proposed model for RNA interference (RNAi). The first step in RNAi is the recognition and processing of the dsRNA into 21-22nt short interfering RNAs (siRNA). The process involves the binding of the dsRNA-processing protein complex to the dsRNA (represented by the blue, sense and green, antisense ovals). This complex mediates the cleavage of the dsRNA into 21-22nt siRNAs with short (1-3nt) 3' overhangs. Step 2: The dsRNA-processing complex remains bound and the siRNAs are then dissociated by a helicase into ssRNAs forming the siRNPs. Step 3: Targeting and degradation of mRNA. Either the edonuclease contained in the siRNP or a recruited exonuclease would then cleave the mRNA:siRNA duplex at target sites in the centre of the 21nt siRNA, leading to depletion of target mRNA (Adapted from Elbashir et al., 2001a).

protein encoded by the *mut-7* gene may be a candidate for this activity (Ketting, 1999).

Step 3: Targeting and cleavage of mRNA

Each small RNA fragment causes site-specific cleavage of the target mRNA at the centre of each 21-23 nt fragment (Elbashir et al., 2001a). The siRNP would bind with the mRNA and either recruit a nuclease that cleaves mRNA or the endonuclease responsible for the dsRNA cleavage may also cleave the target mRNA. Alternatively, strand exchange could occur in siRNP that transiently holds a 21-23nt dsRNA fragment close to the mRNA (Zamore et al., 2000). The cleavage process may also involve genes such as the *C.elegans rde-1* and *rde-4*. The small RNAs may be amplified by an RNA-directed RNA polymerase, for example *ego-1* identified in *C.elegans* (Smardon et al., 2000) or *qde-1* from *N.crassa* (Cogoni and Macino, 1999). It appears that both antisense and sense mRNA can be targeted for degradation by this process (Elbashir et al., 2001a).

Ultimately, the target gene expression is silenced.

5.1.8 Aims

The following chapter is an account of studies conducted to assess the use of dsRNA to perturb the expression of *Xanx-4* in *Xenopus laevis*.

5.2 Results

5.2.1 Production of single stranded and double stranded RNAs.

In order to test whether RNAi could be used to interfere with *Xanx-4* expression in *Xenopus*, a range of *Xanx-4* dsRNAs were prepared. The PCR products, Short (74bp), Long-1 (367bp) and Long-2 (367bp) were generated using the primers shown in figure 5.2 and table 2.3. The *Xanx-4* specific primers incorporated RNA polymerase binding sequences at their 5' ends, allowing for RNA synthesis from the PCR products generated.

The Short and Long-1 PCR products were used as templates to generate the dsRNAs double stranded RNA-Short (dsRNA-S) and double stranded RNA-Long-1 (dsRNA-L1) respectively (figure 5.3). To generate control RNAs, Long-2 PCR product was used to synthesise the single stranded RNA sense strand (ssRNA-Sense) and antisense strand (ssRNA-Asense) (figure 5.4, i and ii). Equimolar amounts of these two strands (ssRNA-Sense and ssRNA-Asense) were combined to produce the single stranded RNAs-not annealed sample (ssRNAs-Nann) (Fig 5.4, iii) and were also combined and annealed to produce the double stranded RNA-annealed sample (dsRNA-Ann) (figure 5.4, iv).

All RNAs were visualised on an agarose gel (figure 5.5A), quantitated by UV absorbance and diluted to 500µg/ml. *Xanx-4* mRNA was transcribed from *SfiI* linearised *Xanx-4*/RN3 construct (appendix 2) using T3 polymerase and diluted to 250µg/ml. For a specificity control, XEZ (Barnett et al., 2001) dsRNA was transcribed using T7 polymerase from XEZ PCR product previously amplified

Figure 5.2

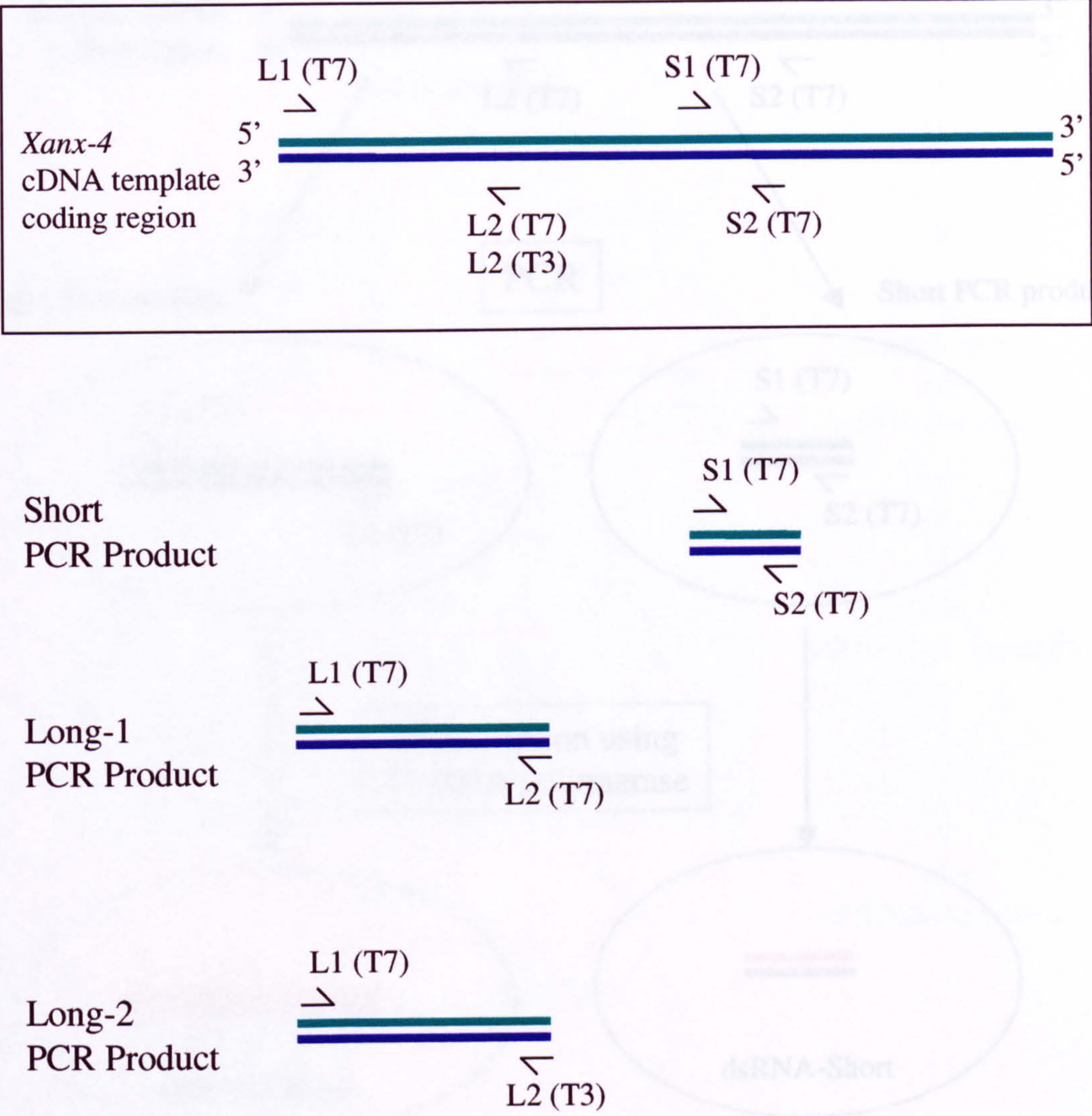


Figure 5.2: PCR products amplified from *Xanx-4* cDNA used to generate dsRNA templates. The position of the primers L1(T7), L2(T7), L2(T3), S1(T7) and S2(T7) on the *Xanx-4* cDNA template coding region is shown in the box. Below shows the combinations of primers used in the PCR to generate the individual PCR products Short, Long-1 and Long-2.

Figure 5.3

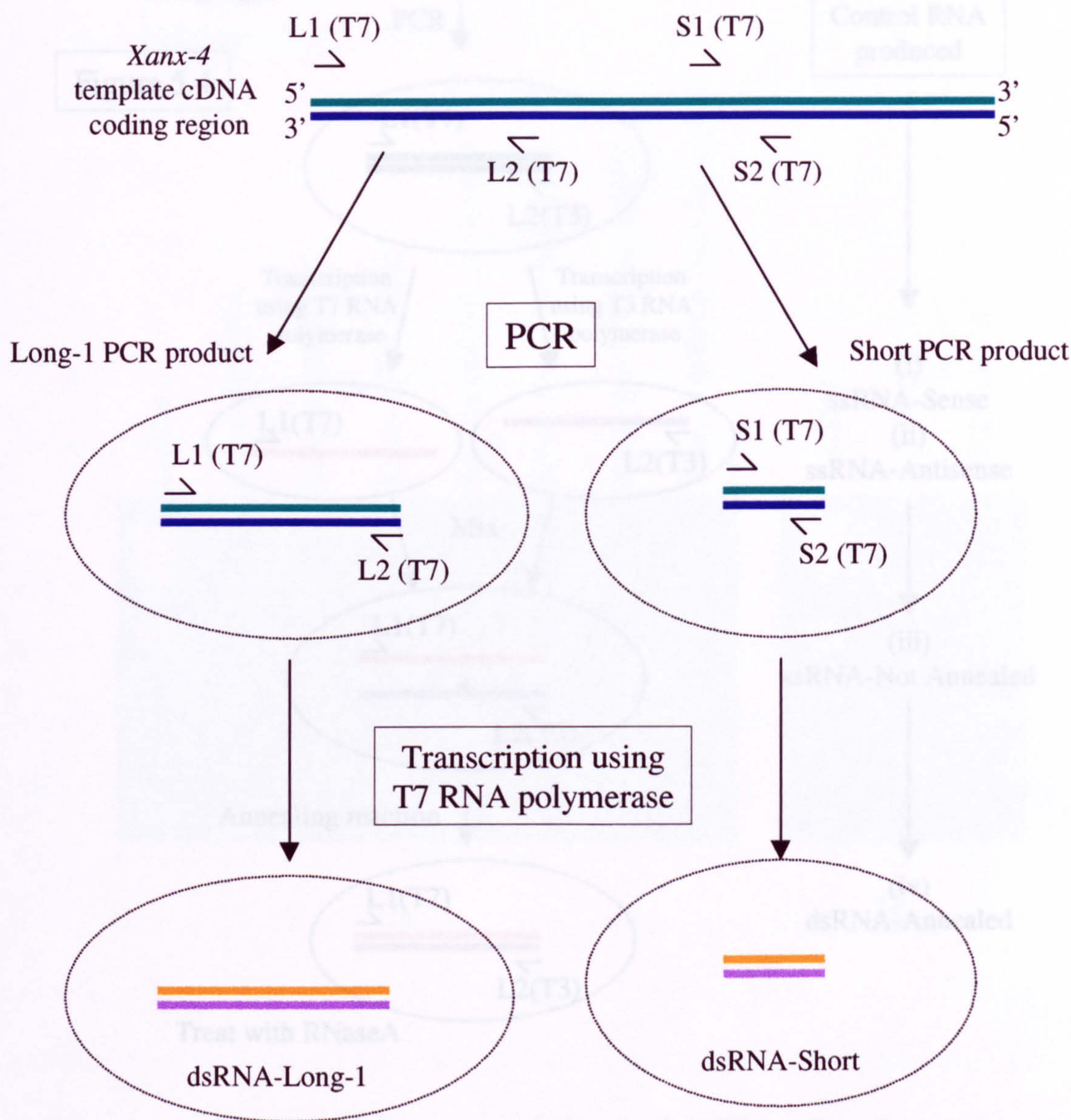


Figure 5.3: Generation of dsRNAs from PCR templates for use in RNAi experiments. The flow diagram demonstrates the process of generating the dsRNA-Long-1 and dsRNA-Short. To synthesise dsRNA-Long-1, Long-1 PCR product is amplified from *Xanx-4* cDNA coding region template using primers L1(T7) and L2(T7) and transcribed using T7 RNA polymerase. To synthesise dsRNA-Short, Short PCR product is amplified from *Xanx-4* cDNA coding region template using primers S1(T7) and S2(T7) and transcribed using T7 RNA polymerase.

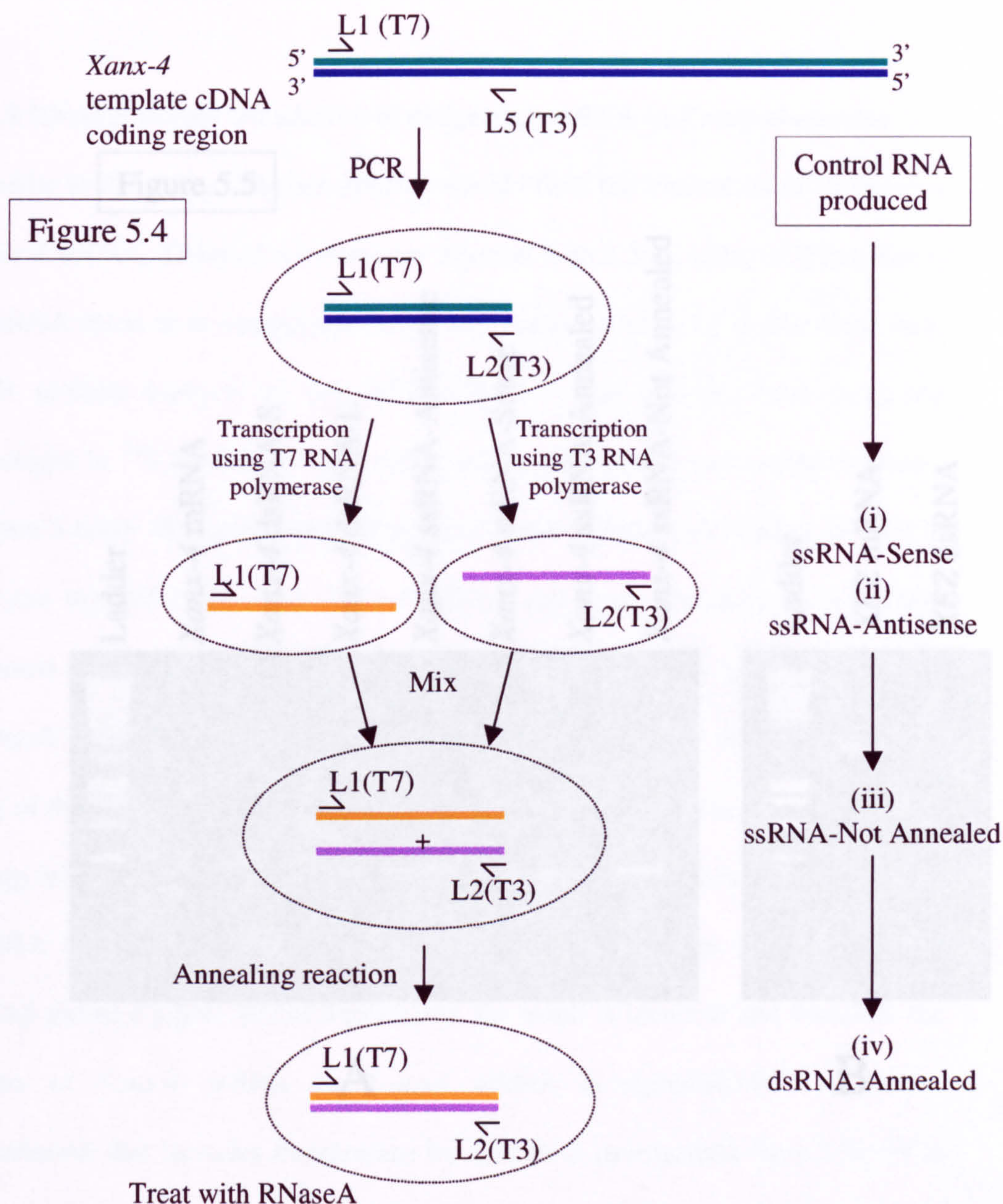


Figure 5.4: Generation of control ssRNAs and dsRNAs. The flow diagram demonstrates the process of generating the control ssRNA-Sense and ssRNA-Antisense, the ssRNA-Not annealed and the dsRNA-Annealed. To synthesise ssRNA-Sense and ssRNA-Antisense, Long-2 PCR product is amplified from *Xanx-4* cDNA coding region template using primers L1(T7) and L2(T3). A transcription reaction using Long-2 PCR product as template and T7 RNA polymerase results in the production of ssRNA-Sense, and using T3 RNA polymerase produces ssRNA-Antisense. Mixing of equal amounts of ssRNA-Sense and ssRNA-Antisense allows the production of ssRNA-Not annealed. The dsRNA-Annealed is prepared by mixing equal amounts of ssRNA-Sense and ssRNA-Antisense and performing an annealing reaction. The dsRNA-Annealed is purified by treatment with RNase A to degrade any contaminating ssRNAs.

Figure 5.5

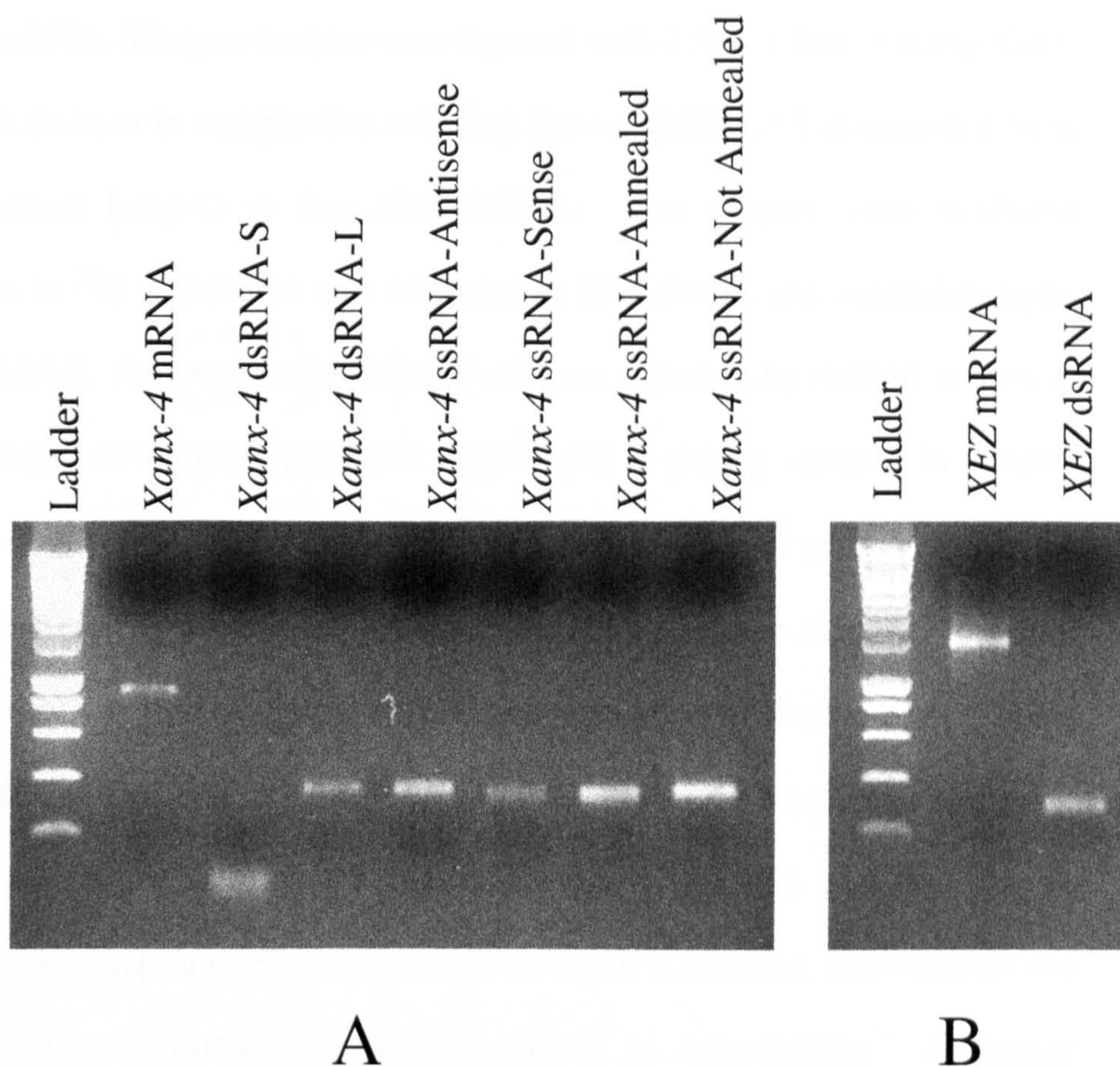


Figure 5.5: The mRNAs, ssRNAs and dsRNAs used in RNAi experiments. An agarose gel showing all the ssRNAs and dsRNAs used in the RNAi experiments, including *Xanx-4* mRNA, dsRNA-Short, dsRNA-Long and control RNAs (A). XEZ mRNA and XEZ dsRNA which, were used as controls (B).

with primers XEZR1 and XEZR2 (table 2.3), visualised on an agarose gel (figure 5.5B) and diluted to 500µg/ml.

5.2.2 RNAi prevents translation of exogenous mRNA in *Xenopus* oocytes.

In order to determine whether dsRNA would effect the translation of exogenous *Xanx-4* mRNA, *Xenopus* oocytes were injected with 2.5ng, 1.0ng or 0.5ng *Xanx-4* mRNA alone or in combination with 5ng *Xanx-4* dsRNA-L1 (transcribed from PCR product Long-1) or 5ng XEZ dsRNA. The oocytes were incubated overnight in ³⁵S methionine and subjected to SDS-PAGE and autoradiography (figure 5.6Ai). Reduction of translation of *Xanx-4* protein by dsRNA is seen in oocytes injected with 1.0ng *Xanx-4* mRNA and is greatly reduced in oocytes injected with 0.5ng *Xanx-4* mRNA. Translation of *Xanx-4* protein in oocytes injected with 2.5ng *Xanx-4* mRNA is unaffected by *Xanx-4* dsRNA. Therefore 5ng of dsRNA is able to significantly reduce translation of *Xanx-4* protein when 0.5ng mRNA is injected. XEZ dsRNA had no effect on the translation of *Xanx-4* mRNA and the interference by *Xanx-4* dsRNA is therefore specific. Figure 5.6Aii shows a repeat of this experiment, the result is identical and therefore the effect of *Xanx-4* dsRNA on *Xanx-4* mRNA is reproducible. A further experiment that includes interference by dsRNA-S (transcribed from 74bp PCR product Short) is shown in figure 5.6B; *Xanx-4* protein translation is perturbed by both of the dsRNAs, showing that in oocytes dsRNA from 74bp to 367bp can be effective in preventing *Xanx-4* translation.

To assess the effect of ssRNAs compared to dsRNAs, on the translation of exogenous *Xanx-4* mRNA, oocytes were injected with 0.5ng *Xanx-4* mRNA

Figure 5.6

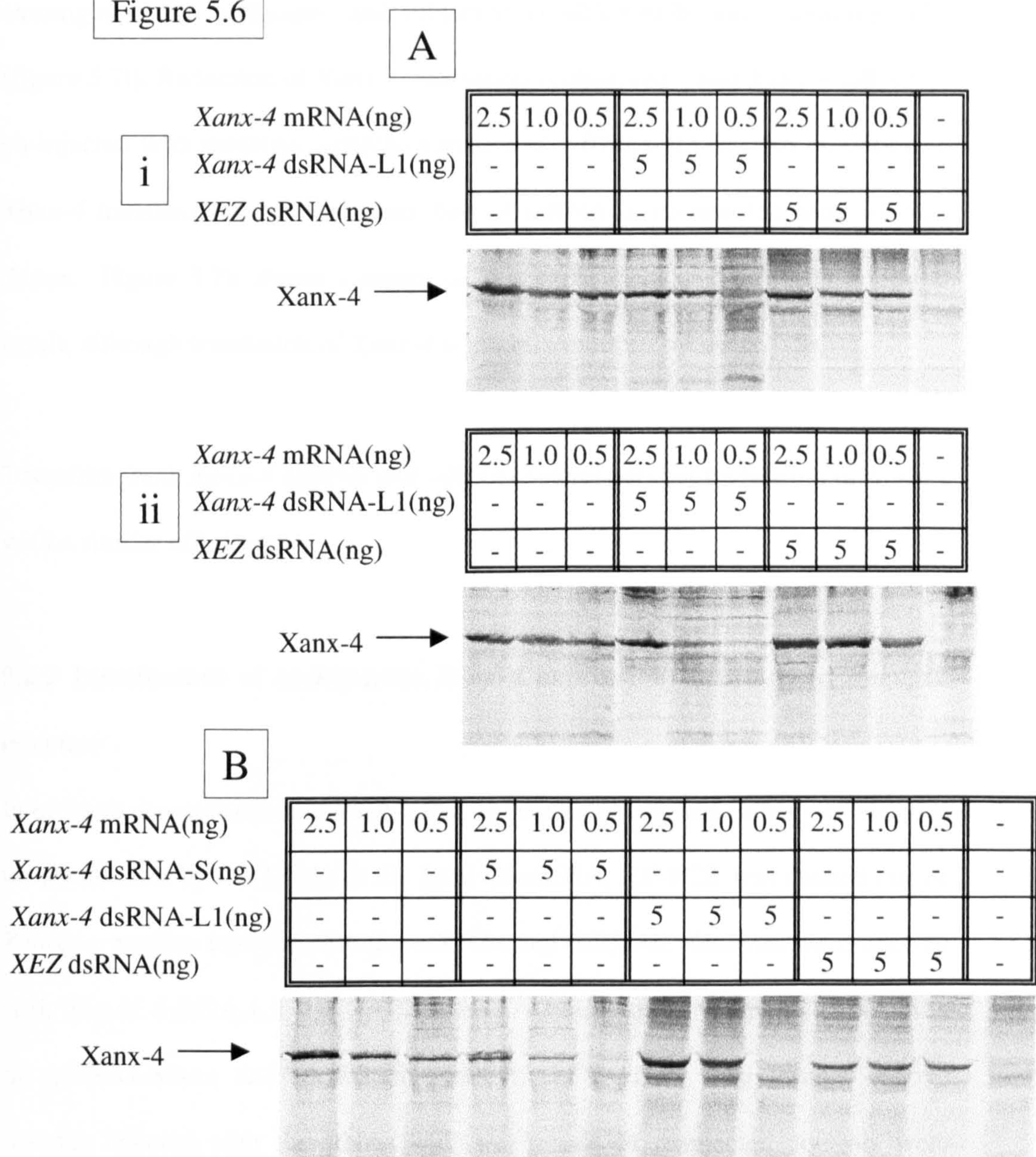


Figure 5.6: *Xanx-4* dsRNA-Long-1 and dsRNA-Short prevents translation of exogenous *Xanx-4* mRNA in *Xenopus* oocytes. *Xenopus* oocytes were injected with 2.5ng, 1.0ng or 0.5ng *Xanx-4* mRNA alone or in combination with 5ng *Xanx-4* dsRNA-L1 or 5ng *XEZ* dsRNA. The oocytes were incubated overnight in ³⁵S methionine and subjected to SDS-PAGE and autoradiography. The results show that dsRNA-Long-1 is able to deplete *Xanx-4* mRNA translation (Ai). It appears that 5ng of *Xanx-4* dsRNA is able to deplete 0.5ng of *Xanx-4* mRNA. *XEZ* dsRNA no effect on translation of *Xanx-4* mRNA. In a repeat of the experiment (Aii) similar results were observed. The results shown in B, demonstrate that *Xanx-4* dsRNA-Short is also capable of depleting *Xanx-4* mRNA translation to a similar extent to that of *Xanx-4* dsRNA-Long-1.

alone or in combination with 5ng dsRNA-L1, dsRNA-S, ssRNA-Asense, ssRNA-Sense, dsRNA-Ann or ssRNAs-NAnn. The oocytes were incubated overnight in ^{35}S methionine and subjected to SDS-PAGE and autoradiography (figure 5.7i). Reduction of *Xanx-4* translation is observed when *Xanx-4* mRNA is co-injected with dsRNAs, ssRNA-Asense and ssRNAs-NAnn. No reduction in *Xanx-4* translation was seen when *Xanx-4* mRNA is co-injected with ssRNA-Sense. Figure 5.7ii shows a repeat of this experiment and provides a similar result, although translation of *Xanx-4* is slightly reduced by ssRNA-Sense.

Therefore, both *Xanx-4* dsRNA and ssRNA-Asense prevent translation of *Xanx-4* with a similar efficiency.

5.2.3 Interference of endogenous *Xanx-4* expression by RNAi in *Xenopus* oocytes.

In order to determine whether the effect on protein expression in oocytes was due to interference by the RNAs at the level of mRNA, RT-PCR was carried out on *Xenopus* oocytes injected with the ssRNAs and dsRNAs. Oocytes were injected with 5ng of dsRNA-L1, dsRNA-S, ssRNA-Asense, ssRNA-Sense, dsRNA-Ann or ssRNAs-NAnn and incubated overnight in BarthX. Two groups of five oocytes injected with the RNAs and two groups of uninjected controls were selected at random and subjected to RT-PCR using *Xanx-4* specific primers (Figure 5.8i). *Xanx-4* expression is much reduced by ssRNA-Asense and ssRNAs-NAnn in one of the two duplicates and slightly reduced in dsRNA-L1 and dsRNA-Ann. However, figure 5.8ii shows a repeat of this experiment where *Xanx-4* expression is slightly reduced only in the dsRNA-S and dsRNA-L1

Figure 5.7

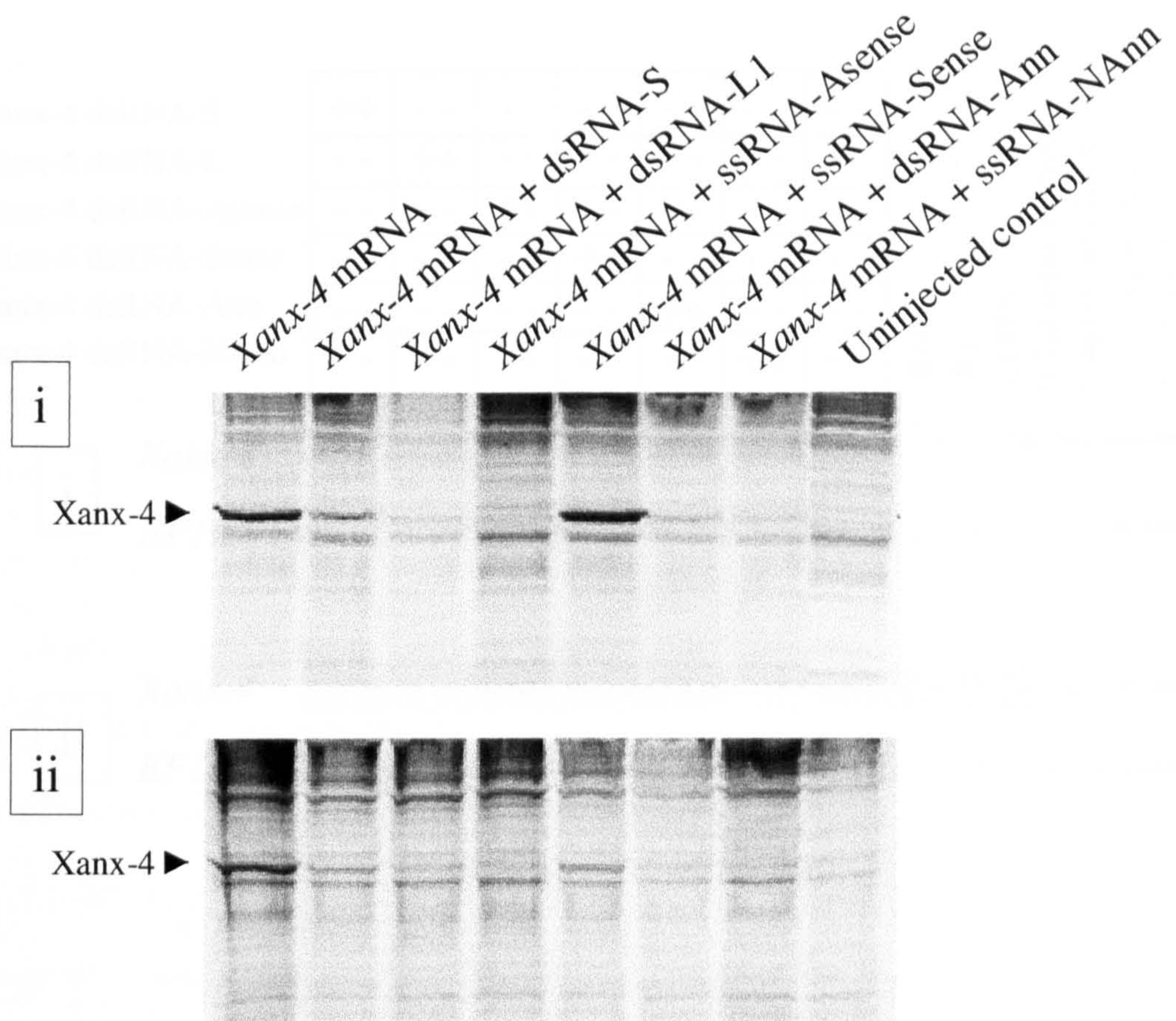


Figure 5.7: The effect of control *Xanx-4* ssRNAs and dsRNAs compared to *Xanx-4* dsRNA-Short and dsRNA-Long-1 on the translation of exogenous *Xanx-4* mRNA in oocytes. *Xenopus* oocytes were injected with 0.5ng *Xanx-4* mRNA alone or in combination with 5ng dsRNA-L1, dsRNA-S, ssRNA-Asense, ssRNA-Sense, dsRNA-Ann or ssRNAs-Nann. The oocytes were incubated overnight in ^{35}S methionine and subjected to SDS-PAGE and autoradiography (i). Reduction of Xanx-4 protein translation is observed when *Xanx-4* mRNA is co-injected with the three dsRNAs, ssRNA-Asense and ssRNAs-Nann. No reduction in Xanx-4 protein translation is seen when *Xanx-4* mRNA is co-injected with ssRNA-Sense. (ii) shows a repeat of this experiment and provides a similar result, although translation of Xanx-4 protein is slightly reduced by ssRNA-Sense.

Figure 5.8

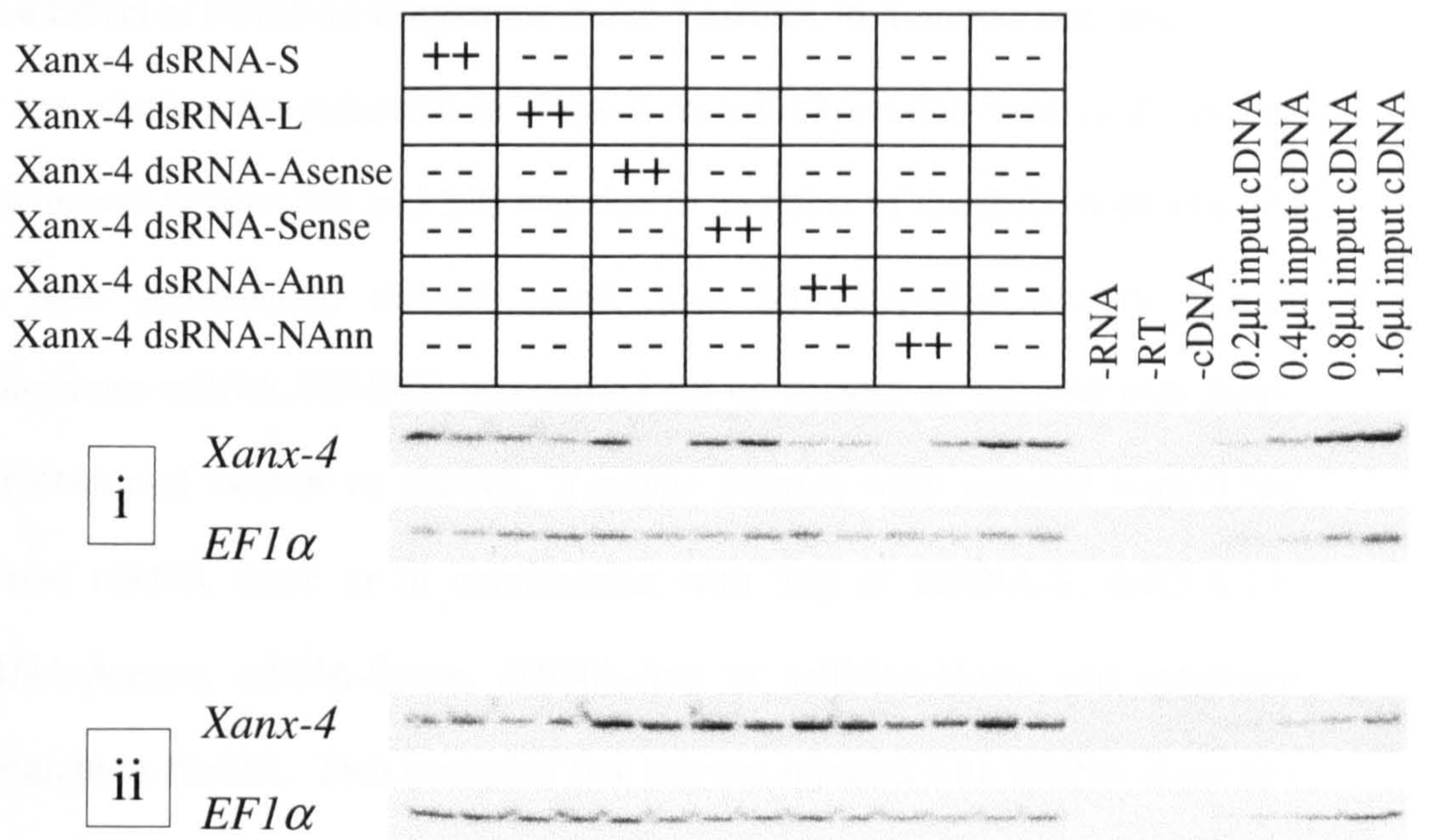


Figure 5.8: Interference of endogenous *Xanx-4* expression by *Xanx-4* dsRNA and ssRNA in *Xenopus* oocytes determined by RT-PCR. Oocytes were injected with 5ng of dsRNA-L1, dsRNA-S, ssRNA-Asense, ssRNA-Sense, dsRNA-Ann or ssRNAs-Nann and incubated overnight in BarthX. Two groups of five oocytes injected with the RNAs and two groups of uninjected controls were selected at random and subjected to RT-PCR using *Xanx-4* specific primers (i). *Xanx-4* expression is much reduced by ssRNA-Asense and ssRNAs-Nann in one of the two duplicates and slightly reduced in dsRNA-L1 and dsRNA-Ann. However, a repeat of this experiment shows *Xanx-4* expression is slightly reduced only in the dsRNA-S and dsRNA-L1 groups and no reduction was seen in ssRNA-Asense or ssRNAs-Nann (ii). *EF1α* was used as a loading control.

groups and no reduction was seen in ssRNA-Asense or ssRNAs-NAnn. Therefore it appears any reduction in *Xanx-4* expression seen in the endogenous mRNA level is very small and not reproducible using oocytes from different frogs.

5.2.4 Effect of RNAi on exogenous *Xanx-4* mRNA in *Xenopus* oocytes.

To test whether the reduction in *Xanx-4* protein expression seen in the oocyte experiments (Figure 5.6 and 5.7) was due to an effect of the dsRNA on injected (*in vitro* synthesised) mRNA alone, with no detectable activity against endogenous mRNA, RT-PCR was carried out on oocytes co-injected with *Xanx-4* mRNA and ssRNA or dsRNA. *Xenopus* oocytes were injected with 0.5ng *Xanx-4* mRNA alone or in combination with 5ng of dsRNA-S, dsRNA-L1, ssRNA-Asense, ssRNA-Sense, dsRNA-Ann or ssRNAs-NAnn and incubated overnight in BarthX. Two groups of five oocytes injected with mRNA alone and in combination with each RNA together with two groups of uninjected controls, were selected at random and subjected to RT-PCR (Figure 5.9i). A slight reduction of *Xanx-4* expression was seen in the groups injected with dsRNA-S, dsRNA-L1 and ssRNAs-NAnn. However, in a repeat experiment (figure 5.9ii) all RNAs lowered the level of mRNA detectable when compared to mRNA alone. It appears that the different RNA samples may indeed have an effect on the *Xanx-4* mRNA level that is detectable, but in a non-reproducible manner.

Figure 5.9

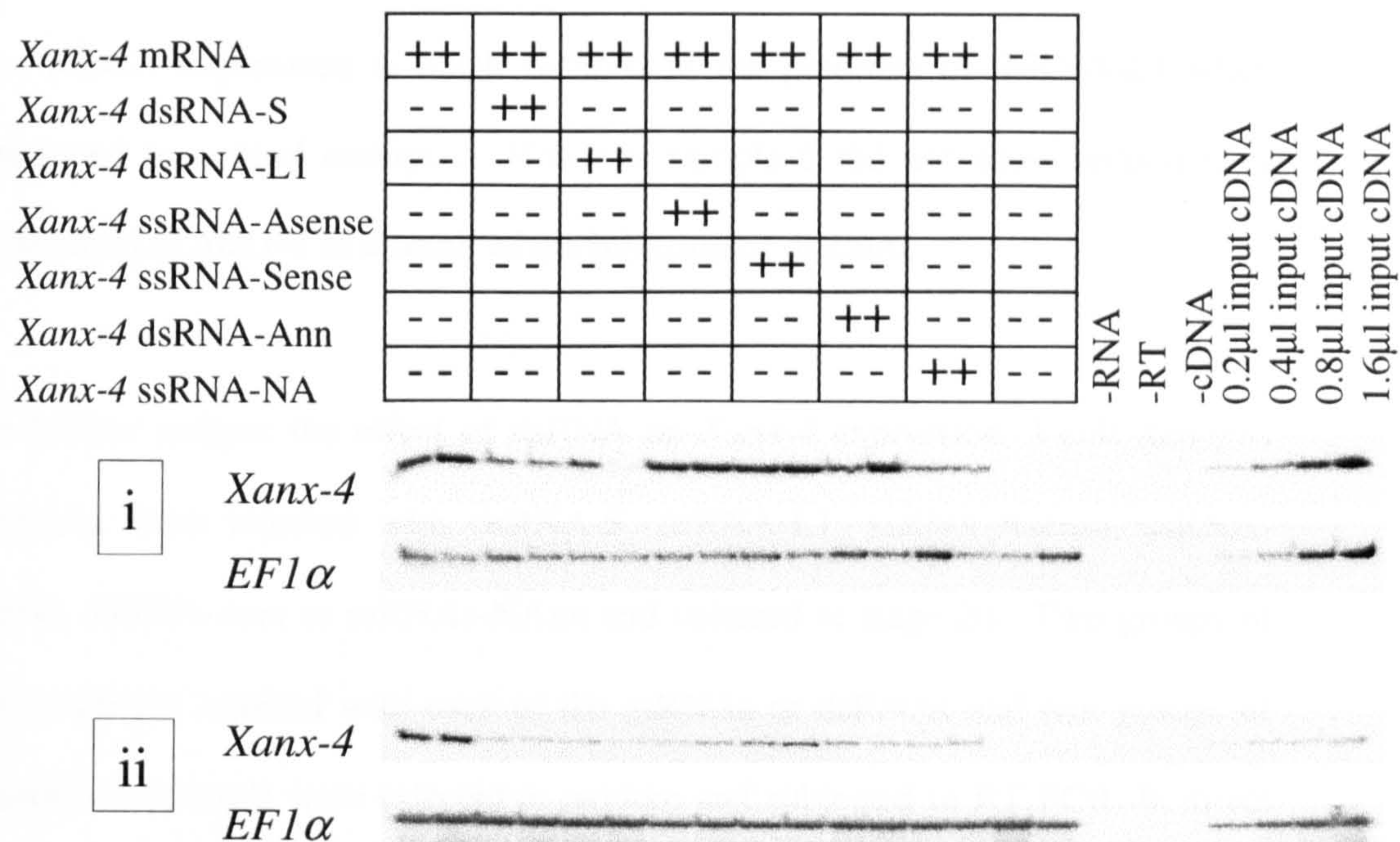


Figure 5.9: The effect of *Xanx-4* dsRNA and ssRNA on exogenous *Xanx-4* mRNA in *Xenopus* oocytes as determined by RT-PCR. *Xenopus* oocytes were injected with 0.5ng *Xanx-4* mRNA alone or in combination with 5ng of *Xanx-4* dsRNA-S, dsRNA-L1, ssRNA-Asense, ssRNA-Sense, dsRNA-Ann or ssRNAs-Nann and incubated overnight in BarthX. Two groups of five oocytes injected with mRNA alone and in combination with each RNA together with two groups of uninjected controls, were selected at random and subjected to RT-PCR (i). A slight reduction of *Xanx-4* expression was seen in the groups injected with dsRNA-S, dsRNA-L1 and ssRNAs-Nann. However, in a repeat experiment (ii) all RNAs lowered the level of mRNA detectable when compared to mRNA alone. *EF1α* was used as a loading control.

5.2.5 Interference of endogenous *Xanx-4* expression by RNAi in *Xenopus* embryos.

To investigate whether dsRNA would have an effect on endogenous *Xanx-4* mRNA expression in embryos, a pilot experiment was carried out. 1-cell *Xenopus* embryos were injected with 5ng dsRNA-L1 and cultured to stage 13. Six groups of two embryos injected with dsRNA and six groups of uninjected controls were selected at random and subjected to RT-PCR. Figure 5.10 shows that *Xanx-4* expression is much reduced in the presence of dsRNA-L1 when compared to control embryos. However sample 5 did not show reduction of expression of *Xanx-4* as a result of the injection of dsRNA.

To further analyse the effect of dsRNA on *Xanx-4* expression, 1-cell *Xenopus* embryos were injected with dsRNA-S, dsRNA-L1, ssRNA-Asense, ssRNA-Sense, dsRNA-Ann or ssRNAs-NAnn and cultured to stage 20. Two groups of five embryos injected with each of the ssRNAs or dsRNAs and two groups of uninjected controls were selected at random and subjected to RT-PCR. In direct contrast to the previous experiment (figure 5.10) figure 5.11i shows that *Xanx-4* expression is unaffected by the different dsRNAs and the ssRNAs. Similarly a repeat experiment (figure 5.11ii), using embryos from different frogs yielded the same result. These experiments suggests that dsRNA may indeed be able to affect levels of gene expression at certain embryonic stages, but in an unreliable and non-reproducible manner.

Figure 5.10

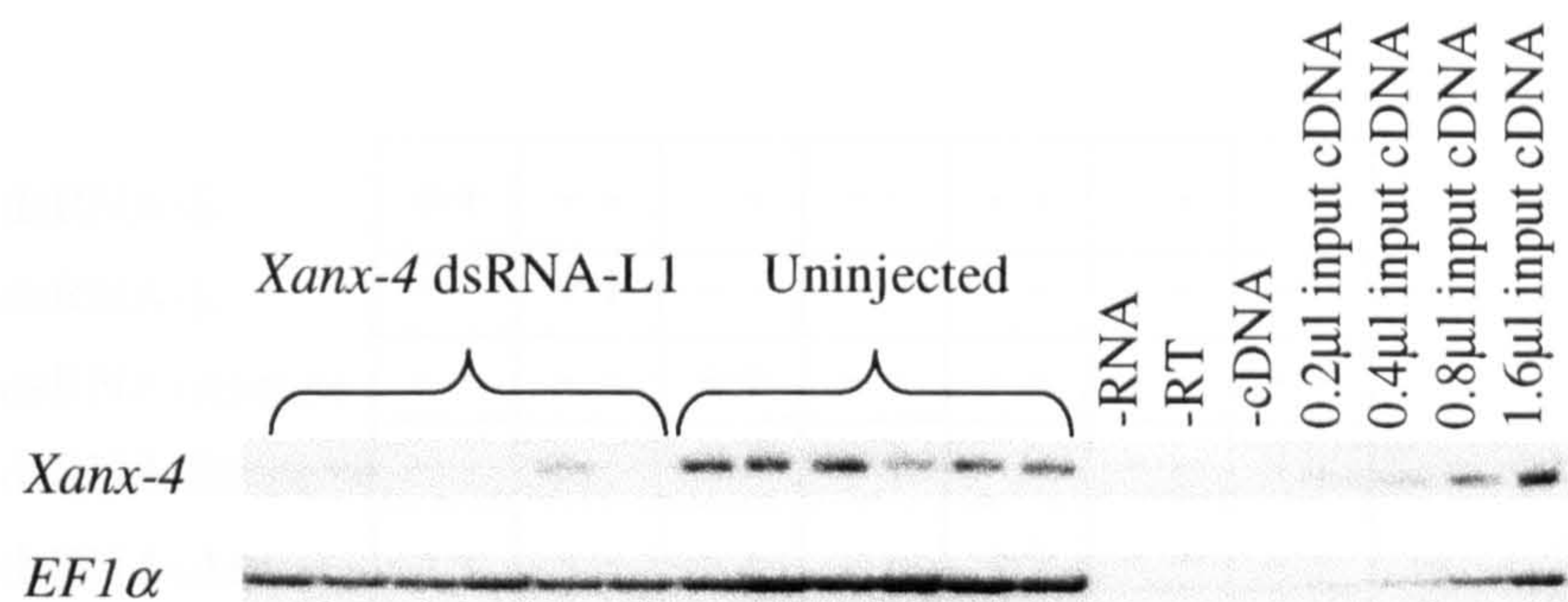


Figure 5.10: The interference of endogenous *Xanx-4* expression by *Xanx-4* dsRNA-Long-1 in stage 13 *Xenopus* embryos determined by RT-PCR. 1-cell *Xenopus* embryos were injected with 5ng *Xanx-4* dsRNA-L1 and cultured to stage 13. Six groups of two embryos injected with *Xanx-4* dsRNA and six groups of uninjected controls were selected at random and subjected to RT-PCR. *Xanx-4* expression is much reduced in the presence of dsRNA-L1 when compared to control. embryos. However sample 5 did not show reduction of expression of *Xanx-4* as a result of the injection of dsRNA. *EF1α* was used as a loading control.

Figure 5.11

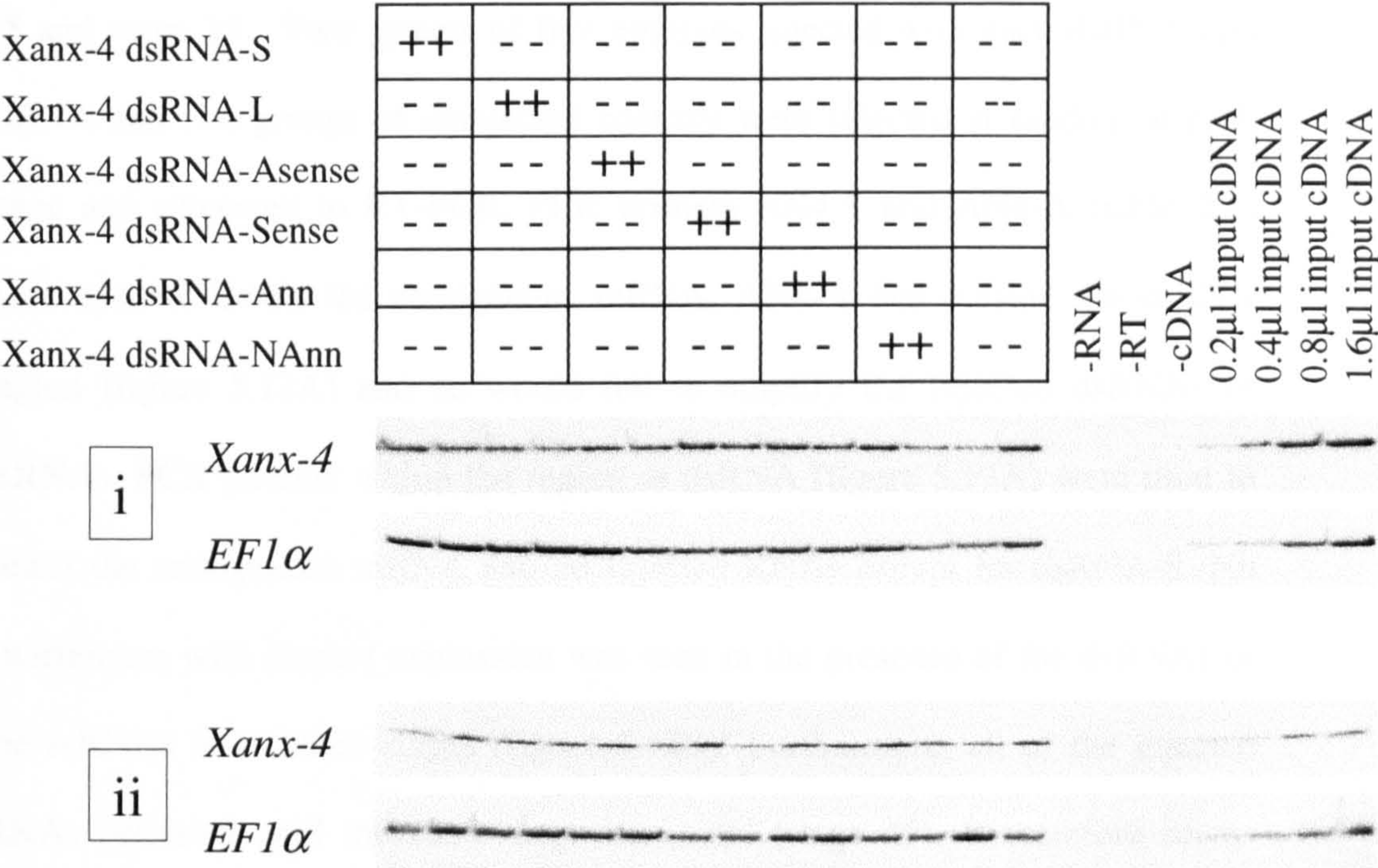


Figure 5.11: The interference of endogenous *Xanx-4* expression by *Xanx-4* dsRNAs and ssRNAs in stage 20 *Xenopus* embryos determined by RT-PCR. 1-cell *Xenopus* embryos were injected with dsRNA-S, dsRNA-L1, ssRNA-Asense, ssRNA-Sense, dsRNA-Ann or ssRNAs-Nann and cultured to stage 20. Two groups of five embryos injected with each ssRNA, ssRNAs or dsRNA and two groups of uninjected controls were selected at random and subjected to RT-PCR (i). In direct contrast to the previous experiment (figure 5.10) this result shows that *Xanx-4* expression is unaffected by the three different dsRNAs, the two ssRNAs and ssRNAs Nann. Similarly a repeat experiment (ii), using embryos from different frogs yielded the same result. *EF1α* was used as a loading control.

5.2.6 Persistence of dsRNA in *Xenopus* embryos

Due to the interference of *Xanx-4* expression by dsRNA observed in embryos harvested at stage 13 (Figure 5.10) and the lack of interference observed in embryos harvested at stage 20 (Figure 5.11), the persistence of dsRNA in *Xenopus* embryos was analysed in embryos at different stages of development. 1-cell *Xenopus* embryos were injected with dsRNA-S, dsRNA-L1, ssRNA-Asense, ssRNA-Sense, dsRNA-Ann or ssRNAs-NAnn and cultured to stage 12.5, stage 25 and stage 35. Two groups of five embryos injected with each dsRNA and ssRNA and two groups of uninjected controls were selected at random at each stage and subjected to RT-PCR. PCR primers AN4-S and AN4-A (table 2.1) were used to detect the endogenous mRNA. AN4-A lies outside the dsRNA region (figure 5.12A) and so would fail to amplify the injected dsRNAs or ssRNAs. PCR primers within the region of dsRNA (figure 5.12A) were used to detect the endogenous mRNA and all injected RNAs except for dsRNA-S. No interference with *Xanx-4* expression was seen in the presence of the dsRNAs or the ssRNAs at all three stages (figure 5.12B). Furthermore, all of the injected RNAs persisted until the latest stage harvested (stage 35). It therefore seems unlikely that the discrepancy between the two previous experiments (Figure 5.10 and 5.11) was due to a lack of persistence of injected dsRNA.

5.2.7 Effect of RNAi on exogenous *Xanx-4* mRNA in *Xenopus* embryos.

Due to the effect of injected dsRNA on exogenous *Xanx-4* mRNA in *Xenopus* oocytes (Figures 5.6 and 5.7), an experiment was performed to ascertain whether dsRNA has an effect on exogenous injected *Xanx-4* mRNA in *Xenopus* embryos. 1-cell *Xenopus* embryos were injected with 0.5ng *Xanx-4* mRNA alone or in

Figure 5.12

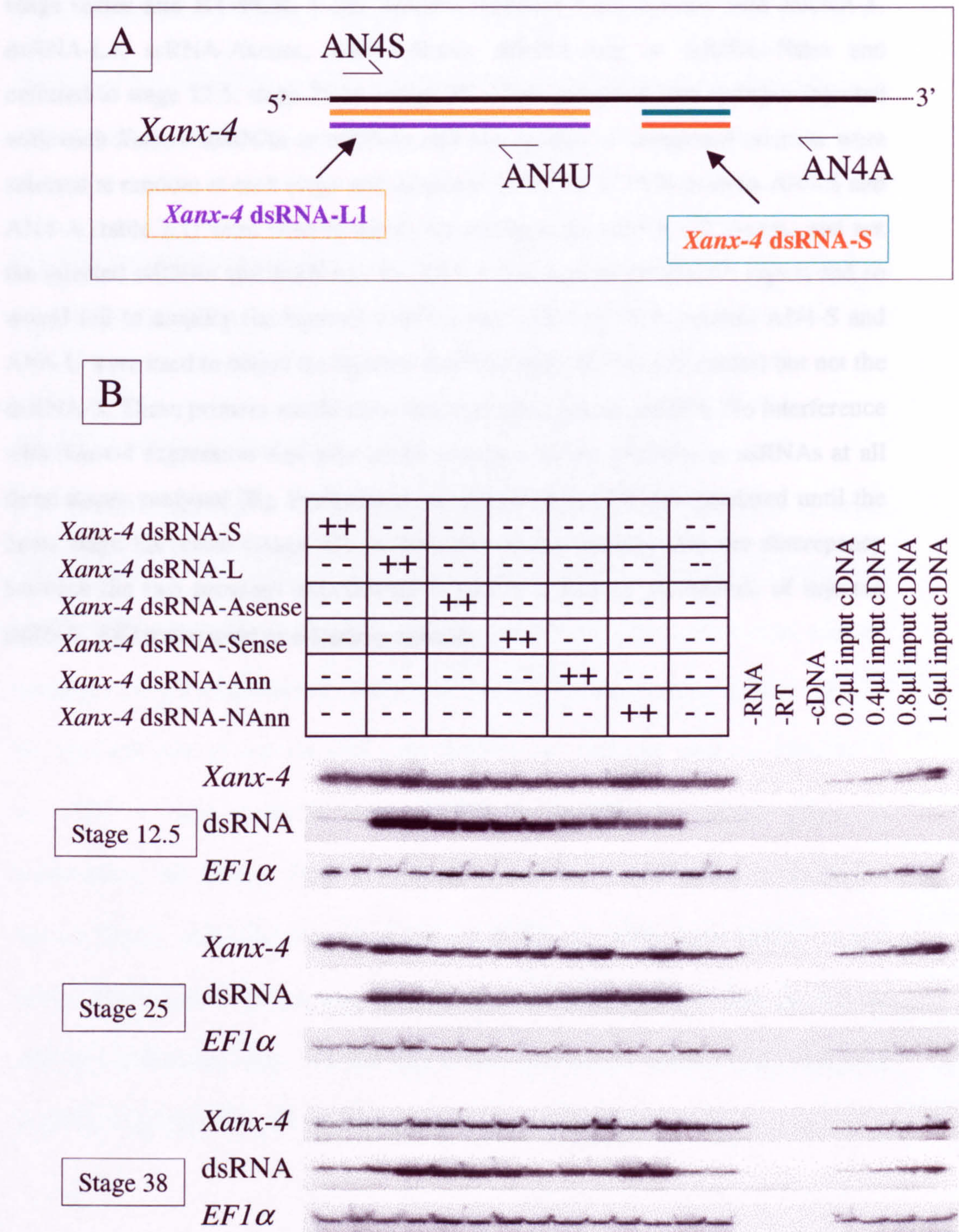


Figure 5.12: Longevity of *Xanx-4* dsRNAs in *Xenopus* embryos determined by a stage series and RT-PCR. 1-cell *Xenopus* embryos were injected with dsRNA-S, dsRNA-L1, ssRNA-Asense, ssRNA-Sense, dsRNA-Ann or ssRNAs-Nann and cultured to stage 12.5, stage 25 and stage 35. Two groups of five embryos injected with each *Xanx-4* dsRNAs or ssRNAs and two groups of uninjected controls were selected at random at each stage and subjected to RT-PCR. PCR primers AN4-S and AN4-A (table 2.1) were used to detect the endogenous mRNA (27 cycles) and not the injected ssRNAs and dsRNAs (A). AN4-A lies outside the dsRNA region and so would fail to amplify the injected dsRNAs and ssRNAs. PCR primers AN4-S and AN4-U were used to detect the injected dsRNAs and ssRNAs (25 cycles) but not the dsRNA-S. These primers would also detect the endogenous mRNA. No interference with *Xanx-4* expression was seen in the presence of the dsRNAs or ssRNAs at all three stages analysed (B). Furthermore all of the injected RNAs persisted until the latest stage harvested (stage 35). It therefore seems unlikely that the discrepancy between the two previous experiments is due to a lack of persistence of injected dsRNA. *EF1 α* was used as a loading control.

combination with 5ng of dsRNA-S, dsRNA-L1, ssRNA-Asense, ssRNA-Sense, dsRNA-Ann or ssRNAs-NAnn and cultured to stage 20. Two groups of five embryos injected with each RNA sample and two groups of uninjected controls were selected at random and subjected to RT-PCR. The level of exogenous *Xanx-4* mRNA was reduced slightly in the presence of all dsRNAs and ssRNAs (figure 5.13i). Similarly a repeat experiment (figure 5.13ii), using embryos from different frogs, yields the same result.

5.3 The use of synthetic short interfering RNA (siRNA) to perturb *Xanx-4* expression in *Xenopus laevis*

5.3.1 The advent of synthetic siRNA

During the course of the dsRNA analyses just described (Section 5.2), work carried out by other groups demonstrated that the RNAi pathway in *Drosophila* involved the cleavage of dsRNAs into 21nt fragments which were then used as templates for the degradation of the target mRNA (Zamore et al., 2000). Due to the apparent lack of success with long dsRNAs in vertebrate species, Elbashir et al., (2001b) used synthetic 21nt dsRNA to specifically induce RNAi in mammalian cell lines. Their success in a number of cell lines (including a human kidney cell line) suggested the possibility of using 21nt dsRNA oligos which may be more potent and specific for vertebrate systems than the longer dsRNAs previously used. To test this in *Xenopus laevis*, siRNA were designed to *Xanx-4* and tested in the following series of experiments.

Figure 5.13

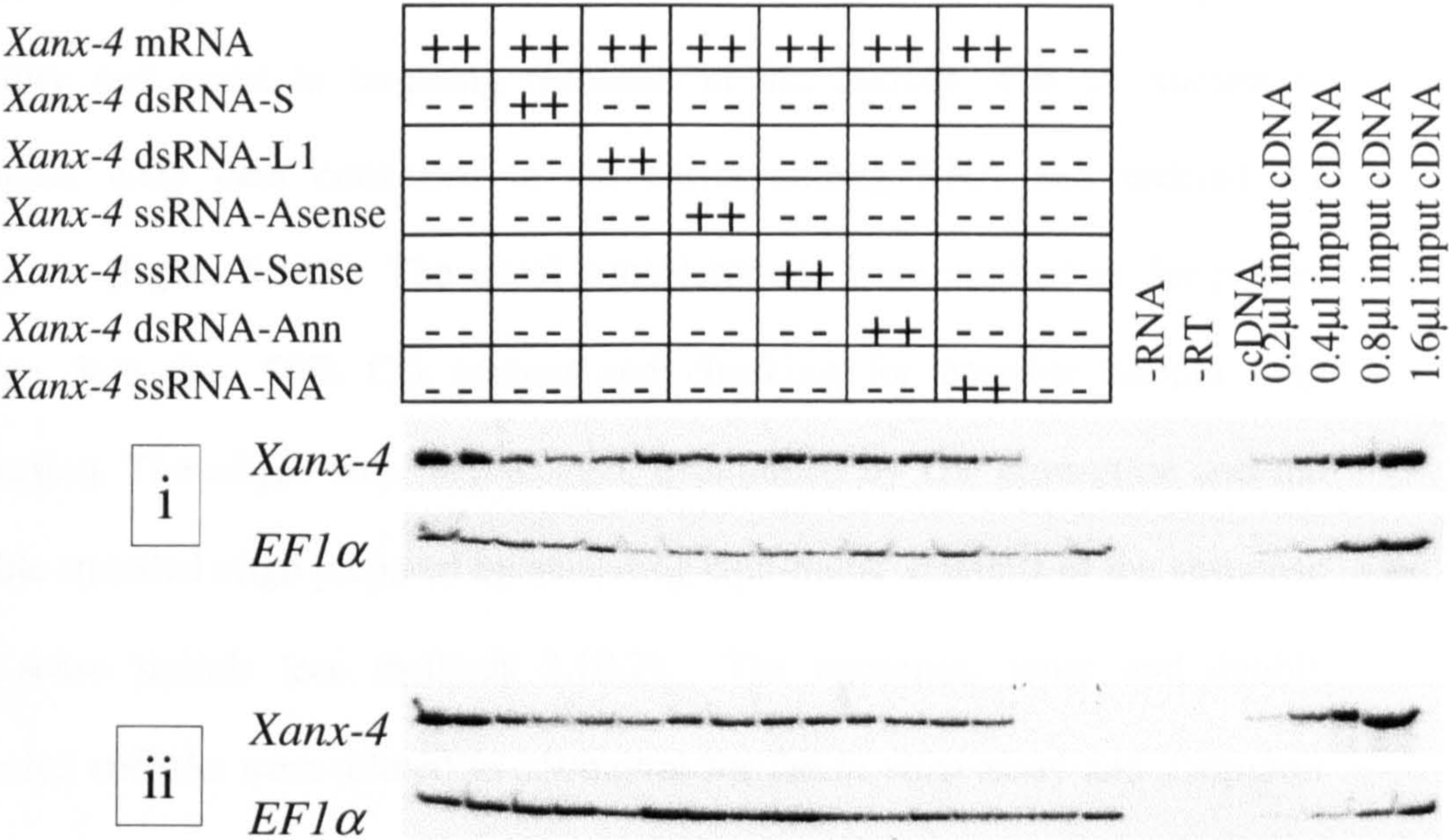


Figure 5.13: The effect of *Xanx-4* dsRNAs and ssRNAs on exogenous *Xanx-4* mRNA in *Xenopus* embryos. 1-cell *Xenopus* embryos were injected with 0.5ng *Xanx-4* mRNA alone or in combination with 5ng of dsRNA-S, dsRNA-L1, ssRNA-Asense, ssRNA-Sense, dsRNA-Ann or ssRNAs-Nann and cultured to stage 20. Two groups of five embryos injected with each RNA sample and two groups of uninjected controls were selected at random and subjected to RT-PCR. The level of exogenous *Xanx-4* mRNA was reduced slightly in the presence of all the three dsRNAs, two ssRNAs and dsRNA-NAnn (i). Similarly a repeat experiment (ii), using embryos from different frogs, yields the same result. *EF1α* was used as a loading control.

5.3.2 The design and preparation of the *Xanx-4* siRNA

The siRNA sequence was designed against the *Xanx-4* 5' coding region, which is the least conserved between annexin family members. This provided gene specificity and reduced the risk of cross-targeting with other annexins in *Xenopus* (figure 5.14). A 23nt region was chosen that contained the sequence 5'-AA-19N-TT-3' in the sense strand, 3'-TT-19N-AA-5' in the antisense strand, thus allowing the design of complementary sense and antisense RNA oligos with two thymine deoxyribose overhangs. These overhangs have been shown to provide stability and assist in targeting (Elbashir et al., 2001b). The 19 nucleotide stretches were then converted to the corresponding RNA and ordered for synthesis (figure 5.13B). The usual considerations were applied as for primer design, less than 50% CG content and checking for possible hairpin loop formation. The oligos were deprotected, quantitated by UV absorption and the double stranded oligo prepared by annealing equi-molar amounts of the antisense and sense strands (see methods 2.10.2). The antisense, sense and double stranded siRNAs were diluted to 250mg/ml for the *in vitro* assay and 250µg/ml for the *in vivo* assays.

5.3.3 Testing the effect of *Xanx-4* siRNA *in vitro*

It has been suggested that the reason for the lack of specificity of dsRNA in vertebrate systems may be due to the effect of dsRNA activating PKR and inducing the interferon response (Tuschl et al., 1999) (see section 5.1 .5.8). To assess whether the *Xanx-4* siRNA would induce non-specific blocking of translation *in vitro* the rabbit reticulocyte lysate systems was employed. Reactions containing 100ng *Xanx-4* mRNA alone or in combination with 1µg

Figure 5.14

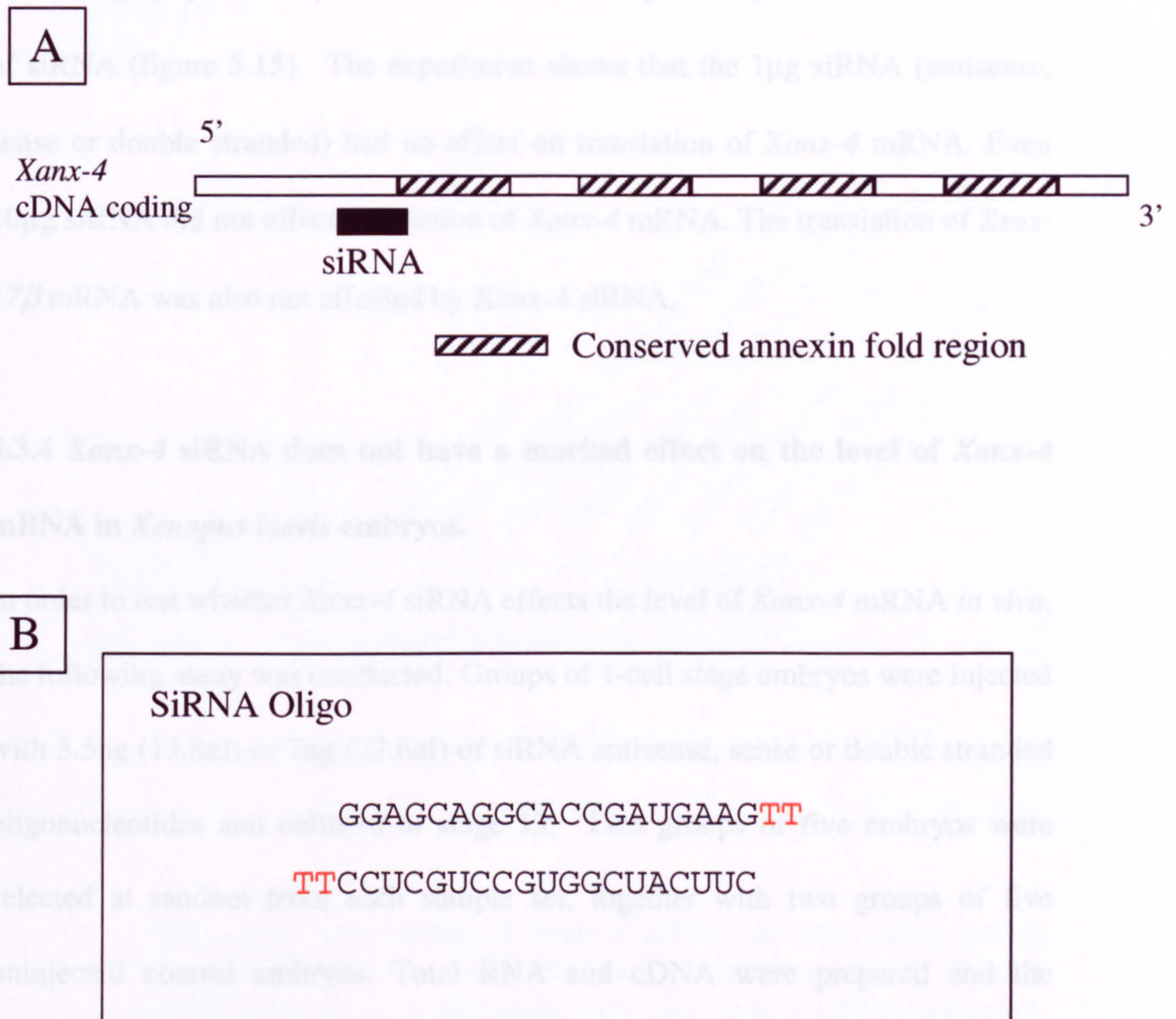


Figure 5.14: The sequence and position of *Xanx-4* siRNA. The siRNA sequence was designed against the *Xanx-4* 5' coding region, which is the least conserved between annexin family members (A). A 23nt region was chosen that contained the sequence 5'-AA-19N-TT-3' in the sense strand, 3'-TT-19N-AA-5' in the antisense strand, thus allowing the design of complementary sense and antisense oligos with two thymine deoxyribose overhangs (red in B). The 19 nucleotide stretches were then converted to the corresponding RNA and ordered for synthesis (B).

Xanx-4 siRNA antisense, sense or double stranded and 10µg *Xanx-4* siRNA double stranded, were incubated and labelled with ³⁵S-methionine according to manufacturer's recommendations. Samples were subjected to SDS-PAGE and autoradiography. *Xsox17β* mRNA was used as a specificity control for the action of siRNA (figure 5.15). The experiment shows that the 1µg siRNA (antisense, sense or double stranded) had no effect on translation of *Xanx-4* mRNA. Even 10µg siRNA did not effect translation of *Xanx-4* mRNA. The translation of *Xsox-17β* mRNA was also not affected by *Xanx-4* siRNA.

5.3.4 *Xanx-4* siRNA does not have a marked effect on the level of *Xanx-4* mRNA in *Xenopus laevis* embryos.

In order to test whether *Xanx-4* siRNA effects the level of *Xanx-4* mRNA *in vivo*, the following assay was conducted. Groups of 1-cell stage embryos were injected with 3.5ng (13.8nl) or 7ng (27.6nl) of siRNA antisense, sense or double stranded oligonucleotides and cultured to stage 13. Two groups of five embryos were selected at random from each sample set, together with two groups of five uninjected control embryos. Total RNA and cDNA were prepared and the samples subjected to RT-PCR, using gene-specific primers, and autoradiography (figure 5.16i). The *Xanx-4* siRNA oligos had no marked effect on the level of *Xanx-4* mRNA detected in any sample tested. The same result was observed in a repeat of the experiment (figure 5.16ii). *ODC* was used as a loading control.

Figure 5.15

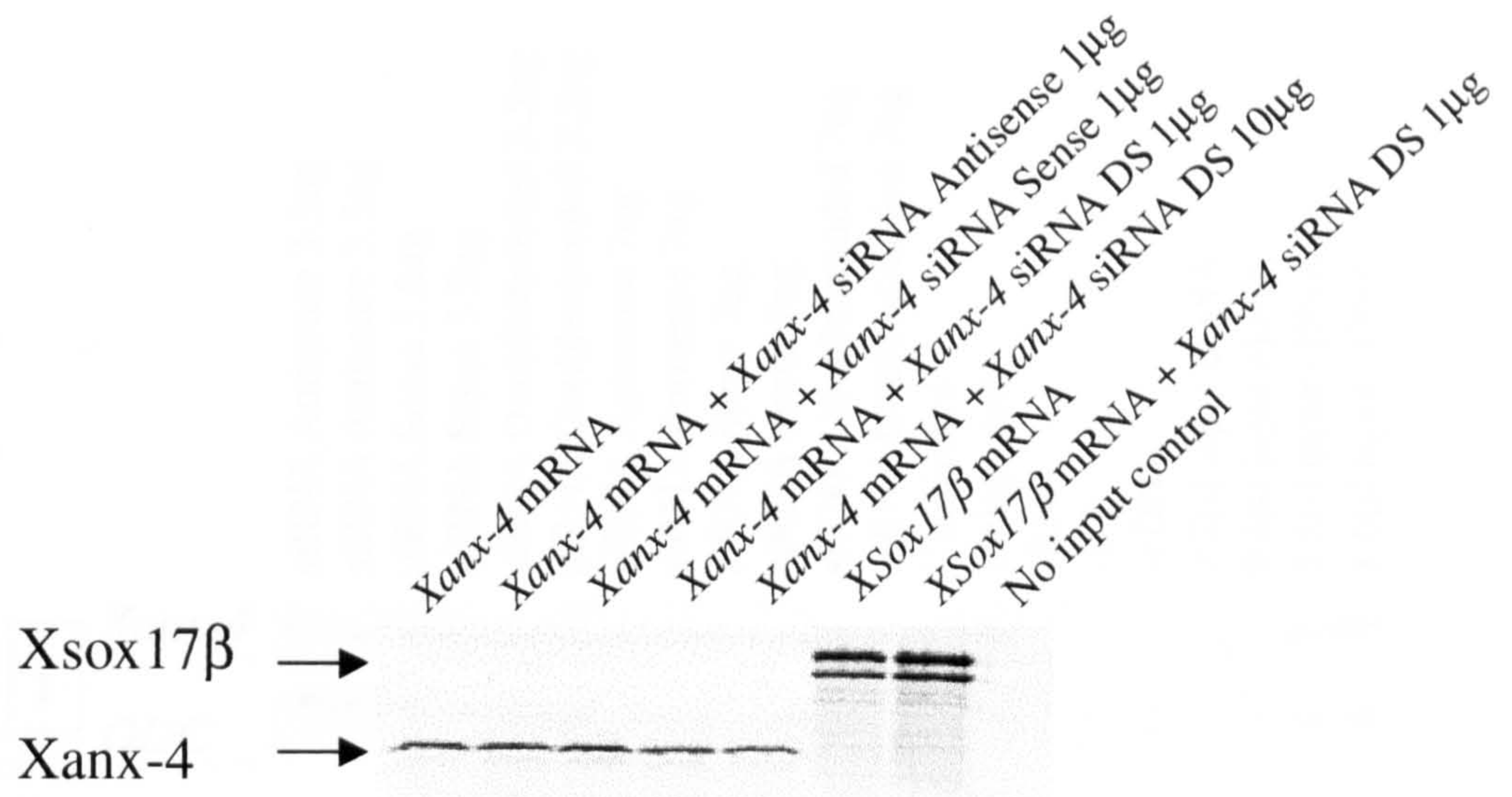


Figure 5.15 The testing of *Xanx-4* siRNA *in vitro* using rabbit reticulocyte lysate system. Reactions containing 100ng *Xanx-4* mRNA alone or in combination with 1μg *Xanx-4* siRNA antisense, sense or double stranded or 10μg *Xanx-4* siRNA double stranded, were incubated and labelled with ³⁵S-methionine according to manufacturer's recommendations. The samples were subjected to SDS-PAGE and autoradiography. *Xsox17β* mRNA was used as a specificity control for any effect of siRNA. The result shows that the 1 μg siRNA (antisense, sense or double stranded) had no effect on translation of *Xanx-4* mRNA. Even 10 μg siRNA did not effect translation of *Xanx-4* mRNA. No effect on translation of *Xsox17β* mRNA was observed.

Figure 5.16

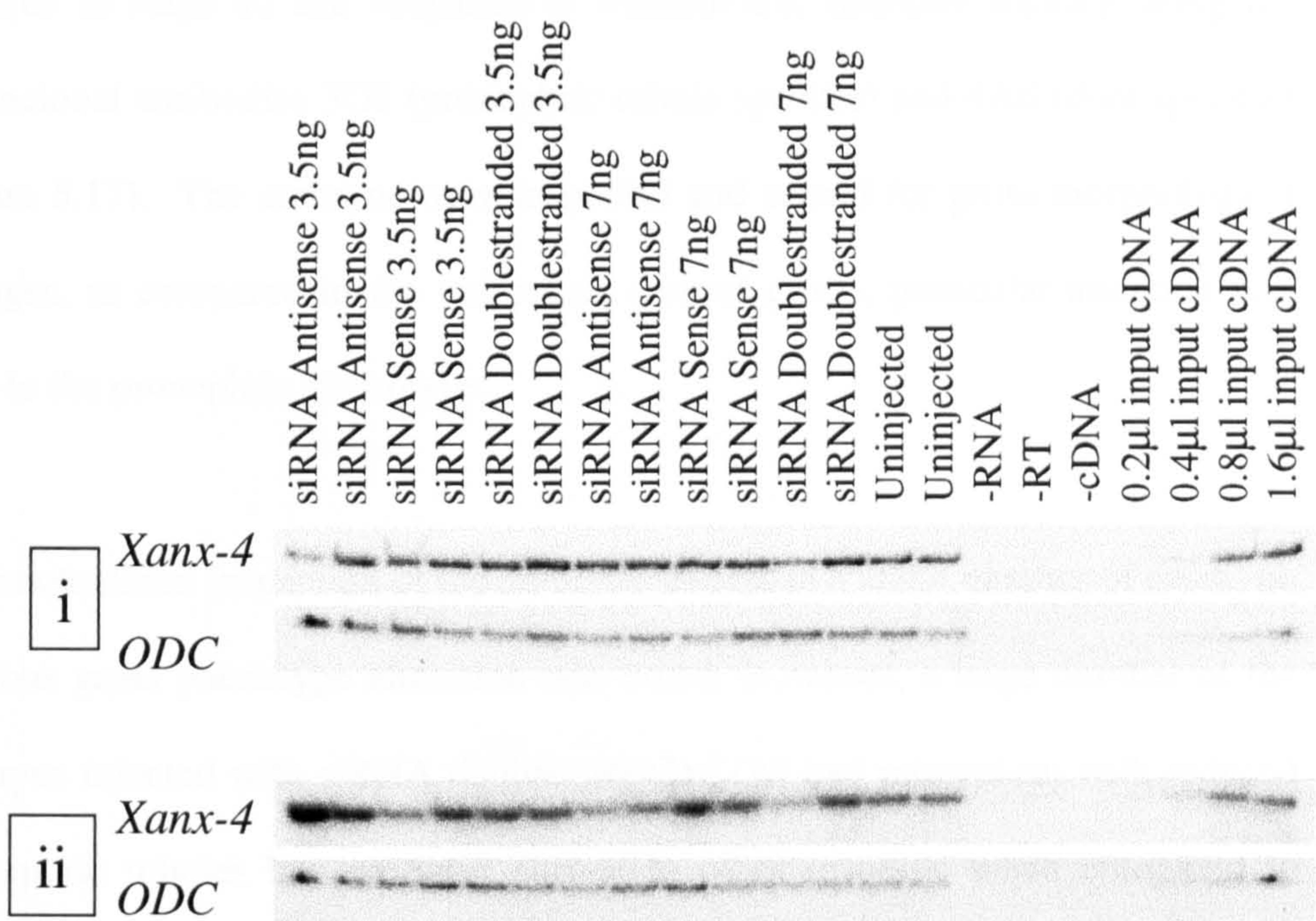


Figure 5.16: The effect of *Xanx-4* siRNA on *Xanx-4* mRNA in *Xenopus laevis* embryos by RT-PCR. Groups of 1-cell stage *Xenopus* embryos were injected with 3.5ng or 7ng of siRNA antisense, sense or double stranded oligonucleotides and cultured to stage 13. Two groups of five embryos were selected at random from each sample set, together with two groups of five uninjected control embryos and subjected to RT-PCR (i). The result shows that *Xanx-4* siRNA oligos had no marked effect on the level of *Xanx-4* mRNA detected in any sample tested. The same result was observed in a repeat of the experiment (ii). *ODC* was used as a loading control.

5.3.5 *Xanx-4* siRNA double stranded produces a reduced tubule phenotype in *Xenopus laevis* embryos.

The remainder of embryos from the experiment described in section 5.3.4 were allowed to develop in order to test whether *Xanx-4* siRNA produces morphological changes in *Xenopus* embryos. The groups of embryos were cultured to stage 40 and subjected to wholemount antibody staining using the monoclonal antibodies 3G8 (pronephric tubule specific) and 4A6 (duct specific) (figure 5.17). The embryos were inspected and scored for gross morphological changes, as compared to the uninjected control group, particular attention was paid to the pronephric phenotype.

On wholemount inspection of the embryos, except in a small number of cases, no obvious gross phenotype alteration was noted. However, a large number of the embryos injected with siRNA double stranded (A) had pronephroi with reduced pronephric tubules but appeared normal in other respects, when compared to embryos injected with siRNA antisense (B) or sense (C) and uninjected controls (D) (Figure 5.17). The scoring categories decided upon were “normal”, “reduced tubules” and “other”. Each pronephros on either side of the embryo was scored as individual and the results for all pronephroi are shown in Figure 5.18.

In the “reduced tubule” category, the tubules appear to be normal in most respects; they are of similar diameter to normal, they are coiled and appear in the normal position but are shorter. Therefore it appears that the pronephroi contain less tubules. An example phenotype associated with the “reduced tubule” category can be seen in figure 5.17A. Most of the embryos injected with siRNA

Figure 5.17

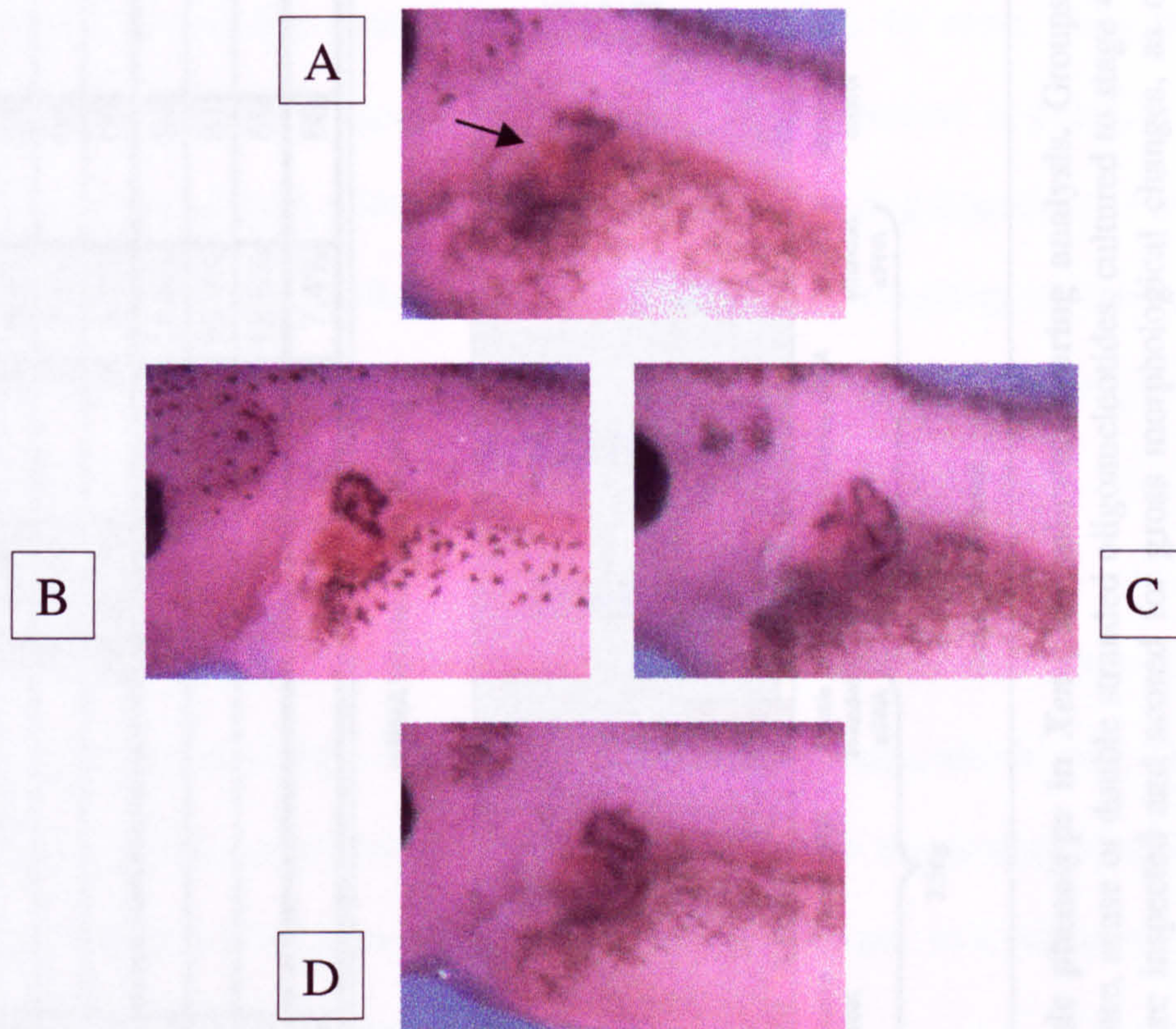
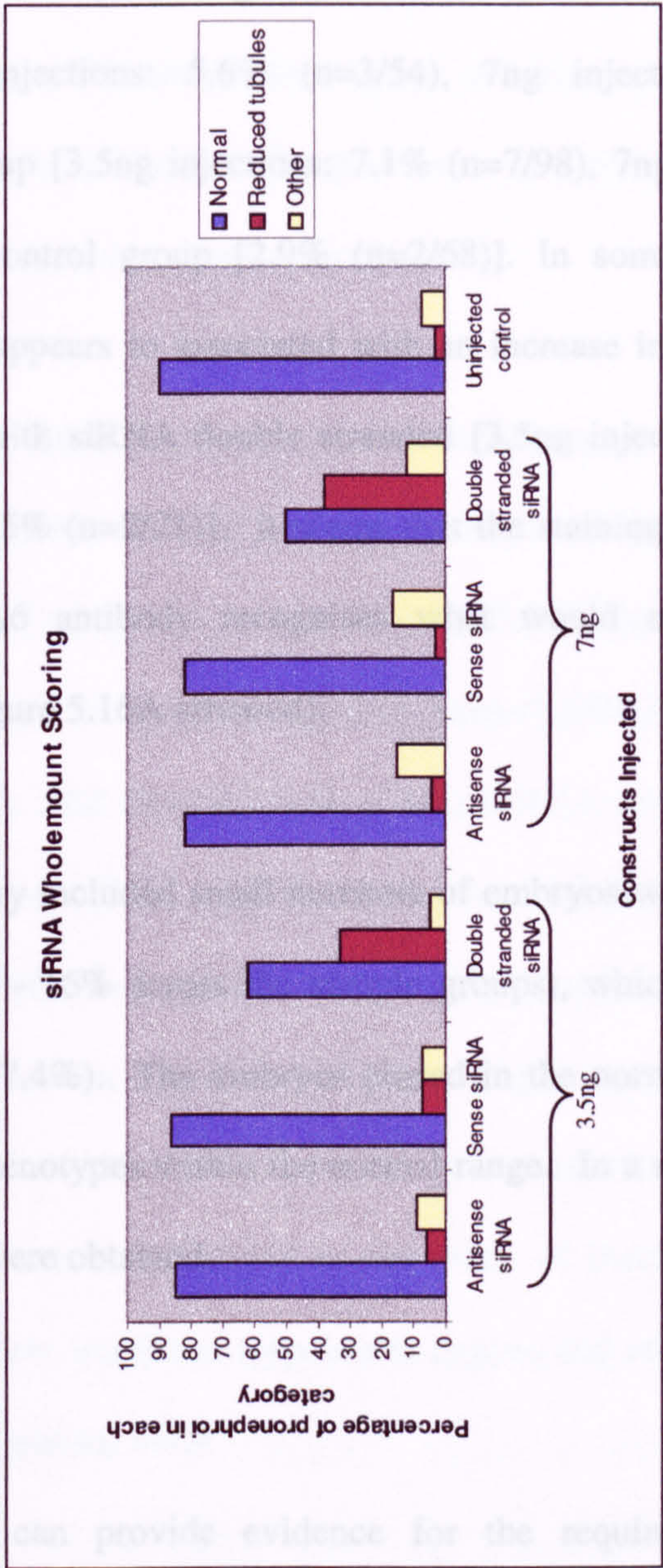


Figure 5.17: Xanx-4 siRNA produces a reduced tubule phenotype in *Xenopus* embryos. Groups of 1-cell stage embryos were injected with 3.5ng or 7ng of siRNA antisense, sense or double stranded oligonucleotides, cultured to stage 40 and subjected to wholemount 3G8 antibody (pronephric tubules, purple) and 4A6 (duct, red) staining. Embryos injected with siRNA double stranded had pronephroi with reduced pronephric tubules (A) when compared to embryos injected with siRNA sense (B), siRNA antisense (C) or uninjected controls (D). In some cases the reduced tubule phenotype appears to be associated with an increase in pronephric duct in embryos injected with siRNA double stranded. It seems that the staining of the duct with the duct-specific 4A6 antibody recognises what would normally be pronephric tubule tissue (A, arrowed).

| Scoring Category | Normal | % | Reduced tubules | % | Other | % | Total | Incr. duct | % |
|-----------------------------|--------|-------|-----------------|-------|-------|-------|-------|------------|------|
| 3.5ng Antisense siRNA | 46 | 85.2% | 3 | 5.6% | 5 | 9.3% | 54 | 0 | 0.0% |
| 3.5ng Sense siRNA | 84 | 85.7% | 7 | 7.1% | 7 | 7.1% | 98 | 0 | 0.0% |
| 3.5ng Double stranded siRNA | 41 | 62.1% | 22 | 33.3% | 3 | 4.5% | 66 | 1 | 4.5% |
| 7ng Antisense siRNA | 44 | 81.5% | 2 | 3.7% | 8 | 14.8% | 54 | 0 | 0.0% |
| 7ng Sense siRNA | 66 | 81.5% | 2 | 2.5% | 13 | 16.0% | 81 | 0 | 0.0% |
| 7ng Double stranded siRNA | 28 | 50.0% | 21 | 37.5% | 7 | 12.5% | 56 | 2 | 9.5% |
| Uninjected control | 61 | 89.7% | 2 | 2.9% | 5 | 7.4% | 68 | 0 | 0.0% |

A



B

Figure 5.18: Xanx-4 siRNA produces a reduced tubule phenotype in *Xenopus* embryos: scoring analysis. Groups of 1-cell stage embryos were injected with 3.5ng or 7ng of siRNA antisense, sense or double stranded oligonucleotides, cultured to stage 40 and subjected to wholemount 3G8 antibody staining. The embryos were inspected and scored for gross morphological changes, as compared to the uninjected control group. Embryos in the siRNA double stranded group had pronephroi with reduced pronephric tubules, when compared to ssRNA injected and uninjected controls. The scoring categories used: normal, reduced tubules and other. Each pronephros was scored as individual and the numerical counts in each group are shown in table A and graphically in B.

antisense (B) and sense (C) displayed normal morphology. The “reduced tubule” phenotype is mainly associated with the siRNA double stranded (3.5ng injections = 33.3%, 7ng injections = 37.5%), although small numbers are also seen in the antisense group [3.5ng injections: 5.6% (n=3/54), 7ng injections: 3.7% (n=2/54)], in the sense group [3.5ng injections: 7.1% (n=7/98), 7ng injections: 2.5% (n=2/81)] and the control group [2.9% (n=2/68)]. In some cases the reduced tubule phenotype appears to associated with an increase in pronephric duct in embryos injected with siRNA double stranded [3.5ng injections: 4.5% (n=1/22), 7ng injections: 9.5% (n=2/21)]. It seems that the staining of the duct with the duct-specific 4A6 antibody recognises what would normally be pronephric tubule tissue (figure 5.16A arrowed).

The “other” scoring category included small numbers of embryos with common aberrant phenotypes (4.5% - 16% across the sample groups), which were also seen in the control group (7.4%). The embryos placed in the normal category were considered to have phenotypes within the normal range. In a repeat of the experiment similar results were obtained.

5.4 Discussion

Loss-of-function analyses can provide evidence for the requirement of a particular gene during the epigenesis of an organism. A number of strategies have been adopted in attempts to interfere with gene expression in *Xenopus laevis*, including antisense RNA, antisense DNA, expression of dominant-negative proteins and the use of antibodies to perturb protein function. These methods have all been used to produce loss-of-function results with varying

degrees of success, none of which is the method of choice for ablating protein expression in *Xenopus* or any other model organism. The recent discovery of RNAi as a potent method of inhibiting the expression of specific genes in various species, in particular in *Drosophila* and *C.elegans*, has provided an opportunity to test a new sequence specific method in *Xenopus laevis* at a time when RNA technologies required credence in vertebrate systems.

5.4.1 RNAi effects on *Xanx-4* mRNA translation in *Xenopus* oocytes

It has been shown that dsRNA of 78bp and 367bp is effective in blocking translation of injected *Xanx-4* mRNA in oocytes (Section 5.2.2; Figure 5.6). The effect of dsRNA in blocking translation of injected *Xanx-4* mRNA in oocytes appears to be specific, since *XEZ* (Barnett et al., 2001) dsRNA does not effect translation of injected *Xanx-4* mRNA. Furthermore, the inhibition of *Xanx-4* translation by both *Xanx-4* dsRNA-S and dsRNA-L1 is highly reproducible. This implies that RNAi can be used for specific interference of protein expression in the *Xenopus* oocyte. Complete block of translation by the interferon response leading to PKR activation, can be ruled out as the mode of blocking *Xanx-4* translation in oocytes since the interferon response is zygotic and other maternal messages are translated at a normal level.

The size of the interfering dsRNAs found to be effective in this study is in good agreement with studies conducted in *C.elegans* (Fire et al., 1998; Parrish et al., 2000), however studies in *Drosophila* show that dsRNAs of less than 100bp often do not activate RNAi (Hammond et al., 2000, Tuschl et al., 1999). The concentration of dsRNA used in this study was 5ng/embryo, this is equal to

0.2 μ M dsRNA-S and 0.04 μ M dsRNA-L1. In the zebrafish assays 15-60pg/embryo (0.04nM) *no tail (ntl)* dsRNA was found to be effective (Wargelius et al., 1999). In the mouse *c-mos* dsRNA at 20pg/embryo (12nM) gave the expected phenotype (Wianny and Zernicka-Goetz, 2000). In *C.elegans* 6x10⁴ molecules/embryo, which calculates as just a few molecules per cell (Fire et al., 1998) and *Drosophila* 25nM (Tuschl et al., 1999).

The ssRNAs, ssRNA-Antisense and ssRNAs-Not Annealed caused suppression of translation of *Xanx-4* mRNA in oocytes (figure 5.7i and 5.7ii). This is probably due to antisense blocking of translation by RNA:DNA hybridisation. Antisense *Xanx-4* was as effective as dsRNA in inhibiting translation of *Xanx-4* protein; this is not observed in *C.elegans* or *Drosophila* where much lower concentrations of dsRNA result in more efficient reduction in protein expression than antisense strategies (Fire et al., 1998; Kennerdell and Carthew, 1998). This would suggest that RNAi is less efficient in *Xenopus* oocytes than in less complex organisms.

The effect observed on *Xanx-4* translation may be due to a mechanism similar to antisense, which might explain why the dsRNAs appear to function with a similar efficiency to the ssRNA antisense. Since dsRNA sometimes led to the detection of a reduction in the level of endogenous and exogenous mRNA, this may reflect a fluctuation in the level of mRNA in response to RNAi. Perhaps the interference occurs at particular levels of intracellular mRNA concentrations or during particular phases of development. The response to RNAi over a specific period of time could be investigated by following the fate of injected GFP

labelled *Xanx-4* mRNA. To look at the effect of RNAi on endogenous *Xanx-4* mRNA over a time course, a transgenic *Xenopus* line expressing *Xanx-4* linked to GFP would need to be constructed.

5.4.2 RNAi effects on *Xanx-4* mRNA translation in embryos

In *Xenopus* embryos specific depletion of endogenous target mRNA by dsRNA occurred in one experiment (figure 5.10) but was not reproducible in two others (5.11i and 5.11ii). In a third experiment (figure 5.12B), no depletion of endogenous *Xanx-4* expression was detected at any stage. It also appears that the ssRNA and dsRNAs persist well beyond stage 35 (figure 5.12B), suggesting that RNAi is not operating in *Xenopus laevis* since interfering dsRNAs are reported to be degraded to 21nt as the first step of the RNAi response. dsRNA does not therefore act reproducibly as a means of specific endogenous mRNA depletion in both oocytes and embryos.

Exogenous *Xanx-4* mRNA is not degraded by RNAi in response to dsRNA (figure 5.13). Since levels of *Xanx-4* protein are reduced in oocytes injected with *Xanx-4* mRNA by dsRNA, it would be interesting to find out whether levels of *Xanx-4* protein are affected by dsRNA in embryos. This could be achieved by injecting embryos with *myc-Xanx-4* mRNA alone or in combination with *Xanx-4* dsRNA and quantifying the *Xanx-4* protein expression by western blotting using an anti-myc antibody. Additionally, in a similar experiment to analyse the effect of RNAi on endogenous protein levels, an antibody would need to be raised to *Xanx-4* protein. During this project, two commercially available antibodies (sc-1930, Santa Cruz and 0590-5096 Biogenesis) and two gifted antibodies (AS17,

Satoh et al., 1997 and BL7B1, Massey et al., 1991a) were extensively tested in western blotting and immunoprecipitation. Although all of these antibodies could detect Xanx-4 in wholemount, none of these could successfully detect Xanx-4 in western blotting or function in immunoprecipitation. Positive control antibodies demonstrated that the techniques used were working effectively.

5.4.3 The effects of *Xanx-4* siRNA in *Xenopus laevis*

It is current opinion that the first step of RNAi involves longer dsRNAs being cleaved into 21nt fragments (siRNA) by RNase III (Elbashir et al., 2001a). These short RNA fragments are able to specifically interfere with gene expression in mammalian cell lines where longer dsRNAs have failed (Elbashir et al., 2001b). It has been shown that viral dsRNA of greater than 30bp induces the interferon response which can lead to blocking of viral and cellular protein synthesis, cell growth is impeded and apoptosis results (Meurs et al., 1990). Tuschl et al., (1999) reported rapid non-specific degradation of mRNA when dsRNA of 505bp was incubated with rabbit reticulocyte lysates; this was suggested to be an interferon response to the longer dsRNA.

The *Xanx-4* siRNA (21nt) did not cause specific or non-specific degradation of mRNA (*Xanx-4* or *Xsox17*) in rabbit reticulocyte lysate, at any concentration tested (figure 5.15). The *Xanx-4* siRNA does not therefore induce RNAi or an interferon response *in vitro*. Similarly, the siRNA did not cause detectable potent and reproducible degradation of *Xanx-4* mRNA in embryos (figure 5.16i and 5.16ii). It seems that siRNA does not invoke the RNAi pathway or the RNAi pathway is not functional in *Xenopus*. It was therefore surprising that injection

of siRNA into embryos resulted in a reduction in pronephric tubules in 31-37% of embryos. It seems likely that this phenotype is caused by a reduction in Xanx-4 protein synthesis by siRNA. It is possible that the injection of siRNAs resulted in a slight reduction in *Xanx-4* mRNA levels and Xanx-4 protein expression, not detectable by the methods employed or at specific stages not analysed by RT-PCR. Further experiments will determine whether Xanx-4 protein levels are depleted in response to siRNA. Northern blot analysis of RNA extracted from embryos injected with siRNA could allow the detection of cleavage products of RNAi. In addition, similar experiments to those of Zamore et al., (2000) could be conducted whereby labelled mRNA is coinjected with siRNA and cleavage products are visualised on an acrylamide gel. The indicator of functional RNAi in this system would be the detection of *Xanx-4* mRNA products of 21nt and/or multiples thereof.

5.4.4 Conclusion

Attempts by two other groups (Nakano et al., 2000; Oelgeschläger et al., 2000) to use RNAi in *Xenopus* resulted in gene specific suppression and aberrant phenotypes, previously associated with the function of the gene in question. It has been shown in this chapter that dsRNA can specifically reduce levels of Xanx-4 protein, and Xanx-4 siRNA causes a reduced pronephric tubule phenotype. However analysis of the effects of dsRNA and siRNA on mRNA levels have proved inconclusive and cast doubt on the mechanism by which the dsRNAs are working. Further studies on RNAi in *Xenopus* will be required before it can be judged a reliable method for interfering with gene expression.

Chapter 6: Perturbation of the expression of *Xanx-4* using morpholino technology

6.1 Introduction

Recently, antisense morpholino technology has been used to deplete endogenous gene expression in a number of organisms by blocking translation of specific genes in early stages of development (for review see Corey and Abrams, 2001; Ekker and Larson, 2001). This contrasts with the previously described RNAi technologies which interfere with transcription (Chapter 5). Morpholino (MO) oligonucleotides possess a non-ionic morpholine backbone rather than a standard ribose sugar backbone of DNA/RNA (figure 6.1). These phosphorodiamidate antisense oligos bind to target mRNA with high affinity and are not recognized by any known cellular binding protein or nuclease (Summerton, 1999). Although MOs bind to complementary RNA sequences by Watson-Crick base-pairing, unlike traditional antisense technology they are not susceptible to degradation by RNaseH. Greater efficacy is thus achieved by a nonclassical antisense approach. These oligos present a non-toxic, relatively inexpensive and reliable method of gene product depletion (Summerton and Weller, 1997). To date, two methods of gene targeting using MOs have been utilised. Firstly, a recent study demonstrated a method of gene knockdown using MOs to inhibit pre-mRNA splicing (Giles et al., 1999). Using this method Draper et al., (2001) demonstrated depletion of FGF8 using a MO that spans an intron/exon boundary; this resulted in the blocking of zygotic, but not maternal, mRNA translation. This method of targetting MO to intron/exon boundaries also allows for the selective depletion of alternative splice variants. The analysis of the effects of MO blocked

Figure 6.1

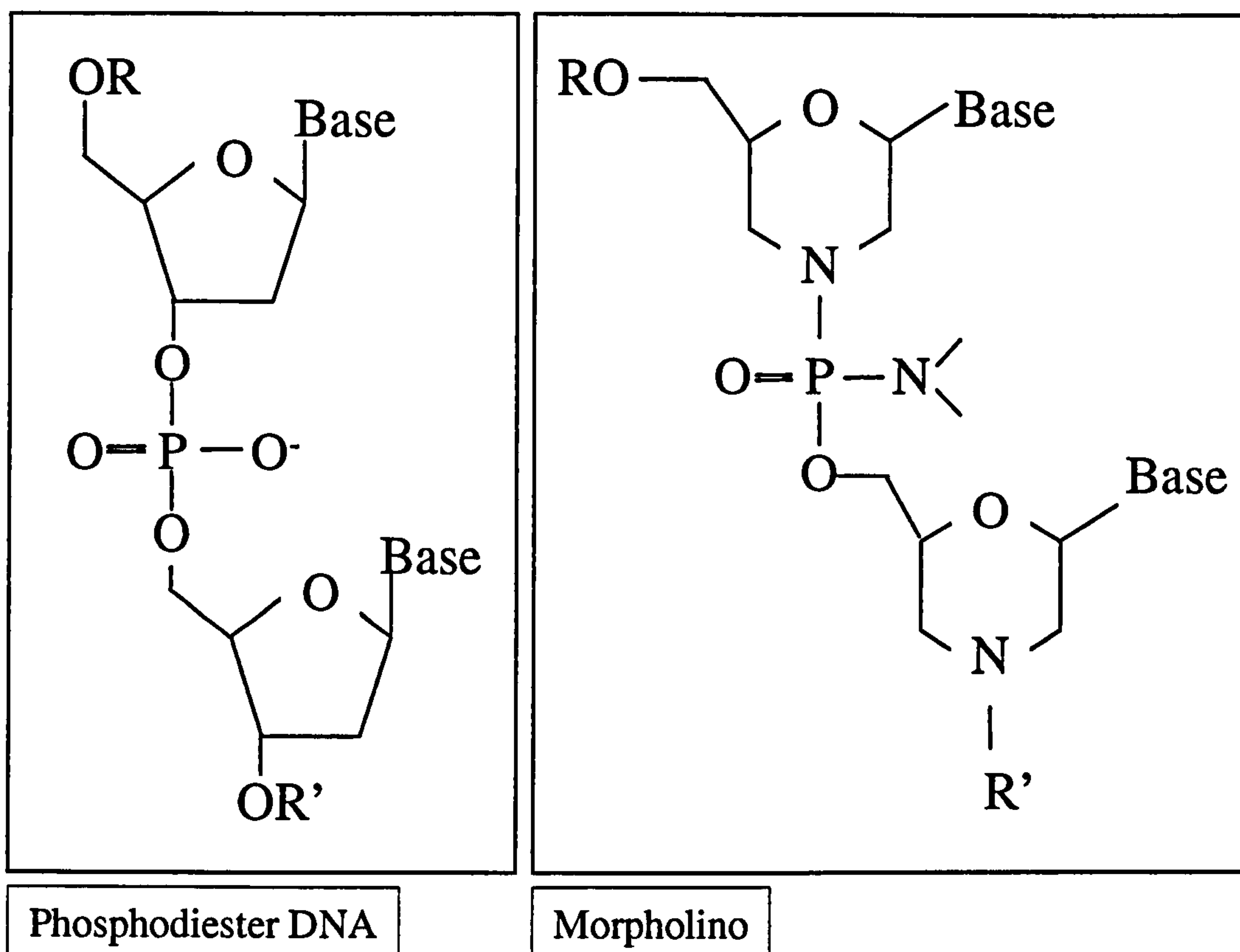


Figure 6.1: The structure of DNA and morpholino oligonucleotides. A morpholino oligo is composed of a series of 6-membered morpholine rings which are joined by non-ionic phosphorodiamidate linkages compared to the 5-membered deoxyribose backbone joined by ionic linkages in DNA. Base refers to adenine, cytosine, guanine or thymine. R and R' denotes continuation of the oligomer chain in the 5' or 3' direction respectively.

splicing has the advantage of not requiring an antibody, it can be detected semi-quantifiably by RT-PCR. The second method involves steric blocking of translation and is at present the most commonly used technique for *in vivo* experiments. The MO is designed to the leader sequence of the mRNA, generally including the start codon. The double stranded RNA:MO complex inhibits scanning of the mRNA by the 40s ribosomal subunit of the ribosome thereby inhibiting translation. This type of approach targets maternal and zygotic mRNA (Summerton, 1999).

6.1.1 The use of morpholinos in *Xenopus*

The first study of the use of morpholinos in *Xenopus* was reported by Heasman et al., (2000). Maternal depletion of β -catenin, a molecule involved in the Wnt pathway, was previously shown to cause embryos to develop without dorsal structures (notochord, somites, neural tube, heads and tails). A similar depletion had been carried out by antisense knockdown in the oocytes that were then subjected to the host-transfer technique (Heasman et al., 1994). This is a very difficult, complex and time consuming process (see previous chapter, section 5.1). Unfortunately, these same antisense oligos could not be used to study zygotic function of β -catenin, as the oligonucleotides were toxic in fertilised eggs. Additionally they are unstable and do not deplete zygotic protein or membrane-associated maternal protein.

In the study of Heasman et al., (2000) the authors injected a morpholino complementary to β -catenin into blastomeres of early *Xenopus* embryos, and demonstrated the depletion of β -catenin protein through neurula stages. The

depletion of both maternal and zygotic gene products occurred. They used targeted injection to show depletion of gene products in different regions of the embryo at different stages. Injection of the MO into dorsal vegetal region of embryos at the 2-cell and 4-cell stage blocks dorsal axis formation and at the 8-cell stage blocks head formation. An injection of MO into A-tier blastomeres at the 32-cell stage causes aberrant cement gland formation. This study showed the use of MO in specific targeting of maternal and zygotic messages allowing the analysis of regionalised, complex pathways. Comparatively, 6-20ng of MO caused the same ventralised phenotype as seen previously with 1ng of phosphorothioate oligo injected into oocytes. The depleted phenotype could be rescued by co-injection with *β-catenin* mRNA (Heasman et al., 2000), a fundamental control for these experiments.

A number of recent studies on wnt signalling pathways using MO have allowed loss-of-function studies to be carried out for previously intractable systems.

The study used a combination of MOs designed to the 5'UTR of two orthologs of *Xfz7* (frizzled genes encode receptors for wnts) and utilised a rescue mRNA without the 5'UTR. The depletion of maternal *Xfz7* (Sumanas & Ekker, 2001) resulted in loss or reduction of anterior structures, confirming a previously suggested role for *Xfz7* in the wnt/ β -catenin dorsoventral axis formation pathway. Later stage *Xfz7*-depleted embryos displayed gastrulation defects, caused by inhibition of convergent extension movements, therefore probably zygotic, as demonstrated by an animal cap cell motility assay (Smith et al., 1990). Both aberrant phenotypes could be rescued by co-injection of *Xfz7* mRNA. Demonstration of a zygotic-only depletion phenotype by injecting MO

into 1-cell stage embryos, probably failed due to a maternal pool of Xfz7 protein already present in the embryo. This study provides the first evidence for a vertebrate Frizzled involvement in both canonical and non-canonical wnt-signalling pathways.

Other studies on the Wnt pathway using the MO technology include that of Deardorff et al., (2001) who showed that Xfz3 is required for Xwnt1 signalling in the formation of the neural crest in *Xenopus laevis* embryos. Tan et al., (2001) have shown that depletion of Kermit using a specific morpholino, blocks neural crest induction by Xfz3 in *Xenopus laevis*; an effect which can be rescued by co-injection with *Kermit* mRNA. The authors suggest that Kermit interacts directly with the cytoplasmic portion of frizzled proteins to modulate their signalling and is required for wnt/frizzled signalling in neural crest development in *Xenopus laevis*.

A number of additional studies have been conducted in *Xenopus laevis*, using MOs as a method to elucidate the function of cloned genes. Schweickert et al., (2001) demonstrated for the first time the requirement of *Pitx1* and *Pitx2* genes for cement gland formation by loss-of-function experiments. In *Drosophila* and *C.elegans* loss-of-function assays have shown that cyclin E, which binds to cdk2 and initiates DNA replication and histone biosynthesis, is responsible for underproliferation in the developing embryo. There are currently no reports of loss-of-function mutations for cyclin E in vertebrates. Audic et al., (2001) demonstrated that cyclin E depletion using cyclin E MO designed to target all three cyclin E forms previously cloned, causes a delay in embryogenesis in

Xenopus laevis embryos. The study demonstrates that an injection of 24ng provides a delay of around 1 stage, 48ng and 96ng around 2-3 stages, at tailbud stage (27) embryos. Injection of control MO at the same level caused no obvious delay. When the uninjected embryos reached stage 39, the MO injected embryos were delayed to stage 35/36 and the control MO injected embryos were delayed one stage. This demonstrates an effect of control MO on the general timing of development of the *Xenopus* embryos at high levels of MO (96ng). This amount of MO is however approximately 24 times higher than the amount routinely used to be effective in *Xenopus*.

Other *Xenopus* studies include functional studies on genes with previously known effects. Retinoic acid receptors (RAR) are able to activate and repress transcription of target genes on recruitment of coactivators and corepressors, depending on the presence of retinoic acid (RA). RAR-mediated signalling is known to be required for patterning along the anterioposterior axis. RARs and corepressors are present in regions where RA is absent (anterior), suggesting unliganded-RARs are acting as repressors in anterior patterning (Koide et al., 2001). Derepression of RARs by injection of a dominant-negative corepressor leads to posteriorisation, as does treatment with RA; an effect which was phenocopied by injection of RAR α morpholino. Injection of wild-type or dominant-negative RAR α rescued the MO phenotype, confirming that RAR functions anteriorly as a transcriptional repressor (Koide et al., 2001). In Dibner et al., (2001) *Xmeis3* was suggested to be involved in the transformation step in neural patterning. It has been suggested that it overcomes anterior neural signalling to enable proper hindbrain cell fate identity. Injection of MO or

Xmeis3-antimorph mRNA, coding for a fusion protein containing Xmeis3 linked to the *Engrailed* transcriptional repressor domain, both caused loss of hindbrain marker expression and an expansion of forebrain markers.

In a comparative study conducted by Nutt et al., (2001) between *Xenopus laevis* and *Xenopus tropicalis* the authors discovered that the inhibitory effect of MO in both *Xenopus* species is long-lived (well into tadpole stages) when using in excess of 1ng MO. The inhibitory effect on translation was also tested and demonstrated to be highly specific. CMV-GFP transgenic lines were used to demonstrate the usefulness of MO in *Xenopus laevis* and *tropicalis*. A GFP-MO was injected into CMV-GFP transgenic 1-cell stage *X.laevis* embryos; 0.1ng-0.4ng did not appreciably deplete GFP, 1ng depleted GFP protein to approximately half at stage 20 but the protein accumulated to virtually normal levels by stage 30. 4ng-40ng of GFP-MO completely knocked down the GFP protein level until reappearance at around stage 40-43. No gross morphological abnormalities were noted in injections of less than or equal to 10ng, however, injections at 20ng resulted in approximately 20% abnormalities and injections at 40ng, 45% abnormalities were observed. In general, the abnormalities seen were antero-posterior truncations and/or microcephaly. A *X.tropicalis* egg is approximately 10-fold smaller than a *X.laevis* egg. Correspondingly a proportionally less quantity of MO provided a similar result in *X.tropicalis* as in *X.laevis*. 1ng injected into *X.tropicalis* blocked translation of *crystallin-GFP* to stage 43 but by stage 47 the GFP fluorescence was indistinguishable from the control. To test the rapidity of dispersal of the oligonucleotide after injection, FITC labelled control MO was injected into the animal pole of one of a 2-cell

stage *Xenopus* embryo and the spread of fluorescence monitored throughout development. The fluorescence was present evenly throughout the injected side of the embryo and so was inherited by daughter cells equally and persisted until stage 43. This suggests that longevity of MO treatment is sufficient to interfere with specific translation well into organogenesis

In a cross-species study Ross et al., (2001) demonstrated that *Twisted gastrulation* (*Tsg*) is a conserved extracellular antagonist of BMP signalling. Overexpression of chordin mRNA in *Xenopus* embryos causes axis duplication (dorsalisation) by inhibition of BMP signalling. MO depletion of *Tsg* in zebrafish causes ventralisation, similar to that produced by chordin mutants. Sub-inhibitory levels of chordin MO and *Tsg* MOs were co-injected into zebrafish embryos, the resultant phenotype demonstrated that they synergistically enhanced blood island expansion (ventralisation).

6.1.2 Zebrafish

Nasevicius and Ekker (2000) reported the first example of MO translational inhibition in zebrafish. They blocked expression from a ubiquitous GFP-transgene, demonstrating that all cells could respond to the MO. The study also involved the targeted depletion of a number of endogenous genes in zebrafish, the resultant morphology of which phenocopied known mutations (*no tail*, *nacre* and *sparce*). The *one-eyed-pinhead* MO demonstrates a limitation in the use of MOs as half of the embryos injected with this MO failed to elicit the loss-of-function phenotype. The authors suggest this could be attributed to polymorphisms in the leader sequence. The authors developed zebrafish models

of human disease targeting the *uroporphyrinogen decarboxylase* gene with a specific MO and produced embryos with hepatoerythropoietic porphyria. Finally, embryos with reduced *sonic hedgehog* (*shh*) and *tiggy-winkle hedgehog* (*twhh*) displayed partial cyclopia and other specific midline abnormalities, providing a zebrafish genetic model for the common human disorder holoprosencephaly. These studies indicated that the MO could indeed specifically deplete maternal and zygotic gene function in zebrafish by interfering specifically with translation and that the aberrant phenotypes could be rescued by coinjection with the appropriate mRNA. During the course of their extensive study, Nasevicius and Ekker (2000) noted an 18% mistargeting rate. This is defined as the fraction of repeated unexpected phenotypes particular to MOs. For example, a phenotype common to the *shh* and *pax-2.1* MOs was that of neural death. Due to the large number of genes required for neural cell survival, it was suggested that this is due to serendipitous homology (Ekker and Larson 2001). As with other types of loss-of-function studies, controls are essential, especially a specific rescue, to allow correct interpretation of any aberrant phenotype observed.

More recently, a host of studies have been reported using MO depletion in zebrafish. These studies have included dissection of induction signalling pathways (Yang et al., 2001; Furthauer et al., 2001; Bauer et al., 2001; Agathon et al., 2001; Erter et al., 2001; Huang et al., 2001), phenocopies of known mutant phenotypes (Kawahara and Dawid, 2001; Yee et al., 2001; Topzewska et al., 2001), confirmation of suggested redundancy (Imai et al., 2001) and differential requirements of specific gene products (Muller et al., 2001). These studies show

that MOs provide a potent, sequence specific depletion of the targeted gene function; they are non-toxic (when used at <30ng/embryo), produce phenocopies of known mutations in a dose-dependent manner and can be successfully rescued using co-injection of mRNA in zebrafish.

Of particular interest, work carried out by Shepherd et al., (2001) demonstrates that Zebrafish GDNF and GFR α expression is consistent with it playing a role in enteric nervous system, motor neuron and kidney development. In mouse and salamander GDNF is suggested to have a role in kidney organogenesis (Durbec et al., 1996; Drawbridge et al., 2000). Interestingly, overexpression of neither GDNF nor GDNF MO had any effect on motor neuron or pronephric development. In contrast, overexpression of GDNF, targeted to somitic tissues, altered the normal axonal guidance, suggesting a role as a chemo attractant. MO knockdown of GDNF caused a 95% reduction in the number of enteric neurons. This effect was not due to apoptosis as using TUNEL labelling, no difference in the number of apoptotic cells was observed in MO injected embryos, at different stages, compared to controls.

6.1.3 Mouse

The only example of MO used in mouse so far is a phenocopy of the mouse *mos* mutation, which has been characterised in null mutants and by RNAi (see chapter 5). In mouse *mos* mutants, the oocytes fail to arrest at metaphase II and undergo parthenogenetic activation. The phenotype of parthenogenetic activation was observed, by injecting the *mos* MO into oocytes to give a frequency of 56% of cases using 340pg MO, 23% of cases using 17pg of *mos* MO and none in control

MO samples. This study demonstrates that the *mos* MO successfully recapitulates the *mos* genetic mutation in mouse (Coonrod et al., 2001).

6.1.4 Chick

Two recent studies have shown that MOs can produce specific depletions of gene expression in the chick. This was achieved by electroporation or microinjection of the MOs *in vivo*. The introduction of an MO specific to *FoxD3* resulted in defects in neural crest segregation and differentiation (Kos et al., 2001) and introduction of an MO specific to *tenascin-C* resulted in defects of neural crest migration (Tucker, 2001).

6.1.5 Sea urchin

Specific MOs have been shown to block translation of target genes in sea urchin. One study suggests a function for *SpKrl* in patterning the vegetal domain by suppressing animal regulatory activities (Howard et al., 2001).

6.1.6 Morpholinos in cell lines and *in vivo/in vitro* for therapeutics

Morpholino-modified antisense oligomers were first tried and tested in cell culture with the intention of designing human therapeutics. Many studies were conducted comparing different types of oligomers for their efficacy (Taylor et al., 1996; Summerton et al., 1997; Stein et al., 1997; Taylor et al., 1998), some time before they were utilised *in vivo*. The success of these initial studies demonstrated a scope in therapeutics for such molecules with specific and predictable effects (Summerton and Weller, 1997). Aberrant splicing of the β -globin gene is the most common mutation causing β -thalassemia in humans.

Lacerra et al., (2000) have shown that aberrant splicing could be corrected by using MOs in β -thalassemic blood cells, and thus expression of defective β -globin genes was repaired and a significant level of Hb A was restored. Arora and Iverson (2001) reported another potential use of MOs in therapeutics. Inhibition of CYP enzymes (enzymes involved in drug metabolism in humans) by MOs could result in safer and more uniform metabolism of clinically relevant drugs. In another study of restenosis (an aberrant proliferative disorder which often follows cardiac surgery), *in vivo* delivery of c-myc MO to four different animal models of restenosis resulted in reduction of the myointimal response (Hudziak et al., 2000; Kiphidze et al., 2001).

6.1.7 Caged RNA/DNA

Ando et al., (2001) have recently reported a new technique for photo-mediated gene activation using another modified nucleic acid analog in zebrafish embryos. The authors demonstrate that a synthetic compound, 6-bromo-4-diazomethyl-7-hydroxycoumarin (Bhc-diazo), can form a covalent bond with the phosphates of the sugar-phosphate backbone of RNA, blocking translation. This process, known as “caging”, is released when the covalently bound RNA is exposed to UV light and results in a partial recovery of translational activity. The protected mRNAs injected are resistant to enzymatic degradation and are therefore more stable than non-caged mRNAs. Since the caged mRNA is highly stable, this technique allows temporal release of injected caged mRNAs at a much later stage than would normally be possible. This conditional expression system allows the induction of dominant-negative mRNAs and simultaneous induction of genes that may act synergistically. This technique, if combined with the MO to produce

caged MOs, could provide a very useful tool to activate the MO at a specific time-point in development.

6.1.8 Summary

In summary, it appears that morpholinos can provide a reliable method of gene knockdown in a number of vertebrate species. They have been shown to phenocopy known mutations and provided answers where conventional antisense or RNAi have failed. Morpholinos show few non-specific effects, although a number of workers have reported increases in toxicity on long term storage of MO. They can be used at a range of concentrations to provide a graded response and can be rescued using mRNA. The following chapter describes the analysis of the results obtained using *Xanx-4* morpholinos to deplete Xanx-4 protein in *Xenopus laevis*.

6.2 Results

6.2.1 *Xanx-4* MO1 blocks translation of *Xanx-4* mRNA

A morpholino oligonucleotide, termed MO1, was designed to be complementary to *Xanx-4* and tested *in vitro* and *in vivo* for its ability to specifically perturb *Xanx-4* translation (Figure 6.2). Due to the lack of anti-annexin IV antibody, that could detect Xanx-4 by western analysis, an *Xanx-4*-myc-tagged expression construct was prepared (section 2.4.5, Table 2.2), the protein product of which could then be detected by western blotting using an anti-myc antibody. The *Xanx-4* cDNA was cloned in frame and upstream of the myc-tag in vector pCS2+MT3 (appendix 3). The myc-tagged *Xanx-4* construct (*myc-Xanx-4*) was

Figure 6.2

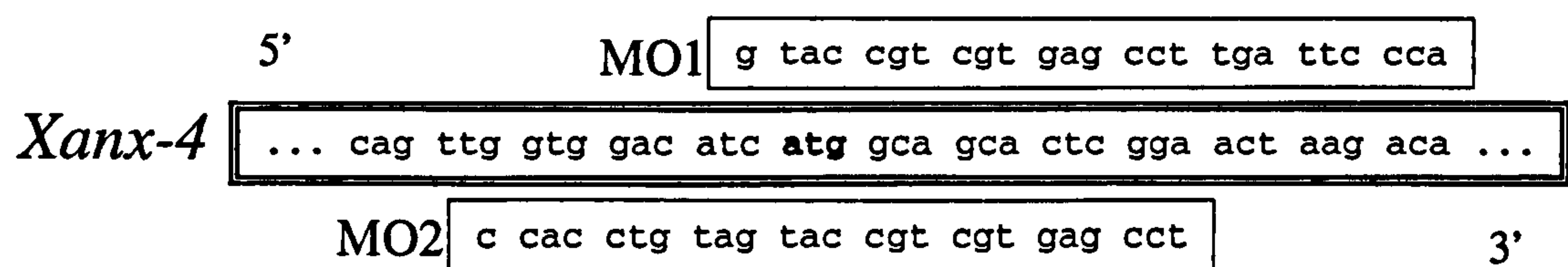


Figure 6.2: The position and sequence of the *Xanx-4* morpholinos MO1 and MO2 in relation to *Xanx-4* coding region. The translation start site (methionine, atg) is in bold type.

linearised with *EcoRI* and transcribed with SP6 RNA polymerase. myc-*Xanx-4* mRNA was diluted to 500µg/ml and used in the following assays to demonstrate the effectiveness and specificity of the *Xanx-4* morpholino (*Xanx-4* MO1) for *Xanx-4* mRNA.

Xanx-4* morpholino specificity *in vitro

Initially the specificity of the *Xanx-4* morpholino was established *in vitro*. Myc-tagged *Sox17β* mRNA (*myc-Xsox17β*, a kind gift of D.Clements, Warwick) was used as a control to test for the *Xanx-4* MO1 specificity. A combination of 100ng of *myc-Xsox17β* mRNA and 100ng of *myc-Xanx-4* mRNA was incubated either alone or in combination with 1µg, 5µg or 10µg of *Xanx-4* MO1 in the reticulocyte lysate system. The lysates were subjected to SDS-PAGE and western blotting using anti-myc antibody (Figure 6.3). Both *myc-Xsox17β* mRNA and *myc-Xanx-4* mRNA were successfully translated at similar levels (lanes 1, 3, 5) but when incubated with 1µg, 5µg or 10µg *Xanx-4* MO1, *myc-Xanx-4* mRNA translation was blocked whereas *myc-Xsox17β* mRNA translation was not (lanes 2, 4, 6 respectively). Lane 7 was no input control sample. The result demonstrates that *Xanx-4* MO1 specifically blocks translation of *Xanx-4* mRNA *in vitro*.

***Xanx-4* MO1 specificity *in vivo*.**

To test the efficacy of *Xanx-4* MO1 *in vivo* the follow experiment was conducted. Embryos were injected at the 1-cell stage with 0.5ng *myc-Xanx4* mRNA alone or in combination with 5ng, 10ng or 20ng *Xanx-4* MO1 and cultured to stage 9, 13 or 21. The embryos were homogenised, fractionated, and

Figure 6.3

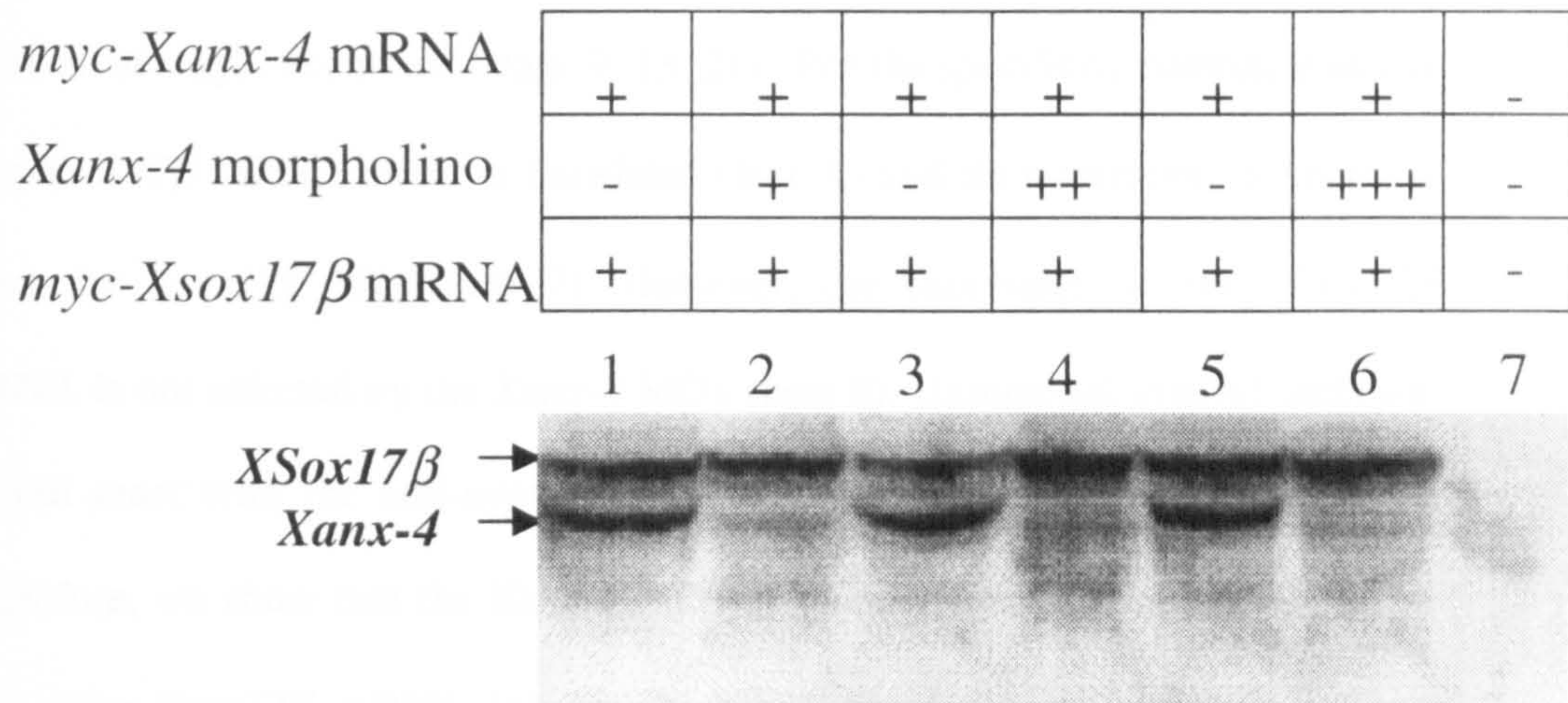


Figure 6.3: *Xanx-4* MO1 specificity *in vitro*. Western blot showing *Xanx-4* MO1 interferes with *in vitro* translation of myc-tagged *Xanx-4* mRNA (*myc-Xanx-4*) and not of myc-tagged *Xsox17 β* mRNA (*myc-Xsox17 β*). The translations were performed in the rabbit reticulocyte lysate system. Lane 1: 100ng *myc-Xanx-4* and 100ng *myc-Xsox17 β* mRNA. Lane 2: 100ng *myc-Xanx-4* and 100ng *myc-Xsox17 β* mRNA and 1 μ g *Xanx-4* MO1. Lane 3: 100ng *myc-Xanx-4* and 100ng *myc-Xsox17 β* mRNA. Lane 4: 100ng *myc-Xanx-4* and 100ng *myc-Xsox17 β* mRNA and 5 μ g *Xanx-4* MO1. Lane 5: 100ng *myc-Xanx-4* and *myc-Xsox17 β* mRNA. Lane 6: 100ng *myc-Xanx-4* and 100ng *myc-Xsox17 β* mRNA and 10 μ g *Xanx-4* MO1. Lane 7: No input mRNA or MO1.

the cytosolic fraction subjected to SDS-PAGE and western blotting using anti-myc antibody. As specificity controls, 0.5ng *myc-Xsox17 β* mRNA was also injected alone or in combination with *Xsox17 β* MO or *Xanx-4* MO1. The results (Figure 6.4) show that *myc-Xanx-4* is translated *in vivo* (lane 1) and that translation is blocked by 5ng (lane 2), 10ng (lane 3) or 20ng (lane 4) *Xanx-4* MO1 at all stages examined (stage 9, 13, 21). For the specificity control, injected *myc-Xsox17 β* mRNA alone is translated (lane 6) and its translation is knocked down by *Xsox17 β* MO (lane 7). However, the expression of *myc-Xsox17 β* mRNA is not affected by the *Xanx-4* MO1 (lane 8). Uninjected, control embryos do not react with the anti-myc antibody at any of the stages tested (lane 5). Therefore, we show that the *Xanx-4* MO1 is specific for *myc-Xanx-4* mRNA *in vivo*. *Myc-Xsox17 β* mRNA injected embryos could not be analyzed at later stages, due to lethality at late gastrula/early neurula stages of this level of message.

6.2.2 *Xanx-4* depletion using MO1 produces pronephric tubules with an enlarged diameter.

In order to examine the activity of *Xanx-4* *in vivo*, MO1 was used to perturb endogenous expression of *Xanx-4*. Embryos were injected at the 1-cell stage with 10ng control MO, 10ng *Xanx-4* MO1 or 0.5ng *Xanx-4* mRNA. The injected embryos were cultured to stage 40 and wholemount antibody stained with 3G8 and 4A6, which are tubule and duct specific monoclonal antibodies, respectively. The wholemount phenotype of each sample group was scored relative to controls (Figure 6.5). Although no obvious effect on pronephric tubule or duct morphology following overexpression of *Xanx-4* mRNA or on injection of

Figure 6.4

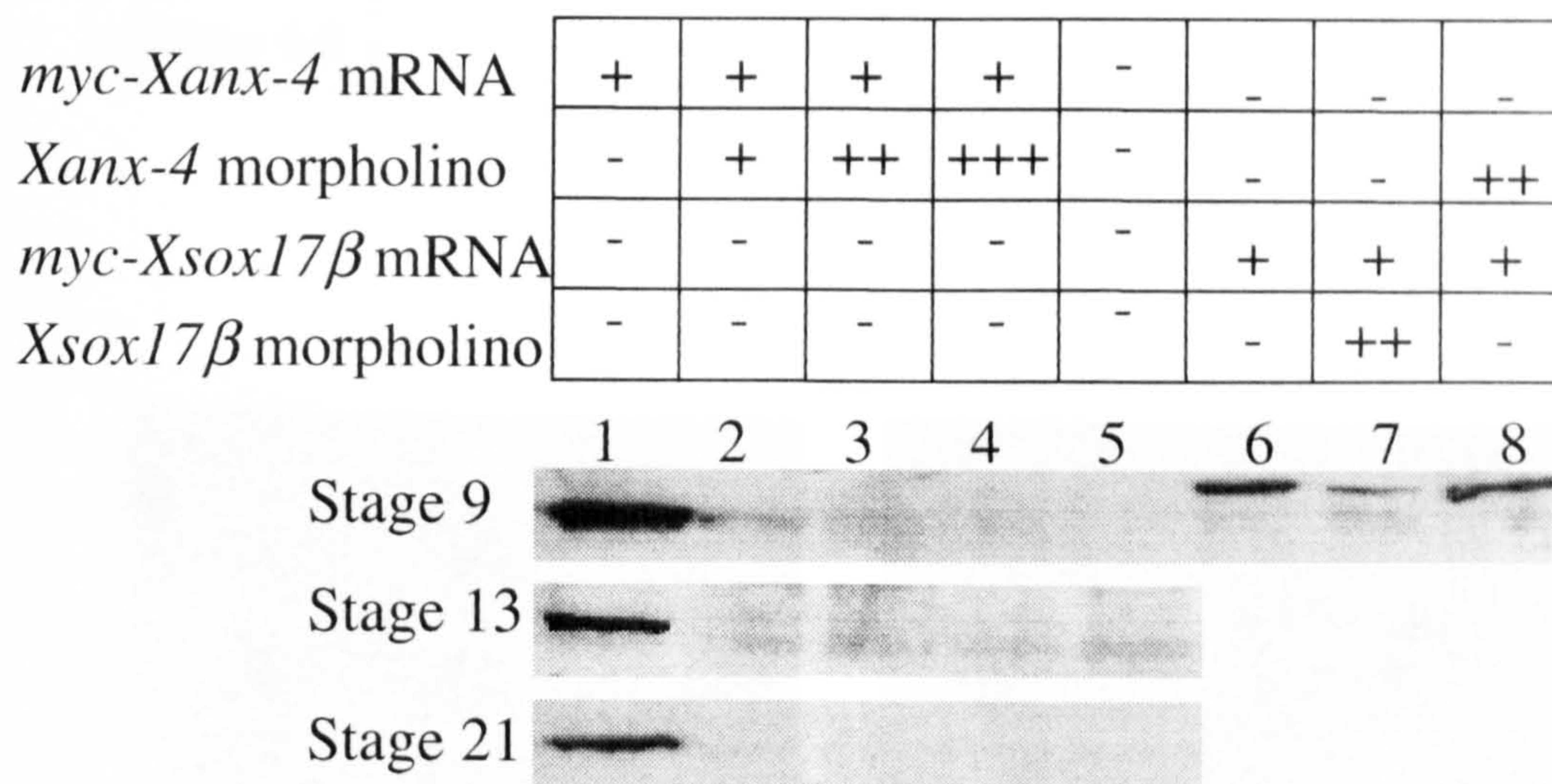


Figure 6.4: *Xanx-4* MO1 specificity *in vivo*. Western blot using anti-myc antibody showing *Xanx-4* MO1 interferes with *in vivo* translation in *Xenopus* embryos of myc-tagged *Xanx-4* mRNA (myc-*Xanx-4*) and not of myc-tagged *Xsox17 β* mRNA (myc-*Xsox17 β*). 1 cell stage *Xenopus* embryos were injected with myc-*Xanx-4* mRNA alone or in combination with *Xanx-4* MO1 and myc-*Xsox17 β* mRNA alone or in combination with *Xsox17 β* MO and cultured to stage 9, 13 and 21. The embryos were homogenised and samples equal to half of an embryo were subjected to SDS-PAGE and western blotting using anti-myc antibody. Lane 1: 0.5ng myc-*Xanx-4* mRNA. Lane 2: 0.5ng myc-*Xanx-4* mRNA and 5ng *Xanx-4* MO. Lane 3: 0.5ng myc-*Xanx-4* mRNA and 10ng *Xanx-4* MO. Lane 4: 0.5ng myc-*Xanx-4* mRNA and 20ng *Xanx-4* MO. Lane 5: Uninjected control. Lane 6: 0.5ng myc-*Xsox17 β* mRNA. Lane 7: 0.5ng myc-*Xsox17 β* mRNA and 10ng *Xsox17 β* MO. Lane 8: 0.5ng myc-*Xsox17 β* mRNA and 10ng *Xanx-4* MO.

Figure 6.5

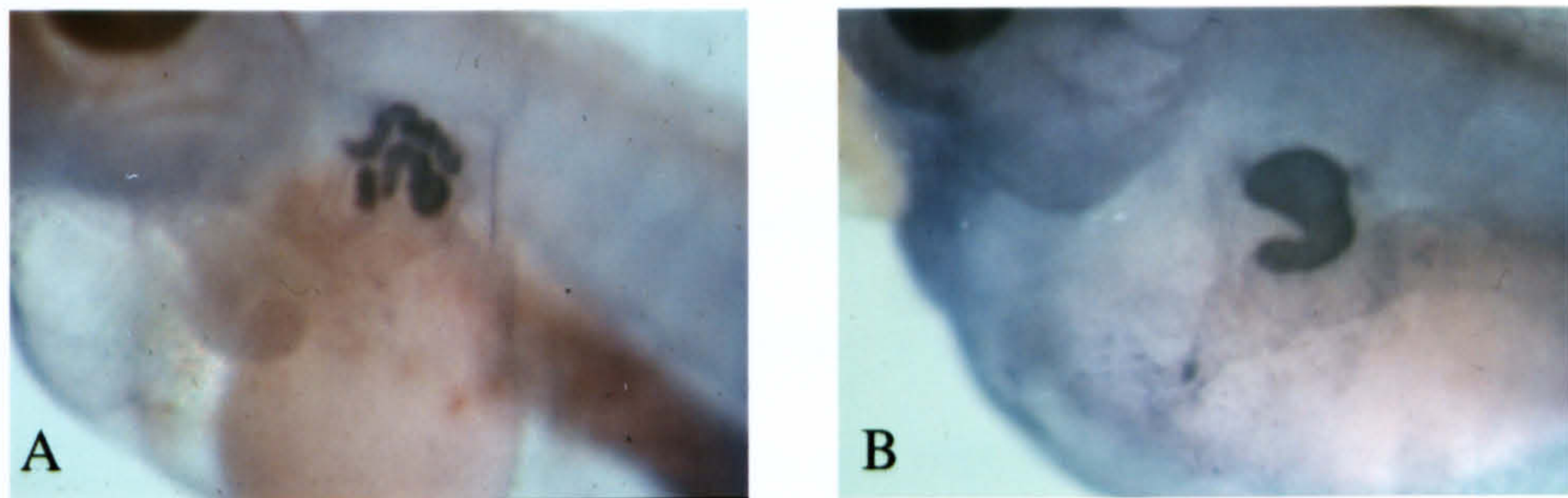


Figure 6.5: Depletion of Xanx-4 in embryos by injection of Xanx-4 MO1 results in pronephric tubules with an enlarged diameter: Wholemount antibody 3G8 staining of stage 40 *Xanx-4* MO1 injected embryos. 1 cell stage *Xenopus* embryos were injected with 10ng of *Xanx-4* MO1, cultured to stage 40 and subjected to wholemount antibody staining with pronephric tubule specific antibody 3G8. A: Normal uninjected control embryo. B: Embryo injected with *Xanx-4* MO shows the shortened, enlarged diameter tubule phenotype.

control MO was observed (116 embryos, 232 pronephroi, figure 6.6), a clear effect on pronephric tubule morphology was observed following *Xanx-4* MO1 injection. The normal, coiled, tubular structure of the pronephric tubules appeared completely disrupted in *Xanx-4* MO1 injected embryos. The effect of the *Xanx-4* MO1 led to the formation of shortened, enlarged and less coiled tubules, figure 6.5B, compared to control figure 6.5A. In some embryos the tubules were reduced in overall size and in some cases missing completely (8/232). A repeat of the experiment yielded a similar result.

In order to investigate the phenotype, a random sample of six immunostained embryos from each treatment group were acrylamide embedded, frozen and cryostat-sectioned at 12µm thickness. The slides were counterstained stained with Hoescht 33258, mounted and compared to un-injected controls. Analysis of the sections revealed that *Xanx-4* MO1 treated embryos (figure 6.7G-I) had tubules that were substantially wider than control un-injected (figure 6.7A-C), control MO injected (figure 6.7D-F), or *Xanx-4* mRNA injected embryos (figure 6.7J-L).

In order to quantify the extent of the *Xanx-4* MO1 phenotype, complete serial sections of the pronephroi from each of the six samples for each treatment were inspected. Approximately 24 sections were counted from each pronephros scored. Tubules were positively identified by the light microscopic identification of 3G8 positive immunostaining and nuclei counted under UV illumination to identify Hoescht staining (figure 6.7). Due to the coiled nature of the pronephric tubules many of the tubule sections could be seen as elongated or oval shaped

Figure 6.6

| Scoring category | Normal | % | Reduced/missing tubules | % | Enlarged tubules | % | Other | % | Total |
|-------------------|--------|-----|-------------------------|---|------------------|-----|-------|-----|-------|
| Control | 42 | 88% | | | 1 | 2% | 3 | 6% | 48 |
| Control MO | 57 | 86% | | | 0 | 0% | 8 | 12% | 66 |
| 10ng Xanx-4 MO1 | 18 | 32% | | | 24 | 43% | 6 | 11% | 56 |
| 0.5ng Xanx-4 mRNA | 48 | 77% | | | 4 | 6% | 8 | 13% | 62 |
| | 165 | | 13 | | 29 | | 25 | | 232 |

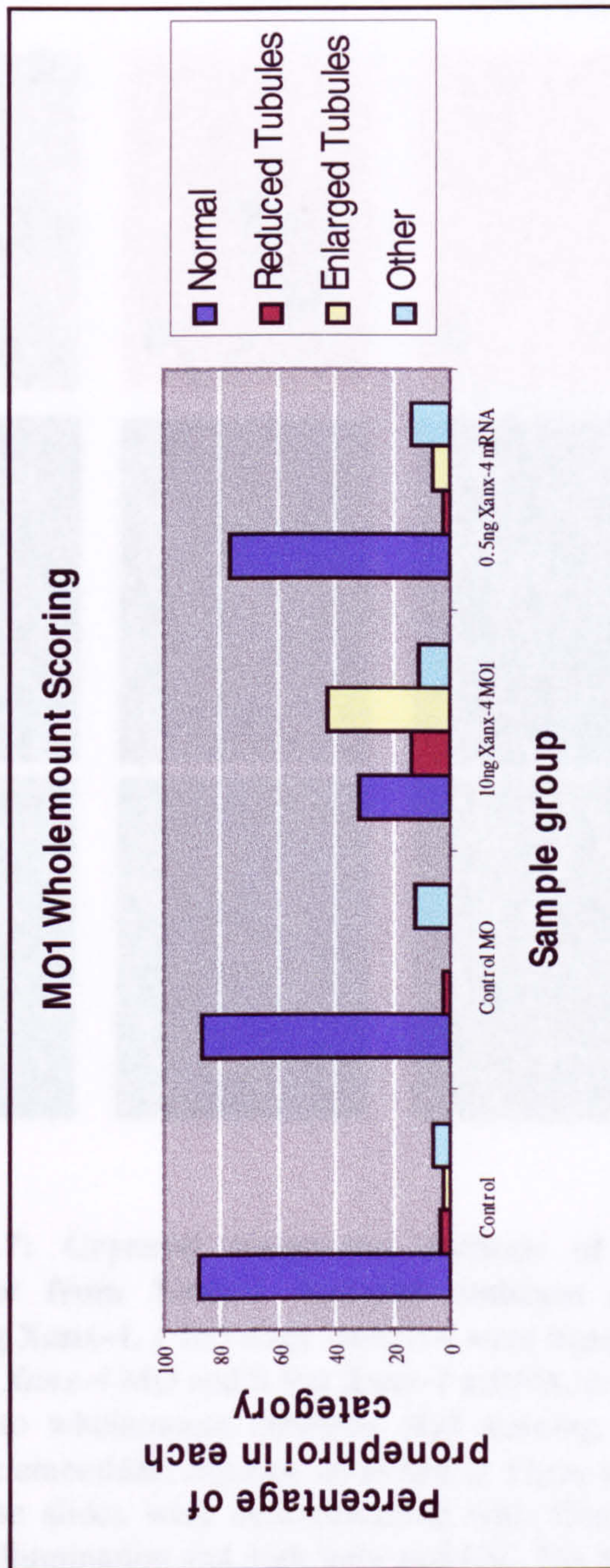


Figure 6.6: Wholemount pronephric phenotype scoring analysis of Xanx-4 depleted embryos and embryos over-expressing Xanx-4. 1-cell stage *Xenopus* embryos were injected with 10ng of *Xanx-4* MO1, 10ng control MO or 0.5ng *Xanx-4* mRNA, cultured to stage 40 and subjected to wholemount antibody staining with pronephric tubule specific antibody 3G8. The embryos were scored for aberrant phenotypes under the following categories, normal, reduced/missing tubules, enlarged tubules (refers to an enlarged diameter, not more or ectopic tubules) and other. The other category refers to naturally occurring phenotypes often observed in *Xenopus* embryos. A: The table shows the actual numerical data from the scoring analysis, the enlarged tubule phenotype was found in 43% (24/56) of *Xanx-4* MO1 injected embryos, 2% (1/48) of control embryos and 6% (4/62) of *Xanx-4* mRNA injected embryos. B: A graphical representation of the data in A.

Figure 6.7

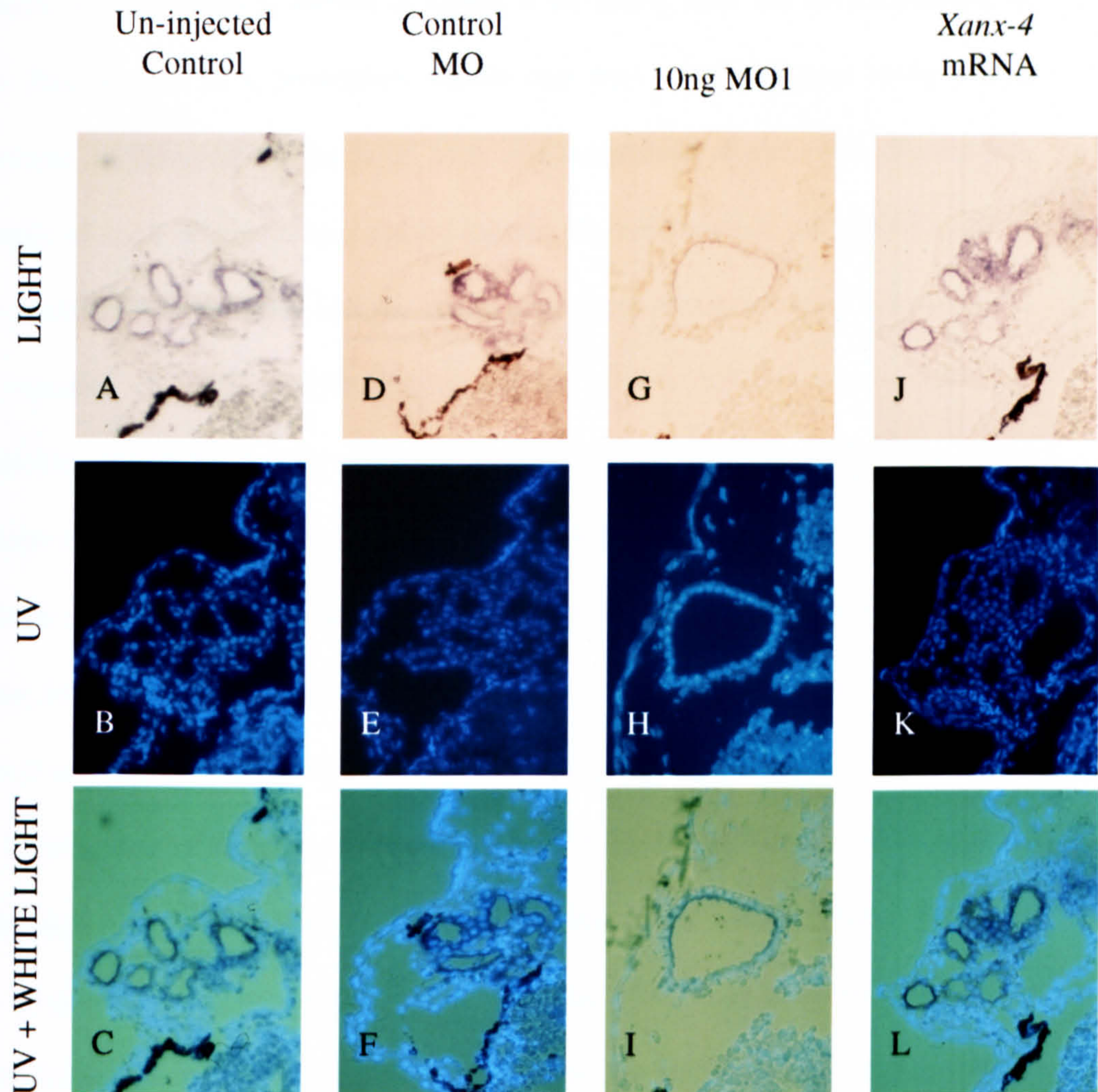


Figure 6.7: Cryostat transverse sections of stage 40 *Xenopus* pronephroi from *Xanx-4* depleted embryos and embryos over-expressing *Xanx-4*. 1 cell stage embryos were injected with 10ng *Xanx-4* MO, 10ng *Xanx-4* MO and 0.5ng *Xanx-4* mRNA, cultured to stage 40 and subjected to wholemount antibody 3G8 staining. The embryos were acrylamide embedded, cryostat sectioned at 12 μ m and lifted on to subbed slides. The slides were counterstained with Hoescht, inspected under light, UV illumination and both light and UV. The figure shows examples of the sections inspected under each light condition. A-C: Un-injected normal controls, D-F sections of embryos injected with 10ng control MO, G-I: sections of embryos injected with 10ng *Xanx-4* MO1, J-L: sections of embryos injected with 0.5ng *Xanx-4* mRNA. The enlarged lumen can clearly be seen in the *Xanx-4* depleted embryos G-I, all other samples appear normal.

cross-sections. A schematic representation of an example section with true transverse (shaded, counted) and a partial longitudinal section (unshaded and arrowed, not counted) is shown in figure 6.8A along with the actual section in 6.8B. Any section of a pronephric tubule that was considered not being a true transverse section, on the basis of such cross-sectional shape, was discounted. All cells of each sectioned pronephric tubule, on both sides of the embryo and in each section were counted and the mean cell count was calculated (Figure 6.9). The number of cells contributing to normal control tubules was remarkably consistent, averaging 9 cells and with a range from 6-15 cells. Inspection of the sections of the *Xanx-4* MO1 injected embryos for the number of cells making up a tubule section, however, revealed that the pronephric tubules had an enlarged lumen, but appeared normal in all other respects. The cells of the tubules retained normal cell integrity and shape, the organisation of the tubule epithelium was one cell in diameter as in normal controls (Figure 6.7). In the *Xanx-4* MO1 injected embryos the average number of cells contributing to the tubule section, however, was 25 and the range was 6-48 (Figure 6.9). The wide range observed reflects the observation that the tubule width at the start and the finish of each tubule domain was of normal size; where the tubules connect with nephrostomes (dorsal) and pronephric duct (ventral). This represents a significant difference from either uninjected control values (mean = 9 and range 5-15), control MO injected values (mean = 9 and range 6-15) or values obtained from *Xanx-4* mRNA injected embryos (mean = 9 and range 6-14). Representative results are presented in figure 6.7 and the mean and standard deviation of the cell counts per tubule section for each sample group are shown in figure 6.9. Duct staining was also

Figure 6.9

Figure 6.8

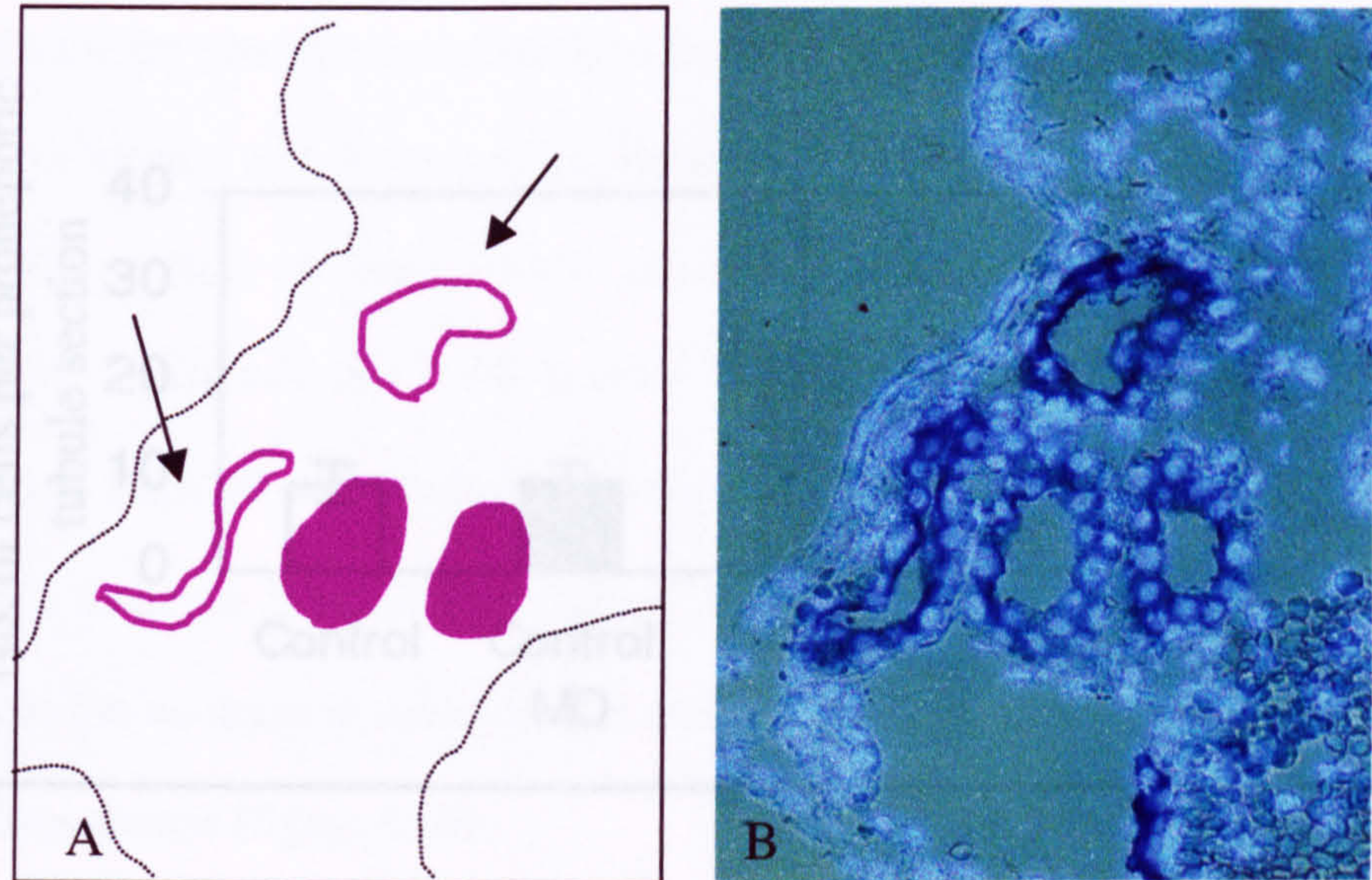


Figure 6.8: A pronephric tubule section and a schematic representation of the same section. The figure illustrates those tubule sections which were included in the analysis and those which were rejected. A: A schematic representation of the sample section in B indicating pronephric tubule section glancing blows (arrowed), unfilled (not counted) and true transverse sections, filled (counted). B: The actual tubule section viewed under a combination of UV and white light, the UV illuminates the Hoescht staining (nuclear DNA) allowing cell count and the white light allows the identification of those cells contributing to the pronephric tubules.

Figure 6.9

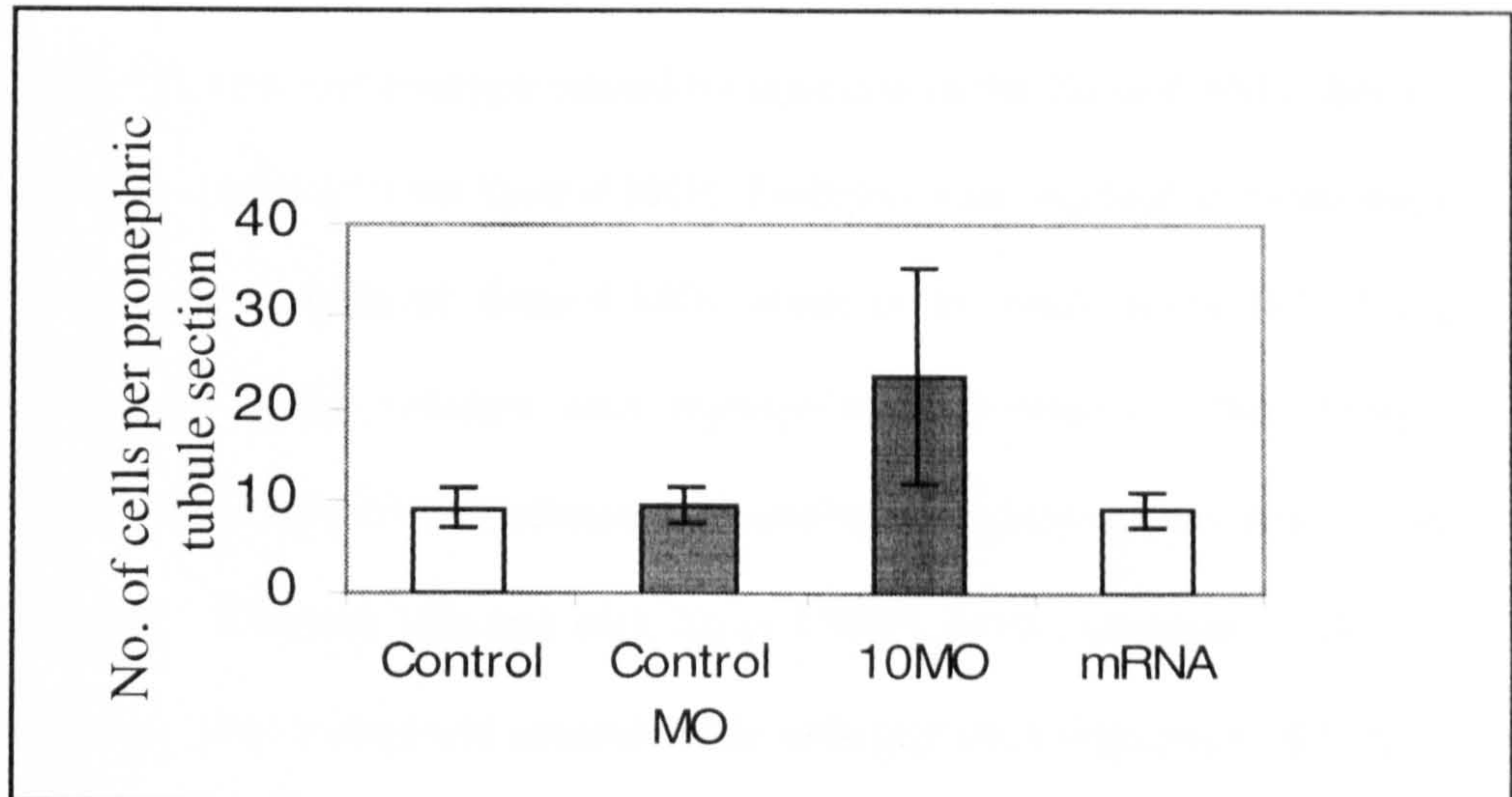


Figure 6.9: Graphical representation of data collected from cell counts of complete serial sections of pronephric tubules from embryos with depleted *Xanx-4* expression or over-expressing *Xanx-4*. 1 cell stage embryos were injected with 10ng control MO (control MO), 10ng *Xanx-4* MO (10MO), 0.5ng *Xanx-4* mRNA (mRNA), cultured to stage 40 and subjected to wholemount antibody 3G8 staining. The embryos were acrylamide embedded, cryostat sectioned at 12 μ m and lifted on to subbed slides. The slides were counterstained with Hoescht, inspected under light and UV illumination and cell counts per pronephric tubule were obtained. The mean number of cells per tubules section in the control, control MO and *Xanx-4* mRNA injected embryos were not significantly different, whereas those embryos injected with 10ng *Xanx-4* MO displayed an enlarged pronephric tubule phenotype. The error bars show 1 standard deviation from the mean.

carried out using specific monoclonal antibody 4A6, no effect on duct morphology was observed.

6.2.3 *Xanx-4* MO1 phenotype can be rescued by co-injection with *Xanx-4* mRNA.

In order to rescue the phenotype caused by injection of the *Xanx-4* MO1, *Xanx-4* mRNA was co-injected with *Xanx-4* MO1. Embryos were injected at 1-cell stage with 5ng, 10ng or 20ng of *Xanx-4* MO1 alone or in combination with 0.5ng *Xanx-4* mRNA. Equal volumes were injected into all embryos. The embryos were cultured to stage 40 and wholemount antibody immunostained with tubule specific 3G8. Embryos injected with *Xanx-4* MO1 were compared to the co-injected and to the un-injected controls. The embryos were examined initially as wholemount specimens (figure 6.10).

As previously described, pronephric tubules of the embryos injected with the *Xanx-4* MO1 (Figure 6.10A,C,E) appeared in general to be wider, shorter and less coiled than those of the normal control embryos (Figure 6.10G), with the most severe aberrant phenotype observed in those embryos injected with the higher concentration of MO1. Those embryos co-injected with 5ng *Xanx-4* MO1 and 0.5ng *Xanx-4* mRNA appeared completely rescued. The pronephric tubules appeared almost normal, (Figure 6.10B). The embryos co-injected with 10ng and 20ng MO1 and 0.5ng *Xanx-4* mRNA showed significant, although incomplete, rescue with the tubules being somewhat less normal and displaying some larger and less coiled tubules (figure 6.10D, F respectively). Seemingly the rescue was

Figure 6.10

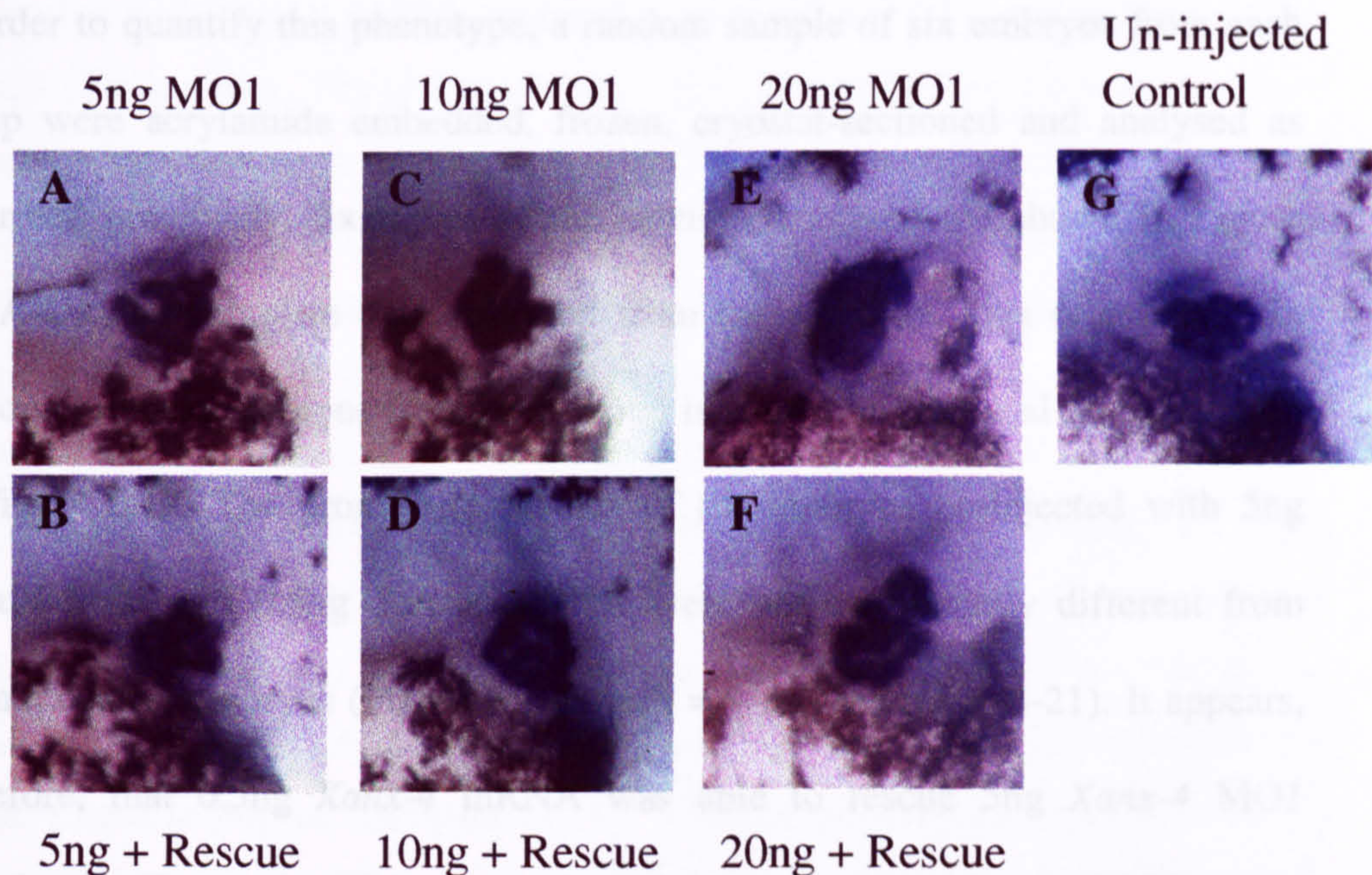


Figure 6.10: The enlarged pronephric tubule phenotype produced by injection of *Xanx-4* MO can be rescued by co-injection with *Xanx-4* mRNA. 1 cell stage embryos were injected with 5ng (A), 10ng (C) or 20ng (E) *Xanx-4* MO1 alone or in combination with 0.5ng *Xanx-4* mRNA (B, D, F respectively) and cultured to stage 40. The embryos were subjected to wholemount antibody 3G8 staining and were scored for phenotypic aberrations. It was seen that those embryos depleted in *Xanx-4* display a shortened, widened and less coiled pronephric phenotype when compared to controls. Those embryos injected with 20ng MO1 display a more severe phenotype than those injected with 10ng MO1 and the least severe phenotype is associated with 5ng MO1 injection. It appears that injection of *Xanx-4* mRNA is able to rescue the enlarged tubule phenotype observed, where co-injection of 0.5ng *Xanx-4* mRNA and *Xanx-4* MO1 (B, D, F) leads to pronephric tubules with a more normal phenotype compared to those injected with MO1 alone (A, C, E).

not complete at the higher concentrations of MO1. Other than the pronephric tubule phenotype described above, the gross phenotype of the embryos in all groups appeared normal.

In order to quantify this phenotype, a random sample of six embryos from each group were acrylamide embedded, frozen, cryostat-sectioned and analysed as described previously. Examples of the sections analysed are shown in Figure 6.11A-U. The complete data collected from the serial sections of each of six randomly chosen embryos from each group is shown in graphical representation in Figure 6.12. The pronephric tubules of the embryos co-injected with 5ng *Xanx-4* MO1 and 0.5ng *Xanx-4* mRNA were not significantly different from normal control embryos (Figure 6.12, mean = 9 and the range 5-21). It appears, therefore, that 0.5ng *Xanx-4* mRNA was able to rescue 5ng *Xanx-4* MO1 completely (Figure 6.11G-I). Those injected with 10ng or 20ng of MO1 were partially rescued by 0.5ng *Xanx-4* mRNA (Figure 6.12, mean 10ng = 12, 20ng = 14 and the ranges both 6-38). Embryos injected with 10ng MO1 and 0.5ng mRNA were rescued to a 5ng MO1 phenotype (compare Figure 6.11M-O to 6.11D-F) and 20ng MO1 and 0.5ng mRNA were rescued to an intermediate phenotype between 10ng and 20ng (Figure 6.11S-U). Similar results were obtained from a repeat experiment.

6.2.4 Analysis of the expression of pronephric molecular markers in *Xanx-4* overexpression and *Xanx-4* morpholino treated embryos.

In order to assess whether overexpression or suppression of *Xanx-4* has an effect on the expression of genes that have been shown to play a role in early kidney

Figure 6.11

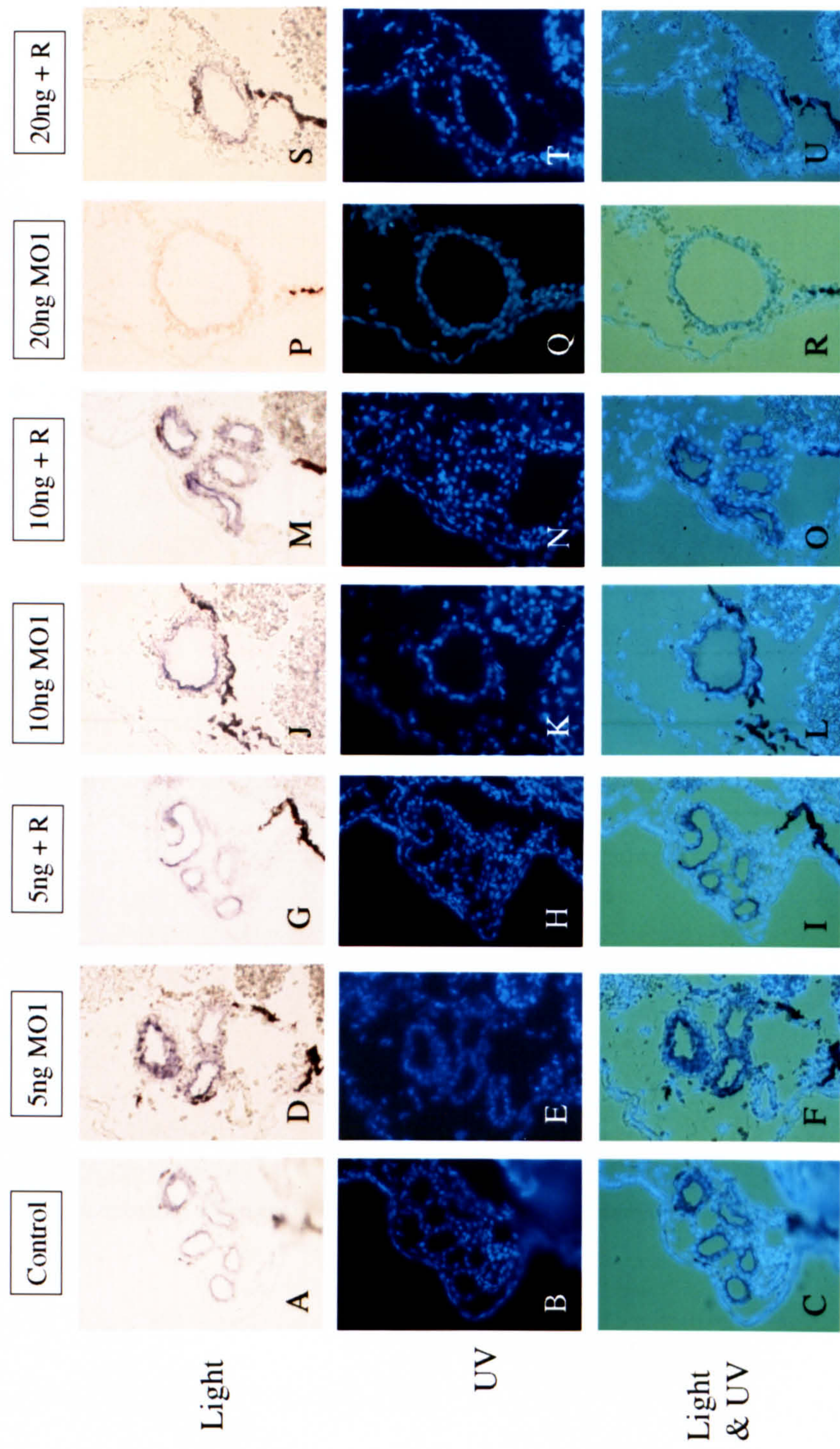


Figure 6.12

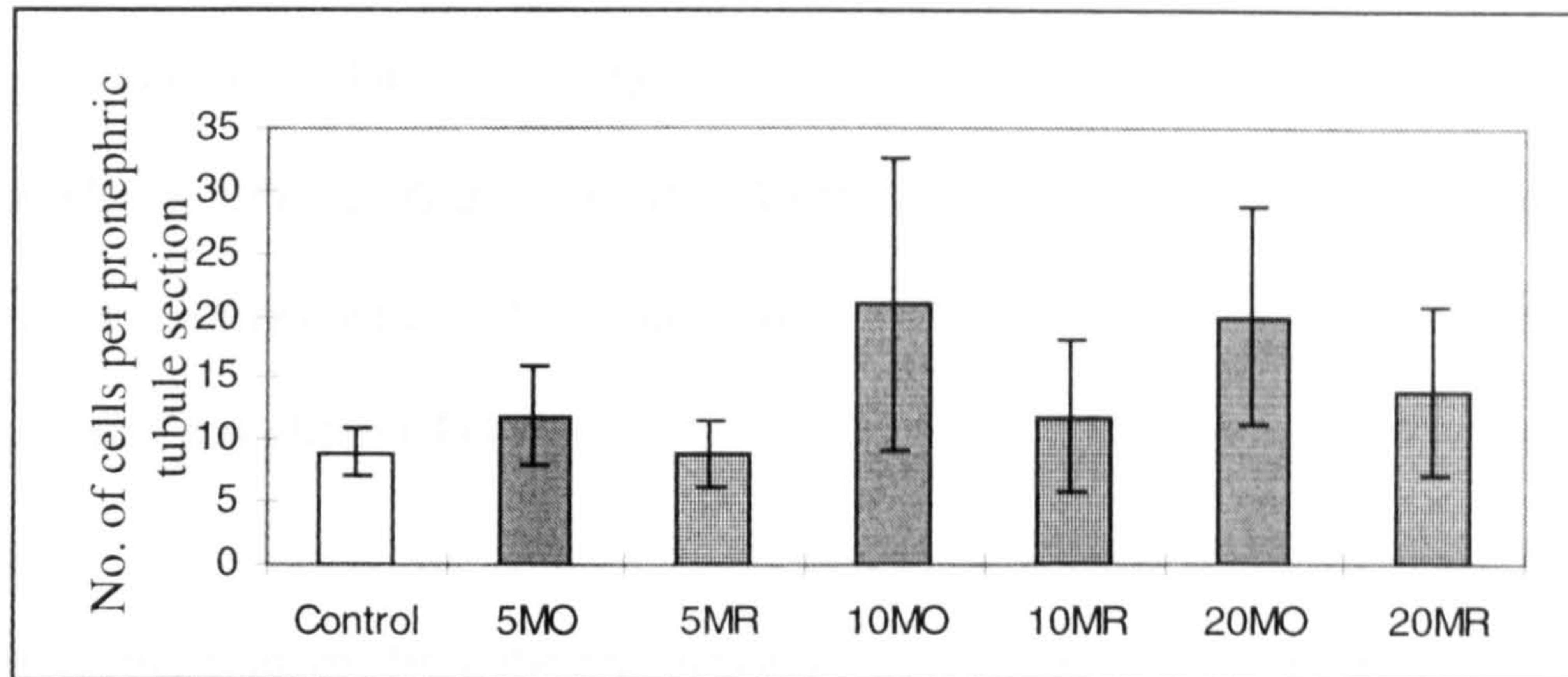


Figure 6.12: Graphical representation of data collected from cell counts of complete serial sections of pronephric tubules from embryos with depleted *Xanx-4* expression or rescued by co-injection of *Xanx-4* mRNA. 1 cell stage embryos were injected with 5ng (5MO), 10ng (10MO) or 20ng (20MO) of *Xanx-4* MO1 alone or in combination with 0.5ng *Xanx-4* mRNA (5MR, 10MR and 20MR respectively), cultured to stage 40 and subjected to wholemount 3G8 antibody staining. The embryos were acrylamide embedded, cryostat sectioned at 12 μ m and lifted on to subbed slides. The slides were counterstained with Hoescht, inspected under light and UV illumination and cell counts per pronephric tubule were obtained. The mean number of cells per tubule section in each of the sample groups was calculated and is presented in the graph. It appears that *Xanx-4* mRNA is able to rescue the enlarged tubule phenotype. 0.5ng of *Xanx-4* mRNA is able to completely rescue the phenotype induced by 5ng MO1 back to normal and partially rescue 10ng and 20ng MO1 phenotypes. The error bars show 1 standard deviation from the mean.

development, semi-quantitative RT-PCR and *in situ* hybridisation was performed using a range of pronephric marker genes. Embryos were injected at the 1-cell stage with 0.5ng *Xanx-4* mRNA or 10ng *Xanx-4* MO1 and cultured to stage 25. Two groups of five embryos from each treatment and two groups of five controls were selected at random and subjected to RT-PCR using primers designed against *Xlim-1*, *XPax-2*, *XPax-8*, *Xwnt-4*, *Xwnt-11* and *xWT-1* (Table 2.1). *EF1 α* is used as a loading control. No obvious effect on RNA expression of any of the marker genes was observed (figure 6.13).

The remaining embryos from the previous experiment, were fixed at stage 27 and subjected to *in situ* hybridisation using RNA probes prepared from cDNA clones of pronephric marker genes *XPax-8*, *Xlim-1* and *xWT-1*. The expression pattern of each marker gene RNA in the embryos injected with *Xanx-4* mRNA and *Xanx-4* MO1 were compared to uninjected control embryos (figure 6.14). No apparent change in *XPax-8* or *Xlim-1* expression pattern was observed in either group with perturbed *Xanx-4* expression, compared to uninjected control. However, a reduced field of *xWT-1* expression was observed in 12/44 of the embryos over-expressing *Xanx-4* compared to controls. This suggests a reduction of glomus tissue. No altered *xWT-1* field of expression was seen in the embryos injected with *Xanx-4* MO1. It seems perturbation of expression of *Xanx-4* is not linked to any of the tubule markers analysed. We also assume from these results that the *Xanx-4* knockout phenotype is not associated with more or less tissue being specified to become pronephric tubule in character.

Figure 6.13

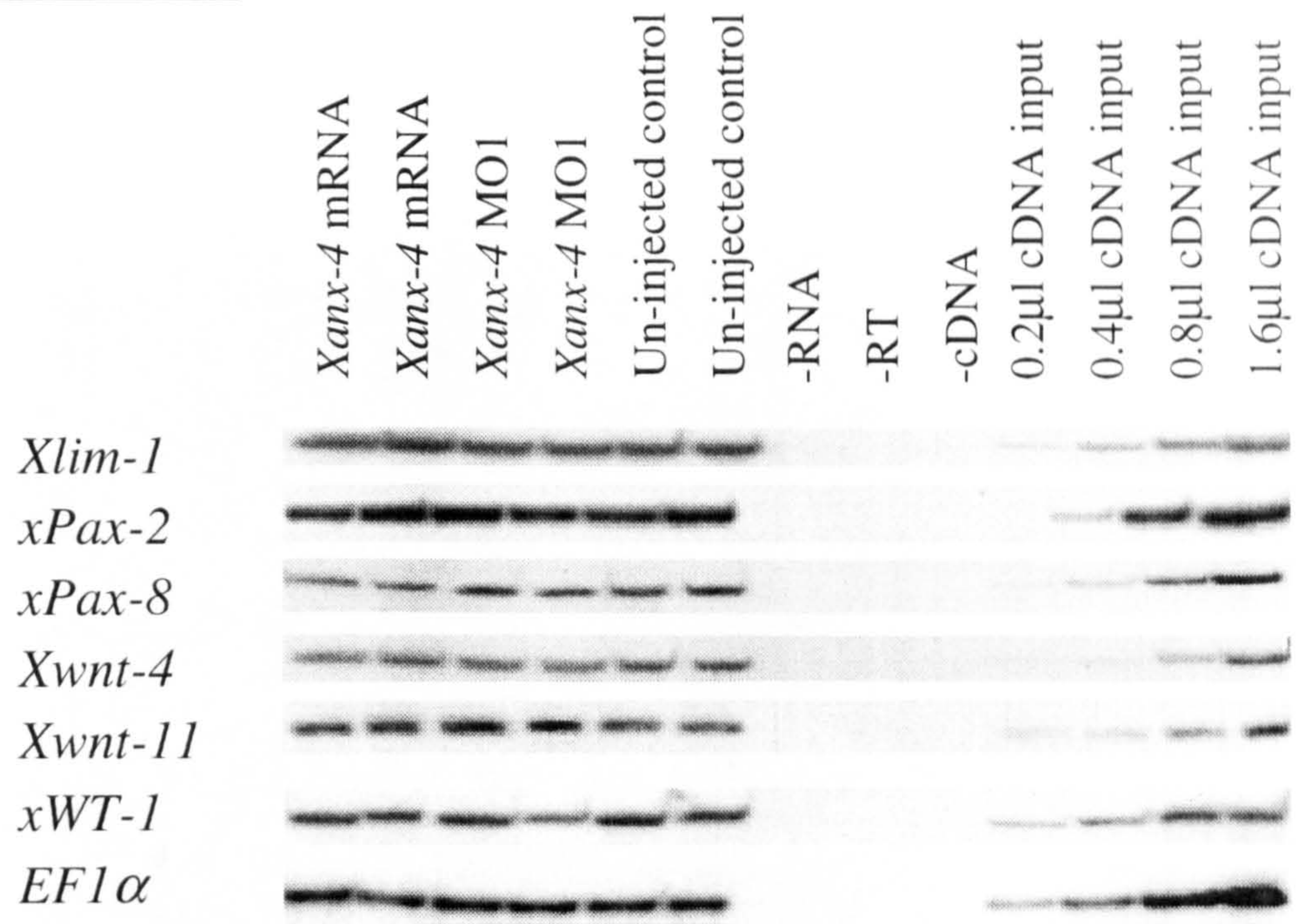


Figure 13: Analysis of the effects of *Xanx-4* depletion or over-expression on the expression of pronephric marker genes by RT-PCR. Embryos were injected at 1 cell stage with 0.5ng *Xanx-4* mRNA or 10ng *Xanx-4* MO and cultured to stage 27. Groups of five embryos were then subjected to RT-PCR using primers designed against a range of pronephric molecular markers. No effect on expression of any of the markers was observed. *EF1α* was used as a loading control.



Figure 14: Analysis of the effects of *Xanx-4* depletion or over-expression on the expression of pronephric marker genes by *in situ* hybridisation. Embryos were injected at 1 cell stage with 0.5ng *Xanx-4* mRNA or 10ng *Xanx-4* MO and cultured to stage 27. The embryos were then subjected to *in situ* hybridisation using specific probes prepared from pronephric molecular markers *Xlim-1* (A, D, G), *XPax-8* (B, E, H) and *xWT1* (C, F, I). No effect on expression of *XPax-8* or *Xlim-1* was observed. However, a reduced field of *xWT1* expression was observed in the embryos injected with *Xanx-4* mRNA (compare C with I).

6.2.5 The issue of a true rescue.

Due to the fact that *Xanx-4* MO1 was positioned mainly in the coding region of *Xanx-4* (figure 6.2) it was suggested that the rescue may not be a true rescue. It was proposed that the action of the injected *Xanx-4* mRNA was of “mopping-up” the MO1. In this way, MO1 would not be available to bind to and block translation of the endogenous message. Concurrently, the injected mRNA would not be available for translation and therefore to rescue the phenotype. A true rescue would involve the MO directed to the endogenous message and the rescue being performed by the protein product of the exogenous mRNA. This type of true rescue requires the MO to be effective against the endogenous message but ineffective against the injected message.

To overcome this issue, two possible approaches were available. Firstly, the MO is designed to the 5'UTR of the target gene mRNA and the 5'UTR is removed from the injected message template prior to *in vitro* transcription. Alternatively, third-base modifications must be made in the exogenous mRNA, so that it is no longer recognised by the MO, but which do not effect its function *in vivo*. A second *Xanx-4* MO (MO2) was ordered against the 5'UTR of the *Xanx-4* cDNA clone. Unfortunately, it was not possible to place an MO in the 5'UTR region, the manufacturer recommended that a MO designed to this region would be ineffective. The next best position (as opposed to MO1) would span the ATG but would contain only 15 complementary nucleotides in the coding region as opposed to 24 in MO1 (figure 6.2). A morpholino is proposed to be ineffective if it contains 6 or less contiguous complementary residues (P. Morcos Gene-tools, pers. comm.). Therefore, in order for MO2 not to recognise the injected *Xanx-4*

mRNA it was necessary to create *Xanx-4* mRNA lacking the 5'UTR and containing two third-base changes in the first 15 nucleotides of the coding region, no more than 6 nucleotides apart. This was carried out using PCR site-directed mutagenesis.

6.2.6 Design and preparation of mutant *Xanx-4* mRNA.

On inspection of the *Xanx-4* cDNA sequence, two third-base modifications were chosen and the corresponding upstream primer (AN4-MUT) designed including an *EcoRI* restriction site 5' of the ATG which would allow removal of the 5'UTR and aid cloning (Figure 6.15, Table 2.2). The *Xanx-4*-MUT cDNA was amplified by PCR (see methods 2.4.5), cloned into expression vector RN3 (appendix 4) and the modifications checked by automated sequencing. *Xanx-4*-MUT mRNA was transcribed using T3 RNA polymerase from *SfiI* linearised *Xanx-4*-MUT/RN3 construct (appendix 4). The mRNA was diluted to 500ug/ml and used in the following assays.

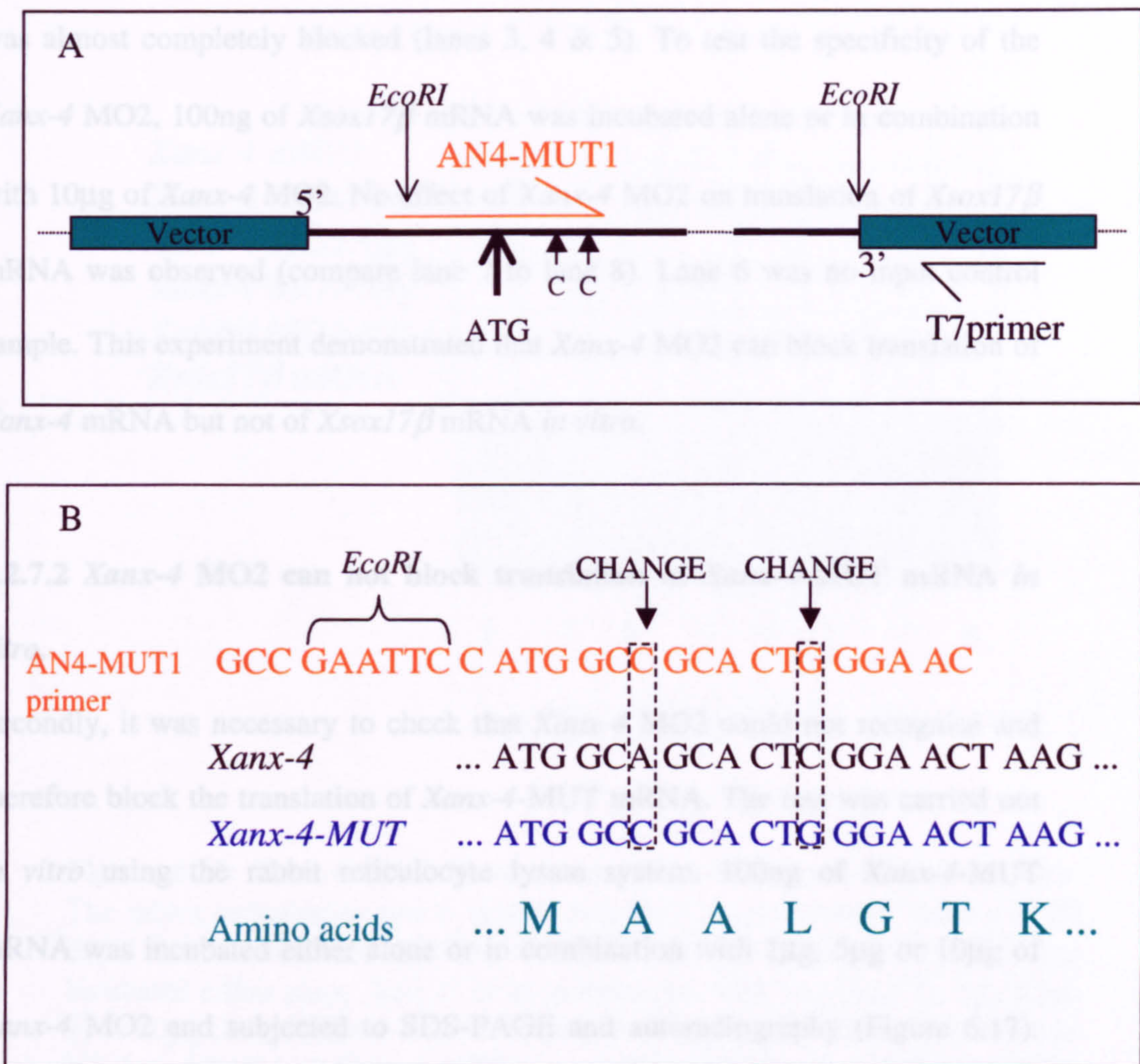
6.2.7 The effectiveness of *Xanx-4* MO2 with *Xanx-4* mRNA and *Xanx-4*-MUT mRNA *in vitro*.

6.2.7.1 *Xanx-4* MO2 blocks translation of *Xanx-4* mRNA *in vitro*.

Firstly, it was necessary to check that the new MO (*Xanx-4* MO2) could block translation of normal *Xanx-4* mRNA. As a simulation of endogenous mRNA *in vivo*, the effectiveness of the *Xanx-4* MO2 was established *in vitro*, using *Xanx-4* MO1 as a positive control for the experiment. 100ng of *Xanx-4* mRNA was incubated either alone or in combination with 1µg of *Xanx-4* MO1 or 1µg, 5µg

or 10µg of *Xanx-4* MO2 in the reticulocyte lysate system. The lysates were subjected to SDS-PAGE and autoradiography (Figure 6.16). The *Xanx-4* mRNA alone was successfully translated (lane 1) and when incubated with 1µg of *Xanx-4* MO1 (lane 2, positive control) or 1µg, 5µg or 10µg *Xanx-4* MO2, translation was almost completely blocked (lanes 3, 4 & 5). To test the specificity of the *Xanx-4* MO2, 100ng of *Xanx-4* mRNA was incubated alone or in combination with 10µg of *Xanx-4* MO1. No effect of *Xanx-4* MO1 on translation of *Xanx-4* mRNA was observed (compare lane 6 with lane 5). Lane 6 was also a positive sample. This experiment demonstrated that *Xanx-4* MO2 can block translation of *Xanx-4* mRNA but not of *Xanx-4* MO1 mRNA in vitro.

Figure 6.15



The *Xanx-4* MUT mRNA alone was successfully translated into a protein of 34kDa, which is in good agreement with *Xanx-4* mRNA (lane 1). When

Figure 6.15: The preparation of *Xanx-4*-MUT mRNA template. A: The AN4-MUT1 upstream primer was designed to the translation start site, incorporating a *EcoRI* restriction enzyme site upstream of the ATG and two third-base changes down-stream of the ATG (CHANGE 1 and CHANGE 2). AN4-MUT1 and T7 primers were used to amplify the *Xanx-4* coding region, allowing the incorporation of the engineered *EcoRI* site and the *EcoRI* site already in *Xanx-4*/pGEM-T Easy construct for cloning into the RN3 vector. The third-base changes achieved are shown in B.

or 10µg of *Xanx-4* MO2 in the reticulocyte lysate system. The lysates were subjected to SDS-PAGE and autoradiography (Figure 6.16). The *Xanx-4* mRNA alone was successfully translated (lane 1) but when incubated with 1µg of *Xanx-4* MO1 (lane 2, positive control) or 1µg, 5µg or 10µg *Xanx-4* MO2, translation was almost completely blocked (lanes 3, 4 & 5). To test the specificity of the *Xanx-4* MO2, 100ng of *Xsox17β* mRNA was incubated alone or in combination with 10µg of *Xanx-4* MO2. No effect of *Xanx-4* MO2 on translation of *Xsox17β* mRNA was observed (compare lane 7 to lane 8). Lane 6 was no input control sample. This experiment demonstrated that *Xanx-4* MO2 can block translation of *Xanx-4* mRNA but not of *Xsox17β* mRNA *in vitro*.

6.2.7.2 *Xanx-4* MO2 can not block translation of *Xanx-4*-MUT mRNA *in vitro*.

Secondly, it was necessary to check that *Xanx-4* MO2 could not recognise and therefore block the translation of *Xanx-4*-MUT mRNA. The test was carried out *in vitro* using the rabbit reticulocyte lysate system. 100ng of *Xanx-4*-MUT mRNA was incubated either alone or in combination with 1µg, 5µg or 10µg of *Xanx-4* MO2 and subjected to SDS-PAGE and autoradiography (Figure 6.17). The *Xanx-4* MUT mRNA alone was successfully translated into a protein of 34kDa, which is in good agreement with *Xanx-4* mRNA (lane 1). When incubated with 1µg, 5µg or 10µg *Xanx-4* MO2, no change in the level of translation of *Xanx-4* MUT mRNA was observed, at any concentration of *Xanx-4* MO2 tested (lanes 4, 5 & 6). This demonstrated that *Xanx-4* MO2 cannot

Figure 6.16

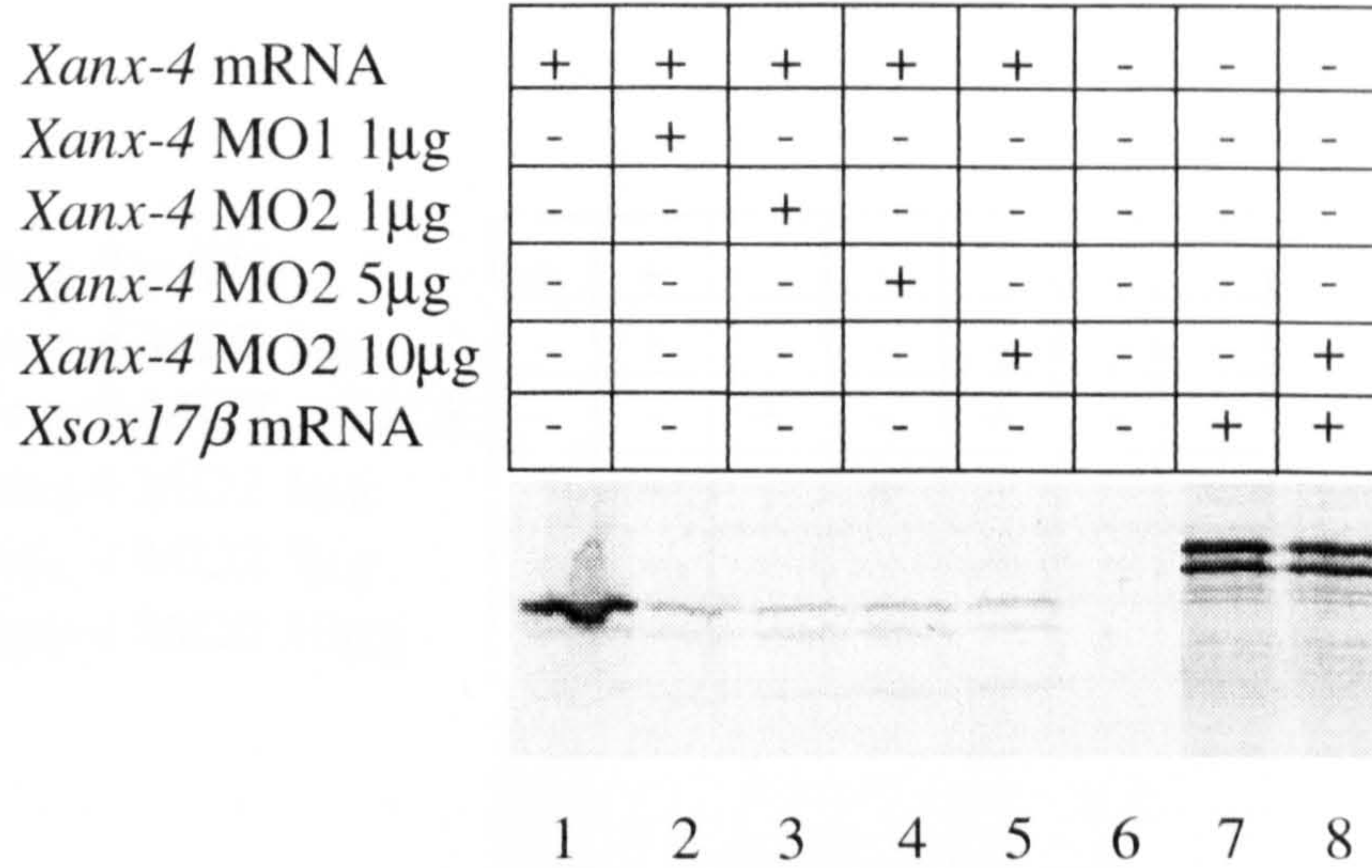


Figure 6.16: *Xanx-4* MO2 blocks translation of *Xanx-4* mRNA *in vitro*. The rabbit reticulocyte lysate system was used to test whether *Xanx-4* MO2 could block translation of *Xanx-4* mRNA. 100ng of *Xanx-4* mRNA was incubated either alone (lane 1) or in combination with 1 μ g (lane 3), 5 μ g (lane 4) or 10 μ g (lane 5) *Xanx-4* MO2. It was observed that the *Xanx-4* MO2 could block translation of *Xanx-4* mRNA at any concentration tested. *Xanx-4* MO1 (lane 2) was used as a positive control. *Xsox17 β* was used as a specificity control. Lane 6 was no input RNA control.

Figure 6.17

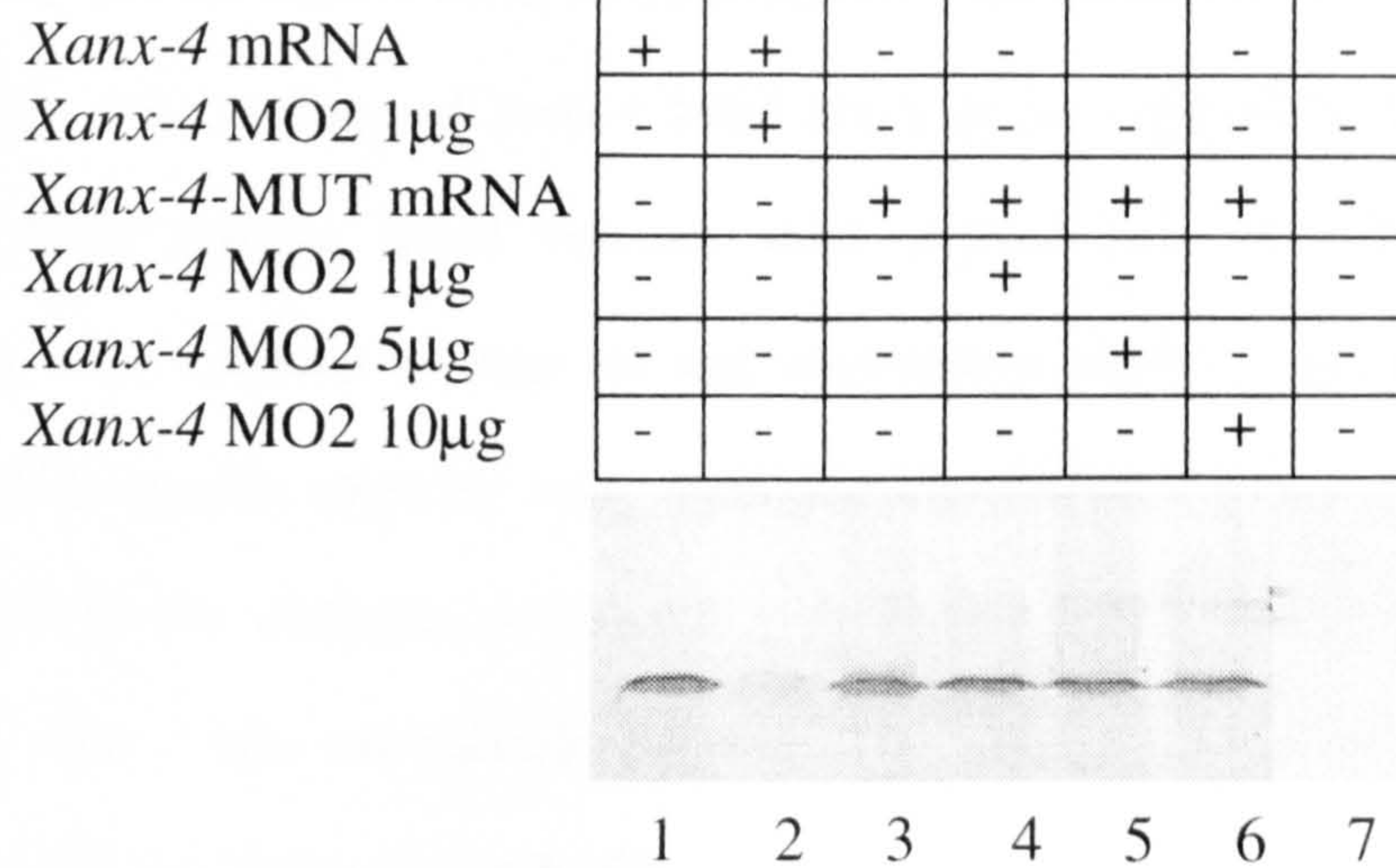


Figure 6.17: *Xanx-4* MO2 does not block translation of *Xanx-4*-MUT mRNA *in vitro*. The rabbit reticulocyte lysate system was used to test whether *Xanx-4* MO2 could block translation of *Xanx-4*-MUT mRNA. 100ng of *Xanx-4* mRNA was incubated alone (lane 1) or in combination with 1μg of *Xanx-4* MO2 (lane 2). The MO2 was able to deplete the translation of *Xanx-4* mRNA. 100ng of *Xanx-4*-MUT mRNA was incubated either alone (lane 3) or in combination with 1μg (lane 4), 5μg (lane 5) or 10μg (lane 6) *Xanx-4* MO2. It was observed that the *Xanx-4* MO2 could not block translation of *Xanx-4*-MUT mRNA at any concentration tested. Lane 7 was no input RNA control.

recognise, and is therefore ineffective at blocking translation of *Xanx-4*-MUT mRNA *in vitro*. Lane 7 was no mRNA input control.

6.2.8 *Xanx-4* MO2 produces the same aberrant pronephric tubule phenotype, observed using *Xanx-4* MO1, which can be rescued by *Xanx-4*-MUT mRNA.

In order to test the *Xanx-4* MO2 *in vivo*, embryos were injected at the 1 cell stage with 5ng, 10ng or 20ng of *Xanx-4* MO2 alone or in combination with 0.5ng *Xanx-4*-MUT mRNA. Equal volumes were injected into all embryos. The embryos were cultured to stage 40 and wholemount antibody immunostained with tubule specific antibody 3G8. Embryos injected with *Xanx-4* MO2 were compared to the embryos co-injected with *Xanx-4* MO2 plus *Xanx-4*-MUT mRNA and to the un-injected controls. The embryos were examined as wholemount specimens (figure 6.18).

The pronephric tubules of the embryos injected with the *Xanx-4* MO2 appeared in general to be wider, shorter and less coiled than those of the normal control embryos, with the most severe aberrant phenotype observed in those embryos injected with the higher concentration of MO2 (compare Figure 6.18A, C and E with G). Those embryos co-injected with 5ng *Xanx-4* MO2 and 0.5ng *Xanx-4*-MUT mRNA appeared completely rescued. The pronephric tubules appeared almost normal (figure 6.18B). The embryos co-injected with 10ng and 20ng MO2 and 0.5ng *Xanx-4*-MUT mRNA showed partial rescue with the tubules being somewhat less normal and displaying some larger and less coiled tubules

Figure 6.18

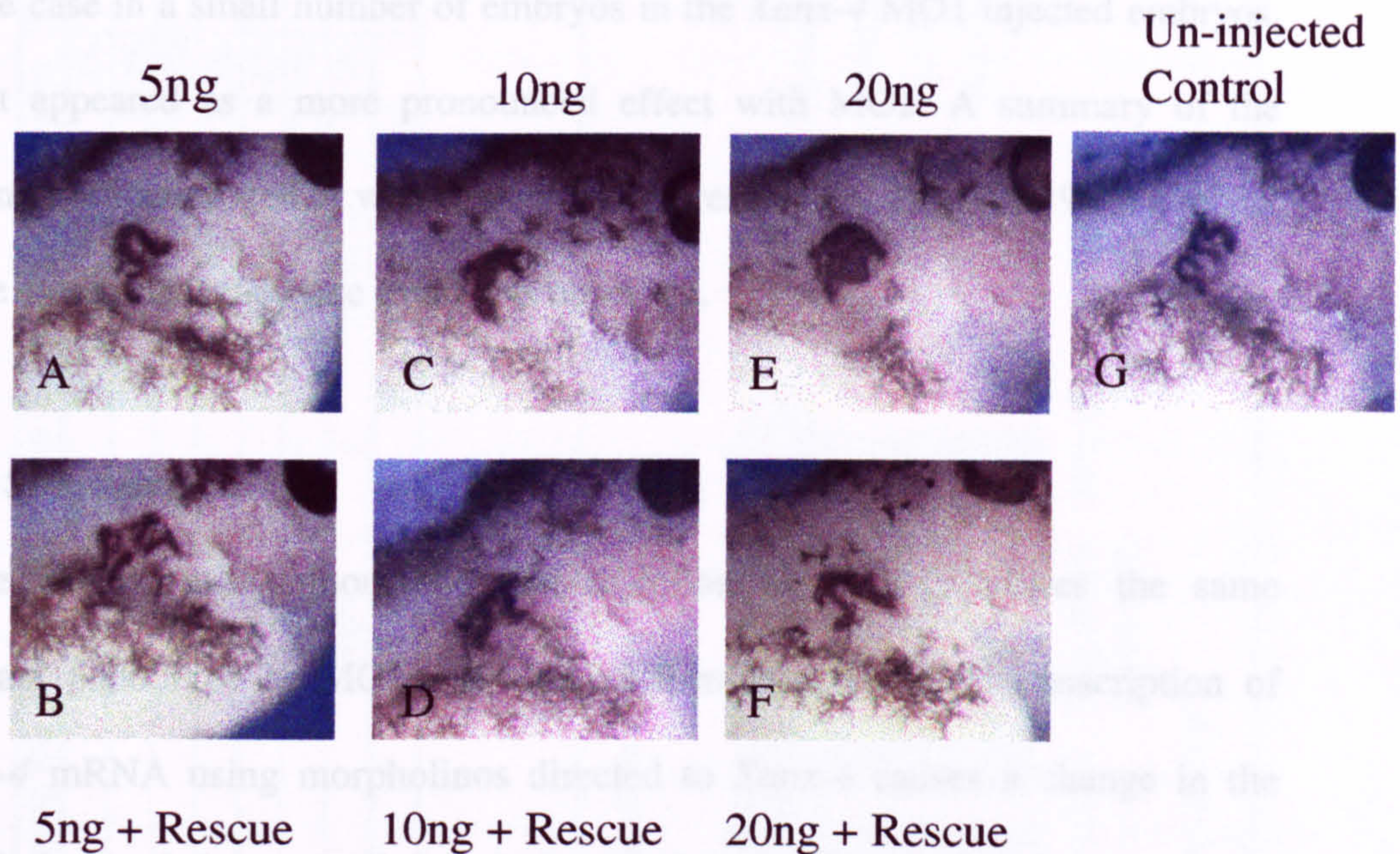


Figure 6.18: *Xanx-4* MO2 produces the same aberrant pronephric tubule phenotype as MO1, which can be rescued by co-injection with *Xanx-4*-MUT, analysed by wholemount antibody 3G8 staining of stage 40 injected embryos. 1-cell stage *Xenopus* embryos were injected with 5ng (A), 10ng (C) or 20ng (E) *Xanx-4* MO2, alone or in combination with *Xanx-4*-MUT mRNA (B, D, F), cultured to stage 40 and subjected to wholemount 3G8 antibody staining. The embryos were compared to normal uninjected control embryos. Embryos injected with *Xanx-4* MO2 show shortened, enlarged diameter tubule phenotype, very similar to the *Xanx-4* MO1 phenotype previously observed. The phenotype appears to become more severe as the concentration of *Xanx-4* MO2 injected increases. *Xanx-4*-MUT mRNA is able to rescue the enlarged tubule phenotype (B, D, F).

(Figure 6.18D and F). In general the results phenocopied the experiment carried out using *Xanx-4* MO1 and *Xanx-4* mRNA. Other than the pronephric tubule phenotype described above, the gross phenotype of the embryos in control and rescue groups appeared normal. Occasionally, embryos injected with *Xanx-4* MO2 alone appeared to be slightly growth retarded, in some cases being around one to two stages behind the control and rescue groups. This was also shown to be the case in a small number of embryos in the *Xanx-4* MO1 injected embryos, but it appeared as a more pronounced effect with MO2. A summary of the scoring is shown together with a graphical representation Figure 6.19. In a repeat of the experiment the same trend was observed.

6.2.9 Summary

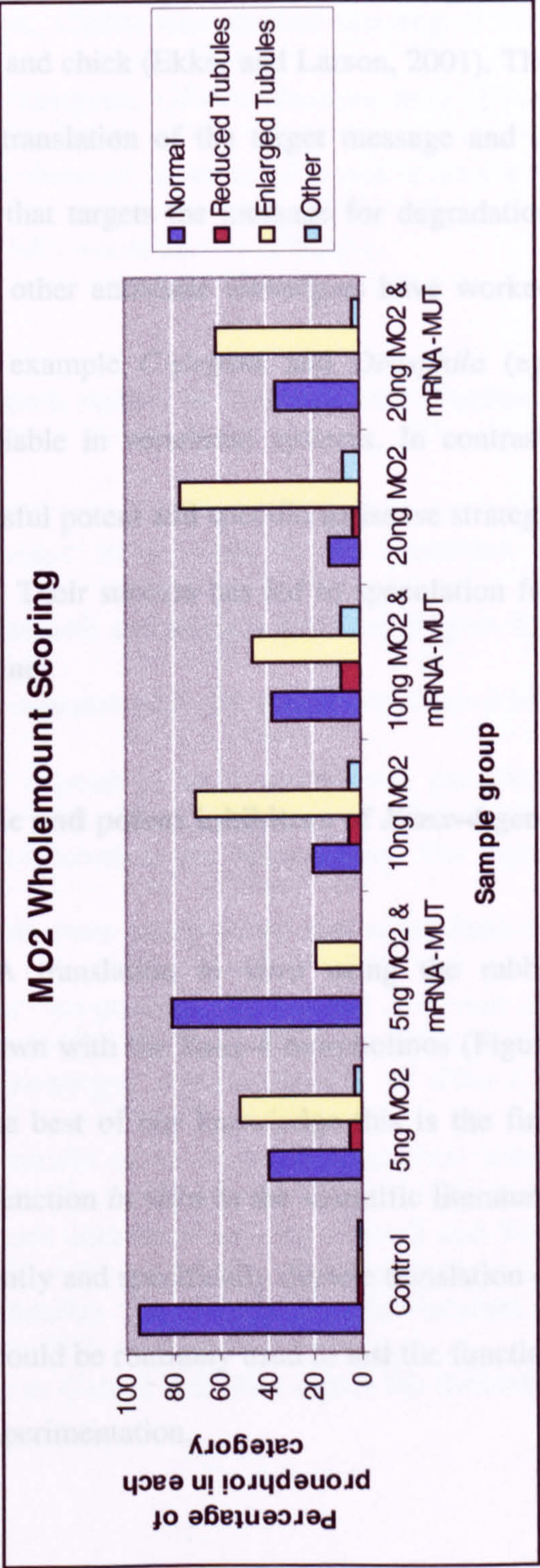
These experiments demonstrate that injection of MO2 produces the same aberrant phenotype as MO1. It also confirms that blocking transcription of *Xanx-4* mRNA using morpholinos directed to *Xanx-4* causes a change in the morphology of the pronephric tubules in *Xenopus laevis*. In some cases the embryos are retarded in stage and in others the pronephros is completely missing. Apart from these observations the embryos appear to be normal in all other respects. The aberrant pronephric tubule phenotype observed is one of shortened, widened and less coiled tubules, the cells appear to be of normal integrity though more cells contribute to a cross-section of the tubule. Either *Xanx-4* or *Xanx-4*-MUT mRNA can rescue the aberrant pronephric tubule phenotype.

Figure 6.19

| Scoring category | Normal | % | Reduced/missing tubules | % | Enlarged tubules | % | Other | % | Total |
|---------------------|--------|-----|-------------------------|----|------------------|-----|-------|----|-------|
| Control | 53 | 95% | 1 | 2% | 1 | 2% | 1 | 2% | 56 |
| 5ng MO2 | 25 | 40% | 3 | 5% | 32 | 52% | 2 | 3% | 62 |
| 5ng MO2 & mRNA-MUT | 39 | 81% | 0 | 0% | 9 | 19% | 0 | 0% | 48 |
| 10ng MO2 | 8 | 20% | 2 | 5% | 28 | 70% | 2 | 5% | 40 |
| 10ng MO2 & mRNA-MUT | 19 | 38% | 4 | 8% | 23 | 46% | 4 | 8% | 50 |
| 20ng MO2 | 4 | 13% | 1 | 3% | 23 | 77% | 2 | 7% | 30 |
| 20ng MO2 & mRNA-MUT | 13 | 36% | 0 | 0% | 22 | 61% | 1 | 3% | 36 |
| | 161 | | 11 | | 138 | | 12 | | 322 |

A

B



6.3 Discussion

Morpholinos are a novel antisense strategy for the perturbation of gene expression. During the course of this work they have been used successfully to specifically interfere with gene expression in a number of model organisms including cell lines, zebrafish, *Xenopus* and chick (Egger and Larson, 2001). The action of the morpholino is to block translation of the target message and is unlike conventional antisense strategy that targets the message for degradation (Corey and Abrams, 2001). Although, other antisense techniques have worked well in less complex organisms, for example *C.elegans* and *Drosophila* (eg. RNAi), they have proven to be unreliable in vertebrate systems. In contrast, morpholinos seem to be the first successful potent and specific antisense strategy employed in more complex organisms. Their success has led to speculation for their use as novel therapeutics in medicine.

6.3.1 *Xanx-4* morpholinos are specific and potent inhibitors of *Xanx-4* gene expression in *Xenopus laevis*.

Specific inhibition of *Xanx-4* mRNA translation *in vitro* using the rabbit reticulocyte lysate system has been shown with the *Xanx-4* morpholinos (Figure 6.3). At the time of writing and to the best of our knowledge this is the first example of the testing of morpholino function *in vitro* in the scientific literature. 1-10 μ g of *Xanx-4* MO was able to potently and specifically deplete translation of 100ng of *Xanx-4* mRNA. This system could be routinely used to test the function and specificity of MO before *in vivo* experimentation.

Specific inhibition of *myc-Xanx-4* mRNA translation was observed in embryos using the *Xanx-4* MO, at all concentrations and stages tested (Figure 6.4). It was found that 5-20ng of *Xanx-4* MO1 was able to deplete translation of 0.5ng of *myc-Xanx-4* mRNA *in vivo* until at least stage 21. This persistence is in agreement with the findings of Nutt et al., (2001) who showed that 4ng of *GFP* MO was able to deplete expression of transgenic *GFP* in *Xenopus* until around stage 38. The highly efficient depletion observed in the *in vitro* and *in vivo* tests systems suggests that lower amounts of MO would also be effective.

6.3.2 *Xanx-4* depletion in *Xenopus laevis* results in enlarged and shortened pronephric tubules.

Depletion of *Xanx-4* protein in *Xenopus laevis* leads to the formation of shortened, less coiled pronephric tubules with an enlarged diameter (Figure 6.5, 7, 11). The severity of the phenotype increases with the amount of *Xanx-4* MO injected (5-20ng). The pronephric duct appears to be of normal size and shape and connects with the posterior common tubule in the normal way. The highly specific effect of *Xanx-4* MOs is evident from observations that apart from the pronephric phenotype embryos appear morphologically normal and that the control MO results in no apparent phenotype. Overexpression of *Xlim-1* in combination with *XPax-2* or *XPax-8* results in an enlarged pronephric tubule phenotype but also results in an increased amount of tubules (Carroll and Vize, 1999). This similarity in phenotypes implies that *Xanx-4* acts downstream of *XPax-2*, *XPax-8* and *Xlim-1*, especially as Carroll and Vize report the formation of ectopic tubules.

6.3.3 A novel strategy for quantitation of pronephric tubule phenotype reveals an increased number of cells in the circumference of the pronephric tubules.

Sectioning of MO injected embryos revealed the tubules were of increased diameter, had a larger lumen but retained a single layer of epithelial cells of normal morphology (Figure 6.7 and 6.11). The novel method of random selection of true transverse sections facilitated the quantitation and comparison of the average number of cells comprising a tubule circumference in normal and effected pronephroi. The average number of cells contributing to a true transverse section of a normal pronephric tubule was found to be 9 with a range of 6-15 and in the *Xanx-4* depleted embryos the average was found to be 25 with a range of 6-48. Detailed inspection of numerous sections of pronephroi revealed that the nephrostomes and duct of depleted embryos were of normal morphology. The wide range of cells contributing to the tubule circumference in depleted embryos reflects that the enlarged tubules were connecting to nephrostomes anteriorly and duct posteriorly, in a normal manner although this has not been fully investigated. An alternative approach to quantifying the phenotype might have measured the circumference of the depleted tubules, however this approach would have been much less informative. Inspection of sections of embryos overexpressing *Xanx-4* revealed that overexpression of *Xanx-4* had no effect on the morphology of the pronephros or the number of cells comprising the tubule circumference. This is in good agreement with the results of chapter 4.

6.3.4 Xanx-4 depleted tubule phenotype can be rescued by *Xanx-4* mRNA.

Co-injection of *Xanx-4* mRNA and MO1 resulted in the rescue of the aberrant tubule phenotype, with 0.5ng of *Xanx-4* mRNA completely rescuing 5ng of MO1 (Figure 6.10). Co-injection of higher amounts of MO resulted in partial rescue of the enlarged tubule phenotype. Complete rescue of the embryos injected with higher amounts of MO (10, 20ng) might have been achieved using increased amounts of mRNA. The rescue of MO1 phenotype with mRNA was deemed to be not a true rescue because the function of the injected mRNA may have been to “mop-up” MO1. It was therefore important to separate the effect of depletion of endogenous message from the effect of rescue by introduction of injected mRNA. This was achieved by designing a second morpholino, MO2 positioned 9bp 5' of MO1 and also by engineering an mRNA mutated by third base wobble to rescue the phenotype. It was found that in the *in vitro* test system, MO2 could block the translation of normal *Xanx-4* mRNA but was impotent in blocking the translation of the mutated mRNA (MUT-mRNA). Injecting MO2 into embryos resulted in an identical phenotype to that produced with MO1 (Figure 6.18), demonstrating that MO2 was as effective in depleting *Xanx-4* mRNA translation as MO1. It also demonstrates that the location chosen for the morpholino to be positioned can be moved without diminishing efficacy. It seems likely that multiple positions proximal to the ATG would be similarly effective. Co-injecting MUT-mRNA and MO2 resulted in a true rescue of the pronephric phenotype (Figure 6.18). This clearly demonstrates that the aberrant phenotype is the result of specific depletion of Xanx-4 protein. Assuming that the alterations to MUT-mRNA did not significantly increase its stability, the ability of MUT-mRNA to rescue the phenotype clearly demonstrates that Xanx-4 protein

translated from injected mRNA persists long enough to exert its function. This represents strong evidence that the lack of *Xanx-4* over-expression phenotype (chapter 4) is not due to lack of persistence of injected *Xanx-4* mRNA or its protein product. The lack of a phenotype associated with over-expression of *Xanx-4* is the result of increased levels of *Xanx-4* protein not having an observable morphological effect. One explanation for this result is that *Xanx-4* may need to interact with other factors to perform its function. Annexins have been shown to have binding partners, in particular members of the S100 family (Garbuglia et al., 2000) and annexin IV has been shown to bind to surfactant protein A in lung epithelia (Sohma et al., 1995).

6.3.5 Pronephric tubule phenotype is a result of morphological perturbation.

The effect of perturbation of *Xanx-4* expression by morpholino injection and *Xanx-4* mRNA over-expression on pronephric marker genes has been analysed. By RT-PCR (Figure 6.12) it has been shown that there is no effect on expression of *Xlim-1*, *XPax-2*, *XPax-8*, *xWnt-4*, *xWnt-11* and *xWT1* by either depletion or over-expression of *Xanx-4*. It therefore seems that perturbation of *Xanx-4* expression by morpholino does not result in a difference in the amount of pronephric tissue specified. With the exception of *xWT1* all other markers used are also expressed in other tissues, it could not be ruled out that overexpression or depletion of *Xanx-4* was effecting non-pronephric domains of expression. For example it is possible that pronephric expression was reduced concurrent with an increase of expression in another domain, the total expression thereby remaining unchanged.

To investigate this possibility wholemount *in situ* hybridisation using *Xlim-1*, *XPax-8* and *xWT1* specific probes was performed on control, *Xanx-4* depleted and *Xanx-4* over-expressing embryos (Figure 6.13). No effect was observed on the pronephric domains of *Xlim-1* and *XPax-8*, although the expression of the glomus specific gene *xWT1* was reduced by over-expression of *Xanx-4*. Due to the similarity of phenotype between *Xanx-4* depletion and *Xlim-1/XPax-2/8* overexpression (Carroll and Vize, 1999), the observation that *Xanx-4* depletion does not effect the amount of pronephric tubule tissue specified provides further evidence that *Xanx-4* is downstream of *Xlim-1/XPax-2/8* in a molecular pathway of tubule specification. Further experiments will examine the effect of over-expression of *Xlim-1* and *XPax-2/8*, alone or in combination, on *Xanx-4* expression.

The effect of *Xanx-4* over-expression on *xWT1* was unexpected as no *Xanx-4* over-expression phenotype was previously observed (chapter 4). The fact that RT-PCR analysis gave similar levels of *xWT1* expression in controls and *Xanx-4* over-expressing embryos suggests that the effect of *Xanx-4* over-expression results in more diffuse expression of *xWT1*. This is consistent with the results observed in the *xWT1 in situ* hybridisation of embryos over-expressing *Xanx-4*, where in some embryos *xWT1* expression was not seen. Further experiments will examine the effect of *Xanx-4* expression on the glomus.

6.3.6 Possible explanations for enlarged tubule phenotype.

It seems unlikely that the enlarged pronephric tubule phenotype seen in embryos injected with *Xanx-4* morpholinos is the result of a defect in the osmotic function

or electrolyte transport of the kidney. A number of mutants identified in the zebrafish genetic screen (Driever et al., 1996) display a pronephric phenotype. Analysis of the mutants (Drummond et al., 1998) revealed that the visible unifying phenotype of all the mutants was the appearance of fluid-filled cysts in the region of the pronephros. These included cyst formation in the glomerulus, duct and tubules. It was suggested that these phenotypes were the result of defects in osmoregulation and electrolyte transport. In mutants displaying cystic tubules the tubule epithelial cells were flattened and distorted by the pressure of fluid in the lumen. These defects were also accompanied by severe axis curvature and general oedema. Since the enlarged pronephric tubule phenotype observed in *Xanx-4* depleted embryos displayed normal tubule epithelial cell morphology, no general oedema or axis curvature, it is unlikely that this phenotype is the result of defective electrolyte transport or osmosis.

Annexins have been shown to bind actin in various systems (Raynal and Pollard, 1994). In an epithelial sheet, each cell has a contractile bundle of actin filaments forming a belt-like structure around the circumference of the cell at the level of the adherens junctions. The tightening of these adhesion belts is known to be involved in the formation of the neural tube in early vertebrate development (Schoenwolf and Smith, 1990). Although tubulogenesis in the formation of the pronephros may be formed by an alternative mechanism, it presumably involves remodelling of the actin cytoskeleton. The enlarged tubules phenotype observed might be the result of failure to mediate actin dependent morphological changes in tubulogenesis. Although annexin IV has not been shown to directly interact with actin in any developmental system, it might be that it exerts its effect

indirectly. The effect of *Xanx-4* depletion on remodelling of the actin cytoskeleton during the formation of the pronephric tubules could be tested by detecting localisation of actin filaments in wholemount with anti-actin antibodies and confocal microscopy.

In normal development, embryos at stage 35 the pronephric tubules formed and appear as the characteristic Tor shape. Further development of the pronephric tubules involves their extension to form the mature highly coiled structure. At stage 35, the embryos depleted in *Xanx-4* expression appear morphologically normal as to their pronephric structure. It therefore seems likely that the enlarged tubule phenotype, with a greater circumference of morphologically normal cells, is the result of a defect in tubule extension between stages 35 and 42. The process of nephrogenesis in the mouse metanephros does not appear to involve active movement of epithelial cells. Although the process of tubulogenesis in the pronephros is not known, the involvement of *Xanx-4* in pronephric tubule extension would probably not be in mediating changes in cell adhesion at adherens junctions if it is assumed that tubule extension does not involve active cell movement. The relationship of calcium in annexin re-localisation could conceivably be involved in the depletion of calcium required to slacken the cell-cell adhesion between cadherins at adherens junctions (De Simone, 1994). A far more likely hypothesis is that depletion of *Xanx-4* expression in pronephric tubules results in defects in direction of epithelial cell division during the extension phase of tubulogenesis. If the extension of pronephric tubules is mediated by directed cell division then a defect causing randomisation of cell division would result in shortened tubules enlarged by a greater number of cells

in the circumference, especially if we assume that cells do not divide to produce a multi-layered epithelium. The aberrant pronephric tubule phenotype observed in embryos depleted of *Xanx-4* expression would fit this hypothesis well. This hypothesis could be tested by analysing direction of cell division in wholemount control and *Xanx-4* depleted embryos using anti- α tubulin antibodies and confocal microscopy. It seems likely that the role of *Xanx-4* in the extension phase of pronephric tubules may be an involvement in the orientation of directed cell division and not in osmotic and/or electrolyte transport, actin re-modelling (*Xanx-4* seems to be required after the tube is formed) or calcium-dependent changes in cell adhesion. Further experiments will help to elucidate this mechanism.

7 Discussion – Annexins and their biological roles and the potential role of *Xanx-4* in pronephric development.

7.1 The annexin family

Annexins are a family of calcium-dependent phospholipid and carbohydrate binding proteins. There are currently 13 annexin family members that have been discovered in vertebrates, invertebrates, fungi and plants (European Annexin Homepage). They share common properties due to their homologous core domain, with approximately 50% amino acid identity in this region between family members. The C-terminal annexin core domain is a 33kDa region composed of four (or eight in respect to annexin VI) highly conserved 70 amino acid repeats (Figure 7.1), including Ca^{2+} and phospholipid binding sites

Figure 7.1

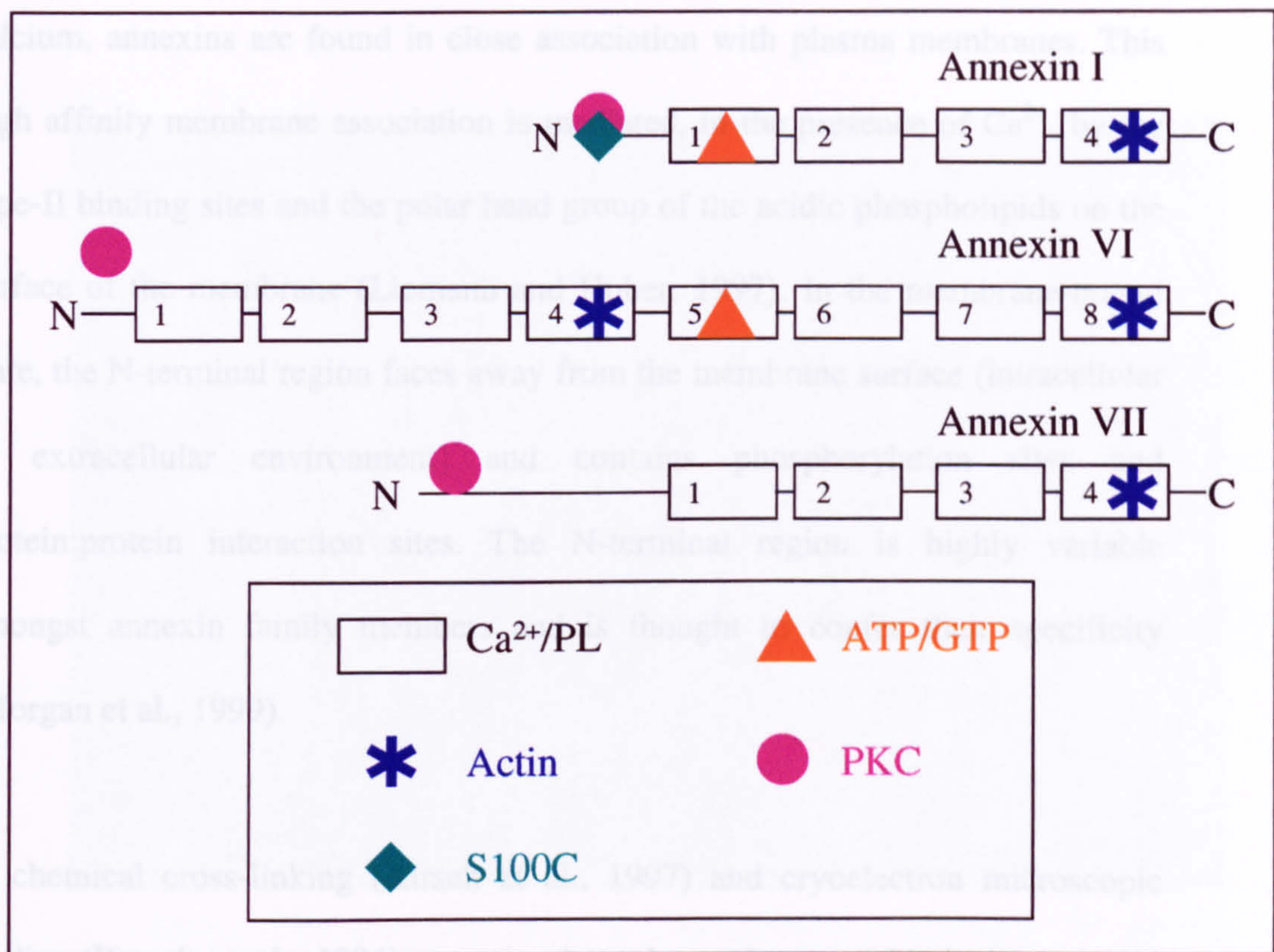


Figure 7.1: Annexin family members share a highly conserved domain structure. A schematic diagram comparing the domain structure of three annexin family members; annexin I, VI and VII. Annexin VI contains six of the highly conserved core domain repeats, whereas annexin I and VII contain four. Ca^{2+}/PL : Calcium and phospholipid binding domains. actin: Actin binding motif, S100C: S-100C binding motif, ATP/GTP: hypothetical binding sites, PKC: Protein kinase C phosphorylation site (Redrawn based on Bandorowicz-Pikula et al., 2001).

(Seaton, 1996). X-ray crystallography studies have revealed that each of the four repeats in the core domain contains five α -helices connected by short loops, in the centre of which is a hydrophilic pore (Figure 7.2). Two loops together form each of the type-II Ca^{2+} binding sites. The core has a globular doughnut shape with the Ca^{2+} binding sites grouped on the convex face. In the presence of calcium, annexins are found in close association with plasma membranes. This high affinity membrane association is mediated, in the presence of Ca^{2+} , by the type-II binding sites and the polar head group of the acidic phospholipids on the surface of the membrane (Liemann and Huber, 1997). In the membrane-bound state, the N-terminal region faces away from the membrane surface (intracellular or extracellular environment) and contains phosphorylation sites and protein:protein interaction sites. The N-terminal region is highly variable amongst annexin family members and is thought to confer their specificity (Morgan et al., 1999).

In chemical cross-linking (Kirsch et al., 1997) and cryoelectron microscopic studies (Pigault et al., 1994) annexins have been shown to bind phospholipid membranes in ordered arrays, and it has been suggested that annexin complexes may function to modify membrane structure. The current excepted model of the mechanism of action of many of the annexins is as follows (Figure 7.3). When intracellular free calcium is low, the annexins are in their soluble and unaggregated resting state. A rise in calcium, subjacent to the membrane, triggers the annexins to rapidly bind to the membrane surface and self-associate. These annexin ordered arrays cause changes in the membrane fluidity, segregation of phospholipids and in the properties of other membrane-bound proteins and

Figure 7.2

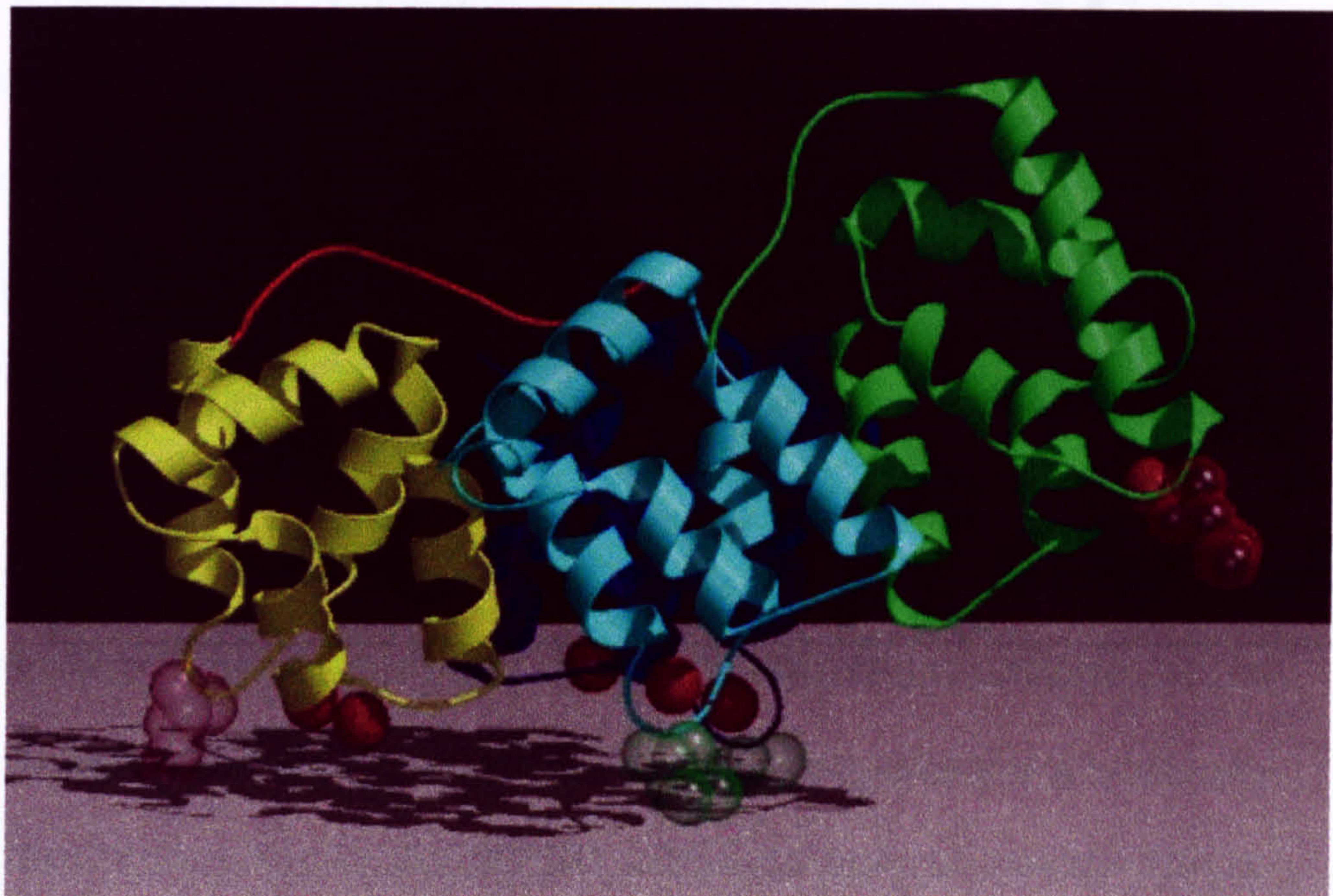


Figure 7.3: Annexins bind to phospholipid membranes in ordered arrays. The model depicts a proposed mechanism of annexin IV inhibition of CaM KII-mediated ion channel activation. In the presence of calcium annexin forms submembrane scaffolding which prevents chloride ion channel phosphorylation and channel opening. In the absence of annexin (shown here competed away using anti-annexin antibody) no aggregates form and the channel is activated. ANX: annexin IV molecules, Ab:

Figure 7.2: Ribbon diagram of the membrane bound form of annexin protein. The four repeats in the core domain are shown in yellow, dark blue, pale blue and green. The red spheres indicate calcium bound to the loop regions. The grey floor shows the plane of the membrane. The N-terminal domain is depicted by the red ribbon (selected from the European Homepage, structure database).

Figure 7.3

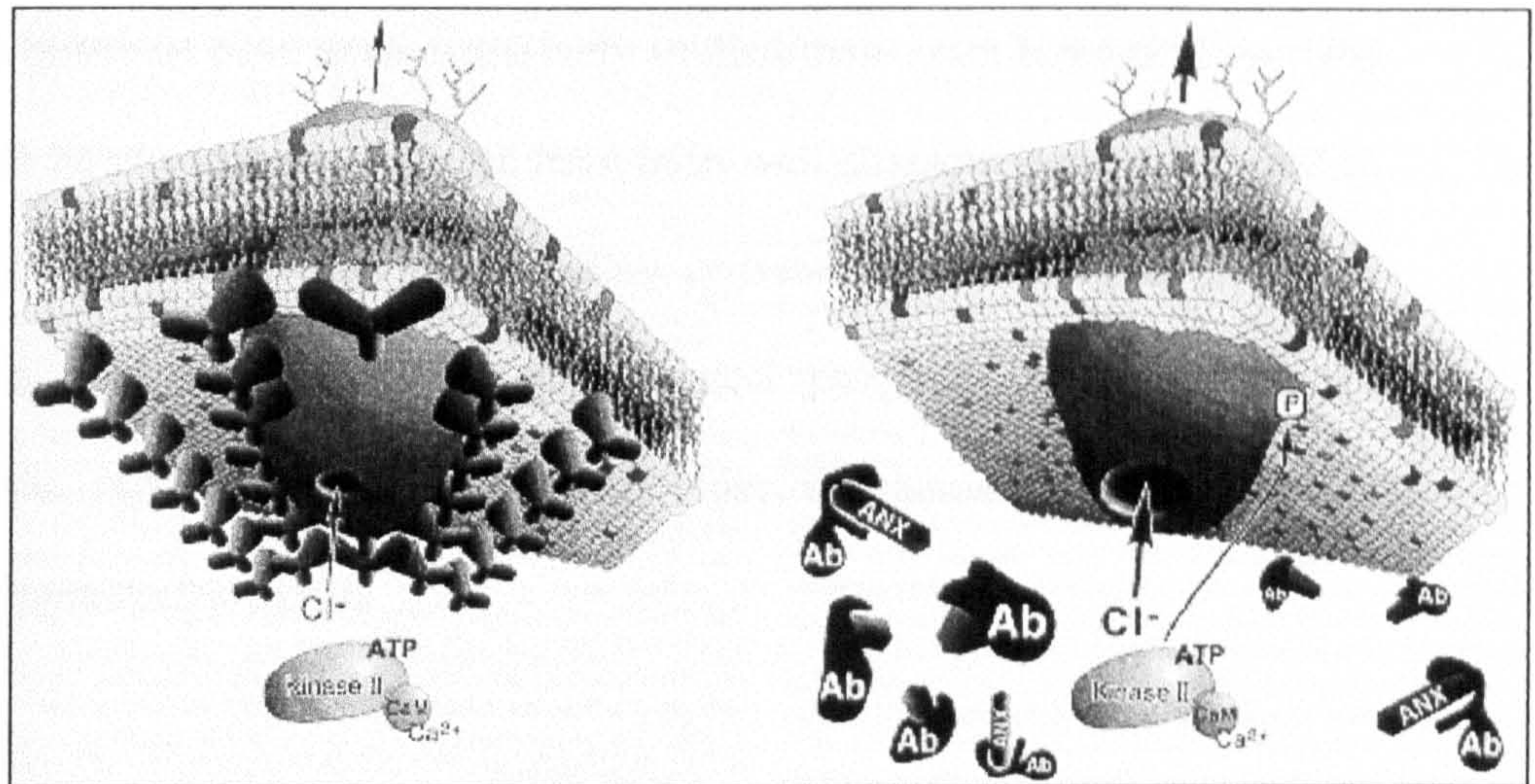


Figure 7.3: Annexins bind to phospholipid membranes in ordered arrays. The model depicts a proposed mechanism of annexin IV inhibition of CaM KII-mediated ion channel activation. In the presence of calcium annexin forms submembrane scaffolding which prevents chloride ion channel phosphorylation and channel opening. In the absence of annexin (shown here competed away using anti-annexin antibody) no aggregates form and the channel is activated. ANX: annexin IV molecules, Ab: antibody (Reproduced from Chen et al., 1994).

enzymes (Oling et al., 2000). This activity may be general enough to account for the many apparent functions of annexins. The mechanism of extracellular annexin action is thought to be similar but that acidic phospholipids would trigger the response rather than a rise in free calcium (Seaton and Dedman, 1998).

Although annexins have been extensively studied their exact biological function remains to be elucidated. Annexins have been well characterised with regard to their tissue localisation and their binding activities and have been shown to participate in a broad range of physiological processes including calcium homeostasis, regulation of ion channel activities, inflammation, anticoagulation and membrane traffic events.

Annexins translocate in response to changes in intracellular calcium.

It is believed that the ability of annexins to shift from a soluble to a membrane bound state upon a rise in free calcium, forms the basis of annexin cellular function. Barwise and Walker (1996) demonstrated that annexins I, II, IV, V and VI are present in human foreskin fibroblasts in distinctive subcellular locations with I, II and VI being cytoplasmic and IV and V being nuclear. On elevation of intracellular calcium the annexins relocate to the plasma (I, II, VI) or nuclear (IV, V) membrane. The authors suggest a role for these annexins in calcium handling, signal transduction and membrane cytoskeletal interactions. Massey-Harroche et al. (1995) demonstrated polarised expression of annexin IV in renal proximal tubules in the rabbit. The localisation of annexin IV was investigated in cultured proximal tubule cells. They found that when the cells were attached to the base

of the culture dish, annexin IV was localised around the nucleus. On further culturing the cells formed domes. Analysis of cells derived from the domes revealed that annexin IV was localised to the basolateral membrane. Eventually when the domes burst and the cells returned to be attached to the dish, annexin IV localisation returned to the nuclear membrane. It is suggested, therefore, that there is a correlation between annexin IV localisation and the organisation of the cytoskeleton and /or cell junctions.

Ion channel activities of the annexins.

A number of annexins have been shown to play a part in intracellular Ca^{2+} signalling by acting as atypical ions channels (Pollard et al., 1992; Burger et al., 1996) and as modulators of ion channel activity (for review see Hawkins et al., 2000). In one particular study Isas et al., (2000) demonstrated that both annexin V and XII are able to reversibly insert into lipid bilayers and form ion channels. The model presented involves the Ca^{2+} and H^+ switching of annexin membrane association. The annexin is a monomer in solution and on presence of free calcium the annexin assembles into trimers on the surface of the membrane. In conditions of low pH major structural reorganisation occurs and the protein inserts into the lipid bilayer. The annexin can be reversibly converted between the three states and the equilibrium is controlled by the concentration of hydrogen and calcium ions. An *in vitro* study using large unilamellar vesicles, the authors demonstrated that annexins I, II, V and VI display, to varying degrees, calcium ion transport activity (Matsuda et al., 1997). Characterisation of the human annexin V ion channel using mutational analysis demonstrated that

the hydrophilic pore, in the centre of the helical bundles, is the ion-conducting pathway (Liemann et al., 1996).

Annexin IV has been shown to have an inhibitory role in the regulation of epithelial calcium-activated chloride ion conductance channel activity. Kaetzel et al.,(1994) introduced exogenous annexin IV protein into a human colon cell line T84 which resulted in the prevention of Ca^{2+} -dependent Cl^- current activation; introduction of anti-annexin IV antibody or oligonucleotides antisense to annexin IV resulted in the enhancement of activation of this current. The authors suggest that the annexin IV plays a role in the modulation of membrane ion channel activity. A further study using the same system, the authors demonstrated that in the presence of free calcium aggregates of annexin IV form a submembrane scaffold, preventing Cl^- channel phosphorylation by Ca^{2+} /calmodulin kinase II (CaM KII) and therefore a reduction in channel open state. This study demonstrates that annexins, cytoplasmic kinases and ion channels can interact to modulate membrane conductance (Chan et al., 1994).

Annexins in membrane fusion events.

Many cellular events are dependent upon membrane fusion mechanisms including fertilisation, cell division and exocytosis and endocytosis. It has been demonstrated that a number of annexins, including I, II, IV and VII, can promote membrane aggregation (Creutz, 1992). Recent studies suggest that annexin I has two separate interaction sites that are involved in membrane binding and aggregation respectively. It has been proposed that annexin I binds to the

phospholipid membrane and forms a laterally aggregated monolayer which directly interacts with a second membrane via its induced hydrophobic interaction site (Bitto et al., 2000). Annexin II has been shown to be essential for exocytosis of lamellar bodies from alveolar epithelial cells of rat lungs which, implicates annexin II in lung surfactant secretion (Liu et al., 1996). Annexin XIIIb has also been implicated in exocytosis in the kidney and lungs (Lafont et al., 1998). Sohma et al., (1995) demonstrated that annexin IV was the major protein bound to the surfactant protein A and lamellar bodies in alveolar type II cells in rat lungs. In a further study in the same system, annexin IV was implicated in exocytosis (Sohma et al., 2001). A medaka annexin, max 3, is present as a maternal pool in unfertilised eggs and has been shown to be able to bind phospholipids and aggregate membrane vesicles. The authors suggest max 3 plays a role in cortical granule exocytosis (Spenneberg et al., 1998).

Annexin II and VI have been implicated in endocytosis. Inhibition of annexin VI by immunodepletion or application of a dominant-negative form of annexin VI blocks endocytosis in an *in vitro* assay using purified fibroblast plasma membranes (Lin et al., 1992). A number of *in vitro* assays have suggested a role for annexin II in the fusion event of endocytosis. One current hypothesis suggests that on binding to protein p11, annexin II can bridge endosomes to the cortex of the cell, through interactions between rafts and the actin cytoskeleton, thus leading to endocytosis (Lecat and Lafont, 1999). Merrifield et al., (2001) have used evanescent-field microscopy to study annexin II-GFP in cells performing pinocytosis. Although no evidence was seen for a role of annexin II in exocytosis, annexin II-GFP was seen to be associated with actin tails propelling

macropinosomes. It was shown by introducing a dominant-negative annexin II construct that annexin II is required for the formation of these macropinocytic rockets. Other annexins have been shown to be associated with the actin cytoskeleton. Tzima et al., (2000) have shown that annexin V binds preferentially to γ -actin but not β -actin in activated platelets. Filipenko and Waisman (2001) have shown by site-directed mutagenesis, that the C-terminus is required for annexin II to bind to F-actin.

Apoptosis and annexin V

Annexin V is routinely used as a marker of apoptosis (van Engeland et al., 1998). Loss of plasma membrane asymmetry, exposing phosphatidylserine (PS) residues on the outer membrane is an early event in apoptosis. Annexin V can strongly and specifically bind PS thus allowing the detection of apoptotic cells with labelled protein or protein plus antibody.

Annexins as nucleotide binding proteins

Annexin V, VI and VII have been shown to bind GTP (Arispe et al., 1996; Bandorowicz-Pikula and Awasthi, 1997; Caohuy et al., 1996). Annexin I has been shown to bind ATP (Han et al., 1998) and cAMP but not GTP or cGMP (Cohen et al., 1995). Ca^{2+} -homeostasis, vesicular transport and signal transduction pathways could be regulated by nucleotide binding to annexins, thereby linking them to cellular energy metabolism. Annexins do not contain the Walker consensus motifs for ATP/GTP binding and are thought to contain a novel ATP/GTP binding fold (review by Bandorowicz-Pikula et al., 2001).

Nucleotide binding domains are thought to be within the repeated domains known to mediate Ca^{2+} and phospholipid binding, ATP/GTP binding to annexins might therefore be regulated by membrane binding (review by Bandorowicz-Pikula et al., 2001). Annexins are thought to undergo conformational changes upon nucleotide binding akin to other ATP-binding proteins (Bandorowicz-Pikula et al., 1997). It is possible that annexins function to modulate activity of other GTP-binding proteins. Annexin VI has been shown to interact with p120^{GAP} , a GTP-binding protein that regulates p21^{ras} by direct interaction (Davis et al., 1996); interestingly p120^{GAP} becomes associated with membranes in response to elevated intracellular Ca^{2+} levels. Annexins have also been found to interact with dynamin (a GTPase involved in endocytosis) (Turpin et al., 1998), synapsin I (an ATP-binding protein in synaptic vesicles) (Inui et al., 1994) and ATP-binding cytoskeletal proteins (Jones et al., 1992; Babiychuk et al., 1999). It has been postulated that annexins might be a new class of GEFs (guanine-nucleotide-exchange factors) or GAPs (GTPase-activating proteins), however annexins probably do not interact with G proteins very specifically and instead regulate interaction of GAPs and/or GEFs with membranes (reviewed by Bandorowicz-Pikula et al., 2001). Additionally, annexin VII has Ca^{2+} -stimulated GTPase activity (Caohuy et al., 1996; Pollard et al., 1998). The intracellular localization of annexin VII is important in exocytotic membrane fusion and secretion in chromaffin cells, it has been proposed that annexin VII is an atypical G protein that is responsible for detecting the Ca^{2+} /GTP signal for exocytosis (Pollard et al., 1998).

In addition to effects on G proteins conferred by GTP binding, annexins are implicated in the G protein mediated phosphoinositide (PI) cascade. This cascade is initiated by the activation of phospholipase C and results in the cleavage of the membrane bound phospholipid PIP₂ into IP₃ (opens calcium channels) and DAG (activates protein kinase C, PKC). PKC phosphorylates many target proteins and is only active in the presence of calcium and phosphatidylserine (reviewed by Nishizuka, 1992). Most annexins are substrates for PKCs with the exception of annexin V (reviewed by Dubois et al., 1996). Mutational analysis of annexin IV has revealed that although phosphorylation by PKC is not required for annexin IV membrane localisation, it is required for vesicle aggregation *in vitro* (Kaetzel et al., 2001).

Anti-inflammatory and anticoagulant activities of annexins.

Annexin I has been shown to function as an anti-inflammatory protein and is upregulated by glucocorticoids (reviewed by Adcock and Ito, 2000). Glucocorticoids are used in the treatment of inflammatory diseases (eg. asthma). Binding of glucocorticoids to a cytosolic glucocorticoid receptor (GR) facilitates translocation to the nucleus resulting in regulation of transcription of target genes. Glucocorticoids have detrimental side-effects that are thought to be caused by undesirable effects on transcription and there is much interest in identifying novel glucocorticoids that induce anti-inflammatory effects without side-effects. A study by Antonicelli et al. (2001) has shown *in vitro* that treatment with dibutyryl cAMP or the glucocorticoid, dexamethasone, results in activation and binding of CREB (CRE-binding protein) to a cAMP response element (CRE) identified in the annexin I promoter.

Annexin II has been shown to act as an anticoagulant by increasing activation of plasmin via interaction directly with plasminogen (inactive plasmin precursor) and with tissue plasminogen activator (activates plasminogen by proteolytic cleavage) (Hajjar et al., 1994; Cesarman et al., 1994). It has been suggested that annexin II forms a platform on the surface of endothelial cells to facilitate binding of plasminogen and tissue plasminogen activator. Patients with acute promyelocytic leukemia (APL) exhibit increased fibrinolysis correlated with increased levels of annexin II expression (Menell et al., 1999). It has also been reported that annexin II tetramers (AII_t) can inhibit fibrinolysis by stimulation of plasmin autodegradation suggesting that AII_t is involved in regulation of plasmin activity on the fibrin clot surface (Kang et al., 1999; Choi et al., 2001).

Annexins in the extracellular matrix

The extracellular matrix contains various proteoglycans and fibrous proteins of two functional types; mainly structural (eg. collagen) and mainly adhesive (eg. fibronectin and laminin). Glycosaminoglycans (GAGs) are usually attached to protein cores forming proteoglycans. Proteoglycans display distinct spatio-temporal expression patterns during development and their GAG side chains interact with a large number of proteins facilitating function in matrix organisation, proliferation, cell adhesion and differentiation. Annexins have been shown to have different GAG binding properties (Ishitsuka et al., 1998) suggesting that annexins may be involved in extracellular processes. A number of annexins have been found in the extracellular milieu. In one particular study it was discovered that annexin I is exported from prostate cells where it was found

to associate with the surface of the cells in a Ca^{2+} dependent manner (Christmas et al., 1991). Although they have been shown to bind to, and insert into phospholipid membranes, secretion of annexins as free molecules seems unlikely as they lack a hydrophobic signal sequence that is normally required for targeting the protein to the endoplasmic reticulum. Interestingly, there are a number of molecules which have been shown to be secreted from cells through a leaderless pathway (Rubartelli et al., 1992). Some annexins (I, II) have been shown to be expressed on the surface of tumor cell lines, suggesting a role for annexins in cell-cell adhesion processes in metastasis (Yeatman et al., 1993; Pencil et al., 1993). Annexins II, V and VI have been shown to bind collagen and have been identified as major components of matrix vesicles (von der Mark and Mollenhauer 1997). Matrix vesicles have a critical role of initiating the mineralisation process during ossification. Types II and X collagen were found to bind to liposomes in the presence of annexin V which stimulated the influx of Ca^{2+} into the liposome. The authors suggest that the role of annexin V is to provide a conductivity pathway for the loading of Ca^{2+} in to matrix vesicles (Kirsch et al., 2000).

7.2 Summary and final discussion

The review of the annexin literature presented in section 8.1 shows that annexins appear to be involved in a wide range of cellular processes. The majority of studies on annexin function have been performed *in vitro* and in order to determine whether these *in vitro* studies are relevant *in vivo*, it will be of great benefit to analyse the function of annexins in developmental systems. To date, two annexin-null mutant mice have been reported. Hawkins et al., (1999) found

that a null mutant mouse for annexin VI had no definable phenotype. Although it was suspected that disruption of annexin VI would effect cardiovascular function the mice had normal heart rate blood pressure and displayed normal cardiovascular responses to septic shock. Therefore the annexin VI gene is not essential for mouse viability and there is probably redundancy between annexins. Interestingly, overexpression of annexin VI with a heart specific promoter results in mice with congestive heart failure (Guteski-Hamblin et al., 1996). Calcium is a primary regulator of cardiac function, the authors suggested that annexin VI is involved in regulation of calcium homeostasis in the heart. Srivastava et al., (1999) found that generation of a null mutant for annexin VII resulted in embryonic death at day 10 as a result of cerebral hemorrhage. Heterozygous annexin VII (+/-) mice were found to be deficient in circulating insulin although insulin was present at 8-10 fold higher concentration in the pancreatic islets. It has long been thought that annexin VII has a role in Ca^{2+} -dependent exocytotic secretion events. The authors showed that lowering the level of annexin VII causes defects in Ca^{2+} signal transduction and insulin secretion. The mechanism of the defect is suggested to be one of depletion of expression of (inositol 1,4,5-triphosphate) IP_3 receptors resulting in reduced release of intracellular calcium and reduced insulin secretion.

It appears therefore that disruption of annexin expression in developmental systems can yield important functional data, although this has not yet been accumulated for annexin IV.

The aim of the subtractive hybridisation screen performed in this laboratory was to identify novel genes involved in pronephric development. The isolation and characterisation of *Xanx-4* has resulted in the identification of a useful marker of pronephric tubules. The only other specific markers for pronephric tubules are *XSMP-30* (Sato et al., 2000) and monoclonal antibody 3G8 (Vize et al., 1995). However, *Xanx-4* is detectable at stage 26 by *in situ*, much earlier than *XSMP-30* and 3G8 and therefore is a more useful marker for the analysis of early pronephric development and presumably has an important functional role. It would be interesting to isolate the zebrafish homologue of *Xanx-4* and ascertain whether it displays pronephric tubule-specific expression. Adult expression of *Xanx-4* is less restricted and is found in many epithelial tissues with particularly high expression in the gall bladder which, may indicate a role in the secretion of bile. The wider expression of *Xanx-4* in adult frogs is in good agreement with expression of annexin IV in higher vertebrates. Characterisation of other annexins in developmental model organisms may reveal similarly highly restricted expression profiles during embryogenesis as *Xanx-4*. In common with *Xenopus annexin II* and *VII* and fish annexins *max1-5*, *Xanx-4* is expressed maternally. This may reflect a role for annexins in the earliest stages of fertilisation and/or development driven by maternal transcripts in lower vertebrates.

In order to determine the function of *Xanx-4* in pronephric tubule development, overexpression and perturbation of gene expression analyses have been performed. *Xanx-4* overexpression results in no mutant phenotype and it has been argued that this is not due to a lack of persistence of exogenous mRNA since the

phenotype induced by injection of *Xanx-4* morpholino can be rescued by *Xanx-4* mRNA. Interestingly, this is opposite to the results of *annexin VI* knockout and overexpression in the mouse, where knockout results in no phenotype and overexpression does. However, expression driven specifically in the pronephros (transgenic) was not carried and might result in a pronephric phenotype. The phenotype observed in *Xenopus* embryos, injected with *Xanx-4* morpholino, is evidence for the requirement of *Xanx-4* during morphogenesis of pronephric tubules. It has been argued that the enlarged tubule phenotype is not the result of osmotic dysfunction. This is supported by the observation that tadpoles do not display general oedema or cystic pronephric components, but this has not been tested directly by physiological measurements. In fact apart from the enlarged tubules tadpoles are otherwise normal; it would be interesting to ascertain whether they are equally viable at later stages of development that is post onset of feeding and into metamorphosis. A number of annexins have been shown to be capable of inserting into membranes, acting as functional ion channels and are also thought to be involved the modulation of ion channel activity. It is therefore possible that the depletion of *Xanx-4* results in defects in ion transport, although this does not seem to effect the function of the pronephros in maintaining water balance. The formation of larger tubules in *Xanx-4* depleted embryos might reflect a defect in rearrangement of the actin cytoskeleton during tubulogenesis. It has been argued that this seems unlikely as the phenotype observed is not manifested until after the tubules are formed, they appear normal at stage 35. The effects of depletion of *Xanx-4* appear during the maturation of the pronephros when the tubules elongate and coil. A further experiment conducted in a stepwise fashion during the stages of pronephric tubule elongation (stages 35-40) could be

conducted to analyse the effect of *Xanx-4* depletion during pronephric maturation.

It has been argued that a defect in the direction of cell division during tubule extension would explain the phenotype seen in *Xanx-4* depleted embryos. The increased number of cells in a tubule circumference being generated by cell division orientated perpendicular to the direction of tubule extension. Consistent with a role for annexins in proliferation, annexin II has been shown to be regulated during cell cycle of CHO and HeLa cells (Chiang et al., 1993) and has also been shown to be required for DNA replication in *Xenopus* egg extracts (Vishwanatha and Kumble, 1993). Additionally, extracellular annexin II has been shown to stimulate proliferation of osteoclast precursors in human marrow cultures (Menaar et al., 1999). Furthermore, phosphorylation of annexin I has been linked to HGF induced proliferation in the A549 lung carcinoma cell line (Skouteris and Schroder, 1996).

Regulation of direction of cell division occurs in the mouse embryo when the morula undergoes the 8-16 cell and 16-32 cell divisions. The morula consists of peripheral polar cells (polarised by microvilli on external surface) and internal apolar cells, dividing polar cells divide conservatively (symmetric) or differentially (asymmetric) to compensate for inequalities in the ratio between the two types of cells (Fleming, 1987). During murine cortical neurogenesis in the ventricular zone, proliferating neural progenitors can divide symmetrically to generate two new progenitors or asymmetrically to generate one new progenitor and one neuronal precursor (Price and Willshaw, 2000). Direction of cell

division is thought to be important in this process and *pax6* null mutant mice have been shown to display altered ratios of symmetric to asymmetric division (D Price, University of Edinburgh pers. comm.). It is therefore possible that direction of cell division is tightly regulated during extension of pronephric tubules. Although a defect in direction of cell division would seem to account for the enlarged tubule phenotype observed in *Xanx-4* depleted embryos, it is difficult to envisage how *Xanx-4* might be involved in such a process. It would seem that a cell division that generated a two-cell thick tubule wall is not normally seen in tubule epithelia. There is a clear polarity in the apical and basal surfaces of the epithelial cells. However, there is currently no evidence suggesting polarity in cells contributing to the length of the tube, rather than the circumference. It could be hypothesised that the lateral junctions of cells contributing to the circumference of the tubule are subjected to different pressure or have differential adhesive properties to the lateral junctions of the same cells that contribute to tubule length. This would introduce an asymmetry or cell shape necessary to control direction of cell division, *Xanx-4* might be implicated in the regulation of this process. Since *Xanx-4* is localised on the apical surface of epithelial tubule cells it seems difficult to envisage how it would contribute to such an asymmetry. It is currently not known whether *Xanx-4* protein is located on the extracellular or intracellular side of the apical membrane, or indeed whether it is a transmembrane protein. There is evidence in the literature for multiple sub-cellular locations for annexin family members. The exact sub-cellular location could be identified by step-wise extraction of *Xanx-4* from pronephric tubule epithelia using calcium chelators and detergents and immunogold electron microscopy. Factors that control the asymmetric expression of

annexin IV are unknown. It would be interesting to analyse the control of the apical localisation of Xanx-4, possibly by site directed-mutagenesis or GFP-labelled truncation mutants. To ascertain whether there is an alteration of cell division in the pronephric tubules of *Xanx-4* depleted embryos it will be necessary to analyse direction of cell division using anti- α tubulin antibodies and confocal microscopy. Initial attempts at anti- α tubulin staining were too non-specific to interpret. It would also be interesting to analyse proliferation during tubule extension to ascertain whether this occurs in discrete regions or throughout the tubule length. If Xanx-4 is implicated in direction of cell division, it could be used to screen for other factors involved in this process. Initial analysis of cell division within the pronephros suggested that low levels of division were occurring in tailbud stages. However, a more complete study needs to be performed.

It has been found that antisense morpholino oligonucleotides are a very efficient and reliable method of interfering with gene expression. This observation is confirmed by the success of other researchers that have reported the use of morpholinos in a number of developmental systems. The use of mutant mRNA in the rescue experiment allowed the depletion of endogenous Xanx-4 to be uncoupled functionally from the rescue event. It is therefore certain that *Xanx-4* MO2 interferes with the expression of *Xanx-4* and not with any non-specific targets.

The efficacy of RNAi has been tested in *Xenopus* oocytes and embryos. Evidence has been presented that RNAi specifically depletes Xanx-4 protein

levels in oocytes. However, due to seemingly inconsistent results on depletion of *Xanx-4* mRNA in both oocytes and embryos, further experimentation would be required to ascertain whether this method of interfering with gene expression can be used routinely. RNAi was tested at a time when no reliable, sequence-specific method of depletion of gene expression was available to developmental biologists working in *Xenopus* and zebrafish. The results presented in this thesis and by other researchers clearly show that antisense morpholino oligonucleotides present a far more reliable method for the interference of gene expression than RNAi. Due to the ability to uncouple the rescue event and the interference event, morpholinos have the advantage of confirming the specific nature of the phenotype observed. The observation that siRNA resulted in a reduced tubule phenotype was unexpected since no reduction in mRNA levels was detected in embryos. Whether this phenotype represents a specific reduction of *Xanx-4* protein remains to be determined. This could be performed by co-injection of siRNA and *myc-Xanx-4* mRNA in *Xenopus* embryos to ascertain whether *Xanx-4* protein levels are reduced. If this phenotype is the result of specific depletion of *Xanx-4* it might be that it represents a milder phenotype to that observed by injection of morpholino. It is worthy of note that *Xanx-4* morpholino injection occasionally results in reduced or missing tubules. Therefore the reduced tubule phenotype induced by siRNA and occasionally by morpholino injection might be the result of increased apoptosis or reduced proliferation in the pronephric tubules. Further experiments will determine whether this is the case.

Further experiments could include overexpression (injection of mRNA) and depletion (morpholino) of other pronephric genes and analysis of their effect on

Xanx-4. This may lead to insights concerning the molecular regulatory cascade of pronephric development. Isolation and characterisation of the *Xanx-4* promoter would allow specific overexpression of genes in the pronephros using transgenic technology. It would also allow creation of *Xanx-4-GFP* transgenic *Xenopus* in which to study the events of pronephrogenesis and would allow imaging of *Xanx-4* protein localisation *in vivo*. Recently, myself and Dr K Massé, have isolated two genomic clones (approximately 18Kb and 15Kb) containing *Xanx-4* coding sequence which are currently being analysed. In order to study the effect of *Xanx-4* on signal transduction pathways (eg. PKC, MAPK) it would be useful to develop a system for pronephros organ culture.

Despite 24 years of intensive research, the precise function of annexins remains enigmatic. Annexins are implicated in human diseases eg. asthma, thrombosis, it is therefore important to elucidate their functions. This study represents the first developmental study on annexin IV. Furthermore, the enlarged tubule phenotype generated by depletion of *Xanx-4* by morpholino injection provides some clues that might guide experimentation to elucidate the function of annexin IV *in vivo*.

Bibliography

Abdelhak, S., Kalatzis, V., Heilig, R., Compain, S., Samson, D., Vincent, C., Weil, D., Cruaud, C., Sahly, I., Leibovici, M., Bitner-Glindzicz, M., Francis, M., Lacombe, D., Vigneron, J., Charachon, R., Boven, K., Bedbeder, P., Van Regemorter, N., Weissenbach, J. and Petit, C. (1997) A human homologue of the *Drosophila eyes absent* gene underlies Branchio-Oto-Renal (BOR) syndrome and identifies a novel gene family. *Nat. Genet.* 15, 157-164.

Adcock, I. M. and Ito, K. (2000) Molecular mechanisms of corticosteroid actions. *Monaldi Arch. Chest Dis.* 55(3), 256-66.

Agathon, A., Thisse, B. and Thisse, C. (2001) Morpholino Knock-Down of Antivin1 and Antivin2 Upregulates Nodal Signaling. *Genesis* 30, 178-182.

Agius, E., Oelgeschlager, M., Wessely, O., Kemp, C. and De Robertis, E. M. (2000) Endodermal Nodal-related signals and mesoderm induction in *Xenopus*. *Development* 127(6),1173-83.

Ali, S. M., Geisow, M. J. and Burgoyne, R. D. (1989) A role for calpactin in calcium-dependent exocytosis in adrenal chromaffin cells. *Nature* 340, 313-315.

Amaya, E., Musci, T. J. and Kirschner, M. W. (1991) Expression of a dominant negative mutant of the FGF receptor disrupts mesoderm formation in *Xenopus* embryos. *Cell* 66, 257-270.

Ando, H., Furuta, T., Tsien, R. Y. and Okamoto, H. (2001) Photo-mediated gene activation using caged RNA/DNA in zebrafish embryos. *Nat. Genet.* 28(4), 317-25.

Antonicelli, F., De Coupade, C., Russo-Marie, F. and Le Garrec, Y. (2001) CREB is involved in mouse annexin A1 regulation by cAMP and glucocorticoids. *Eur. J. Biochem.* 268(1), 62-9.

Ariizumi, T. and Asashima, M. (2001) *In vitro* induction systems for analyses of amphibian organogenesis and body patterning. *Int. J. Dev. Biol.* 45, 273-9.

Arispe, N., Rojas, E., Genge, B. R., Wu, L. N. and Wuthier, R. E. (1996) Similarity in calcium channel activity of annexin V and matrix vesicles in planar lipid bilayers. *Biophys. J.* 71(4), 1764-1775.

Arora, V. and Iversen, P. L. (2001) Redirection of drug metabolism using antisense technology. *Curr. Opin. Mol. Ther.* 3(3), 249-57.

Artavanis-Tsakonas, S., Rand, M. D. and Lake, R. J. (1999) Notch signaling: cell fate control and signal integration in development. *Science.* 284(5415), 770-6

Assaad, F. F., Tucker, K. L. and Signer, E. R. (1993) Epigenetic repeat-induced gene silencing (RIGS) in Arabidopsis. *Plant Mol. Biol.* 22, 1067-1085.

Audic, Y., Boyle, B., Slevin, M. and Hartley, R. S. (2001) Cyclin E morpholino delays embryogenesis in *Xenopus*. *Genesis* 30(3), 107-9.

Babiychuk, E. B., Palstra, R. J., Schaller, J., Kampfer, U. and Draeger, A. (1999) Annexin VI participates in the formation of a reversible, membrane-cytoskeleton complex in smooth muscle cells. *J. Biol. Chem.* 274(49), 35191-5.

Bahramian, M. A. and Zarbl, H. (1999) Transcriptional and Posttranscriptional Silencing of Rodent $\alpha 1(I)$ Collagen by a Homologous Transcriptionally Self-Silenced Transgene. *Mol. Cell Biol.* 19, 274-283.

Bandorowicz-Pikula, J. and Awasthi, Y. C. (1997) Interaction of annexins IV and VI with ATP. An alternative mechanism by which a cellular function of

these calcium- and membrane-binding proteins is regulated. *FEBS Lett.* 409(2), 300-6.

Bandorowicz-Pikula, J., Buchet, R. and Pikula, S. (2001) Annexins as nucleotide-binding proteins: facts and speculations. *Bioessays* 23(2), 170-8.

Bandorowicz-Pikula, J., Wrzosek, A., Pikula, S. and Awasthi, Y. C. (1997) Fluorescence spectroscopic studies on interactions between liver annexin VI and nucleotides-a possible role for a tryptophan residue. *Eur. J. Biochem.* 248(1), 238-44.

Barnett, M. W., Old, R. W. and Jones, E. A. (1998) Neural induction and patterning by fibroblast growth factor, notochord and somite tissue in *Xenopus*. *Dev. Growth Differ.* 40(1), 47-57.

Barnett, M. W., Seville, R. A., Nijjar, S., Old, R. W. and Jones, E. A. (2001) *Xenopus Enhancer of Zeste (XEZ)*; an anteriorly restricted *polycomb* gene with a role in neural patterning. *Mech. Dev.* 102, 157-167.

Barstead, R. (2001) Genome-wide RNAi. *Curr. Opin. Chem. Biol.* 5, 63-66.

Barwise, J. L. and Walker, J. H. (1996) Annexins II, IV, V and VI relocate in response to rises in intracellular calcium in human foreskin fibroblasts. *J. Cell Sci.* 109 (Pt 1), 247-55.

Bass, B. L. (2000) Double-stranded RNA as a template for gene silencing. *Cell* 101, 235-238.

Bass, B. L. and Weintraub, H. (1987) A Developmentally Regulated Activity That Unwinds RNA Duplexes. *Cell* 48, 607-613.

Bassez, T., Paris, J., Omilli, F., Dorel, C. and Osborne, H. B. (1990) Post-transcriptional regulation of ornithine decarboxylase in *Xenopus laevis* oocytes. *Development* **110**(3), 955-62.

Bauer, H., Lele, Z., Rauch, G. J., Geisler, R. and Hammerschmidt, M. (2001) The type I serine/threonine kinase receptor Alk8/Lost-a-fin is required for Bmp2b/7 signal transduction during dorsoventral patterning of the zebrafish embryo. *Development* **128**(6), 849-58.

Bement, W. M. and Capco, D. G. (1989) Activators of protein kinase C trigger cortical granule exocytosis, cortical contraction and cleavage furrow formation in *Xenopus laevis* oocytes and eggs. *J. Cell Biol.* **108**, 885-892.

Bernstein, E., Caudy, A. A., Hammond, S. M. and Hannon, G. J. (2001) Role for a bidentate ribonuclease in the initiation step of RNA interference. *Nature* **409**, 363-366.

Bitto, E. and Cho, W. (1998) Roles of individual domains of annexin I in its vesicle binding and vesicle aggregation: a comprehensive mutagenesis study. *Biochemistry* **37**, 10231-10237.

Bitto, E., Li, M., Tikhonov, A. M., Schlossman, M. L. and Cho, W. (2000) Mechanism of annexin I-mediated membrane aggregation. *Biochemistry* **39**(44), 13469-77.

Bollerot, K., Angelier, N. and Coumailleau, P. (2001) Molecular cloning and embryonic expression of the *Xenopus Arnt* gene. *Mech. Dev.* **108**(1-2), 227-31.

Bosher, J. M. and Labouesse, M. (2000) RNA interference: genetic wand and genetic watchdog. *Nat. Cell Biol.* **2**, E31-E36.

Bosher, J. M., Dufourcq, P., Sookhareea, S. and Labousse, M. (1999) RNA interference can target pre-mRNA : consequences for gene expression in a *Caenorhabditis elegans* operon. *Genetics* **153**, 1245-1256.

Boustead, C. M., Brown, R. and Walker, J. H. (1993) Isolation, characterisation and localisation of annexin V from chicken liver. *Biochem. J.* **291**, 601-608.

Brand, M., Heisenberg, C. P., Jiang, Y. J., Beuchle, D., Lun, K., FurutaniSeiki, M., Granato, M., Haffter, P., Hammerschmidt, M., Kane, D. A., Kelsh, R. N., Mullins, M. C., Odenthal, J., vanEeden, F. J. M. and NussleinVolhard, C. (1996) Mutations in zebrafish genes affecting the formation of the boundary between midbrain and hindbrain. *Development* **123**, 179-190, Sp. Iss.

Brändli, A. W. (1999) Towards a molecular anatomy of the *Xenopus* pronephric kidney. *Int. J. Dev. Biol.* **43**, 381-95. Review.

Brennan, H. C., Nijjar, S. and Jones, E. A. (1999) The specification and growth factor inducibility of the pronephric glomus in *Xenopus laevis*. *Development* **126**(24), 5847-56.

Brennan, H. C., Nijjar, S. and Jones E. A. (1998) The specification of the pronephric tubules and duct in *Xenopus laevis*. *Mech. Dev.* **75**(1-2), 127-37.

Brink, R. A. (1956) A genetic change associated with the R locus in maize which is directed and potentially reversible. *Genetics* **41**, 872-889.

Burger, A., Berendes, R., Liemann, S., Benz, J., Hofmann, A., Gottig, P., Huber, R., Gerke, V., Thiel, C., Romisch, J. and Weber, K. (1996) The crystal structure and ion channel activity of human annexin II, a peripheral membrane protein. *J. Mol. Biol.* **257**(4), 839-47.

Call, K. M., Glaser, T., Ito, C. Y., Buckler, A. J., Pelletier, J., Haber, D. A., Rose, E. A., Kral, A., Yeger, H., Lewis, W. H., Jones, C. and Housman, D. E. (1990) Isolation and characterization of a zinc finger polypeptide gene at the human chromosome 11 Wilms' tumor locus. *Cell*. **60**(3), 509-20.

Caohuy, H., Srivastava, M. and Pollard, H. B. (1996) Membrane fusion protein synexin (annexin VII) as a Ca^{2+} /GTP sensor in exocytotic secretion. *Proc. Natl. Acad. Sci. U. S. A.* **93**(20), 10797-802.

Capdevila, J. and Johnson, R. L. (2000) Hedgehog signaling in vertebrate and invertebrate limb patterning. *Cell. Mol. Life Sci.* **57**(12), 1682-94

Caplen, N. J., Fleenor, J., Fire, A. and Morgan, R. A. (2000) dsRNA-mediated gene silencing in cultured *Drosophila* cells: a tissue culture model for the analysis of RNA interference. *Gene* **252**, 95-105.

Carmeliet, P. (1999) Basic Concepts of (Myocardial) Angiogenesis: Role of Vascular Endothelial Growth Factor and Angiopoietin. *Curr. Interv. Cardiol. Rep.* **1**(4), 322-335.

Carroll, T. J. and Vize, P. D. (1999) Synergism between *Pax-8* and *lim-1* in embryonic kidney development. *Dev Biol.* **214**(1), 46-59.

Carroll, T. J. and Vize, P. D. (1996) Wilms' tumor suppressor gene is involved in the development of disparate kidney forms: evidence from expression in the *Xenopus* pronephros. *Dev Dyn.* **206**(2), 131-8.

Carroll, T. J. and Vize, P. D. (1999) Synergism between *Pax-8* and *lim-1* in embryonic kidney development. *Dev. Biol.* **214**, 46-59.

Carroll, T. J., Wallingford, J. B. and Vize, P. D. (1999) Dynamic patterns of gene expression in the developing pronephros of *Xenopus laevis*. *Dev Genet.* **24**(3-4), 199-207.

Cerutti, L., Mian, N. and Bateman, A. (2000) Domains in gene silencing and cell differentiation proteins: the novel PAZ domain and redefinition of the Piwi domain. *Trends Biochem. Sci.* **25**, 481-482.

Cesarman, G. M., Guevara, C. A. and Hajjar, K. A. (1994) An endothelial cell receptor for plasminogen/tissue plasminogen activator (t-PA). II. Annexin II-mediated enhancement of t-PA-dependent plasminogen activation. *J. Biol. Chem.* **269**(33), 21198-203.

Chan, H. C., Kaetzel, M. A., Gotter, A. L., Dedman, J. R. and Nelson, D. J. (1994) Annexin IV inhibits calmodulin-dependent protein kinase II-activated chloride conductance. A novel mechanism for ion channel regulation. *J. Biol. Chem.* **269**(51), 32464-8.

Chan, T. C., Takahashi, S. and Asashima, M. (2000) A role for *Xlim-1* in pronephros development in *Xenopus laevis*. *Dev Biol.* **228**(2), 256-69.

Chen, W. S., Manova, K., Weinstein, D. C., Duncan, S. A., Plump, A. S., Prezioso, V. R., Bachvarova, R. F. and Darnell, J. E. (1994) Disruption of the *hnf-4* gene, expressed in visceral endoderm, leads to cell-death in embryonic ectoderm and impaired gastrulation of mouse embryos. *Genes Dev.* **8** (20), 2466-2477.

Chiang, Y., Schneiderman, M. H. and Vishwanatha, J. K. (1993) Annexin II expression is regulated during mammalian cell cycle. *Cancer Res.* **53**(24), 6017-21.

Choi, K. S., Fitzpatrick, S. L., Filipenko, N. R., Fogg, D. K., Kassam, G., Magliocco, A. M. and Waisman, D. M. (2001) Regulation of plasmin-dependent fibrin clot lysis by annexin II heterotetramer. *J. Biol. Chem.* **276**(27), 25212-21.

Christmas, P., Callaway, J., Fallon, J., Jones, J. and Haigler, H. T. (1991) Selective secretion of annexin 1, a protein without a signal sequence, by the human prostate gland. *J. Biol. Chem.* **266**(4), 2499-507.

Chuang, C. F. and Meyerowitz, E. M. (2000) Specific and heritable genetic interference by double-stranded RNA in *Arabidopsis thaliana*. *Proc. Natl. Acad. Sci. USA* **97**, 4985-4990.

Chuong, C. M., Patel, N., Lin, J., Jung, H. S. and Widelitz, R. B. (2000) Sonic hedgehog signaling pathway in vertebrate epithelial appendage morphogenesis: perspectives in development and evolution. *Cell Mol. Life Sci.* **57**(12), 1672-81.

Cleaver, O. and Krieg, P. A. (1998) VEGF mediates angioblast migration during development of the dorsal aorta in *Xenopus*. *Development* **125**(19), 3905-14

Clemens, J. C., Worby, C. A., Simonson-Leff, N., Muda, M., Maehama, T., Hemmings, B. A. and Dixon J. E. (2000) Use of double-stranded RNA interference in *Drosophila* cell lines to dissect signal transduction pathways. *Proc. Natl. Acad. Sci. USA* **97**, 6499-6503.

Clements, D., Friday, R. V. and Woodland, H. R. (1999) Mode of action of VegT in mesoderm and endoderm formation. *Development* **126**(21), 4903-11.

Cogoni, C. and Macino, G. (1997) Isolation of quelling-defective (*qde*) mutants impaired in posttranscriptional transgene-induced gene silencing in *Neurospora crassa*. *Proc. Natl. Acad. Sci. USA* **94**, 10233-10238.

Cogoni, C. and Macino, G. (1999) Gene silencing in *Neurospora crassa* requires a protein homologous to RNA-dependent RNA polymerase. *Nature* **399**, 166-169.

Cogoni, C., Irelan, J. T., Schumacher, M., Schmidhauser, T. J., Selker, E. U. and Macino, G. (1996) Transgene silencing of the *al-1* gene in vegetative cells of *Neurospora* is mediated by a cytoplasmic effector and does not depend on DNA-DNA interactions or DNA methylation. *EMBO.J.* **15**, 3153-3163.

Cohen, B. E., Lee, G., Arispe, N. and Pollard, H.B. (1995) Cyclic 3'-5'-adenosine monophosphate binds to annexin 1 and regulates calcium-dependent membrane aggregation and ion channel activity. *FEBS Lett.* **377**, 444-450.

Coonrod, S. A., Bolling, L. C., Wright, P. W., Visconti, P. E. and Herr, J. C. (2001) A Morpholino Phenocopy of the Mouse *mos* Mutation. *Genesis* **30**(3), 198-200.

Corey, D. R. and Abrams, J. M. (2001) Morpholino antisense oligonucleotides: tools for investigating vertebrate development. *Genome Biol.* **2**(5), REVIEWS 1015.

Cornish, J. A., Kloc, M., Decker, G. L., Reddy, B. A, Etkin, L. D. (1992) *Xlcaax-1* is localized to the basolateral membrane of kidney tubule and other polarized epithelia during *Xenopus* development. *Dev. Biol.* **150**(1), 108-20.

Creutz, C. E. (1992) The annexins and exocytosis. *Science* **258**(5084), 924-31.

Dale, L. and Slack, J. M. W. (1987) Fate map of the 32-cell stage of *Xenopus laevis*. *Development.* **99**, 527-551.

Dalmay, T., Hamilton, A., Rudd, S., Angell, S. and Baulcombe, D. C. (2000) An RNA-dependent RNA polymerase gene in *Arabidopsis* is required for posttranscriptional gene silencing mediated by a transgene but not by a virus. *Cell* **101**, 543-553.

Davies, J. A. and Brändli, A. W. (1997) The kidney Development Database. World Wide Web URL: <http://www.ana.ed.ac.uk/anatomy/database/kidbase/kidhome.html>.

Davis, A. J., Butt, J. T., Walker, J. H., Moss, S.E. and Gawler, D. J. (1996) The Ca^{2+} -dependent lipid binding domain of P120GAP mediates protein-protein interactions with Ca^{2+} -dependent membrane-binding proteins. Evidence for a direct interaction between annexin VI and P120GAP. *J. Biol. Chem.* **271**(40), 24333-6. Erratum in: *J. Biol. Chem.* (1996) **271**(52), 33705.

Deardorff, M. A., Tan, C., Saint-Jeannet, J. P. and Klein, P. S. (2001) A role for *frizzled 3* in neural crest development. *Development* **128**(19), 3655-63.

Demartis, A., Maffei, M., Vignali, R., Barsacchi, G. and Desimone, V. (1994) Cloning and developmental expression of lfb3/hnf1-beta transcription factor in *xenopus-laevis*. *Mech. Dev.* **47** (1), 19-28

DeSimone, D. W. (1994) Adhesion and matrix in vertebrate development. *Curr. Opin. Cell Biol.* **6**(5), 747-51.

Dibner, C., Elias, S. and Frank, D. (2001) XMeis3 protein activity is required for proper hindbrain patterning in *Xenopus laevis* embryos. *Development* **128**(18), 3415-26.

Draper, B. W., Morcos, P. A. and Kimmel, C. B. (2001) Inhibition of Zebrafish *fgf8* Pre-mRNA Splicing With Morpholino Oligos: A Quantifiable Method for Gene Knockdown. *Genesis* **30**, 154-156.

Drawbridge, J. and Steinberg, M. S. (1996) Morphogenesis of the axoloti pronephric duct: a model system for the study of cell migration *in vivo*. *Int.J.Dev.Biol.* **40**, 709-713.

Drawbridge, J., Meighan, C. M. and Mitchell, E. A. (2000) GDNF and GFRalpha-1 are components of the axoloti pronephric duct guidance system. *Dev.Biol.* **228**(1), 116-124.

- Dressler, G. R. (1999)** Kidney development branches out. *Dev Genet.* 24(3-4), 189-93. Review.
- Driever, W., Solnica-Krezel, L., Schier, A. F., Neuhauss, S. C., Malicki, J., Stemple, D. L., Stainier, D. Y., Zwartkruis, F., Abdelilah, S., Rangini, Z., Belak, J. and Boggs, C. (1996)** A genetic screen for mutations affecting embryogenesis in zebrafish. *Development* 123,37-46.
- Drummond, I. A. (2000)** The zebrafish pronephros: a genetic system for studies of kidney development. *Pediatr Nephrol.* 14(5), 428-35. Review.
- Drummond, I. A., Majumdar, A., Hentschel, H., Elger, M., Solnica-Krezel, L., Schier, A. F., Neuhauss, S. C., Stemple, D. L., Zwartkruis, F., Rangini, Z., Driever, W. and Fishman, M. C. (1998)** Early development of the zebrafish pronephros and analysis of mutations affecting pronephric function. *Development* 125(23), 4655-67.
- Du, S. J., Purcell, S. M., Christian, J. L., McGrew, L. L. and Moon, R. T. (1995)** Identification of distinct classes and functional domains of *Wnts* through expression of wild-type and chimeric proteins in *Xenopus* embryos. *Mol.Cell.Biol.* 15, 2625-2634.
- Dubois, T., Oudinet, J. P., Mira, J. P. and Russo-Marie, F. (1996)** Annexins and protein kinases C. *Biochim. Biophys. Acta.* 1313(3), 290-4.
- Dudley, A. T., Lyons, K. M. and Robertson, E. J. (1995)** A requirement for bone morphogenetic protein-7 during development of the mammalian kidney and eye. *Genes Dev.* 9(22), 2795-807.
- Durbec, P., Marcos-Gutierrez, C. V., Kilkenny, C., Grigoriou, M., Wartiovaara, K., Suvanto, P., Smith, D., Ponder, B., Costantini, F., Saarma, M. et al. (1996)** GDNF signalling through the Ret receptor tyrosine kinase. *Nature* 381(6585), 789-93.

Ekker, S. C. and Larson, J. D. (2001) Morphant Technology in Model Developmental Systems. *Genesis*. 30, 89-93.

Ekker, S. C., McGrew, L. L., Lai, C. J., Lee, J. J., von Kessler, D. P., Moon, R. T. and Beachy, P. A. (1995) Distinct expression and shared activities of members of the hedgehog gene family of *Xenopus laevis*. *Development* 121(8), 2337-47.

Elbashir, S. M., Lendeckel, W. and Tuschl, T. (2001a) RNA interference is mediated by 21- and 22-nucleotide RNAs. *Genes Dev.* 15, 188-200.

Elbashir, S. M., Harborth, J., Lendeckel, W., Yalcin, A., Weber, K. and Tuschl, T. (2001b) Duplexes of 21-nucleotide RNAs mediate RNA interference in cultured mammalian cells. *Nature* 411, 494-498.

Erter, C. E., Wilm, T. P., Basler, N., Wright, C. V. and Solnica-Krezel, L. (2001) Wnt8 is required in lateral mesendodermal precursors for neural posteriorization *in vivo*. *Development* 128(18), 3571-83.

European Annexin Homepage. <http://www24.brinkster.com/annexins/>

Fales, D. (1935) Experiments on the development of the pronephros of *Amblystoma punctatum*. *J.Exp. Zool.* 72, 147-173.

Favor, J., Sandulache, R., Neuhauser-Klaus, A., Pretsch, W., Chatterjee, B., Senft, E., Wurst, W., Blanquet, V., Grimes, P., Sporle, R. and Schughart, K. (1996) The mouse Pax2^{Neu} mutation is identical to a human PAX2 mutation in a family with renal-coloboma syndrome results in development defects of the brain, ear, eye and kidney. *Proc. Natl. Acad. Sci USA*. 93, 13870-13875.

Filipenko, N. R. and Waisman, D. M. (2001) The C terminus of annexin II mediates binding to F-actin. *J. Biol. Chem.* 276(7), 5310-5.

Filippov, V., Solovyev, V., Filippov, M. and Gill, S. S. (2000) A novel type of RNase III family proteins in eukaryotes. *Gene* **245**, 213-221.

Fire, A. (1999) RNA-triggered gene silencing. *Trends in Genet.* **15** (9), 358-363.

Fire, A., Xu, S., Montgomery, M. K., Kostas, S. A., Driver, S. E. and Mello, C. C. (1998) Potent and specific genetic interference by double-stranded RNA in *Caenorhabditis elegans*. *Nature* **391**, 806-811.

Fleming, T. P. (1987) A quantitative analysis of cell allocation to trophectoderm and inner cell mass in the mouse blastocyst. *Dev. Biol.* **119**(2), 520-31.

Fraser, A. G., Kamath, R. S., Zipperlen, P., Martinez-Campos, M., Sohrmann, M. and Ahringer, J. (2000) Functional genomic analysis of *C.elegans* chromosome 1 by systematic RNA interference. *Nature* **408**, 325-330.

Furthauer, M., Reifers, F., Brand, M., Thisse, B. and Thisse, C. (2001) sprouty4 acts *in vivo* as a feedback-induced antagonist of FGF signaling in zebrafish. *Development* **128**(12), 175-186.

Garbuglia, M., Verzini, M., Hofmann, A., Huber, R. and Donato, R. (2000) S100A1 and S100B interactions with annexins. *Biochim Biophys Acta.* **1498**(2-3), 192-206.

Giles, R. V., Spiller, D. G., Clark, R. E. and Tidd, D. M. (1999) Antisense morpholino oligonucleotide analog induces missplicing of C-myc mRNA. *Antisense Nucleic Acid Drug Dev.* **9**(2), 213-20.

Gonczy, P., Echeverri, C., Oegema, K., Coulson, A., Jones, S. J. M., Copley, R. R., Duperon, J., Oegema, J., Brehm, M., Cassin, E., Hannak, E., Kirkham, M., Pichler, S., Flohrs, K., Goessen, A., Leidel, S., Alleaume, A-M., Martin, C., Ozlu, N., Bork, P. and Hyman, A. A. (2000) Functional

genomic analysis of cell division in *C. elegans* using RNAi of genes on chromosome 111. *Nature* **408**, 331-336.

Graf, J. D. and Kobel, H. R. (1991) Genetics of *Xenopus laevis*. In *Xenopus laevis: Practical Uses in Cell and Molecular Biology* (Kay, B.K. and Peng, H.B., Eds.) *Academic Press, San Diego*. pp. 19-34.

Graff, J. M., Bansal, A. and Melton, D. (1996) *Xenopus* Mad Proteins Transduce Distinct Subsets of Signals for the TGF β Superfamily. *Cell* **85**, 479-487.

Green, J. B. and Smith, J. C. (1990) Graded changes in dose of a *Xenopus* activin A homologue elicit stepwise transitions in embryonic cell fate. *Nature* **347**(6291), 391-4.

Green, J. B., Howes, G., Symes, K., Cooke, J. and Smith, J. C. (1990) The biological effects of XTC-MIF: quantitative comparison with *Xenopus* bFGF. *Development* **108**(1), 173-83.

Gunteski-Hamblin, A. M., Song, G., Walsh, R. A., Frenzke, M., Boivin, G. P., Dorn, G. W. 2nd., Kaetzel, M. A., Horseman, N. D. and Dedman, J. R. (1996) Annexin VI overexpression targeted to heart alters cardiomyocyte function in transgenic mice. *Am. J. Physiol.* **270**(3 Pt 2), H1091-100.

Gura, T. (2000) A silence that speaks volumes. *Nature* **404**, 804-808.

Gurdon, J. B., Harger, P., Mitchell, A. and Lemaire, P. (1994) Activin signalling and response to a morphogen gradient. *Nature* **371**(6497), 487-92.

Hajjar, K. A., Jacovina, A. T. and Chacko, J. (1994) An endothelial cell receptor for plasminogen/tissue plasminogen activator. I. Identity with annexin II. *J. Biol. Chem.* **269**(33), 21191-7.

- Hamilton, A. and Baulcombe, D. (1999)** A species of small antisense RNA in posttranscriptional gene silencing in plants. *Science* **286**, 950-951.
- Hammond, S. M., Bernstein, E., Beach, D. and Hannon, G. J. (2000)** An RNA-directed nuclease mediates post-transcriptional gene silencing in *Drosophila* cells. *Nature* **404**, 293-296.
- Hamre, K. M., Keller-Peck, C. R., Campbell, R. M., Peterson, A. C., Mullen, R. J. and Goldowitz, D. (1996)** Annexin IV is a Marker of Roof and Floor Plate Development in the Murine CNS. *J.Comp.Neurol.* **368**, 527-537.
- Han, H-Y., Lee, Y-H., Oh, J-Y., Na, D-S. and Lee, B-J. (1998)** NMR analyses of the interactions of human annexin 1 with ATP, Ca^{2+} , and Mg^{2+} . *FEBS. Lett.* **425**, 523-527.
- Harland RM. (1991)** In situ hybridization: an improved whole-mount method for *Xenopus* embryos. *Methods Cell Biol.* **36**, 685-95.
- Harlow, E. and Lane, D. (1998)** *Antibodies: A laboratory manual*. Cold Spring Harbor Laboratory Press, Cold Spring Harbor, New York.
- Hawkins, T. E., Merrifield, C. J. and Moss, S. E. (2000)** Calcium signaling and annexins. *Cell Biochem. Biophys.* **33(3)**, 275-96.
- Hawkins, T. E., Roes, J., Rees, D., Monkhouse, J. and Moss, S. E. (1999)** Immunological development and cardiovascular function are normal in annexin VI null mutant mice. *Mol. Cell Biol.* **19(12)**, 8028-32.
- Heasman, J., Crawford, A., Goldstone, K., Garner-Hamrick, P., Gumbiner, B., McCrea, P., Kintner, C., Noro, C. Y. and Wylie, C. (1994)** Overexpression of cadherins and underexpression of beta-catenin inhibit dorsal mesoderm induction in early *Xenopus* embryos. *Cell* **79(5)**, 791-803.

- Heasman, J., Kofron, M. and Wylie, C. (2000)** Beta-catenin signaling activity dissected in the early *Xenopus* embryo: a novel antisense approach. *Dev Biol.* **222**(1), 124-34.
- Heller, N. and Brändli, A. W. (1997)** *Xenopus Pax-2* displays multiple splice forms during embryogenesis and pronphric development. *Mech. Dev.* **69**, 83-104.
- Hemmati-Brivanlou A. and Melton D. A. (1992)** A truncated activin receptor inhibits mesoderm induction and formation of axial structures in *Xenopus* embryos. *Nature* **359**, 609-614.
- Holewa, B., vonStrandmann, E.P., Zapp, D., Lorenz, P. and Ryffel, G.U. (1996)** Transcriptional hierarchy in *Xenopus* embryogenesis: HNF4 a maternal factor involved in the developmental activation of the gene encoding the tissue specific transcription factor HNF1 alpha (LFB1). *Mech. Dev.* **54** (1), 45-57.
- Hoppler, S., Brown, J. D. and Moon, R. T. (1996)** Expression of a dominant-negative Wnt blocks induction of MyoD in *Xenopus* embryos. *Genes Dev.* **10**, 2805-2817.
- Howard, E. W., Newman, L. A., Oleksyn, D. W., Angerer, R. C. and Angerer, L. M. (2001)** SpKrl: a direct target of beta-catenin regulation required for endoderm differentiation in sea urchin embryos. *Development* **128**(3), 365-75.
- Hsu, H. J., Wang, W. D. and Hu, C. H. (2001)** Ectopic expression of negative ARNT2 factor disrupts fish development. *Biochem. Biophys. Res. Commun.* **282**(2), 487-92.
- Huang, H., Ningai, L. and Lin, S. (2001)** *Pdx-1* Knockdown Reduces Insulin Promoter Activity in Zebrafish. *Genesis* **30**, 134-136.

- Hudson C., Clements, D., Friday R. V., Stott D. and Woodland, H. R. (1997) *Xsox17 α* and - β Mediate Endoderm Formation in *Xenopus*. *Cell* **91**, 397-405.
- Hudziak, R. M., Summerton, J., Weller, D. D. and Iversen, P. L. (2000) Antiproliferative effects of steric blocking phosphorodiamidate morpholino antisense agents directed against c-myc. *Antisense Nucleic Acid Drug Dev.* **10**(3), 163-76.
- Imai, Y., Gates, M.A., Melby, A.E., Kimelman, D., Schier, A.F. and Talbot, W.S. (2001) The homeobox genes *vox* and *vent* are redundant repressors of dorsal fates in zebrafish. *Development* **128**(12), 2407-20.
- Inui, M., Watanabe, T. and Sobue, K. (1994) Annexin VI binds to a synaptic vesicle protein, synapsin 1. *J. Neurochem.* **63**, 1917-1923.
- Isas, J. M., Cartailier, J. P., Sokolov, Y., Patel, D. R., Langen, R., Luecke, H., Hall, J. E. and Haigler, H. T. (2000) Annexins V and XII insert into bilayers at mildly acidic pH and form ion channels. *Biochemistry* **39**(11), 3015-22.
- Ishitsuka, R., Kojima, K., Utsumi, H., Ogawa, H. and Matsumoto, I. (1998) Glycosaminoglycan binding properties of annexin IV, V, and VI. *J. Biol. Chem.* **273**(16), 9935-41.
- Ivanenkov, V. V., Gerke, V., Minin, A. A., Plessmann, U. and Weber, K. (1993) Transduction of Ca²⁺ signals upon fertilization of eggs; identification of an S-100 protein as a major Ca²⁺-binding protein. *Mech. Dev.* **42**, 151-158.
- Ivanenkov, V. V., Weber, K. and Gerke, V. (1994). The expression of different annexins in the fish embryo is developmentally regulated. *FEBS Lett.* **352**, 227-230.

- Izant, J. G. and Bryson, L. J. (1991)** *Xenopus* Annexin II (Calpactin I) Heavy Chain Has a Distinct Amino Terminus. *J. Biol. Chem.* **266**, 18560-18566.
- Jones, P. G., Moore, G. J. and Waisman, D. M. (1992)** A nonapeptide to the putative F-actin binding site of annexin-II tetramer inhibits its calcium-dependent activation of actin filament bundling. *J. Biol. Chem.* **267**(20), 13993-7.
- Jorgensen, A. J., Bennekou, P., Eskensen, K. and Kirstensen, B. I. (1997)** Annexins from Ehrlich ascites cells inhibit the calcium-activated chloride current in *Xenopus laevis* oocytes. *Eur. J. Physiol.* **434**, 261-266.
- Jost, M., Thiel, C., Weber, K. and Gerke, V. (1992).** Mapping of three unique Ca^{2+} -binding sites in human annexin II. *Eur. J. Biochem.* **207**, 923-930.
- Kaetzel, M. A., Harzarika, P. and Dedman, J. R. (1989)** Differential tissue expression of three 35-kDa annexin calcium-dependent phospholipid-binding proteins. *J. Biol. Chem.* **264**, 14463-14470.
- Kaetzel, M. A., Chan, H. C., Dubinsky, W. P., Dedman, J. R. and Nelson, D. J. (1994)** A role for annexin IV in epithelial cell function. Inhibition of calcium-activated chloride conductance. *J. Biol. Chem.* **269**(7), 5297-302.
- Kaetzel, M. A., Mo, Y. D., Mealy, T. R., Campos, B., Bergsma-Schutter, W., Brisson, A., Dedman, J. R. and Seaton, B. A. (2001)** Phosphorylation mutants elucidate the mechanism of annexin IV-mediated membrane aggregation. *Biochemistry* **40**(13), 4192-9.
- Kamath, R. S., Martinez-Campos, M., Zipperlen, P., Fraser, A. G. and Ahringer, J. (2000)** Effectiveness of specific RNA-mediated interference through ingested double-stranded RNA in *Caenorhabditis elegans*. *Gen.Biol.* **2**(1), research 0002.1-0002.10.

- Kang, H. M., Choi, K. S., Kassam, G., Fitzpatrick, S. L., Kwon, M., Waisman, D. M.** (1999) Role of annexin II tetramer in plasminogen activation. *Trends Cardiovasc. Med.* **9**(3-4), 92-102.
- Karpen, G. H.** (1994) Position-effect variegation and the new biology of heterochromatin. *Curr. Opin. Genet. Dev.* **4**, 281-291.
- Kawahara, A. and Dawid, I. B.** (2001) Critical role of *biklf* in erythroid cell differentiation in zebrafish. *Curr Biol.* **11**(17), 1353-7.
- Kennerdell, J. R. and Carthew, R. W.** (1998) Use of dsRNA-mediated genetic interference to demonstrate that *frizzled* and *frizzled 2* Act in the wingless pathway. *Cell* **95**, 1017-1026.
- Kennerdell, J. R. and Carthew, R. W.** (2000) Heritable gene silencing in *Drosophila* using double-stranded RNA. *Nat. Biotechnol.* **18**, 896-898.
- Ketting, R. F. and Plasterk, R. H.** (2000) A genetic link between co-suppression and RNA interference in *C. elegans*. *Nature* **404** (6775), 296-8.
- Ketting, R. F., Haverkamp, T. H., van Luenen, H. G. and Plasterk, R. H.** (1999) Mut-7 of *C. elegans*, required for transposon silencing and RNA interference, is a homolog of Werner syndrome helicase and RnaseD. *Cell* **99**, 133-141.
- Kipshidze, N., Moses, J., Shankar, L. R. and Leon, M.** (2001) Perspectives on antisense therapy for the prevention of restenosis. *Curr. Opin. Mol. Ther.* **3**(3), 265-77.
- Kirsch, T., Harrison, G., Golub, E. E. and Nah, H. D.** (2000) The roles of annexins and types II and X collagen in matrix vesicle-mediated mineralization of growth plate cartilage. *J. Biol. Chem.* **275**(45), 35577-83.

Kirsch, T., Nah, H. D., Demuth, D. R., Harrison, G., Golub, E. E., Adams, S. L. and Pacifici, M. (1997) Annexin V-mediated calcium flux across membranes is dependent on the lipid composition: implications for cartilage mineralization. *Biochemistry* **36**(11), 3359-67.

Kispert, A., Vainio, S. and McMahon, A. P. (1998) *Wnt-4* is a mesenchymal signal for epithelial transformation of metanephric mesenchyme in the developing kidney. *Development* **125**(21), 4225-34.

Kluge, B. and Fischer, A. (1991) The pronephros of the early ammocoete larva of lamprets (cyclostomata, petromyzontes)-Fine-structure of the renal tubules. *Cell and tissue research*. **263**(3), 515-528.

Kohlhase, J., Wischermann, A., Reichenbach, H., Froster, U. and Engel, W. (1998) Mutations in the SALL1 putative transcription factor gene cause Townes-Brocks syndrome. *Nat. Gen.* **18**, 81-83.

Koide, T., Downes, M., Chandraratna, R. A., Blumberg, B. and Umesono, K. (2001) Active repression of RAR signaling is required for head formation. *Genes Dev.* **15**(16), 2111-21.

Kojima, K., Utsumi, H., Ogawa, H. and Matsumoto, I. (1994) Highly polarised expression of carbohydrate-binding protein p33/41 (annexin IV) on the apical plasma membrane of epithelial cells in renal proximal tubules. *FEBS Letters*. **342**, 313-318.

Kos, R., Reedy, M. V., Johnson, R. L. and Erickson, C. A. (2001) The winged-helix transcription factor FoxD3 is important for establishing the neural crest lineage and repressing melanogenesis in avian embryos. *Development* **128**(8), 1467-79.

Kreidberg, J. A., Sariola, H., Loring, J. M., Maeda, M., Pelletier, J., Housman, D. and Jaenisch, R. (1993) *WT-1* is required for early kidney development. *Cell* 74(4), 679-91.

Kreig, P. A. and Melton, D. A. (1987) *In vitro* RNA synthesis with SP6 RNA polymerase. *Methods Enzymol.* 155, 397-415.

Kroll, K. L., and Amaya, E. (1996) Transgenic *Xenopus* embryos from sperm nuclear transplantations reveal FGF signaling requirements during gastrulation. *Development* 122(10), 3173-83.

Ku, M. and Melton, D. A. (1993) *Xwnt-11*: a maternally expressed *Xenopus wnt* gene. *Development* 119(4), 1161-73.

Lacerra, G., Sierakowska, H., Carestia, C., Fucharoen, S., Summerton, J., Weller, D. and Kole, R. (2000) Restoration of hemoglobin A synthesis in erythroid cells from peripheral blood of thalassemic patients. *Proc. Natl. Acad. Sci. U.S.A.* 97(17), 9591-6.

Lafont, F., Lecat, S., Verkade, P. and Simons, K. (1998) Annexin XIIIb associates with lipid microdomains to function in apical delivery. *J. Cell Biol.* 142(6), 1413-27.

Lallier, T. E., Whittaker, C. A. and DeSimone, D. W. (1996) Integrin alpha 6 expression is required for early nervous system development in *Xenopus laevis*. *Development.* 122(8), 2539-54.

Latinkic, B. V. and Smith, J. C. (1999) *Goosecoid* and *mix.1* repress *Brachyury* expression and are required for head formation in *Xenopus*. *Development* 126, 1769-1779.

Lecat, S. and Lafont, F. (1999) Annexins and their interacting proteins in membrane traffic. *Cell Biol. Biophys.* 207, 133-140.

- Levi, G., Gumbiner, B. and Thiery, J. P. (1991)** The distribution of E-cadherin during *Xenopus laevis* development. *Development* **111**(1), 159-69.
- Li, Y-X., Farrell, M. J., Liu, R., Mohanty, N. and Kirby, M. L. (2000)** Double-stranded RNA injection produces null phenotypes in zebrafish. *Dev.Biol.* **217**, 394-405.
- Liemann, S. and Huber, R. (1997)** Three-dimensional structure of annexins. *Cell Mol. Life Sci.* **53**(6), 516-21.
- Liemann, S., Benz, J., Burger, A., Voges, D., Hofmann, A., Huber, R. and Gottig, P. (1996)** Structural and functional characterisation of the voltage sensor in the ion channel human annexin V. *J. Mol. Biol.* **258**(4), 555-61.
- Lin, H. C., Sudhof, T. C. and Anderson, R. G. (1992)** Annexin VI is required for budding of clathrin-coated pits. *Cell.* **70**(2), 283-91.
- Lindbo, J. A. and Dougherty, W. G. (1992)** Pathogen-derived resistance to a potyvirus: immune and resistant phenotypes in transgenic tobacco expressing altered forms of a potyvirus coat protein nucleotide sequence. *Mol. Plant-Microbe Interact.* **5**, 143-153.
- Liu,L., Wang, M., Fisher, A. B. and Zimmerman, U. J. (1996)** Involvement of annexin II in exocytosis of lamellar bodies from alveolar epithelial type II cells. *Am. J. Physiol.* **270**(4 Pt 1), L668-76.
- Lohmann, J. U., Endl, I. and Bosch, T. C. G. (1999)** Silencing of developmental genes in *Hydra*. *Dev.Biol.* **214**, 211-214.
- Lynn, K., Fernandez, A., Aida, M., Sedbrook, J., Tasaka, M., Masson, P. and Barton, M. K. (1999)** The *PINHEAD/ZWILLE* gene acts pleiotropically in

Arabidopsis development and has overlapping functions with the *ARGONAUTE1* gene. *Development* **126**, 469-481.

Lyon, M. F. (1961) Gene action in the X-chromosome of the mouse (*Musculus L*). *Nature* **190**, 372-373

Majumdar, A. and Drummond, I. A. (2000) The zebrafish floating head mutant demonstrates podocytes play an important role in directing glomerular differentiation *Dev Biol.* **222**(1), 147-57.

Majumdar, A., Lun, K., Brand, M. and Drummond, I. A. (2000) Zebrafish no isthmus reveals a role for *pax2.1* in tubule differentiation and patterning events in the pronephric primordia. *Development* **127**(10), 2089-98.

Marcos-Gutierrez, C. V., Wilson, S. W., Holder, N. and Pachnis, V. (1997) The zebrafish homologue of the ret receptor and its pattern of expression during embryogenesis. *Oncogene* **14**(8), 879-89.

Massey, D., Traverso, V. and Maroux, S. (1991a) Lipocortin IV Is a Basolateral Cytoskeleton Constituent of Rabbit Enterocytes. *J. Biol. Chem.* **266**, 3125-3130.

Massey, D., Traverso, V., Rigal, A. and Maroux, S. (1991b). Cellular and Subcellular localisation of Annexin IV in rabbit intestinal epithelium, pancreas and liver. *Biol. Cell* **73**, 151-156.

Massey-Harroche, D., Traverso, V., Mayran, N., Francou, V., Vandewalle, A. and Maroux, S. (1995) Changes in expression and subcellular localization of annexin IV in rabbit kidney proximal tubule cells during primary culture. *J. Cell Physiol.* **165**(2), 313-22.

Massey-Harroche, D., Mayran, N., Maroux, S. (1998) Polarized localizations of annexins I, II, VI and XIII in epithelial cells of intestinal, hepatic and pancreatic tissues. *J. Cell Sci.* **111**, 3007-3015.

Matsuda, R., Kaneko, N. and Horikawa, Y. (1997) Presence and comparison of Ca^{2+} transport activity of annexins I, II, V, and VI in large unilamellar vesicles. *Biochem. Biophys. Res. Commun.* **237**(3), 499-503.

Mattioni, T., Louvion, J.F., and Picard, D. (1994) Regulation of protein activities by fusion to steroid binding domains. *Methods Cell Biol.* **43 Pt A**, 335-52.

Mayran, N., Traverso, V., Maroux, S. and Massey-Harroche, D. (1996) Cellular and subcellular localizations of annexins I, IV, and VI in lung epithelia. *Am. J. Physiol.* **270**, L863-L871.

McLaughlin, K. A., Rones, M. S. and Mercola, M. (2000) Notch regulates cell fate in the developing pronephros. *Dev Biol.* **227**(2), 567-80.

Mead, P. E., Brivanlou, I. H., Kelly, C. M. and Zon, L. I. (1996) BMP-4-responsive regulation of dorsal-ventral patterning by the homeobox protein Mix.1. *Nature* **382**, 357-360.

Menaa, C., Devlin, R. D., Reddy, S. V., Gazitt, Y., Choi, S. J. and Roodman, G. D. (1999) Annexin II increases osteoclast formation by stimulating the proliferation of osteoclast precursors in human marrow cultures. *J. Clin. Invest.* **103**(11), 1605-13.

Menell, J. S., Cesarman, G. M., Jacovina, A. T., McLaughlin, M. A., Lev, E. A., Hajjar, K. A. (1999) Annexin II and bleeding in acute promyelocytic leukemia. *Comment in: N Engl J Med.* **340**(13), 1035-6.

Merrifield, C. J., Rescher, U., Almers, W., Proust, J., Gerke, V., Sechi, A. S. and Moss, S. E. (2001) Annexin 2 has an essential role in actin-based macropinocytic rocketing. *Curr. Biol.* 11(14), 1136-41.

Meurs, E. F., Chong, K., Galabru, J., Thomas, N. S., Kerr, I. M., Williams, B. R. G. and Hovanessian, A. G. (1990) Molecular cloning and characterization of the human double-stranded RNA-activated protein kinase induced by interferon. *Cell* 62, 379-390.

Misquitta, L. and Paterson, B. M. (1999) Targeted disruption of gene function in *Drosophila* by RNA interference (RNA-i): A role for *nautilus* in embryonic somatic muscle formation. *Proc. Natl. Acad. Sci. USA* 96, 1451-1456.

Mitchell, T. S. and Sheets, M. D. (2001) The fgfr pathway is required for the trunk-inducing functions of spemann's organizer. *Dev Biol.* 237(2), 295-305.

Mobjerg, N., Larsen, E. H. and Jespersen, A. (2000) Morphology of the kidney in larvae of *Bufo viridis* (Amphibia, Anura, Bufonidae) *J.Morphol.* 245(3), 177-95.

Mohun, T. J., Taylor, M. V., Garrett, N. and Gurdon, J. B. (1989) The CArG promoter sequence is necessary for muscle-specific transcription of the cardiac actin gene in *Xenopus* embryos. *EMBO J.* 8(4), 1153-61.

Montgomery, M. K., Xu, S. and Fire, A. (1998) RNA as a target of double-stranded RNA-mediated genetic interference in *Caenorhabditis elegans*. *Proc. Natl. Acad. Sci. USA* 95, 15502-15507.

Moody, S. A. (1987) Fates of the Blastomeres of the 32-cell-stage *Xenopus* Embryo. *Dev. Biol.* 122, 300-319.

Morgan, R. O. and Fernandez, M. P. (1997) Annexin gene structures and molecular evolutionary genetics. *Cell Mol. Life Sci.* 53, 508-515.

Morgan, R. O., Jenkins, N. A., Gilbert, D. J., Copeland, N. G., Balsara, B. R., Testa, J. R. and Fernandez, M. P. (1999) Novel human and mouse annexin A10 are linked to the genome duplications during early chordate evolution. *Genomics* 60(1), 40-9.

Moriya, N., Uchiyama, H. and Asashima, M. (1993) Induction of pronephric tubules by activin and retinoic acid in presumptive ectoderm of *Xenopus laevis*. *Dev. Growth Differ.* 35, 123-128.

Moriya, N., Komazaki, S., Takahashi, S., Yokota, C. and Asashima, M. (2000) *In vitro* pancreas formation from *Xenopus* ectoderm treated with activin and retinoic acid. *Dev. Growth Differ.* 42(6), 593-602.

Mourrain, P., Beclin, C., Elmayan, T., Feuerbach, F., Godon, C., Morel, J.B., Jouette, D., Lacombe, A.M., Nikic, S., Picault, N., Remoue, K., Sanial, M., Vo, T.A. and Vaucheret, H. (2000) Arabidopsis SGS2 and SGS3 genes are required for posttranscriptional gene silencing and natural virus resistance. *Cell*. 101, 533-542.

Mowbray, C., Hammerschmidt, M. and Whitfield, T. T. (2001) Expression of BMP signalling pathway members in the developing zebrafish inner ear and lateral line. *Mech. Dev.* 108(1-2), 179-84.

Muller, F., Lakatos, L., Dantonel, J., Strahle, U. and Tora, L. (2001) TBP is not universally required for zygotic RNA polymerase II transcription in zebrafish. *Curr. Biol.* 11(4), 282-7.

Murre, C., Bain, G., van Dijk, M. A., Engel, I., Furnari, B. A., Massari, M. E., Matthews, J. R., Quong, M. W., Rivera, R. R. and Stuver, M. H. (1994) Structure and function of helix-loop-helix proteins. *Biochem. Biophys. Acta*. 1218(2), 129-35.

Naciff, J. M., Kaetzel, M. A., Behbehani, M. M. and Dedman, J. R. (1996) Differential expression of annexins I-VI in the rat dorsal root ganglia and spinal cord. *J. Comp. Neurol.* **368**, 356-370.

Nakano, H., Amemiya, S., Shiokawa, K. and Taira, M. (2000) RNA Interference for the Organizer-Specific Gene *Xlim-1* in *Xenopus* Embryos. *Biochem. Biophys. Res. Commun.* **274**, 434-439.

Napoli, C., Lemieux, C. and Jorgensen, R. (1990) Introduction of a chimeric chalcone synthase gene into petunia results in reversible co-suppression of homologous gene in trans. *Plant Cell* **2**, 279-289.

Nasevicius, A. and Ekker, S. C. (2000) Effective targeted gene 'knockdown' in zebrafish. *Nat. Genet.* **26**(2), 216-20.

NCBI GenBank <http://www.ncbi.nlm.nih.gov>.

Ngo, H., Tschudi, C., Gull, K. and Ulla, E. (1998) Double-stranded RNA induces m RNA degradation in *Trypanosoma brucei*. *Proc. Natl. Acad. Sci. USA* **95**, 14687-14692.

Nicholson, A. W. (1999) Function, mechanism and regulation of bacterial ribonucleases. *FEMS Microbiol. Rev.* **23**, 371-390.

Nieuwkoop, P. D. (1969) The formation of mesoderm in Urodelean amphibians. Induction by the edoderm. *Wilhelm Roux's Arch. EntwMech. Org.* **162**, 341-373.

Nieuwkoop, P. D. and Faber, J. (1994) Normal table of *xenopus laevis* (daudin): a systematical and chronological survey of the development from the fertilized egg till the end of metamorphosis. Garland Publishing, Inc., New York and London.

Nishizuka, Y. (1992) Intracellular signaling by hydrolysis of phospholipids and activation of protein kinase C. *Science* 258(5082), 607-14.

Nutt, S. L., Bronchain, O. J., Hartley, K. O. and Amaya, E. (2001) Comparison of morpholino based translational inhibition during the development of *Xenopus laevis* and *Xenopus tropicalis*. *Genesis* 30(3), 110-3.

Oates, A. C., Bruce, A. E. E. and Ho, R. K. (2000) Too much interference: injection of double-stranded RNA has nonspecific effects in the zebrafish embryo. *Dev. Biol.* 224, 20-28.

Oelgeschläger, M., Larrain, J., Geissert, D. and De Robertis, E. (2000) The evolutionarily conserved BMP-binding protein Twisted gastrulation promotes BMP signalling. *Nature* 405, 757-763.

Oling, F., Santos, J. S., Govorukhina, N., Mazeres-Dubut, C., Bergsma-Schutter, W., Oostergetel, G., Keegstra, W., Lambert, O., Lewit-Bentley, A. and Brisson A. (2000) Structure of membrane-bound annexin A5 trimers: a hybrid cryo-EM - X-ray crystallography study. *J. Mol. Biol.* 304(4), 561-73.

Onuma, Y., Nishinakamura, R., Takahashi, S., Yokota, T. and Asashima, M. (1999) Molecular cloning of a novel *Xenopus spalt* gene (*Xsal-3*). *Biochem Biophys Res Commun* 264(1), 151-6.

Osterloh, D., Wittbrodt, J. and Gerke, V. (1998) Characterization and Developmentally Regulated Expression of Four Annexins in the Killifish *Medaka*. *DNA and Cell Biology* 17, 835-847.

Palauqui, J-C., Elmayan, T., Pollien, J.-M. and Vaucheret, H. (1997) Systemic acquired silencing: transgene specific post-transcriptional silencing is transmitted by grafting from silenced stocks to non-silenced scions. *Embo.J.* 16, 4738-4745.

Park, Y.D., Papp, I., Moscone, E. A., Iglesias, V. A., Vaucheret, H., Matzke, A. J. M. and Matzke, M. A. (1996) Gene silencing mediated by promoter homology occurs at the level of transcription and results in meiotically heritable alterations in methylation and gene activity. *Plant J.* **9**, 183-194.

Parr, B. A. and McMahon, A. P. (1994) *Wnt* genes and vertebrate development. *Curr. Opin. Genet. Dev.* **4**(4), 523-8.

Parrish, S. Fleenor, J. Xu, S., Mello, C. and Fire, A. (2000) Functional anatomy of a dsRNA trigger: differential requirement for the two trigger strands in RNA interference. *Mol. Cell.* **6**, 1077-1087.

Pencil, S. D., Toh, Y. and Nicolson, G. L. (1993) Candidate metastasis-associated genes of the rat 13762NF mammary adenocarcinoma. *Breast Cancer Res. Treat.* **25**(2), 165-74.

Peng, Y., Kok, K. H., Xu, R. H., Kwok, K. H., Tay, D., Fung, P. C., Kung, H. F., Lin, M. C. (2000) Maternal cold inducible RNA binding protein is required for embryonic kidney formation in *Xenopus laevis*. *FEBS Lett.* **482**(1-2), 37-43.

Pfeffer, P. L., Gerster, T., Lun, K., Brand, M. and Busslinger, M. (1998) Characterization of three novel members of the zebrafish *Pax2/5/8* family: dependency of *Pax5* and *Pax8* expression on the *Pax2.1* (*noi*) function. *Development* **125**(16), 3063-74.

Pierce, S. B. and Kimelman, D. (1995) Regulation of Spemann organizer formation by the intracellular kinase Xgsk-3. *Development* **121**, 755-765.

Pigault, C., Follenius-Wund, A., Schmutz, M., Freyssinet, J. M. and Brisson, A. (1994) Formation of two-dimensional arrays of annexin V on phosphatidylserine-containing liposomes. *J. Mol. Biol.* **236**(1), 199-208.

- Plasterk, R. H. A. and Ketting, R. F. (2000) The silence of the genes. *Curr. Op. Gen. Dev.* 10, 562-567.
- Pollard, H. B., Caohuy, H., Minton, A. P. and Srivastava, M. (1998) Synexin (annexin VII) hypothesis for Ca^{2+} /GTP-regulated exocytosis. *Adv. Pharmacol.* 42, 81-7.
- Pollard, H. B., Guy, H. R., Arispe, N., de la Fuente, M., Lee, G., Rojas, E. M.,
Pollard, J. R., Srivastava, M., Zhang-Keck, Z. Y., Merezhinskaya, N.,
Caohuy, H., Burns, A. L. and Rojas, E. M. (1992) Calcium channel and membrane fusion activity of synexin and other members of the Annexin gene family. *Biophys. J.* 62(1), 15-8.
- Pontoglio, M., Prie, D., Cheret, C., Doyen, A., Leroy, C., Froguel, P., Velho, G., Yaniv, M. and Friedlander, G. (2000) HNF1alpha controls renal glucose reabsorption in mouse and man. *EMBO Rep.* 1(4), 359-65.
- Price, D. J. and Willshaw, D. J. (2000) Mechanisms of Cortical Development. Chapt.2. Early development of the telencephalon. *Oxford Science Publications.*
- Raynal, P. and Pollard, H. B. (1994). Annexins: the problem of assessing the biological role for a gene family of multifunctional calcium-and phospholipid-binding proteins. *Biochim. Biophys. Acta.* 1197, 63-93.
- Rebagliati, M. R. and Melton, D. A. (1987) Antisense RNA injections in fertilised frog eggs reveal an RNA duplex unwinding activity. *Cell* 48, 599-605.
- Romano, N. and Macino, G. (1992) Quelling transient inactivation of gene expression in *Neurospora crassa* by transformation with homologous sequences. *Mol. Microbiol.* 6, 3343-3353.

Ross, J. J., Shimmi, O., Vilmos, P., Petryk, A., Kim, H., Gaudenz, K., Hermanson, S., Ekker, S. C., O'Connor, M. B. and Marsh, J. L. (2001) Twisted gastrulation is a conserved extracellular BMP antagonist. *Nature* 410(6827), 479-83.

Rubartelli, A., Bajetto, A., Allavena, G., Wollman, E. and Sitia, R. (1992) Secretion of thioredoxin by normal and neoplastic cells through a leaderless secretory pathway. *J. Biol. Chem.* 267(34), 24161-4.

Ruiz, I., Altaba, A., Choi, T. and Melton, D. A. (1991) Expression of the Xhox3 homeobox protein in *Xenopus* embryos; Blocking its early function suggests the requirement of Xhox3 for normal posterior development. *Dev. Growth Differ.* 33, 651-669.

Safer, A. M., Tytler, P. and El-Sayed, N. (1982) The structure of the head of the kidney in the mudskipper, *Periophthalmus koelreuteri*. *J. Morphol.* 174, 121-131.

Sakakibara, N., Gasa, S., Kamio, K., Makita, A. and Koyanagi, T. (1987). Association of elevated sulfatides and sulfotransferase activities with human renal cell carcinoma. *Cancer Res.* 49, 335-339.

Sambrook, J., Fritsch, E. F. and Maniatis, T. (1989) Molecular cloning: a laboratory manual, 2nd ed. Cold Spring Harbor laboratory Press, Cold Spring Harbor, N.Y.

Sanchez, M. P., Silos-Santiago, I., Frisen, J., He, B., Lira, S. A. and Barbacid, M. (1996) Renal agenesis and the absence of enteric neurons in mice lacking GDNF. *Nature* 382(6586), 70-3.

Sanchez Alvarado, A. S. and Newmark, P. A. (1999) Double-stranded RNA specifically disrupts gene expression during planarian regeneration. *Proc. Natl. Acad. Sci. USA* **96**, 5049-5054.

Sanyanusin, P., Schimmenti, L. A., McNoe, L. A., Ward, T. A., Pierpont, M. I., Sullivan, M. J., Dobyns, W. B. and Eccles, M. R. (1995) Mutation of the *PAX2* gene in a family with optic nerve colo renal anomalies and vesicoureteral reflux. *Nat. Genet.* **9**(4), 358-64.

Sarafian, T., Pradel, L. A., Henry, J. P., Aunis, D. and Bader, M. F. (1991). The participation of annexin II (calpactin I) in calcium-evoked exocytosis requires protein kinase C. *J. Cell. Biol.* **114**, 1135-1147.

Sato, A., Asashima, M., Yokota, T. and Nishinakamura, R. (2000) Cloning and expression pattern of a *Xenopus* pronephros-specific gene, *XSMP-30*. *Mech. Dev.* **92**(2), 273-5.

Satoh, A., Takayama, E., Kojima, K., Ogawa, H., Katsura, Y., Kina, T. and Matsumoto, I. (1997) Characterisation of Human p33/41 (Annexin IV), a Ca^{2+} Dependent Carbohydrate-Binding Protein with Monoclonal Anti-annexin IV Antibodies, AS11 and AS17. *Biol. Pharm. Bull.* **20**, 224-229.

Saxén, L. (1987) Organogenesis of the kidney. *Cambridge: Cambridge University Press.*

Schiebel, W., Pelissier, T., Riedel, L., Thalmeir, S., Schiebel, R., Kempe, D., Lottspeich, F., Sanger, H. L. and Wassenger, M. (1998) Isolation of an RNA-directed RNA polymerase-specific cDNA clone from tomato. *Plant Cell.* **10**, 2087-2101.

Schmidt, A., Palumbo, G., Bozzetti, M. P., Tritto, P., Pimpinelli, S. and Schafer, U. (1999) Genetic and molecular characterisation of *sting*, a gene

involved in crystal formation and meiotic drive in the male germ line of *Drosophila melanogaster*. *Genetics* **151**, 749-760.

Schoenwolf, G. C. and Smith, J. L. (1990) Mechanisms of neurulation: traditional viewpoint and recent advances. *Development*. **109**, 243-270.

Schuchardt, A., D'Agati, V., Pachnis, V. and Costantini, F. (1996) Renal agenesis and hypodysplasia in ret-k- mutant mice result from defects in ureteric bud development. *Development* **122**(6), 1919-29

Schweickert, A., Deissler, K., Blum, M. and Steinbeisser, H. (2001) Pitx1 and Pitx2c are required for ectopic cement gland formation in *Xenopus laevis*. *Genesis* **30**(3), 144-8.

Seaton, B. A. and Dedman, J. R. (1998). Annexins. *BioMetals* **11**, 399.

Seaton, B. A. (1996) Annexins: molecular structure to cellular function. R.G. Landes Company. Austin, Texas.

Serluca, F. C. and Fishman, M. C. (2001) Pre-pattern in the pronephric kidney field of zebrafish. *Development* **128**(12), 2233-41.

Seufert, D. W., Brennan, H. C., DeGuire, J., Jones, E. A. and Vize, P. D. (1999) Developmental basis of pronephric defects in *Xenopus* body plan phenotypes. *Dev. Biol.* **215**(2), 233-42.

Shawlot, W. and Behringer, R. R. (1995) Requirement for *Lim1* in head organizer function. *Nature* **374**, 425-430.

Shepherd, I. T., Beattie, C. E. and Raible, D. W. (2001) Functional analysis of zebrafish GDNF. *Dev. Biol.* **231**(2), 420-35.

- Shi, D. L., Goisset, C. and Boucaut, J. C. (1998)** Expression of *Xfz3*, a *Xenopus* frizzled family member, is restricted to the early nervous system. *Mech. Dev.* **70**(1-2), 35-47.
- Shibata, M., Ono, H., Hikasa, H., Shinga, J. and Taira, M. (2000)** *Xenopus* crescent encoding a Frizzled-like domain is expressed in the Spemann organizer and pronephros. *Mech. Dev.* **96**(2), 243-6.
- Shuttleworth, J. and Colman, A. (1988)** Antisense oligonucleotide-directed cleavage of mRNA in *Xenopus* oocytes and eggs. *EMBO.J.* **7**(2), 427-434.
- Simonneau, L., Broders, F. and Thiery, J. P. (1992)** N-cadherin transcripts in *Xenopus laevis* from early tailbud to tadpole. *Dev. Dyn.* **194**(4), 247-60.
- Sirvastava, M., Zhang-Keck, Z-Y., Caohuy, H., McPhie, P. and Pollard, H. (1996)** Novel isoforms of synexin in *Xenopus laevis*: multiple tandem PGQM repeats distinguish mRNAs in specific adult tissues and embryonic stages. *Biochem. J.* **316**, 729-735.
- Sive, H. L., Grainger, R. M. and Harland, R. M. (2000)** Early Development of *Xenopus laevis*. A laboratory manual, Cold Spring Harbor laboratory Press, Cold Spring Harbor, N.Y.
- Skouteris, G. G. and Schroder, C. H. (1996)** The hepatocyte growth factor receptor kinase-mediated phosphorylation of lipocortin-1 transduces the proliferating signal of the hepatocyte growth factor. *J. Biol. Chem.* **271**(44), 27266-73.
- Smardon, A., Spoerke, J., Stacey, S., Klein, M., Mackin, N. and Maine, E. (2000)** EGO-1 is related to RNA-directed RNA polymerase and functions in germ-line development and RNA interference in *C. elegans*. *Curr.Biol.* **10**, 169-178.

- Smith, J. C., Price, B. M., Van Nimmen, K. and Huylebroeck, D. (1990)** Identification of a potent *Xenopus* mesoderm-inducing factor as a homologue of activin A. *Nature* **345** (6277), 729-31.
- Smithers, L., Haddon, C., Jiang, Y. and Lewis, J. (2000)** Sequence and embryonic expression of deltaC in the zebrafish. *Mech. Dev.* **90**(1), 119-23.
- Sohma, H., Matsushima, N., Watanabe, T., Hattori, A., Kuroki, Y. and Akino, T. (1995)** Ca²⁺-dependent binding of annexin IV to surfactant protein A and lamellar bodies in alveolar type II cells. *Biochem. J.* **312**, 175-181.
- Sohma, H., Creutz, C. E., Gasa, S., Ohkawa, H., Akino, T. and Kuroki, Y. (2001).** Differential lipid specificities of the repeated domains of annexin IV. *Biochim. Biophys. Acta.* **1546**, 205-215.
- Sohma, H., Ohkawa, H., Akino, T. and Kuroki, Y. (2001)** Binding of annexins to lung lamellar bodies and the pma-stimulated secretion of annexin v from alveolar type ii cells. *J. Biochem. (Tokyo).* **130**(3), 449-55.
- Spenneberg, R., Osterloh, D. and Gerke V. (1998)** Phospholipid vesicle binding and aggregation by four novel fish annexins are differently regulated by Ca²⁺. *Biochim. Biophys. Acta.* **1448**(2), 311-9.
- Srivastava, M., Zhang-Keck, Z. Y., Caohuy, H., McPhie, P. and Pollard, H. B. (1996)** Novel isoforms of synexin in *Xenopus laevis*: multiple tandem PGQM repeats distinguish mRNAs in specific adult tissues and embryonic stages. *Biochem. J.* **316** (Pt 3), 729-35.
- Srivastava, M., Atwater, I., Glasman, M., Leighton, X., Goping, G., Caohuy, H., Miller, G., Pichel, J., Westphal, H., Mears, D., Rojas, E. and Pollard, H. B. (1999)** Defects in inositol 1,4,5-trisphosphate receptor expression, Ca(2+) signaling, and insulin secretion in the anx7(+/-) knockout mouse. *Proc. Natl. Acad. Sci. U.S.A.* **96**(24), 13783-8.

Stark, K., Vainio, S., Vassileva, G. and McMahon, A. P. (1994) Epithelial transformation of metanephric mesenchyme in the developing kidney regulated by *Wnt-4*. *Nature* **372**(6507), 679-83

Stein, D., Foster, E., Huang, S. B., Weller, D. and Summerton, J. (1997) A specificity comparison of four antisense types: morpholino, 2'-O-methyl RNA, DNA, and phosphorothioate DNA. *Antisense Nucleic Acid Drug Dev.* **7**(3),151-7.

Steinbach, O. C., Wolffe, A. P. and Rupp, R. A. W. (1997) Somatic linker histones cause loss of mesodermal competence in *Xenopus*. *Nature* **389**, 395-402.

Steinbeisser, H., Fainsod, A., Niehrs, C., Sasai, Y. and De Robertis, E. M. (1995) The role of *gsc* and *BMP-4* in dorsal-ventral patterning of the marginal zone in *Xenopus*: a loss-of -function study using antisense RNA. *EMBO. J.* **14**, 5230-5243.

Stryer, L. (1995) Biochemistry. New York: *W.H. Freeman and Company*.

Sumanas, S. and Ekker, S. C. (2001) *Xenopus frizzled-7* Morphant Displays Defects in Dorsoventral Patterning and Convergent Extension Movements during Gastrulation. *Genesis* **30**, 119-122.

Summerton J. (1999) Morpholino antisense oligomers: the case for an RNase H-independent structural type. *Biochim. Biophys. Acta.* **1489**(1), 141-58.

Summerton, J. and Weller, D. (1997) Morpholino antisense oligomers: design, preparation, and properties. *Antisense Nucleic Acid Drug Dev.* **7**(3), 187-95. Review.

Summerton, J., Stein, D., Huang, S. B., Matthews, P., Weller, D. and Partridge, M. (1997) Morpholino and phosphorothioate antisense oligomers

compared in cell-free and in-cell systems. *Antisense Nucleic Acid Drug Dev.* **7**(2), 63-70.

Svoboda, P., Stein, P., Hayashi, H. and Schultz, R. M. (2000) Selective reduction of dormant maternal mRNAs in mouse oocytes by RNA interference. *Development* **127**, 4147-4156.

Tabara, H., Grishok, A. and Mello, C. C. (1998) RNAi in *C.elegans*: soaking in the genome sequence. *Science* **282**, 430-431.

Tabara, H., Sarkissian, M., Kelly, W. G., Fleenor, J., Grishok, A., Timmons, L., Fire, A. and Mello, C. C. (1999) The *rde-1* gene, RNA interference, and transposon silencing in *C. elegans*. *Cell* **99**, 123-132.

Taira, M., Jamrich, M., Good, P. J. and Dawid, I. B. (1992) The *LIM* domain-containing homeo box gene *Xlim-1* is expressed specifically in the organizer region of *Xenopus* gastrula embryos. *Genes Dev.* **6**, 356-366.

Taira, M., Otani, H., Jamrich, M. and Dawid, I. B. (1994) Expression of the *LIM* class homeobox gene *Xlim-1* in pronephros and CNS cell lineages of *Xenopus* embryos is affected by retinoic acid and exogastrulation. *Development* **120**(6), 1525-36.

Tan, C., Deardorff, M. A., Saint-Jeannet, J. P., Yang, J., Arzoumanian, A. and Klein, P. S. (2001) Kermit, a frizzled interacting protein, regulates frizzled 3 signaling in neural crest development. *Development* **128**(19), 3665-74.

Tavernarakis, N., Wang, S. L., Dorovkov, M., Ryazanov, A. and Driscoll, M. (2000) Heritable and inducible genetic interference by dsRNA. *Nat. Genet.* **24**, 180-183.

- Taylor, M. F., Paulauskis, J. D., Weller, D. D. and Kobzik, L. (1996)** *In vitro* efficacy of morpholino-modified antisense oligomers directed against tumor necrosis factor-alpha mRNA. *J. Biol. Chem.* **271**(29), 17445-52.
- Taylor, M. F., Paulauskis, J. D., Weller, D. D. and Kobzik, L. (1997)** Comparison of efficacy of antisense oligomers directed toward TNF-alpha in helper T and macrophage cell lines. *Cytokine* **9**(9), 672-81.
- Taylor, M. F., Weller, D. D. and Kobzik, L. (1998)** Effect of TNF-alpha antisense oligomers on cytokine production by primary murine alveolar macrophages. *Antisense Nucleic Acid Drug Dev.* **8**(3), 199-205.
- Timmons, L. and Fire, A. (1998)** Specific interference by ingested dsRNA. *Nature* **395**, 854.
- Topczewska, J. M., Topczewski, J., Shostak, A., Kume, T., Solnica-Krezel, L. and Hogan, B. L. (2001)** The winged helix transcription factor Foxc1a is essential for somitogenesis in zebrafish. *Genes Dev.* **15**(18), 2483-93.
- Torres, M., Gómez-Pardo, E., Dressler, G. R. and Gruss, P. (1995)** Pax-2 controls multiple steps of urogenital development. *Development* **121**, 4057-4065.
- Tucker, R. P. (2001)** Abnormal neural crest cell migration after the in vivo knockdown of tenascin-C expression with morpholino antisense oligonucleotides. *Dev. Dyn.* **222**(1), 115-9.
- Turpin, E., Russo-Marie, F., Dubois, T., de Paillerets, C., Alfsen, A. and Bomsel, M. (1998)** In adrenocortical tissue, annexins II and VI are attached to clathrin coated vesicles in a calcium-independent manner. *Biochim. Biophys. Acta.* **1402**(2), 115-30.

- Tuschl, T., Zamore, P. D., Lehmann, R., Bartel, D. P. and Sharp, P. A. (1999) Targeted mRNA degradation by double-stranded RNA in vitro. *Genes Dev.* **13**, 3191-3197.
- Tytler, P. (1988) Morphology of the pronephros of the juvenile brown trout, *Salmo trutta*. *J.Morphol.* **19**, 189-204.
- Tzima, E., Trotter, P. J., Orchard, M. A. and Walker, J. H. (2000) Annexin V relocates to the platelet cytoskeleton upon activation and binds to a specific isoform of actin. *Eur. J. Biochem.* **267**(15), 4720-30.
- Ui-Tei, K., Zenno, S., Miyata, Y. and Saigo, K. (2000) Sensitive assay of RNA interference in *Drosophila* and chinese hamster cultured cells using firefly luciferase gene as target. *FEBS Lett.* **479**, 79-82.
- Ungar, A. R. , Kelly, G. M. and Moon, R. T. (1995) Wnt4 affects morphogenesis when misexpressed in the zebrafish embryo. *Mech. Dev.* **52**(2-3), 153-64.
- Uochi, T. and Asashima, M. (1998) *XCIRP* (*Xenopus* homolog of cold-inducible RNA-binding protein) is expressed transiently in developing pronephros and neural tissue. *Gene* **211**(2), 245-50.
- Uochi, T. and Asashima M. (1996) Sequential gene expression during pronephric tubule formation in vitro in *Xenopus* ectoderm. *Dev. Growth Differ.* **38**, 625-634
- van Blokland, R., Van der Geest, N., Mol, J. N. M. and Kooter, J. M. (1994) Transgene-mediated suppression of chalcone synthase expression in *Petunia hybrida* results from an increase in RNA turnover. *Plant J.* **6**, 861-877.
- van Engeland, M., Nieland, L. J., Ramaekers, F. C., Schutte, B. and Reutelingsperger, C. P. (1998) Annexin V-affinity assay: a review on an

apoptosis detection system based on phosphatidylserine exposure. *Cytometry* **31**(1), 1-9.

van West, P., Kamoun, S., van't Klooster, J. W. and Govers, F. (1999) Internuclear gene silencing in *Phytophthora infestans*. *Mol. Cell* **3**, 339-348.

Vaucheret, H., Beclin, C., Elmayan, T., Feuerbach, F., Godon, C., Morel, J-B., Mourrain, P., Palauqui, J-C. and Vernhettes, S. (1998) Transgene-induced gene silencing in plants. *Plant J.* **16**(6), 651-659.

Vishwanatha, J. K. and Kumble, S. (1993) Involvement of annexin II in DNA replication: evidence from cell-free extracts of *Xenopus* eggs. *J. Cell Sci.* **105** (Pt2), 533-40.

Vize, P. D., Jones, E. A. and Pfister, R. (1995). Development of the *Xenopus* pronephric system. *Dev. Biol.* **171**, 531-540.

Vize, P. D., Melton, D. A., Hemmati-Brivanlou, A., Harland, R. M. (1991) Assays for gene function in developing *Xenopus* embryos. *Methods Cell Biol.* **36**, 367-87.

Vize, P. D., Seufert, D. W., Carroll, T. J. and Wallingford, J. B. (1997) Model systems for the study of kidney development: use of the pronephros in the analysis of organ induction and patterning. *Dev. Biol.* **188**(2), 189-204. Review.

Voinnet, O., Vain, P., Angell, S. and Baulcombe, D.C. (1998) Systemic spread of sequence-specific transgene RNA degradation in plants is initiated by localized introduction of ectopic promotorless DNA. *Cell* **95**, 177-187.

Vojtek, A. B. and Hollenberg, S. M. (1995) Ras-Raf interaction: two-hybrid analysis. *Methods Enzymol.* **255**, 331-42.

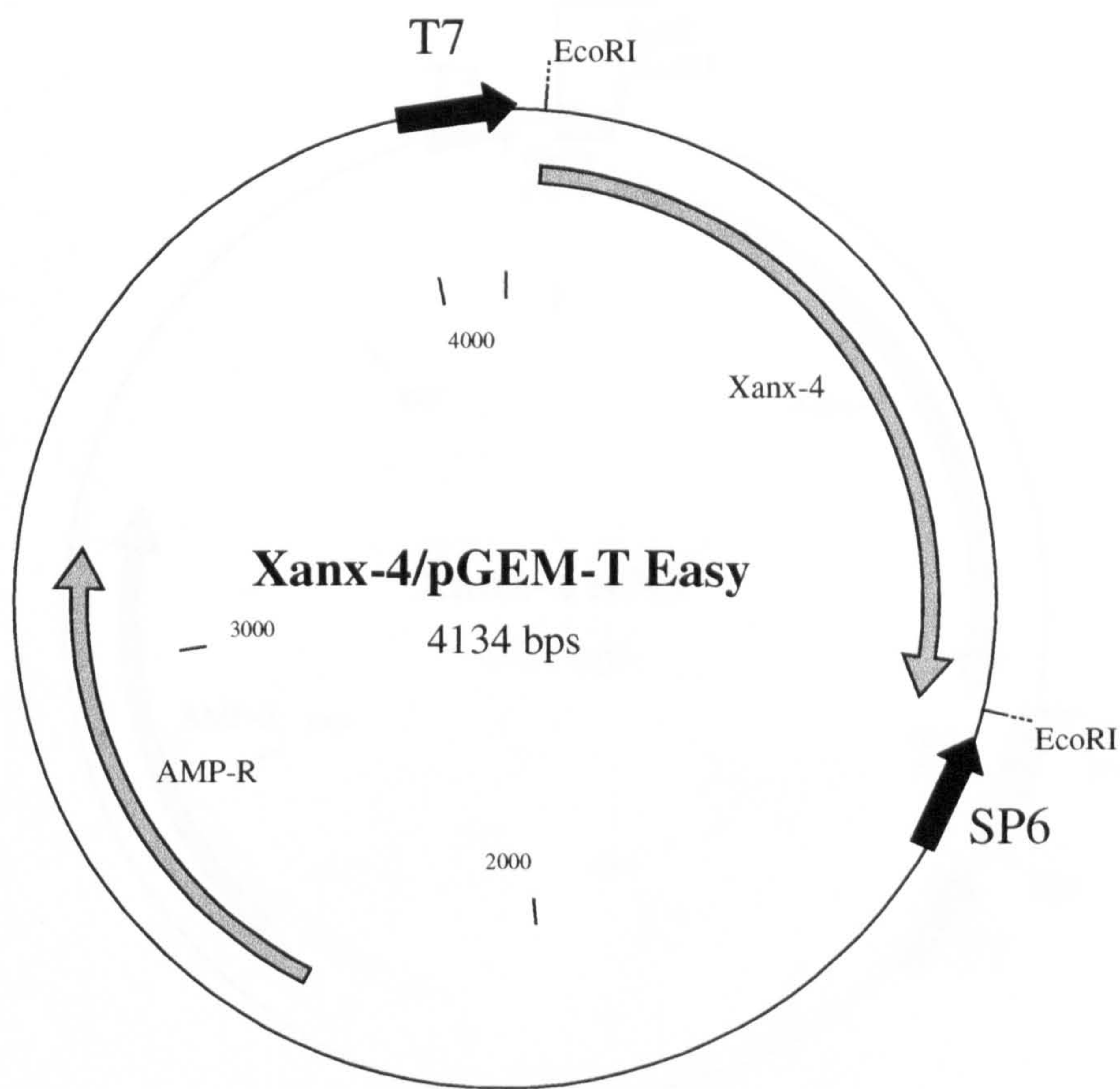
- von der Mark, K. and Mollenhauer, J. (1997) Annexin V interactions with collagen. *Cell Mol. Life Sci.* **53**(6), 539-45.
- Vukicevic, S., Kopp, J.B., Luyten, F.P. and Sampath, T.K. (1996) Induction of nephrogenic mesenchyme by osteogenic protein 1 (bone morphogenetic protein 7). *Proc. Natl. Acad. Sci. USA* **93**(17), 9021-6.
- Wallingford, J. B., Carroll, T. J. and Vize, P. D. (1998) Precocious Expression of the Wilms' Tumor Gene *xWT1* Inhibits Embryonic Kidney Development in *Xenopus laevis*. *Dev. Biol.* **202**, 103-112.
- Wang, S., Krinks, M., Kleinwaks, L. and Moos, M. Jr. (1997) A novel *Xenopus* homologue of bone morphogenetic protein-7 (BMP-7). *Genes Funct.* **1**(4), 259-71.
- Wargelius, A., Ellingson, S. and Fjose, A. (1999) Double-stranded RNA induces specific developmental defects in zebrafish embryos. *Biochem. Biophys. Res. Commun.* **263**, 156-161.
- Wassenegger, M., Heimes, S., Riedel, L. and Sanger, H. L. (1994) RNA-directed *de novo* methylation of genomic sequences in plants. *Cell* **76**, 567-576.
- Weber, H., Strandmann, E. P.V. , Holewa, B., Bartkowski, S., Zapp, D., Zoidl, C. and Ryffel, G. U. (1996) Regulation and function of the tissue-specific transcription factor *HNF1 alpha (LFB1)* during *Xenopus* development. *Int. J. Dev. Biol.* **40** (1), 297-304
- Wianny, F. and Zernicka-Goetz, M. (2000) Specific interference with gene function by double-stranded RNA in early mouse development. *Nat. Cell Biol.* **2**, 70-75.
- Wice, B. M. and Gordon, J. I. (1992). A strategy for isolation of cDNAs encoding proteins affecting annexin intestinal epithelial cell growth and

- differentiation: Characterization of a novel gut specific N-myristoylated annexin. *J. Cell Biol.* **116**, 405-422.
- Wild, W., von Strandmann, E. P., Nastos, A., Senkel, S., Lingott-Frieg, A., Bulman, M., Bingham, C., Ellard, S., Hattersley, A. T. and Ryffel, G. U. (2000) The mutated human gene encoding hepatocyte nuclear factor 1 beta inhibits kidney formation in developing *Xenopus* embryos. *Proc. Natl. Acad. Sci. USA* **97**(9), 4695-4700.
- Wilson, R. and Mohun, T. (1995) XIdx, a dominant negative regulator of bHLH function in early *Xenopus* embryos. *Mech. Dev.* **49**, 211-222.
- Witta, S. E. and Sato, S. M. (1997) XIPOU 2 is a potential regulator of Spemann's Organizer. *Development* **124**(6), 1179-89.
- Wu, H., Xu, H., Miraglia, L. J. and Crooke, S. T. (2000) Human RNase III is a 160 kDa protein involved in preribosomal RNA processing. *J. Biol. Chem.* **17**, 17.
- Yang, Z., Liu, N. and Lin, S. (2001) A zebrafish forebrain-specific zinc finger gene can induce ectopic *dlx2* and *dlx6* expression. *Dev. Biol.* **231**(1), 138-48.
- Yeatman, T. J., Updyke, T. V., Kaetzel, M. A., Dedman, J. R. and Nicolson, G. L. (1993) Expression of annexins on the surfaces of non-metastatic and metastatic human and rodent tumor cells. *Clin. Exp. Metastasis.* **11**(1), 37-44.
- Yee, N. S., Yusuf, S. and Pack, M. (2001) Zebrafish *pdx1* Morphant Displays Defects in Pancreas Development and Digestive Organ Chirality, and Potentially Identifies a Multipotent Pancreas Progenitor Cell. *Genesis* **30**, 137-140.
- Young, G. P. H., Young, J. D-E., Deshpande, A. K., Goldstein, M., Koide, S. S. and Cohn, Z. A. (1984). A Ca^{2+} -activated channel from *Xenopus laevis* oocyte membranes reconstituted into planar bilayers. *Cell Biol.* **81**, 5155-5159.

Zamore, P. D., Tuschl, T., Sharp, P. A. and Bartel, D. P. (2000). RNAi: Double-stranded RNA directs the ATP-dependent cleavage of mRNA at 21 to 23 Nucleotide Intervals. *Cell* 101, 25-33.

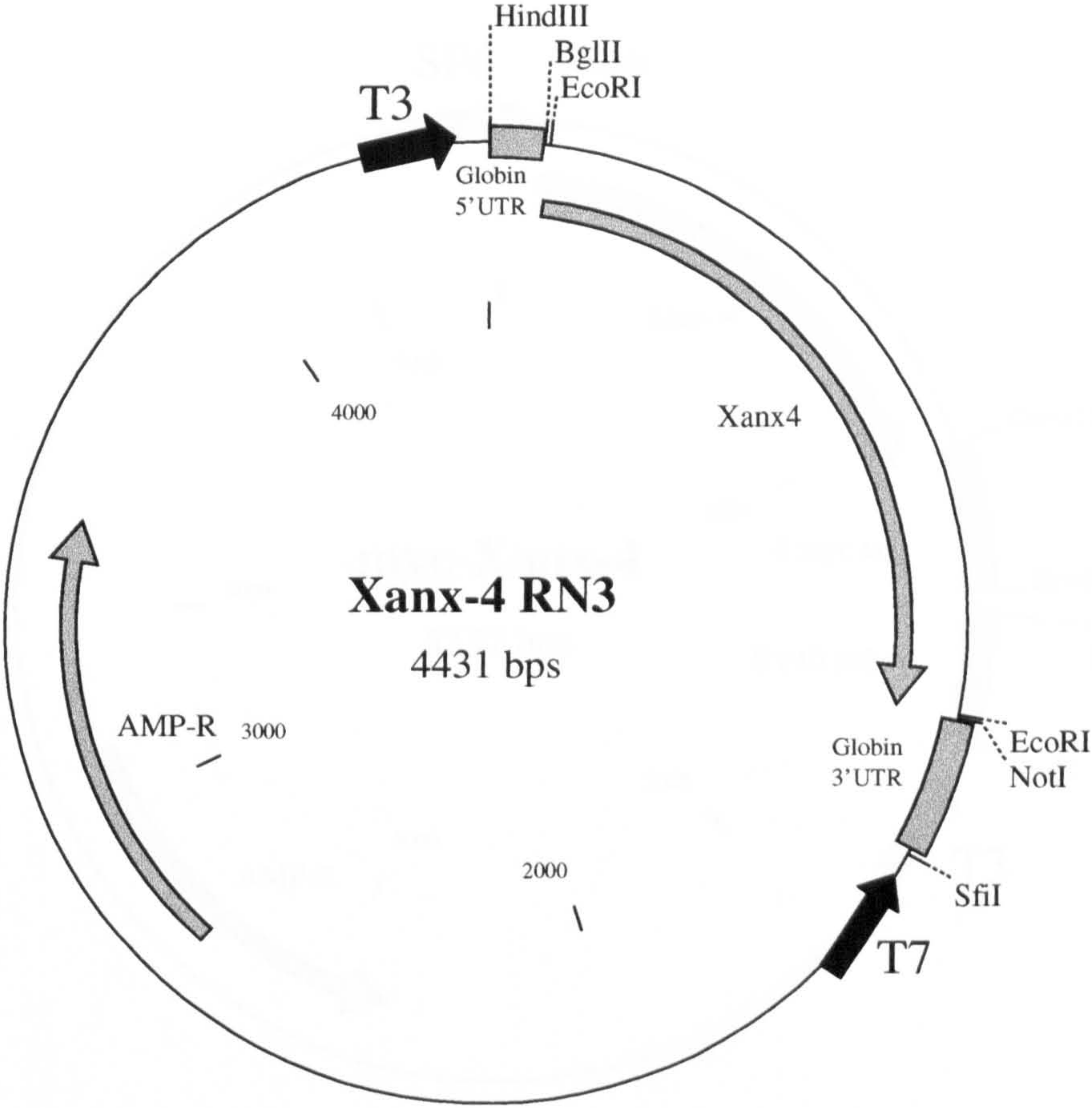
Zhou, A., Paranjape, J. M., Der, S. D., Williams, B. R. G. and Silverman, R. H. (1999). Interferon action in triply deficient mice reveals the existence of alternative antiviral pathways. *Virology* 258, 435-440.

Appendix 1



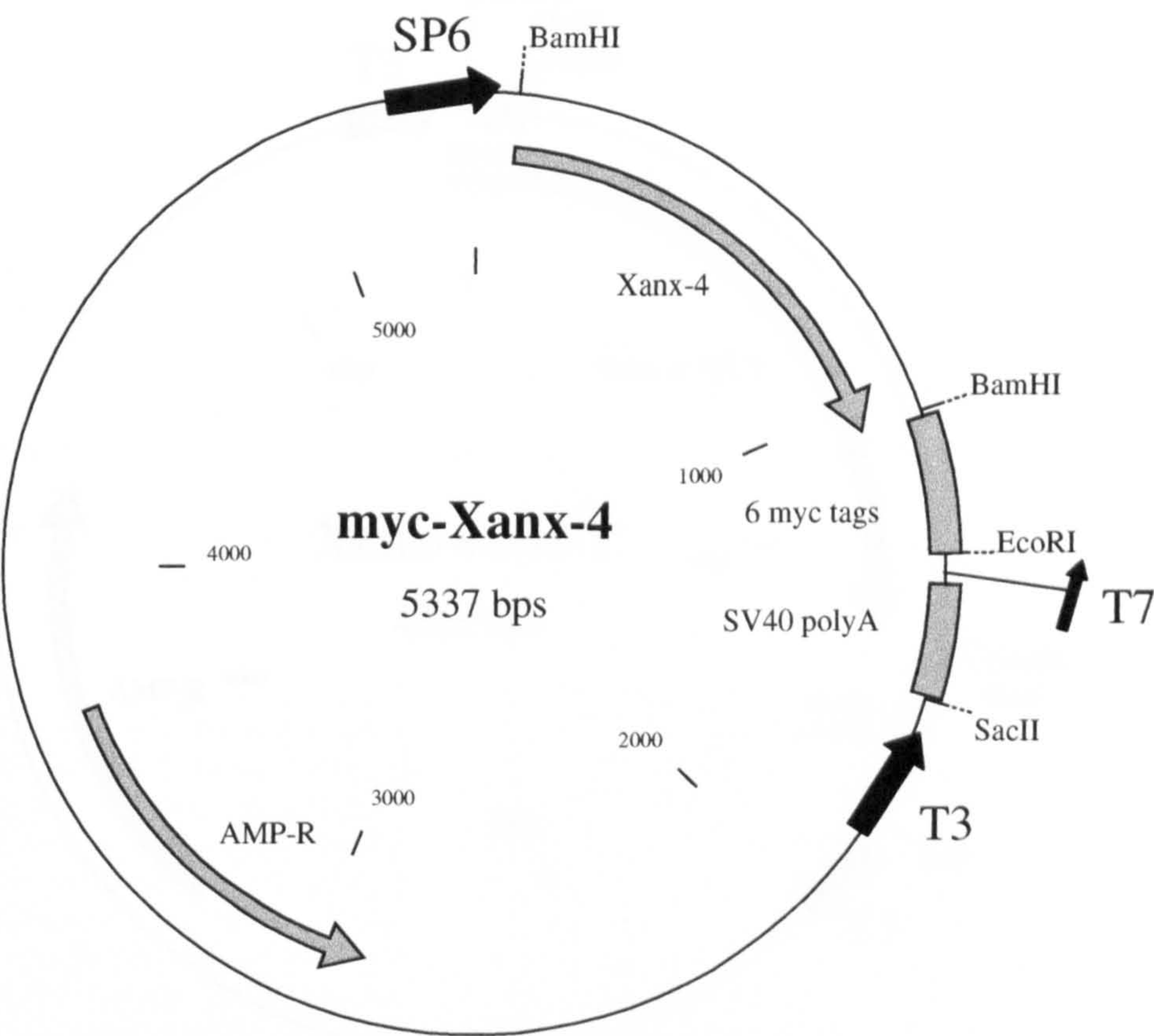
Plasmid: Xanx-4/pGEM-T Easy
Insert: Xanx4 coding region 1.131kb
Vector: pGEM-T Easy 3kb

Appendix 2



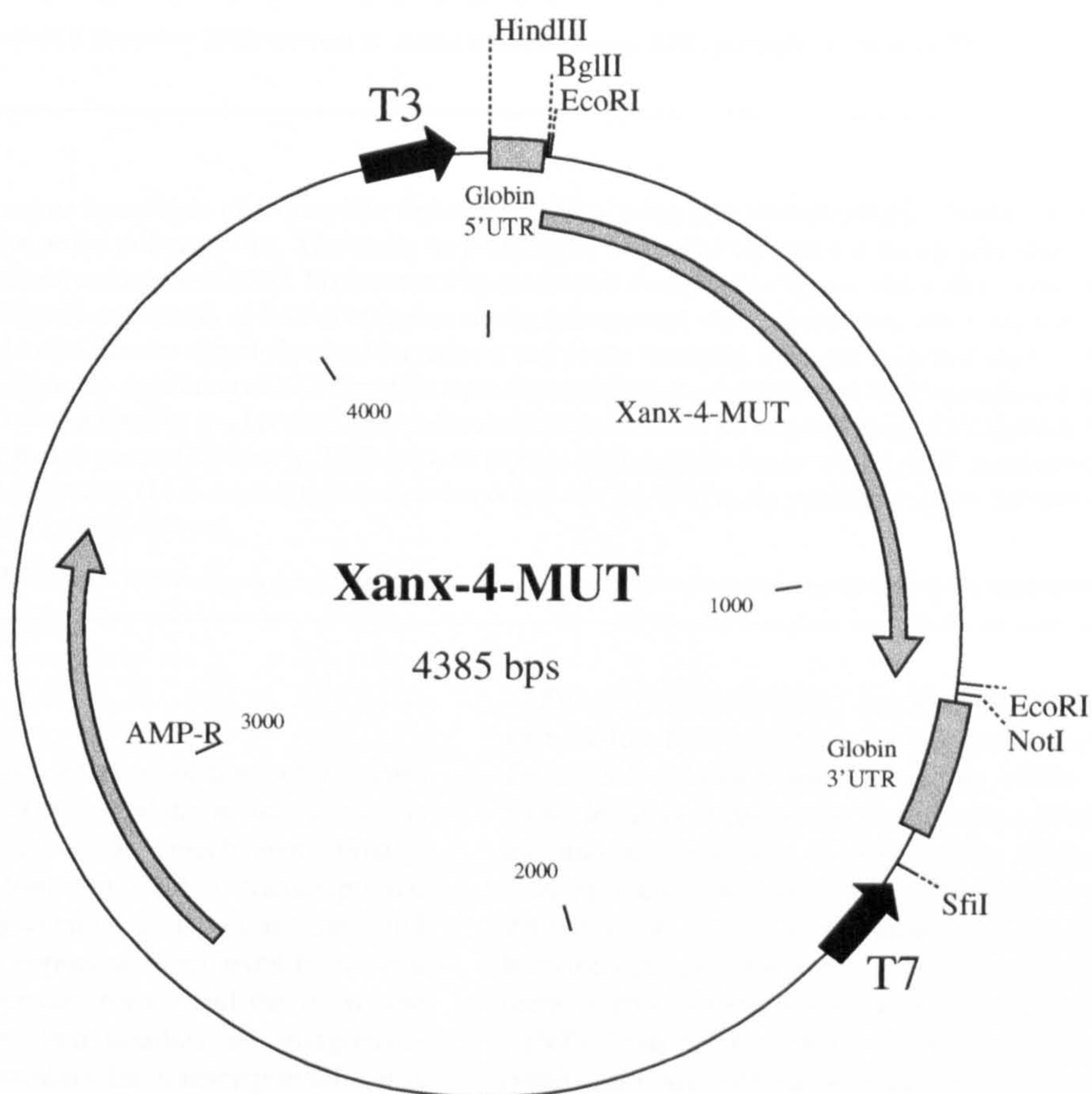
Plasmid: Xanx-4 RN3
Insert: Xanx4 coding region 1.131kb
Vector: RN3 3.3kb

Appendix 3



Plasmid: myc-Xanx-4
Insert: Xanx4 coding region 970bp
Vector: pCS3+MT 4367bp

Appendix 4



Plasmid: Xanx-4-MUT
Insert: Xanx4 coding region 1085bp
Vector: RN3 3.3kb

**CONTAINS
PULLOUTS**

Xenopus Enhancer of Zeste (XEZ); an anteriorly restricted polycomb gene with a role in neural patterning

M.W. Barnett, R.A. Seville, S. Nijjar, R.W. Old, E.A. Jones*

Cell and Molecular Development Group, Department of Biological Sciences, University of Warwick, Coventry CV4 7AL, UK

Received 5 December 2000; received in revised form 18 January 2001; accepted 29 January 2001

Abstract

We have identified the *Xenopus* homologue of *Drosophila Enhancer of Zeste* using a differential display strategy designed to identify genes involved in early anterior neural differentiation. *XEZ* codes for a protein of 748 amino acids that is very highly conserved in evolution and is 96% identical to both human and mouse *EZ(H)2*. In common with most other *Xenopus Pc-G* genes and unlike mammalian *Pc-G* genes, *XEZ* is anteriorly restricted. Zygotic expression of *XEZ* commences during gastrulation, much earlier than other anteriorly localized *Pc-G* genes; expression is restricted to the anterior neural plate and is confined later to the forebrain, eyes and branchial arches. *XEZ* is induced in animal caps overexpressing *noggin*; up-regulation of *XEZ* therefore represents a response to inhibition of BMP signalling in ectodermal cells. We show that the midbrain/hindbrain junction marker *En-2*, and hindbrain marker *Krox-20*, are target genes of *XEZ* and that *XEZ* functions to repress these anteroposterior marker genes. Conversely, *XEZ* does not repress the forebrain marker *Otx-2*. *XEZ* overexpression results in a greatly thickened floor of the forebrain. These results implicate an important role for *XEZ* in the patterning of the nervous system. © 2001 Elsevier Science Ireland Ltd. All rights reserved.

Keywords: *Enhancer of zeste*; *EZ(H)2*; *enx-1*; *Xenopus*; Anterior neural plate; Repression; Polycomb-group; Neural induction; Anteroposterior patterning

1. Introduction

The temporal and spatial regulation of homeobox genes during the development of *Drosophila melanogaster* is thought to take place via a two step mechanism. Firstly, expression is initiated by transiently acting transcriptional activators and repressors (gap and segmentation genes) and secondly, maintenance of expression is achieved by protein products of the *trithorax group* (*trx-G*) and the *polycomb group* (*Pc-G*) genes. These two families act antagonistically; the *trx-G* proteins maintain the transcriptional status of activated homeobox genes and the *Pc-G* proteins maintain inactivated genes in a silent state (reviewed in Orlando and Paro, 1995). *Pc-G* proteins form multimeric protein complexes at transcriptionally inactive chromatin sites and are believed to be responsible for maintaining target genes in a silent state (Franke et al., 1992; DeCamillis et al., 1992; reviewed by Pirrotta, 1997). The mechanism underlying this silencing is unknown although it has been suggested that it could involve the formation of highly condensed chromatin domains similar to heterochromatin (Paro and Hogness, 1991).

Enhancer of zeste [*E(z)*] was first identified as a dominant gain-of-function modifier of the *zeste1-white* interaction in *Drosophila* (Kalisch and Rasmuson, 1974). The X-linked *white* locus is required for pigmentation of the *Drosophila* eye and its expression is repressed by the *z1* allele of the *zeste* (*z*) locus (Jack and Judd, 1979; Gelbart and Wu, 1982; Zachar et al., 1985). *E(z)* mutants also produce homeotic transformations caused by ectopic expression of segment identity genes of the Antennapedia and Bithorax complexes (ANT-C and BX-C). This is a phenotype seen in *Pc* (*polycomb*) gene mutants and was the observation that led to the initial classification of *E(z)* as a *Pc-G* gene (Jones and Gelbart, 1990).

E(Z) has been shown to co-localize with other *Pc-G* proteins, as part of a multimeric protein complex, at many chromosome sites (Carrington and Jones, 1996). In *Drosophila*, *E(Z)* protein has been shown to be required for suppressor of *zeste* (2) [*Su(z)2*] and Posterior sex combs (*psc*) proteins to associate with chromosomes (Rastelli et al., 1993). Furthermore, *E(Z)* protein has been shown to directly interact and co-localise with the *Pc-G* protein, *ESC* (extra sex combs) at multiple chromosomal sites (Tie et al., 1998). The signals that initiate *Pc-G* gene silencing are currently unknown, but are thought to be strongly correlated with the initial transcriptional status of a target gene

* Corresponding author.

E-mail address: eoliver-jones@bio.warwick.ac.uk (E.A. Jones).

when Pc-G silencing is implemented (Poux et al., 1996; Pirrotta, 1997).

In vertebrates, the homologues of E(Z) and ESC, EZ(H)2 (human Enhancer of Zeste homologue 2) and EED (embryonic ectoderm development), are also able to directly interact (Sewalt et al., 1998). In a recent study of the EED/EZ(H)2 protein complex, it was suggested that Pc-G repression of transcription involves histone deacetylation via a direct interaction between EED and histone deacetylase proteins (van der Vlag and Otte, 1999).

Although E(z) has been classified as a Pc-G protein, there is also evidence that it can act as a Trx-G protein (LaJeunesse and Shearn, 1996). Trx-G proteins are characterized by the presence of a SET domain at their C-termini and all E(Z) homologues characterized in *Drosophila* and other species also contain SET domains (Goodrich et al., 1997; Grossniklaus et al., 1998; Jones and Gelbart, 1990; Tschiersch et al., 1994; Holdeman et al., 1998; Hobert et al., 1996a). At different developmental stages and in different tissues E(Z) can be involved in either the activation or repression of a given homeotic selector gene. The SET domain may determine whether E(z) acts as either a *trx-G* or *Pc-G* gene (LaJeunesse and Shearn, 1996).

Enhancer of zeste is highly conserved in evolution and is found in plants, insects, nematodes and vertebrates (Goodrich et al., 1997; Grossniklaus et al., 1998; Jones and Gelbart, 1990; Holdeman et al., 1998; Hobert et al., 1996a). It is interesting that the only *Pc-G* genes identified in *C.elegans* are homologues of E(z) and *esc* (*mes-2* and *mes-6* respectively) (Holdeman et al., 1998; Korf et al., 1998), suggesting that these genes can function independently of other *Pc-G* genes in nematodes, and possibly also function at least partially independently in flies and vertebrates. Two homologues of *Enhancer of zeste* have been isolated in mice and humans, EZ(H)1 (also termed *enx-2*) (Abel et al., 1996; Ogawa et al., 1998) and EZ(H)2 (also termed *enx-1*) (Chen et al., 1996; Hobert et al., 1996a). During *Drosophila* and mouse early embryogenesis expression of *Pc-G* genes is uniform, their spatially defined range of action is thought to be refined by the localized expression of other transcriptional regulators (Paro 1990; Pearce et al., 1992; Alkema et al., 1995). EZ(H)2 is ubiquitously expressed at very early stages of mouse embryogenesis but in later development becomes restricted to organs of haematopoietic activity and the nervous system (Hobert et al., 1996a). It has also been shown that the proto-oncogene product, Vav, which plays a critical role in haematopoietic signal transduction, interacts specifically with EZ(H)2 via the Box 2 and Box 3 regions (Hobert et al., 1996b). Studies in cell lines suggest that EZ(H)2 is necessary for proliferation in haematopoietic cells (Fukuyama et al., 2000). EED and BMI-1 have an antagonistic role in haematopoietic cell proliferation; EED repressing and BMI-1 enhancing proliferation. (Lessard et al., 1999). BMI-1 enhances proliferation by repressing the *ink4a* locus (Jacobs et al., 1999); the gene products of the *ink4a* locus, p16INK4a and p19ARF, antag-

onize the formation and activation of cyclin D-CDK4 complexes (reviewed by Vidal and Koff, 2000). It has been suggested that EZ(H)2 might interfere with the repressive effect of EED by interacting with EED (Fukuyama et al., 2000). Furthermore, EZ(H)1 expression has been shown to be elevated in Neuro-2a cells induced to undergo neuronal differentiation in response to serum deprivation (Ogawa et al., 1998). Less differentiated cells were observed to produce higher levels of EZ(H)1 protein than more highly differentiated cells, suggesting that EZ(H)1 functions at early stages of neuronal differentiation.

Xenopus *Pc-G* genes show more spatially restricted patterns of expression than seen in higher vertebrates and are all expressed in the nervous system (Reijnen et al., 1995; Yoshitake et al., 1999). To date four *Pc-G* genes, *XPolycomb* (*XPc2*), *Xbmi-1*, *Xenopus Polycomblike-1* (*XPcl1*) and *Xenopus Polycomb homologue* (*XPc1*) have been cloned in *Xenopus laevis* (Reijnen et al., 1995; Yoshitake et al., 1999; Strouboulis et al., 1999). All four genes are expressed at high levels maternally and expression declines around the time of gastrulation. It has been shown that *XPc1* mRNA is masked until the blastula stage, being complexed with storage mRNPs, and *XPc1* protein is first detected in embryonic nuclei in gastrula-stage embryos (Strouboulis et al., 1999). Zygotic expression of *XPc2*, *Xbmi-1*, *XPcl1* and *XPc1* begins at stages 15, 19, 19 and 22 respectively. Both *Xbmi-1* and *XPcl1* are restricted to anterior domains of expression; *Xbmi-1* is restricted to the head and anterior spinal cord whilst *XPcl1* is restricted to brain and eyes (Reijnen et al., 1995; Yoshitake et al., 1999). *XPc2* is expressed along the anteroposterior axis in the nervous system and mesoderm (Reijnen et al., 1995) whilst spatial expression data for *XPc1* is not available. Anterior neural defects have been produced by overexpressing *Xenopus* *Pc-G* genes (Yoshitake et al., 1999). Overexpression of *Xbmi-1* or *XPcl1* results in thickening of the roof and floor plates of the forebrain and midbrain and represses expression of *En-2*. *XPc1* has been shown to mediate gene repression but in contrast to EED, this repression has been shown to be independent of histone deacetylase activity (Strouboulis et al., 1999).

In an attempt to isolate novel genes expressed early during neural differentiation, we have exploited the *Xenopus* animal cap system. Anterior neural differentiation is induced in *Xenopus* when BMP-signalling is inhibited by the secreted proteins noggin, chordin, follistatin, Xnr3 or cerberus (Zimmerman et al., 1996; Piccolo et al., 1996; Temura et al., 1998; Hansen et al., 1997; Piccolo et al., 1999). *Xenopus* animal caps can be induced to undergo anterior neural differentiation by dissociating the caps in saline lacking divalent cations, a mechanism that is believed to work by washing away BMPs which promote epidermal differentiation. We have used differential display to screen for genes that are upregulated when animal caps undergo dissociation. RNA fingerprints of animal caps dissociated and processed immediately were compared to RNA finger-

prints from caps dissociated and incubated over a range of times. One of the clones identified was *Xenopus Enhancer of Zeste (XEZ)*. Unlike other known *Xenopus Pc-G* genes, *XEZ* is not expressed maternally. Zygotic expression of *XEZ* commences much earlier than other *Xenopus Pc-G* genes, is restricted to the anterior nervous system, and represents an early response to inhibition of BMP signalling. This study also identifies *En-2* and *Krox-20* as target genes of *XEZ*.

2. Results and discussion

2.1. Cloning and sequence analysis of *Xenopus laevis* Enhancer of zeste (*XEZ*)

In order to identify novel genes expressed early during anterior neural differentiation, we used differential display to screen for genes upregulated when animal caps undergo dissociation. Animal caps were removed from Stage 9 *Xenopus* embryos and disaggregated in Barth's A saline lacking divalent cations. Differential display was performed using cDNA, reverse transcribed from RNA isolated from disaggregated cells, taken at time 0 and samples taken after 3, 12 and 24 h of dissociation. Differentially expressed transcripts were identified by the appearance of new bands following disaggregation. One of the bands identified, termed P1B, was detected after 3 h of dissociation and when cloned was found to be 198bp in length. P1B showed significant similarity to the 3' UTR of *human enhancer of zeste homologue 2 [EZ(H)2]* and was used as a probe to

screen a stage 10.5 *Xenopus laevis* λZAP cDNA library. This resulted in the isolation of a clone of 2772bp (accession number: AF351126) containing an ORF of 2244bp that is 80% identical to human *EZ(H)2*. The clone, termed *XEZ*, codes for a protein of 748 amino acids (Fig. 1A). *XEZ* shows high evolutionary conservation, being overall 96% identical to both mouse and human *EZ(H)2*, 66% identical to both mouse and human *EZ(H)1* and 57% identical to *Drosophila Enhancer of Zeste [E(z)]* at the amino acid level. In common with Enhancer of Zeste homologues in mammals, insects, nematodes and plants, *XEZ* contains a C-terminally located SET domain. *XEZ* also contains the CXC domain (Hobert et al., 1996a), conserved between insects and mammals in which the spacing of 17 cysteine residues is conserved (Fig. 1B).

2.2. Temporal expression profile of *XEZ*

We have performed RT-PCR to show the temporal expression profile of *XEZ* (Fig. 2). Levels of *XEZ* mRNA were analysed in the unfertilized egg and at a number of embryonic stages between 32-cell stage and stage 41 using *XEZ* gene specific primers. In contrast to *XPolycomb*, *Xbmi-1* and *Xenopus Polycomb-like (XPcl1)* which are expressed at high levels maternally (Reijnen et al., 1995; Yoshitake et al., 1999), maternal expression of *XEZ* was not detected. Zygotic expression of *XEZ* commences at low levels in the late blastula, increasing at mid- to late-gastrula stages, peaking in the early neurula and is still detectable at stage 41. The onset of zygotic *XEZ* expression is much earlier

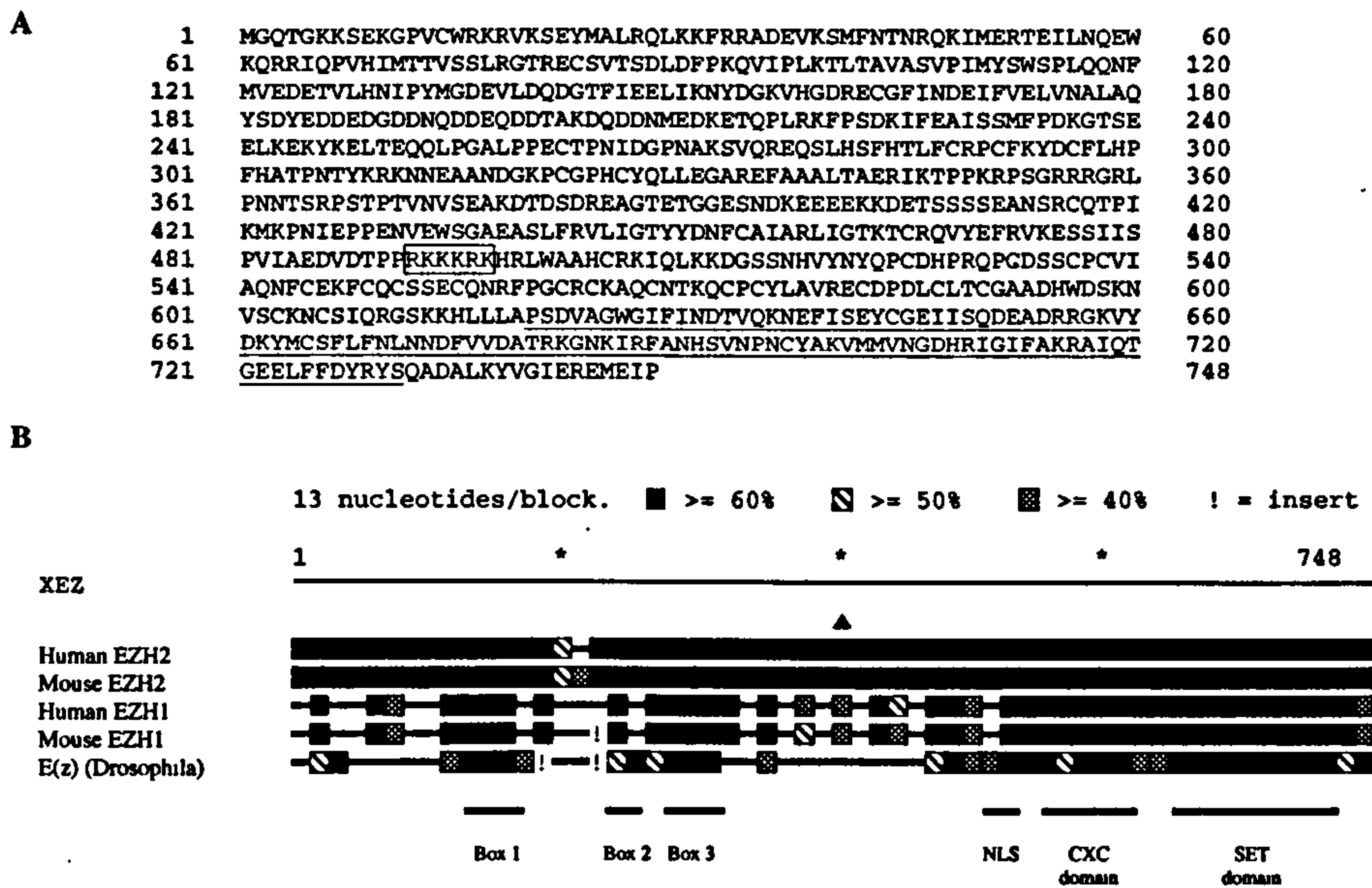


Fig. 1. (A) Predicted polypeptide sequence of *XEZ* (ORF 2244bp) 748 amino acids. The nuclear localisation sequence (NLS) is boxed and the SET domain is underlined. (B) Comparison of *XEZ* protein sequence with mouse, human and *Drosophila* homologues. Human *EZ(H)2* and *EZ(H)1*, mouse *EZ(H)2* and *EZ(H)1* and *Drosophila E(Z)* were compared to *XEZ* protein sequence using Align Plus Version 3.0. Each block represents 13 amino acids and identity to *XEZ* is shown as greater than 60%, greater than 50%, greater than 40% or less than 40% (shown as line). Box 2 and 3 are part of the region which interacts with the Vav proto-oncogene product. NLS is the nuclear localization sequence. CXC domain is found in *E(Z)* homologues and consists of a cysteine-rich domain in which the spacing of 17 cysteine residues is conserved between insects and mammals. The C-terminally located SET domain is conserved between Trx-G proteins.

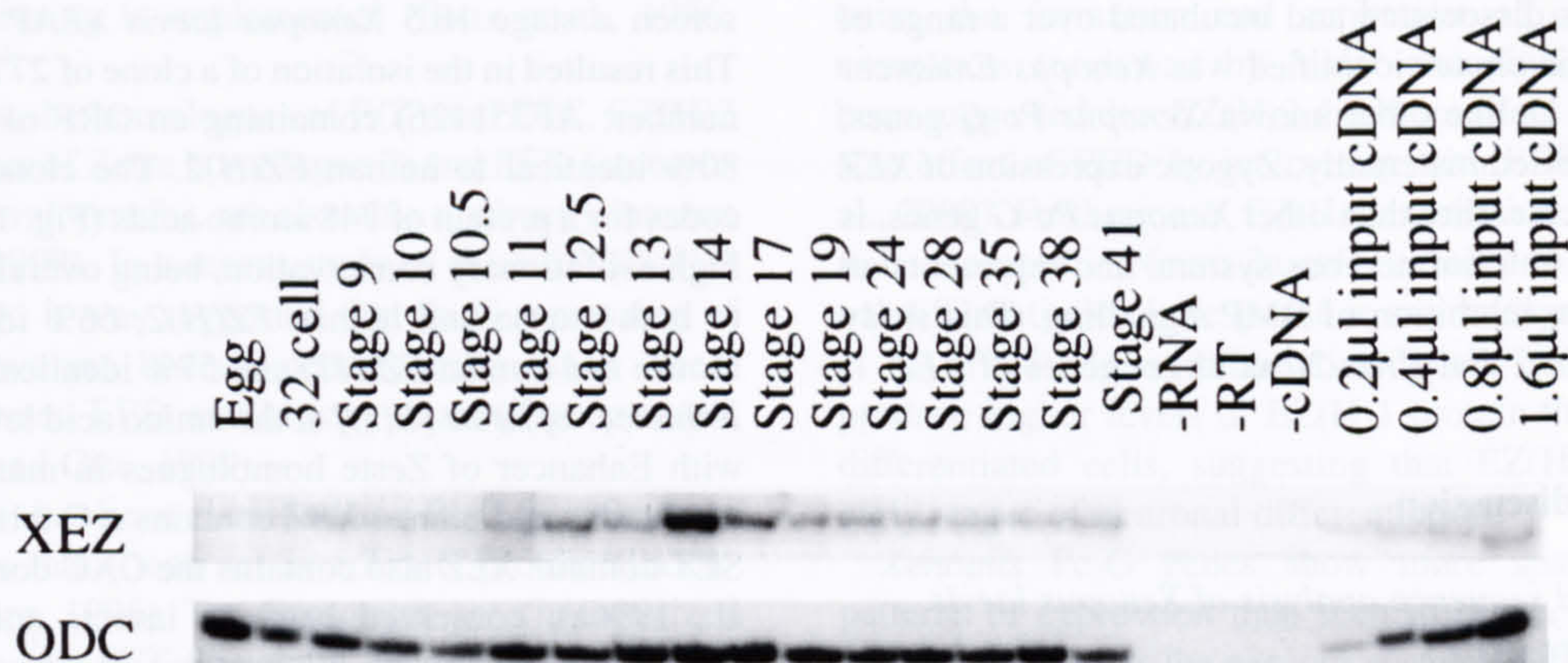


Fig. 2. Temporal expression profile of *XEZ*. RT-PCR showing expression pattern of *XEZ* transcripts in *Xenopus laevis* unfertilised egg and embryo stages. Significant maternal expression is not detected. Zygotic expression of *XEZ* commences at low levels in the late blastula stages, increasing at mid to late gastrula stages, peaking in the early neurula stages and is still detectable at stage 41. Stage 41 cDNA is used for the linearity control and ODC is used as a loading control.

than other *Xenopus* *Pc-G* genes; zygotic expression of *XPolycomb* is first detected at early neurula stage (Stage 15) whereas *Xbmi-1* and *XPcll* are first detected in the late neurula embryo (Stage 19) (Reijnen et al., 1995; Yoshitake et al., 1999).

2.3. Expression of *XEZ* is restricted to the anterior nervous system

Wholemount in situ hybridization shows that expression of *XEZ* is restricted to the anterior nervous system from stage 14 to 27 (Fig. 3A–C). In the stage 20 and 27 embryos this anterior neural expression appears graded, with the

strongest expression in the most anterior regions (Fig. 3B,C). *XPcll* and *Xbmi-1* are similarly both restricted to anterior domains of expression at tailbud stages, whereas *Xpolycomb* is expressed along the entire anteroposterior axis (Reijnen et al., 1995; Yoshitake et al., 1999). Expression of *XEZ* later becomes restricted to the forebrain, eye and branchial arches in the Stage 35 tadpole (Fig. 3D). *XEZ* expression is not detected in the midbrain and hindbrain. In contrast, *XPcll* is expressed in the forebrain, midbrain, hindbrain, anterior spinal cord and eye at Stage 33 (Yoshitake et al., 1999). Expression of *XEZ* is highest in the first branchial arch, less in the second arch and is greatly reduced in the third and fourth arches.

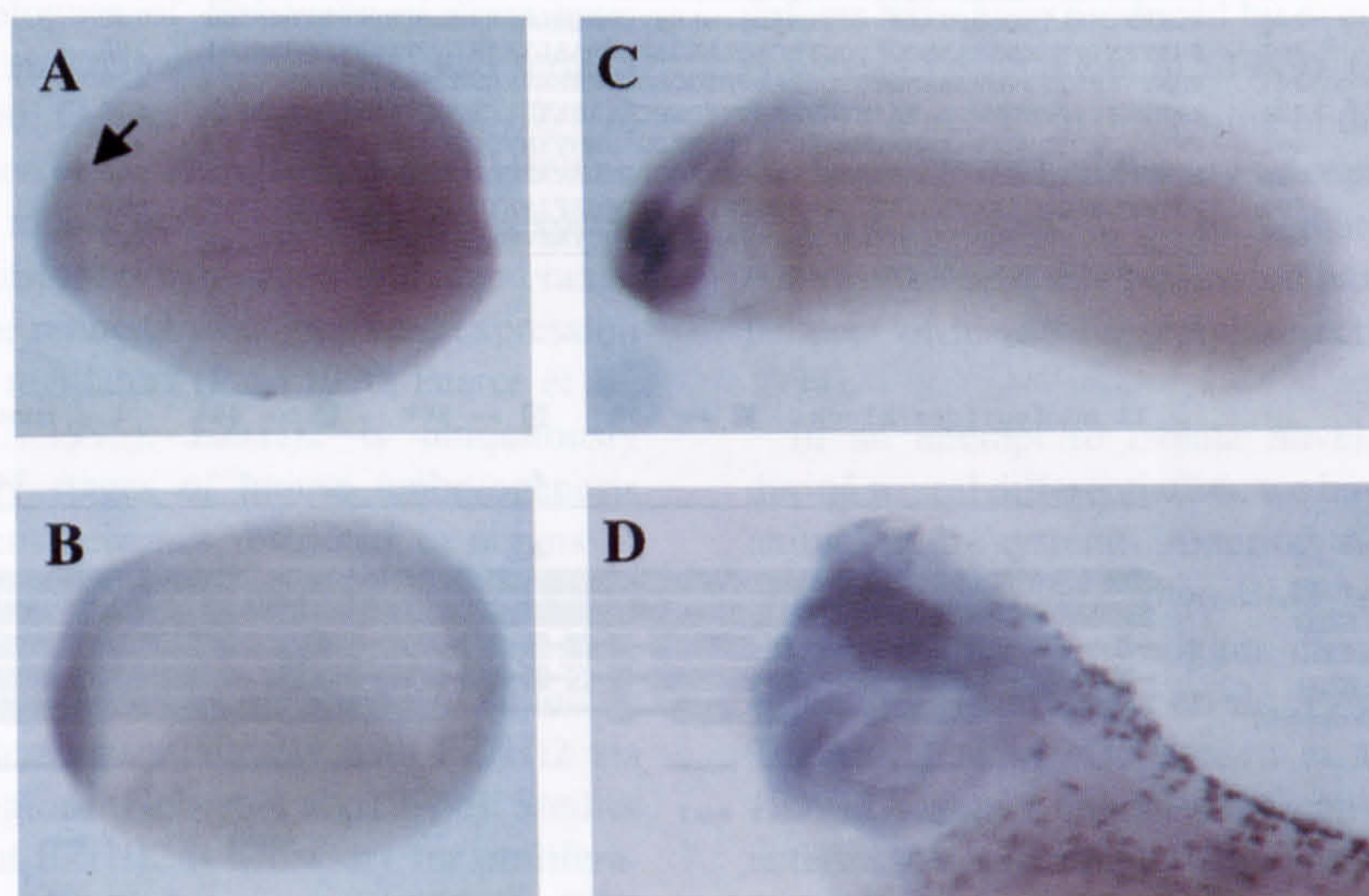


Fig. 3. Wholemount in situ hybridisation of *XEZ*. Wholemount in situ hybridisation of *XEZ* DIG labelled antisense RNA probe shows that expression of *XEZ* is restricted to the anterior nervous system. (A) Stage 14 embryo expression is restricted to the anterior nervous system (indicated by arrow) (B) Stage 20 embryo and (C) Stage 27 embryo, the *XEZ* transcripts are detected in the anterior nervous system. In (B) and (C) the expression pattern appears to be graded with the strongest expression in the most anterior regions. (D) Stage 35 embryo shows that expression of *XEZ* later becomes restricted to the forebrain, eye and branchial arches. The *XEZ* expression is highest in the first branchial arch, less in the second and is greatly reduced in the third and fourth arches. The sense probe control showed no staining pattern (data not shown).

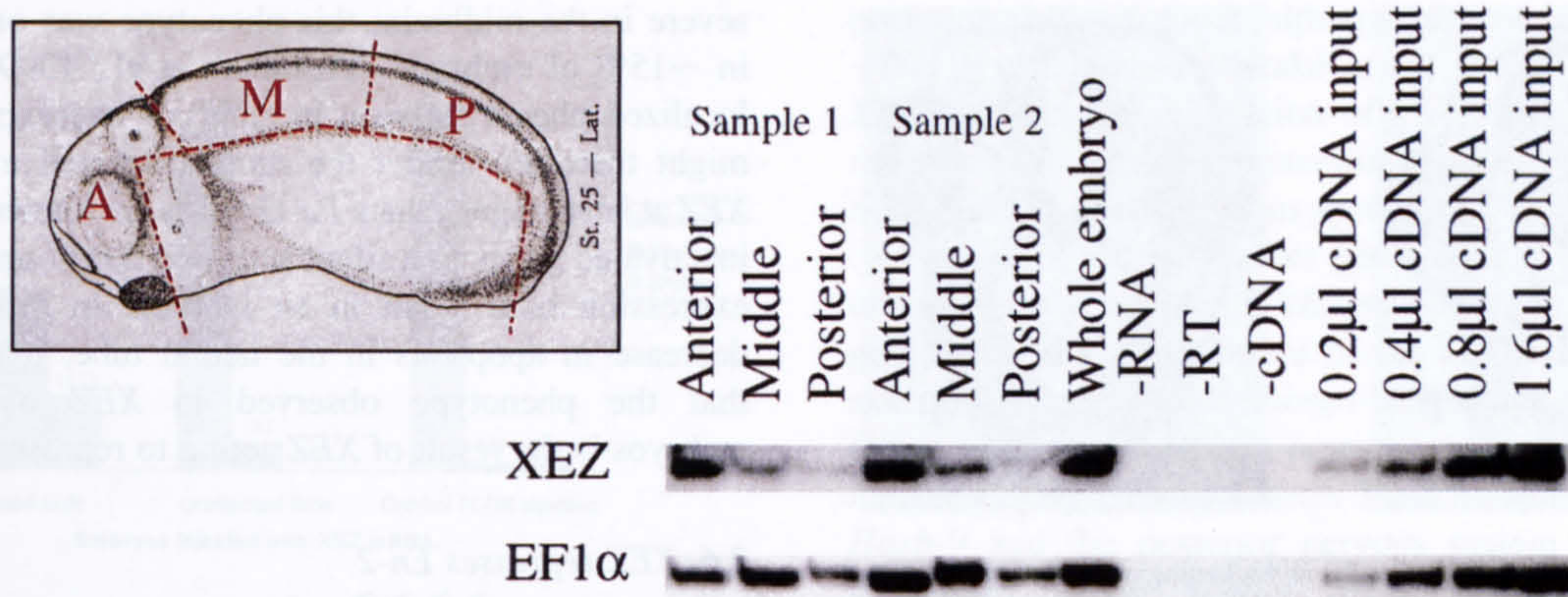


Fig. 4. *XEZ* expression is anteriorly restricted. Dissection series of stage 25 *Xenopus laevis* embryos analysed by RT-PCR. Stage 25 embryos were dissected as shown in the insert picture into three equivalent axial pieces, A, anterior; M, middle; P, posterior; the endoderm was removed. Duplicate samples 1 and 2 both consisted of 5 embryos. Analysis shows the expression of *XEZ* is highest in the anterior nervous system, is reduced in the middle section and is barely detectable in the posterior in both dissected embryo pools. Whole embryo control cDNA at stage 25 was used for the linearity and *EF1α* was used as a loading control. Since the sections of neural tissue were equal in terms of regional identity, but only approximately equivalent in terms of amount of biological material, it is not reasonable to equalize loading of cDNA between samples (as shown by the *EF1α* signal).

The spatial expression of *XEZ* was further analysed by dissecting the nervous system from stage 25 embryos and cutting into three equivalent sized pieces (Anterior, Middle and Posterior). RT-PCR analysis showed that expression of *XEZ* is highest in the anterior tissue, is reduced in the middle section and is barely detectable in the posterior tissue (Fig. 4), supporting the observation that expression of *XEZ* is anteriorly restricted and graded posteriorly.

2.4. *XEZ* is induced by *noggin*

Since *XEZ* was isolated from a differential screen that selected for genes upregulated when BMP signalling is removed from animal cap cells, the expression of *XEZ* was analysed in animal caps from embryos injected with *noggin* mRNA which induces anterior neural markers. One-cell stage embryos were injected with approximately

0.8 ng *noggin* mRNA and cultured to stage 9. Animal caps were taken and cultured to Stage 13, 20, 28 and 32. RT-PCR analysis showed that at stage 13, *XEZ* expression is highly induced in *noggin* injected caps compared to a much lower level of expression in control caps (Fig. 5). However, the high level of expression is not maintained and *XEZ* expression is only slightly increased in animal caps overexpressing *noggin* analysed at Stage 20, 28 and 32.

2.5. Overexpression of *XEZ* results in thickening of the floor plate in the forebrain

Injection of an RNA into *Xenopus* embryos is often used to assess the developmental consequences due to overexpression of a gene. The function of *XEZ* in the anterior nervous system was investigated by targeted injection of *XEZ* mRNA. Approximately 0.4 ng of *XEZ* mRNA was

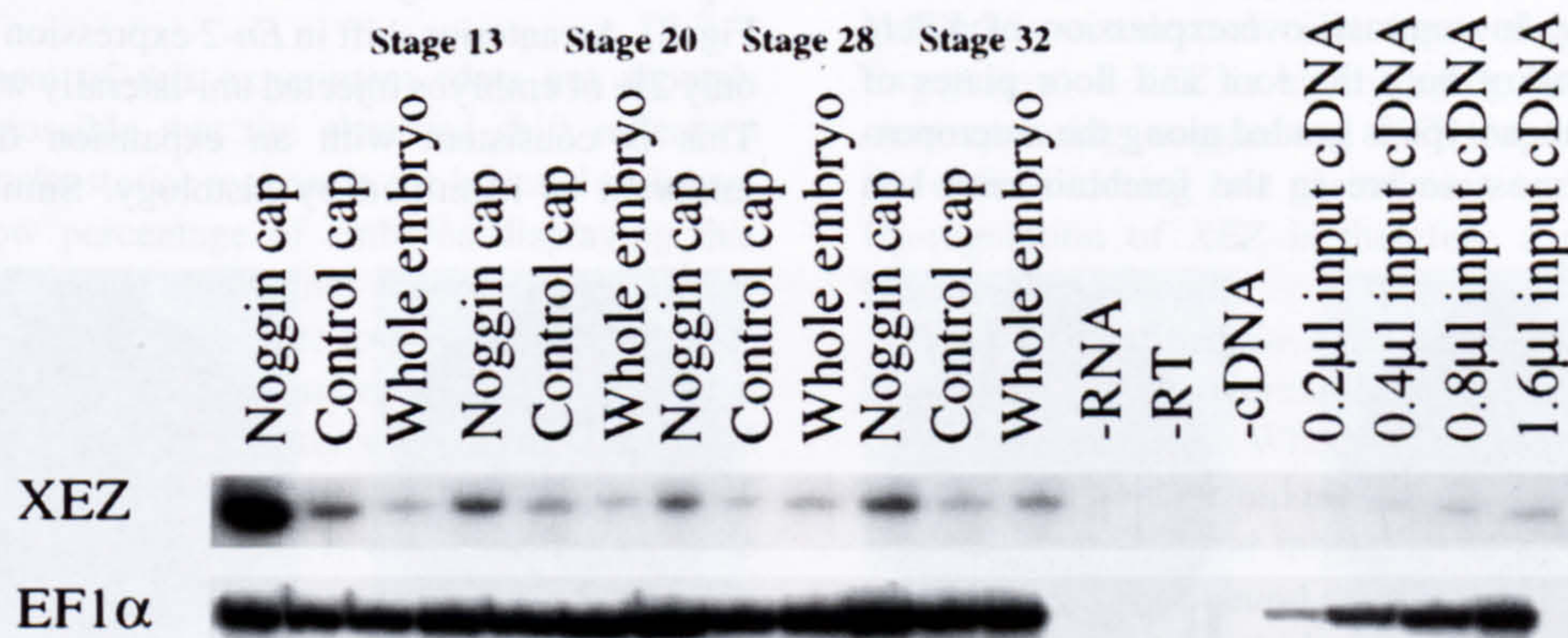


Fig. 5. *XEZ* is induced by *noggin*. RT-PCR showing induction of *XEZ* in *noggin*-injected animal caps. Animal caps were taken from stage 9 embryos previously injected at the 1 cell stage with *noggin* mRNA. The animal caps were cultured to stage 13, 20, 28 and 32. RT-PCR analysis shows that at stage 13 *XEZ* expression is highly induced in *noggin* animal caps compared to a much lower level of expression in control animal caps. However, this high level of expression is not maintained and *XEZ* expression is only slightly higher in animal caps overexpressing *noggin* compared to control caps at stages 20, 28 and 32. Stage 32 whole embryo cDNA was used as input for the linearity and *EF1α* was used as a loading control.

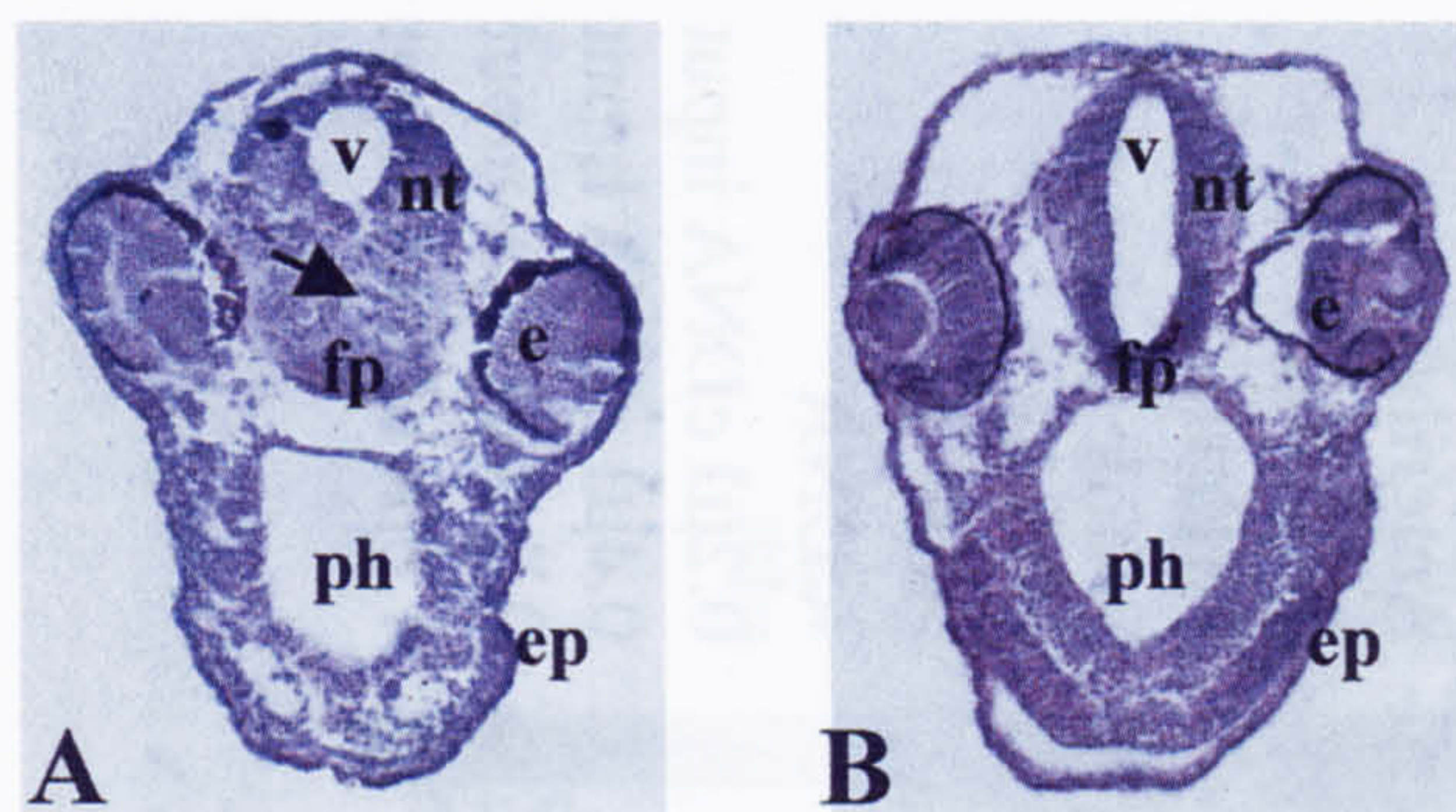


Fig. 6. Overexpression of *XEZ* results in thickening of the floor plate region in the forebrain of in *Xenopus laevis* embryos. Embryos were injected with *XEZ* mRNA and cultured to stage 37. The embryos were then wax embedded, sectioned at 6 μ m and stained with eosin and hematoxylin. (A) Section shows thickening of the floor of the midbrain (arrow) compared to (B) a normal control embryo. v, ventricle; nt, neural tube; fp, floor plate; ph, pharynx; ep, epidermis; e, eye.

injected into both dorsal blastomeres (total of 0.8 ng) at the 4-cell stage and the resulting tadpoles were inspected for morphological alterations compared to uninjected controls. Apart from a slight uneven appearance to the epidermis, no obvious gross phenotype alteration was noted. The tadpoles were then sectioned at stage 37 to examine the effects on the morphology of the internal structure, and in particular of the nervous system being the main region of *XEZ* gene expression. Tadpoles consistently showed thickening of the floor plate region in the midbrain (Fig. 6) (phenotype observed in 12/12 specimens, in randomly chosen embryos from two independent experiments). Thickening of the floor plate region appeared to occur at the expense of the ventricle, which may possibly be an expansion of the sonic hedgehog expressing floor plate domain. Sections through the nervous system of the tadpoles at different anterior/posterior registers were inspected. Apart from the apparent thickening in the floor plate region the phenotype of the tadpoles in section appeared normal. Control injected embryos showed no such thickening. In contrast, overexpression of *XPc11* results in thickening of both the roof and floor plates of the brain and this phenotype is graded along the anteroposterior axis, being most severe in the forebrain and less

severe in the midbrain; this phenotype was only observed in ~15% of embryos (Yoshitake et al., 1999). The more localized phenotype seen in embryos overexpressing *XEZ* might therefore reflect the more restricted expression of *XEZ* at later stages. Since *Pc-G* genes are known to maintain inactivated genes in a silent state and *XPc11* and *XEZ* overexpression both result in an increase in proliferation or decrease in apoptosis in the neural tube, it seems likely that the phenotype observed in *XEZ* overexpressing embryos is the result of *XEZ* acting to repress target genes.

2.6. *XEZ* represses *En-2*

Having observed phenotypic effects of overexpression of *XEZ* in the midbrain region, the midbrain-hindbrain junction marker *En-2* was chosen to further analyse the role of *XEZ* in the anterior nervous system and to assess the ability of *XEZ* to affect the expression of genes that mark the pattern of the anteroposterior neural axis. Uni-lateral injection was decided upon in order to compare left side versus right side. Two-cell stage embryos were co-injected uni-laterally with 0.8ng *XEZ* and FLDX to mark the injected side. Embryos were cultured to late neurula stage (Stage 19) and the injected side recorded. Sorted embryos were then fixed and subjected to wholemount in situ hybridization with the midbrain-hindbrain junction marker *En-2*. Repression of expression of *En-2* on the side injected with *XEZ* mRNA was seen in 48% of embryos (Figs. 7A,C, and 8A,B). Occasional embryos showed complete loss of the *En-2* expression on the injected side (Fig. 7A). The level of *En-2* expression was scored as repressed on the injected side when it was deemed as being outside the range of normal variation as assessed by analysis of control embryos. In contrast, repression of *En-2* on the injected side was observed in only 2% of embryos injected uni-laterally with the fluorescent tracer FLDX alone. Uni-lateral overexpression of *XEZ* also resulted in an anterior shift of *En-2* expression on the injected side in 20% of embryos (Fig. 7B, Fig. 8). An anterior shift in *En-2* expression was observed in only 2% of embryos injected uni-laterally with FLDX alone. This is consistent with an expansion of tissue in the midbrain as identified by histology. Similar results were

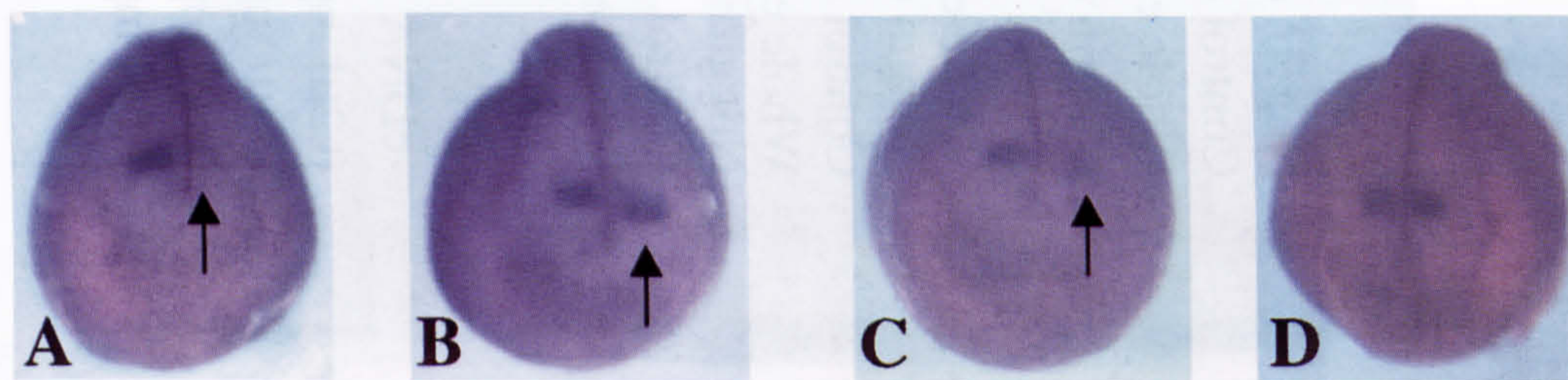


Fig. 7. Repression of *En-2* by *XEZ*. Embryos were uni-laterally co-injected at the two cell stage with *XEZ* mRNA and FLDX. The FLDX was used as a marker for the injected side. The embryos were cultured to stage 19 and subjected to wholemount in situ hybridisation using an *En-2* antisense RNA DIG-labelled probe. The injected side is indicated by an arrow. (A) Complete ablation of *En-2* expression on *XEZ* injected side. (B) Anterior shift of *En-2* expression on *XEZ* injected side. (C) Repression of *En-2* expression on *XEZ* injected side. (D) Normal control. The *En-2* sense control probe showed no staining pattern (data not shown).

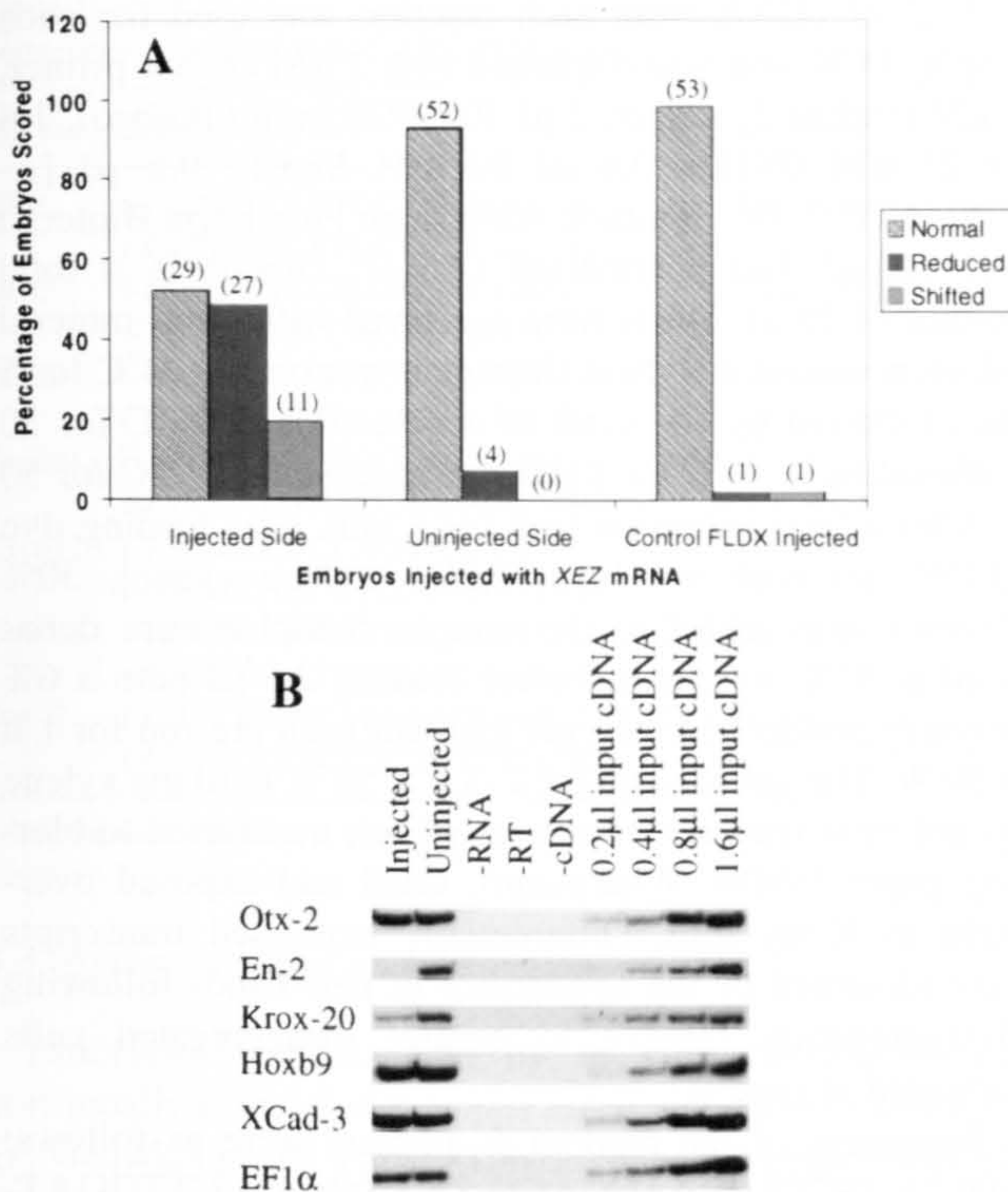


Fig. 8. *XEZ* represses *En-2*. (A) *Xenopus laevis* embryos were uni-laterally co-injected at the 2-cell stage with *XEZ*mRNA and FLDX. The embryos were cultured to stage 19 and subjected to wholemount in situ hybridisation using the midbrain-hindbrain junction marker *En-2* antisense RNA probe. The embryos were scored as having reduced expression of *En-2* when the level of *En-2* staining was lower (or absent) than control embryo normal variation. The embryos showing reduced-expression were also scored for any shift in the anterior or posterior register of the *En-2* marker staining relative to the uninjected side. Numbers in brackets are actual numerical scores. (B) *XEZ* represses *En-2*, *Krox-20* but not other neural markers. Embryos were injected at the 1 cell stage with *XEZ*mRNA, cultured to stage 19 and subjected to RT-PCR. The figure shows that the expression of *En-2* and *Krox-20* are repressed compared to uninjected control, but other neural markers are not affected. *EF1α* was used as a loading control and the uninjected sample used for linearity input cDNA.

obtained on repeat of this experiment (data not shown). Although it is possible that the observed shift reflects a change in anterior/posterior register in the injected embryos, the relatively low percentage of embryos displaying this phenotype suggests that this is not the case. The effects observed are more likely to be due to mechanical perturbation caused by increased cell numbers in this region. If a change in anterior/posterior register were to occur it would be expected to result in a posterior shift as the domain of expression of *XEZ* was increased. It was interesting to note that, on comparison of left side versus right side in respect to the gross phenotype, the injected side tended to appear somewhat enlarged and the epidermis seemed rather uneven and disorganised. This was not readily apparent in the sectioned embryos. Overexpression of *Pcll* also results in repression of *En-2*, but was only observed in 15% of embryos. In contrast, overexpression of *Pcll* results in a

posterior shift of *En-2*, although this was only seen in ~8% of embryos (Yoshitake et al., 1999). The ability of *XEZ* to affect the expression of *En-2* more strongly may reflect the much earlier expression of *XEZ* in the more anterior elements of the nervous system.

A range of neural marker genes was chosen to further investigate the ability of *XEZ* to affect the expression of genes that mark the pattern of the anteroposterior neural axis. The marker genes chosen were the forebrain marker *Otx-2*, midbrain-hindbrain junction marker *En-2*, hindbrain marker *Krox-20* (rhombomeres 3 and 5), spinal cord marker *Hoxb-9* and the posterior nervous system and posterior mesoderm marker *Xcad-3*. 1-cell stage embryos were injected with 0.8 ng *XEZ*mRNA, cultured to stage 19 and subjected to RT-PCR. The results show that *XEZ* does indeed repress *En-2* expression but also shows a repression of *Krox-20*. Other marker genes were not affected (Fig. 8B). A further round of in situ hybridization was then carried out on stage 19 embryos which had been uni-laterally co-injected with 0.8 ng *XEZ* mRNA and FLDX (as before), sorted and probed with the neural marker genes. No obvious effects on the level of expression or the anteroposterior specification of *Otx-2*, *Hoxb-9* and *Xcad-3* were observed (data not shown).

2.7. Summary

We have cloned *XEZ*, the *Xenopus* homologue of *Drosophila Enhancer of Zeste* by a differential display strategy designed to identify genes involved in early anterior neural differentiation. *XEZ* is very highly conserved between *Xenopus* and mammals being 96% identical at the amino acid level to both mouse and human *EZ(H)2*. Unlike in mammals, where *EZ(H)2* and other *Pc-G* genes exhibit ubiquitous expression during early embryogenesis, *XEZ* is restricted to the anterior neural plate and expression is later restricted to the forebrain, eyes and branchial arches. *XEZ* was cloned using a strategy designed to identify genes upregulated in ectodermal cells deprived of BMP signalling. Expression of *XEZ* is highly upregulated in animal caps overexpressing *noggin* and *XEZ* expression increases in the embryo during late gastrulation and early neurulation. Up-regulation of *XEZ* is therefore a response to neural induction in *Xenopus*.

We have identified *En-2* and *Krox-20* as targets of *XEZ* by demonstrating that overexpression of *XEZ* results in repression of these genes. Whether this repression is direct or indirect is currently unknown. Interestingly, *Otx-2* is not repressed by *XEZ* and might indicate that the function of *XEZ* in the anterior neural plate is to inhibit posteriorization of anterior neural tissue. Anterior neuronal differentiation is normally delayed in comparison to posterior neuronal differentiation (Papalopulu and Kintner, 1996) and *XEZ* might be involved in the mechanism that facilitates this delay of differentiation. Furthermore, overexpression of *XEZ* results in thickening of the floor plate region of the

forebrain, a phenotype that may be caused by *XEZ* enhancing proliferation in the anterior nervous system. Since *EZ(H)2* is necessary for proliferation in haematopoietic cells (Fukuyama et al., 2000) and *EED* represses proliferation in haematopoiesis, it would be interesting to identify *Xenopus EED* and characterize its role in neural development. Further work will ascertain whether overexpression of *XEZ* enhances proliferation or decreases apoptosis in the forebrain, and the target genes involved in these processes will be identified.

3. Experimental procedures

3.1. Differential display

Animal caps were removed from stage 9 *Xenopus laevis* embryos by manual dissection and washed three times in calcium and magnesium free Barth X (CFMF), and disaggregated by placing on polyHEMA plates in CFMF. Undisaggregated pigmented cells were removed, only fully disaggregated pigmented and inner epidermal cells were used for sample collection. The first sample was taken after 30 min when the cells were fully disaggregated, and thereafter +3, +12 and +24 h. Total RNA was prepared as described below. 150 µl XTB buffer (300 mM NaCl, 20 mM Tris, pH 7.5, 1 mM EDTA, pH 8, 1% SDS) and 45 µg proteinase K (Boehringer) was added to each sample and cells, homogenized by pipetting, were then incubated at 37°C for 15 min. Five micrograms glycogen was added, samples were phenol extracted and ethanol precipitated at –20°C for 30 min. Following centrifugation for 20 min in a benchtop microcentrifuge, dried pellets were taken up in 30 µl SP6 transcription buffer (Gibco) containing 10U DNase I (Boehringer) and 10U placental RNase Inhibitor (Boehringer). Samples were incubated at 37°C for 15 min, 120 µl of XTB buffer containing 45 µg proteinase K was added and incubated at 37°C for an additional 20 min. Following phenol extraction and phenol/chloroform extraction, samples were ethanol precipitated at room temperature for no more than 30 min. After centrifugation in benchtop microcentrifuge for 20 min at 4°C, pellets were washed with 70% ethanol, dried and resuspended in 10 µl RNase-free H₂O. A small portion of each sample was used for spectrophotometric quantification, and 2 µg total RNA used to synthesize first-strand cDNA. Total RNA was combined with 2 µM of the anchor primer [(dT)12A, (dT)12C or (dT)12G] in a total volume of 11.4 µl and incubated at 70°C for 10 min, followed by chilling on ice. After addition of 4 µl first strand synthesis buffer (Gibco), 2 µl 100 mM DTT and 1.6 µl dNTPs, samples were incubated at 37°C for 10 min. 1 µl Superscript II reverse transcriptase (Gibco) was added, followed by incubation at 37°C for 1 hour. Samples were heated at 95°C for 5 min, placed on ice for 2 min and stored at –20°C before use in differential display PCR.

1 µl of cDNA from each reaction was used for each display PCR, and was combined with 2 µM anchor primer, 2 µM random 5' primer, 2 µl 10× PCR buffer (Gibco), 1.6 µl 25 µM dNTPs, 0.6 µl 50 mM MgCl₂, 0.5 µl [α-³⁵S]dATP (1000 Ci/mmol; Amersham Pharmacia Biotech) and 0.5 µl Taq polymerase (2.5 U; Gibco) in a total volume of 20 µl. Tubes were overlaid with 30 µl mineral oil, incubated in a Hybaid Omnigene machine at 94°C for 5 min, followed by 40 cycles of denaturation at 94°C for 30 s, annealing at 40°C for 2 min and extension at 72°C for 30 s. After a final extension step for 5 min, 4 µl loading dye (0.25% bromophenol blue, 0.25% xylene cyanol, 30% glycerol) was added to the sample. Samples were denatured at 95°C for 5 mins before loading 2.5 µl onto a 6% polyacrylamide/7 M urea gel that had been pre-run for 1 h at 50 W. The gel was run for 2–3 h at 50 W until the xylene cyanol front reached the bottom of gel, transferred to blotting paper (3MM; Whatmann), dried and exposed overnight to X-ray film. Differentially expressed transcripts were identified by the appearance of new bands following disaggregation relative to control disaggregated cells harvested at time 0.

Sequences of the random 5' primers were as follows: DD1: 5'-GCTTACAACGAGG-3'; DD2: 5'-GCTTGGATTGGTC-3'; DD3: 5'-GCTCTTTCTACCC-3'; DD4: 5'-GCTTTTGGCTCC-3'; DD5: 5'-GCTGGAACCAATC-3'; DD6: 5'-GCTAAACTCCGTC-3'; DD7: GCTTCGATACAGG-3'; DD8: 5'-GCTTGGTAAAGGG-3'; DD9: 5'-GCTTCGGTCATAG-3'; DD10: 5'-GCTGGTACTAAGG-3'; DD11: 5'-GCTTACCTAAGCG-3'; and DD12: 5'-GCTCTGCTTGATG-3'.

Gel regions corresponding to bands representing candidate cDNAs were excised using sterile scalpels and transferred to sterile 0.5 ml microcentrifuge tubes. 100 µl H₂O was added, followed by heating to 95°C for 20 min. Samples were ethanol precipitated at –70°C for 20 min, centrifuged in a benchtop microcentrifuge, pellets washed with 70% ethanol, dried and resuspended in 10 µl H₂O.

PCR products recovered from the gel were cloned using the pGEM-T Vector system (Promega).

3.2. Library screening and sequencing

Whole embryo stage 10.5 λZAP II library was plated at a density of 2.5×10^5 plaques on 25 cm² plates and duplicate plaque lifts taken on Hybond N+ (Amersham) nylon filters. Probe was made by random-primed synthesis (Feinberg and Vogelstein, 1984), using the P1B fragment indicated in the text, and hybridized in 0.1% SDS, 5× SSC, 0.1% BSA, 0.1% poly vinyl-pyrrolidone, 0.1% Ficoll (type 400) at 62°C. The first wash was performed at 62°C in 2× SSC, 0.1% SDS, followed by washes in 1× SSC/0.1% SDS, 0.5× SSC/0.1% SDS and 0.2× SSC/0.1% SDS. The *XEZ* clone was excised from λZAP II vector and sequencing was carried out on both strands using an Applied Biosystems 373A instrument.

Table 1
Sequences of primers used for RT-PCR analysis^a

| Marker | Sequence (5' to 3') | Reference |
|--------------|--|----------------------|
| XEZ | f-ACACTCACTGCTGTAGCCTC r-CCTGCTCATCGTCTTGATTG | This work |
| ODC | f-GGAGCTGCAAGTTTGGAGA r-TCAGTTGCCAGTGTGGTC | Bassez et al., 1990 |
| EFl α | f-CAGATTGGTGTGCTGGATATGC r-CACTGCCTTGATGACTCCTA | Mohun et al., 1989 |
| Hoxb9 | f-TACTTACGGGCTTGGCTGGA r-AGCGTGTAACCAGTGGCTG | Wright et al., 1990 |
| Krox-20 | f-AACCGCCCCAGTAAGACC r-GTGTCAGCCTGTCCTGTTAG | Bradley et al., 1993 |
| Xcad-3 | f-ACCGAGCGATTCCAGTTC r-CAGTGAATCCGGTGGAAAC | This work |
| Otx-2 | f-CATCGGACATAAAGCAGCTCATC r-CTTCCCTCCTCTGTTTCCTCG | Lai et al., 1995 |

^a f, forward primers; r, reverse primers.

3.3. Embryo culture and dissection

Embryos were obtained by in vitro fertilisation of hormonally stimulated *Xenopus laevis* and staged according to Nieuwkoop and Faber (1967). Standard embryological procedures were used as described by Jones and Woodland (1986). Embryos were dejellied in 2% cysteine hydrochloride, pH8 and cultured in 1/10 BarthX. Dissected animal caps were cultured in BarthX or Ca²⁺ and Mg²⁺ free BX depending on whether disaggregation was required, and staged using whole embryo controls. Whole embryo dissections were performed (Fig. 4, insert) in BarthX using an eyelash knife.

3.4. mRNA synthesis and microinjection

The complete XEZ cDNA was removed from pBluescript SK- and cloned into the pCS2+ vector at the *EcoRI* and *XhoI* sites. XEZ mRNA was synthesized from XEZ/pCS2+ plasmid template, linearized by cutting with *Sac II*, using the mMessage mMachine (SP6 polymerase, Ambion). All micro-injections were carried out with RNA diluted to approximately 25 μ g/ml. Approximately 0.8 ng (36 nl) was injected into the one cell embryo or one or two blastomeres at the two cell stage (as specified in the text) of dejellied embryos under 5% Ficoll in BarthX.

3.5. RT-PCR

Total RNA from whole embryos was isolated and used for RT-PCR as described by Barnett et al., 1998. Primers used in this study are shown in Table 1.

3.6. Wholemount in situ hybridization

The wholemount in situ hybridization procedure used was as described in Harland, 1991. The embryos were fixed in MEMFA (0.5 M MOPS, pH 7.4, 100 mM EGTA, 1 mM MgSO₄, 4% formaldehyde) and hybridised with RNA

probes produced from cDNA clones. The XEZ antisense probe was transcribed with T7 RNA polymerase from a sub-clone of 1415bp of XEZ in pBluescript KS+. The *engrailed* antisense probe was transcribed with T3 RNA polymerase from a full-length clone of 1.5Kb in pBluecript KS+ (a gift from A. Hemmati-Brivanlou, Rockefeller University, NY). Probes were synthesized and labelled using a DIG labelling kit (Boehringer) and visualised using anti-DIG-alkaline phosphatase secondary and NBT/BCIP for the colour reaction according to manufacturer's recommendations (Boehringer).

3.7. Histological analysis

Tadpoles were fixed in MEMFA at Stage 37 and dehydrated in an ascending series of ethanol to 100%. The samples were cleared in Histoclear II (Lamb) and incubated first in 1:1 Histoclear II:Paraplast Xtra (Sigma) at 60°C for 30 minutes and then transferred to molten Paraplast Xtra and incubated overnight. The samples were embedded on a cushion of Paraplast Xtra, allowed to cool, sectioned (6 μ m) and collected on to subbed slides. The sections were then cleared with Histoclear II and stained using 20% Harris hematoxylin solution (Sigma) and 1% eosin (BHD).

Acknowledgements

We thank Hugh Woodland for the gift of the *Xenopus* cDNA library, Surinder Bhamra for the in situ hybridization and histology and Bob Taylor for maintenance of breeding frogs. This work was supported by the Wellcome Trust (MWB and RWO) and the BBSRC (RAS, SN and EAJ).

References

- Abel, K.J., Brody, L.C., Valdes, J.M., Erdos, M.R., McKinley, D.R., Castilla, L.H., Merajver, S.D., Couch, F.J., Friedman, L.S., Ostermeyer, E.A., Lynch, E.D., King, M.-C., Welsh, P.L., Osbourne-Lawrence, S., Spillman, M., Bowcock, A.M., Collins, F.S., Weber, B.L., 1996. Characterisation of EZH1, a Human homolog of *Drosophila Enhancer of zeste* near BRCA1. *Genomics* 37, 161–171.
- Alkema, M.J., van der Lugt, N.M., Bobeldijk, R.C., Berns, A., van Lohuizen, M., 1995. Transformations of axial skeleton due to overexpression of bmi-1 in transgenic mice. *Nature* 374, 724–727.
- Barnett, M.W., Old, R.W., Jones, E.A., 1998. Neural induction and patterning by fibroblast growth factor, notochord and somite tissue in *Xenopus*. *Dev. Growth Differ.* 40, 47–57.
- Bassez, T., Paris, J., Omilli, F., Dorel, C., Osborne, H.B., 1990. Post-transcriptional regulation of ornithine decarboxylase in *Xenopus laevis* oocytes. *Development* 110, 955–962.
- Bradley, L.C., Snape, A., Bhatt, S., Wilkinson, D.G., 1993. The structure and expression of the *Xenopus* Krox-20 gene: conserved and divergent patterns of expression in rhombomeres and neural crest. *Mech. Dev.* 40, 73–84.
- Carrington, E.A., Jones, R., 1996. The *Drosophila* Enhancer of zeste gene encodes a chromosomal protein: examination of wild-type and mutant protein distribution. *Development* 122, 4073–4083.
- Chen, H., Rossier, C., Antonarakis, S.E., 1996. Cloning of human homo-

- logue of the *Drosophila* Enhancer of zeste gene (EZH2) that maps to chromosome 21q22.2. Genomics 38, 30–37.
- DeCamillis, M., Cheng, N.S., Pierre, D., Brock, H.W., 1992. The polyhomeotic gene of *Drosophila* encodes a chromatin protein that shares polytene chromosome-binding sites with Polycomb. Genes Dev. 6, 223–232.
- Feinberg, A., Vogelstein, B., 1984. A technique for radiolabelling DNA restriction endonuclease fragments to high specific activity. Anal. Biochem. 137, 266–267.
- Franke, A., DeCamillis, M., Zink, D., Cheng, N., Brock, H.W., Paro, R., 1992. Polycomb and polyhomeotic are constituents of a multimeric protein complex in chromatin of *Drosophila melanogaster*. EMBO J. 11, 2941–2950.
- Fukuyama, T., Otsuka, T., Shigematsu, H., Uchida, N., Arima, F., Ohno, Y., Iwasaki, H., Fukuda, T., Niho, Y., 2000. Proliferative involvement of ENX-1, a putative human Polycomb gene, in haematopoietic cells. Br. J. Haematol. 108, 842–847.
- Gelbart, W.M., Wu, C.T., 1982. Interactions of zeste mutations with loci exhibiting transvection effects in *Drosophila melanogaster*. Genetics 102, 179–189.
- Goodrich, J., Puangsomlee, P., Martin, M., Long, D., Meyerowitz, E.M., Coupland, G., 1997. A Polycomb-group gene regulates homeotic gene expression in Arabidopsis. Nature 386, 44–51.
- Grossniklaus, U., Vielle-Calzada, J-P., Hoepfner, M.A., Gagliano, W.B., 1998. Maternal control of embryogenesis by MEDEA, a polycomb group gene in Arabidopsis. Science 280, 446–450.
- Hansen, C.S., Marion, C.D., Steele, K., George, S., Smith, W.C., 1997. Direct neural induction and selective inhibition of mesoderm and epidermis inducers by Xnr3. Development 124, 483–492.
- Harland, R., 1991. In Situ Hybridisation: An Improved Whole-Mount Method for *Xenopus* Embryos. Methods Cell Biol. 36, 685–695.
- Hobert, O., Sures, I., Ciossek, T., Fuchs, M., Ullrich, A., 1996a. Isolation and developmental expression analysis of Enx-1, a novel mouse Polycomb gene. Mech. Dev. 55, 171–184.
- Hobert, O., Jallal, B., Ullrich, A., 1996b. Interaction of Vav with ENX-1, a putative transcriptional regulator of homeobox gene expression. Mol. Cell. Biol. 16, 3066–3073.
- Holdeman, R., Nehrt, S., Strome, S., 1998. MES-2, a maternal protein essential for viability of the germline in *Caenorhabditis elegans*, is homologous to a *Drosophila* Polycomb group protein. Development 125, 2457–2467.
- Jack, J.W., Judd, B.H., 1979. Allelic pairing and gene regulation: a model for the zeste-white interaction in *Drosophila melanogaster*. Proc. Natl. Acad. Sci. USA 76, 1368–1372.
- Jacobs, J.J.L., Kieboom, K., Marino, S., DePinho, R.A., van Lohuizen, M., 1999. The oncogene and Polycomb-group gene bmi-1 regulates cell proliferation and senescence through the ink4a locus. Nature 397, 164–168.
- Jones, R.S., Gelbart, W.M., 1990. Genetic analysis of the Enhancer of zeste locus and its role in gene regulation in *Drosophila melanogaster*. Genetics 126, 185–199.
- Jones, E.A., Woodland, H.R., 1986. Development of the ectoderm in *Xenopus* – tissue specification and the role of cell association and division. Cell 44, 345–355.
- Kalisch, W.E., Rasmuson, B., 1974. Changes of zeste phenotype induced by autosomal mutations in *Drosophila melanogaster*. Hereditas 78, 97–104.
- Korf, I., Fan, Y., Strome, S., 1998. The Polycomb group in *Caenorhabditis elegans* and maternal control of germline development. Development 125, 2469–2478.
- Lai, C.-J., Ekker, S.C., Beachy, P.A., Moon, R.T., 1995. Patterning of the neural ectoderm of *Xenopus laevis* by the amino terminal product of hedgehog autoproteolytic cleavage. Development 121, 2349–2360.
- LaJeunesse, D., Shearn, A., 1996. E(z): a polycomb group gene or a trithorax group gene? Development 122, 2189–2197.
- Lessard, J., Schumacher, A., Thorsteinsdottir, U., van Lohuizen, M., Magnuson, T., Sauvageau, G., 1999. Functional antagonism of the Polycomb-Group eed and Bmi1 in hemopoietic cell proliferation. Genes Dev 13, 2691–2703.
- Mohun, T.J., Taylor, M.V., Garrett, N., Gurdon, J.B., 1989. The CARG promoter sequence is necessary for muscle-specific transcription of the cardiac actin gene in *Xenopus laevis* embryos. EMBO J. 8, 1153–1161.
- Nieuwkoop, P.D., Faber, J., 1967. Normal table of *Xenopus laevis* (Daudin), 2nd Ed. North Holland, Amsterdam.
- Ogawa, M., Hiraoka, Y., Taniguchi, K., Aiso, S., 1998. Cloning and expression of a Human/mouse Polycomb group gene, ENX-2/Enx-2. Biochem. Biophys. Acta. 1395, 151–158.
- Orlando, V., Paro, R., 1995. Chromatin multiprotein complexes involved in the maintenance of transcription patterns. Curr. Opin. Gen. Dev. 5, 174–179.
- Papalopulu, N., Kintner, C., 1996. A posteriorising factor, retinoic acid, reveals that anteroposterior patterning controls the timing of neuronal differentiation in *Xenopus* neuroectoderm. Development. 122, 3409–3418.
- Paro, R., 1990. Imprinting a determined state into the chromatin of *Drosophila*. Trends. Genet 6, 416–421.
- Paro, R., Hogness, D.S., 1991. The Polycomb protein shares a homologous domain with a heterochromatin-associated protein of *Drosophila*. Proc. Natl. Acad. Sci. USA. 88, 263–267.
- Pearce, J.J., Singh, P.B., Gaunt, S.J., 1992. The mouse has a Polycomb-like chromobox gene. Development 114, 921–929.
- Piccolo, S., Sasai, Y., Lu, B., De Robertis, E.M., 1996. Dorsoventral patterning in *Xenopus*: inhibition of ventral signals by direct binding of chordin to BMP-4. Cell 86, 589–598.
- Piccolo, S., Agius, E., Leyns, L., Bhattacharyya, S., Grunz, H., Bouwmeester, T., De Robertis, E.M., 1999. The head inducer Cerberus is a multifunctional antagonist of Nodal, BMP and Wnt signals. Nature 397, 707–710.
- Pirrotta, V., 1997. Chromatin-silencing mechanisms in *Drosophila* maintain patterns of gene expression. Trends Genet. 13, 314–318.
- Poux, S., Kostic, C., Pirrotta, V., 1996. Hunchback-independent silencing of late Ubx enhancers by a Polycomb Group Response Element. EMBO J. 15, 4713–4722.
- Rastelli, L., Chan, C.S., Pirrotta, V., 1993. Related chromosome binding sites for zeste, suppressors of zeste and polycomb group proteins in *Drosophila* and their dependence on Enhancer of zeste function. EMBO J. 12, 1513–1522.
- Reijnen, M.J., Hamer, K.M., den Blaauwen, J.L., Lambrechts, C., Schoneveld, I., van driel, R., Otte, A.P., 1995. Polycomb and bmi-1 homologs are expressed in overlapping patterns in *Xenopus* embryos and are able to interact with each other. Mech. Dev. 53, 35–46.
- Sewalt, R.G.A.B., van der Vlag, J., Gunster, M.J., Hamer, K.M., den Blaauwen, J.L., Satijn, D.P.E., Hendrix, T., van Driel, R., Otte, A.P., 1998. Characterisation of interactions between the mammalian Polycomb-group proteins Enx-1/EZH2 and EED suggests the existence of different mammalian polycomb-group protein complexes. Mol. Cell. Biol. 18, 3586–3595.
- Strouboulis, J., Damjanovski, S., Vermaak, D., Meric, F., Wolffe, A.P., 1999. Transcriptional repression by XPc1, a new polycomb homolog in *Xenopus laevis* embryos, is independent of histone deacetylase. Mol. Cell. Biol. 19, 3958–3968.
- Temura, S., Yamamoto, T.S., Takagi, C., Uchiyama, H., Natsume, T., Shimasaki, S., Sugino, H., Ueno, N., 1998. Direct binding of follistatin to a complex of bone-morphogenetic protein and its receptor inhibits ventral and epidermal cell fates in early *Xenopus* embryo. Proc. Natl. Acad. Sci. USA 95, 9337–9342.
- Tie, F., Furuyama, T., Harte, P.J., 1998. The *Drosophila* Polycomb group proteins ESC and E(Z) bind directly to each other and co-localise at multiple chromosomal sites. Development 125, 3483–3496.
- Tschiersch, B., Hofmann, A., Krauss, V., Dorn, R., Korge, G., Reuter, G., 1994. The protein encoded by the *Drosophila* position-effect variegation suppressor gene Su(var)3-9 combines domains of antagonistic regulators of homeotic gene complexes. EMBO J. 16, 3822–3831.
- van der Vlag, J., Otte, A.P., 1999. Transcriptional repression mediated by

the human polycomb-group protein EED involves histone deacetylation. *Nat Genet.* 23, 474–478.

Vidal, A., Koff, A., 2000. Cell-cycle inhibitors: three families united by a common cause. *Gene* 247, 1–15.

Wright, C.V.E., Morita, E.A., Wilkin, D.J., de Robertis, E.M., 1990. The *Xenopus* Xlhbbox 6 homeo protein, a marker of posterior neural induction, is expressed in proliferating neurons. *Development* 109, 225–234.

Yoshitake, Y., Howard, T.L., Christian, J.L., Hollenberg, S.M., 1999.

Misexpression of Polycomb-group proteins in *Xenopus* alters anterior neural development and represses neural target genes. *Dev. Biol.* 215, 375–387.

Zachar, Z., Chapman, C.H., Bingham, P.M., 1985. On the molecular basis of transvection effects and the regulation of transcription. *Cold Spring Harbor Symp. Quant. Biol.* 50, 337–346.

Zimmerman, L.B., De Jesus-Escobar, J.M., Harland, R.M., 1996. The Spemann organizer signal noggin binds and inactivates bone morphogenetic protein 4. *Cell* 86, 599–606.